
Holocene landscape history of southern Portugal

William Fletcher
Trinity College
University of Cambridge

This dissertation is submitted for the
degree of Doctor of Philosophy.

This dissertation is the result of my own work and includes nothing which is the outcome of work done in collaboration except where specifically indicated in the text.

This dissertation does not exceed 80,000 words, excluding appendices and the bibliography.

Summary

To date, southern Portugal, and especially the Algarve region, has been the focus of only limited palaeoecological research. In particular, the scarcity of dated pollen studies has meant that inferences regarding the vegetation history of the Algarve and related aspects of landscape evolution have had to be drawn from distant sites. The pursuit of palaeoecological research has been hindered by the lack of suitable sites for pollen analysis. This dissertation contributes to the understanding of Holocene palaeoenvironmental change in the Algarve region with new palynological data from three boreholes drilled in intertidal, estuarine settings. In a region without natural lakes, estuarine sediments deposited during the Holocene marine transgression represent a valuable resource for pollen analysis.

Presented in the dissertation are the methods and results of sedimentary and palynological analyses of AMS ^{14}C dated sediment sequences from the estuaries of the Guadiana, Arade and Boina rivers. Sediment analyses, including loss-on-ignition, particle-size analysis and magnetic susceptibility, are used to characterise sedimentary units within the sequences and permit an interpretation of changing environments of deposition during the Holocene. The sedimentary analyses contribute to the understanding of the evolution of the Arade/Boina and Guadiana estuaries and changes in the littoral zone, and are critical to the investigation of palynological material preserved within the cores.

Pollen analysis of the estuarine sediments provides detailed palaeoecological information regarding changes in local and wetland environments within the estuarine settings, and for vegetation events in the wider landscape between *c.* 13,000 and 2,000 cal BP. Critical to the analysis are both taxonomic precision and the rigorous discrimination of wetland and non-wetland taxa. Based on the new pollen records, this dissertation provides the first account of Holocene vegetation history for the Algarve. Identified at the three sites is an early and mid-Holocene woodland vegetation characterised by *Pinus*, evergreen and deciduous oaks (*Quercus* spp.), and associated understorey shrubs and herbs. After *c.* 5000 cal BP, dramatic declines in arboreal pollen are recorded, associated with an increase in moor and heath taxa, notably Ericaceae and Cistaceae. The results permit a re-evaluation of the debated role of anthropogenic impact on the Algarve landscape.

Finally, the results of both sedimentary and pollen analyses are placed in the wider regional context of the Iberian peninsula. Considered in the dissertation are: a) the timing and nature of changes in coastal environments during the Holocene transgression, b) the impact of sea-level change on wetland environments, c) the characteristics of the early and mid-Holocene vegetation, and d) the evidence for major deforestation during prehistoric times.

Acknowledgements

I acknowledge with gratitude the financial support of the NERC studentship which made this study possible, and the support of Trinity College and the Philip Lake Fund of the Department of Geography. I am grateful for the guidance and support of my supervisor, Harriet Allen, throughout the course of the Ph.D., both in Cambridge and during visits to Portugal, and for her assistance in reading drafts of this thesis. Many thanks also go to the other members of my advisory committee, Phil Gibbard and Charly French, for their helpful comments. I would like to extend my gratitude to Tomasz Boski for providing access to the samples which form the basis of the research, and for his enthusiasm and advice.

I am also very grateful for the help of many people who provided advice, assistance and discussion in all manner of areas. Many thanks to Steve Boreham for practical instruction, in-depth discussion and problem-solving at every stage of the Ph.D., and to Chris Rolfe for his assistance on many occasions during the laboratory work. I am indebted to Jose Mateus and Paula Quieroz for their advice and comments on my research during a visit to Lisbon, and for their generosity in sharing their ideas and written work with me. I am very grateful to Will Simonson for providing valuable information about the Algarve flora, and for numerous helpful comments on my work, and to the other members of the A Rocha conservation centre for providing a base for exploration, the use of their library, and for much practical support. Thanks also to Charles Turner and Martin Head for their assistance in palynological matters; Richard Preece, Tom Meijer and Jan Light for mollusc identifications; Ian Lawson for accompanying me to Portugal for the first field visit; Tony Stevenson, Tim van der Schriek, Dave Passmore and Peter James for helpful comments at the start of the Ph.D.; James Brassington for help with satellite images and discussions in the Algarve; Allen Coombes and Robert Page for providing botanical specimens for pollen reference; Catarina and Luis Ferreira, and Pedro Barros for helpful discussions regarding the geography and archaeology of the Algarve.

A thank you is owed to all the members of the Quaternary Palaeoenvironments Group, for discussion, encouragement and friendship over the several years since I first began the M.Phil. in Quaternary Science. In particular, I am grateful to Stijn de Schepper, Vasiliki Margari, Maria Papanikolaou and Phil Hughes for their good humour and companionship, willingness to look down a microscope, and for providing lots of feedback on ideas and problems. Looking back, I would like to thank Marco Madella and the members of the Pitt-Rivers laboratory for fostering an interest in all things botanical.

Finally, I will always be grateful for the loving support of my family, for looking after me especially in the last few months, for my dad's help in printing out the thesis, for my mum's care and kindness; and to my good friend, Magnus Marsden, for all the years of mutual support and encouragement; and to Nicky Milner, for proofreading and good advice, constant emotional support, and unfailing confidence since the beginning.

Contents

1	Introduction	1
1.1	Aims and objectives	2
1.2	Rationale	3
1.3	Choice of sites and methods	7
1.4	Palynology of estuarine sediments	10
1.5	Structure of the thesis	11
2	Study areas	13
2.1	Algarve: a general overview	13
2.1.1	Geology and landforms	15
2.1.2	Climate	18
2.1.3	Flora	21
2.2	Guadiana estuary	25
2.2.1	Physiographic setting	25
2.2.2	Hydrodynamic setting	26
2.2.3	Sediment supply	27
2.2.4	Modern Sedimentary environments	28
2.2.5	Sedimentary infill	29
2.2.6	Study site: core CM5, Beliche-Guadiana	31
2.3	Boina-Arade estuary	32
2.3.1	Physiographic setting	32
2.3.2	Study site: core P2, Arade	35
2.3.3	Study site: core P5, Boina	35
3	Methodology	36
3.1	Sample collection and preparation	36
3.1.1	Sampling strategy	36
3.1.2	Sample collection and storage	37
3.1.3	Subsampling and preparation for analysis	38
3.2	Methods for sediment analyses	38
3.2.1	Loss-on-ignition	38
3.2.2	Particle size analysis	42
3.2.3	Magnetic Susceptibility	45
3.3	Methods for pollen analysis	47
3.3.1	Pollen preparation	47
3.3.2	Pollen counting and identification	47
3.3.3	Calculation of pollen concentrations	50
3.4	Radiocarbon data	50
4	Core lithology and results of sediment analyses	51
4.1	CM5 Guadiana	51
4.1.1	Core lithology (CM5)	51
4.1.2	Loss-on-ignition (CM5)	53
4.1.3	Particle size analysis (CM5)	55
4.1.4	Magnetic susceptibility (CM5)	56
4.1.5	Shell content (CM5)	57

4.2	P2 Arade	57
4.2.1	Core lithology (P2)	57
4.2.2	Loss-on-ignition (P2)	59
4.2.3	Particle size analysis (P2)	60
4.2.4	Magnetic susceptibility (P2)	61
4.2.5	Shell content (P2).....	62
4.3	P5 Boina	62
4.3.1	Core lithology	62
4.3.2	Loss-on-ignition (P5)	65
4.3.3	Particle size analysis (P5)	66
4.3.4	Magnetic susceptibility (P5)	67
4.3.5	Shell content (P5).....	68
5	Radiocarbon chronology and age-depth models	94
5.1	Introduction	94
5.2	Radiocarbon dates	94
5.2.1	Sample material and sources of error	95
5.2.2	Calibration	100
5.3	Age-depth models	103
5.3.1	CM5 Guadiana	104
5.3.2	P2 Arade	107
5.3.3	P5 Boina	110
5.4	Sedimentation trends and sea-level history	112
6	Discussion: sediment properties	117
6.1	On the interpretation of sedimentary parameters	117
6.1.1	Organic content	117
6.1.2	Carbonate content	119
6.1.3	Particle Size	120
6.1.4	Magnetic susceptibility	126
6.2	CM5 Guadiana	131
6.2.1	Organic and carbonate content	131
6.2.2	Particle Size	132
6.2.3	Magnetic susceptibility	137
6.3	P2 Arade	140
6.3.1	Organic and carbonate content	140
6.3.2	Particle Size	141
6.3.3	Magnetic Susceptibility	145
6.4	P5 Boina	147
6.4.1	Organic and carbonate content	147
6.4.2	P5 Particle Size	148
6.4.3	P5 Magnetic susceptibility	151
6.5	Characterisation of the infill sequences: summary	153
7.1	Presentation of the pollen data	155
7.1.1	Pollen types and nomenclature	155
7.1.2	Construction of the pollen diagrams	157
7.1.3	Order of taxa in the diagrams	162
7.1.4	Summary diagrams	162
7.1.5	Pollen zonation	163
7.2	Description of the pollen results	165

7.2.1	CM5 Guadiana	166
7.2.2	P2 Arade	177
7.2.3	P5 Boina	179
8	Discussion: pollen data	201
8.1	On the interpretation of pollen percentage data	201
8.2	CM5 Guadiana	212
8.2.1	Late-glacial vegetation, c. 13,000–11,860 cal BP	212
8.2.2	Early Holocene vegetation, c. 11,860–8960 cal BP	215
8.2.3	Holocene forest conditions, c. 8960–5200 cal BP	217
8.2.4	A mid-Holocene deforestation event, c. 7760–7350 cal BP	220
8.2.5	Indications of anthropogenic impact, c. 5200–1430 cal BP	221
8.2.6	Agricultural indicators	223
8.2.7	Saltmarsh development, c. 5200–1430 cal BP	227
8.2.8	Dinoflagellates and other micro-fossils	227
8.3	P2 Arade	228
8.4	P5 Boina	231
9	Integration	234
9.1	Estuarine evolution and environments of deposition	234
9.1.1	Beliche-Guadiana (Core CM5)	234
9.1.2	Boina-Arade estuary (Cores P2 and P5)	247
9.1.3	Summary: Holocene changes in the estuarine domain	255
9.2	Vegetation history and landscape changes	256
9.2.1	Late-glacial	256
9.2.3	Mid-Holocene	261
9.2.4	Late Holocene	264
9.3	Evaluation and prospects for future research	267
10	Conclusions	271
	Bibliography	277
	Appendix A. Beliche surface pollen samples	300
	Appendix B. Table of pollen types.	312

List of Figures

1.1. Location of Holocene pollen records from the southwestern Iberian peninsula	4
2.1. Map of southern Portugal and location of study areas.	14
2.2. Geological sketch map of southern Portugal.	15
2.3. Distribution of thermotypic stages and rainfall in southern Portugal	18
2.4. Map of the Guadiana estuary, showing hydrodynamic domains.	26
2.5. Schematic cross section of the Guadiana infill	30
2.6. Geology of the Portimão area	33
3.1. Strategic sequence of analyses for small sediment samples	37
4.1. Core lithology and sample depths, CM5	69
4.2. Loss-on-ignition results, CM5	71
4.3. Biplots of loss-on-ignition results, CM5	72
4.4. Particle size distribution, organics and carbonates removed, CM5	73
4.5. Particle size summary, organics and carbonates removed, CM5	74
4.6. Magnetic susceptibility results, CM5	75
4.7. Biplot of χ_{lf} vs. $\chi_{fd}\%$, CM5.	75
4.8. Shell content of sediment samples, CM5	76
4.9. Core lithology and sample depths, P2.	77
4.10. Loss-on-ignition results, P2	79
4.11. Biplot of organic matter vs. CaCO_3 content, P2	80
4.12. Particle size distribution, organics and carbonates removed, P2	81
4.13. Particle size summary, organics and carbonates removed, P2	82
4.14. Magnetic susceptibility results, P2	83
4.15. Biplot of χ_{lf} vs. $\chi_{fd}\%$, P2	83
4.16. Shell content of sediment samples, P2	84
4.17. Core lithology and sample depths, P5	85
4.18. Loss-on-ignition results, P5	87
4.19. Biplots of loss-on-ignition results, P5	88
4.20. Particle size distribution, organics and carbonates removed, P5	89
4.21. Particle size summary, organics and carbonates removed, P5	90
4.22. Gravel content and integrated particle size data, P5	91
4.23. Magnetic susceptibility results, P5	92
4.24. Biplot of χ_{lf} vs. $\chi_{fd}\%$, P5.....	92
4.25. Shell content of sediment samples, P5	93
5.1. Age-depth model, CM5	105
5.2. Age-depth model, P2	108

5.3. Age-depth model, P5	109
5.4. General sedimentation trend in the CM5, P2 and P5 cores	114
6.1. The Pejrup ternary diagram for estuarine sediments	123
6.2. Template for biplot of mean grain size vs. sorting	125
6.3. Particle size histograms for three samples from core CM5	133
6.4. Pejrup ternary diagram, CM5 sand/silt/clay data	134
6.5. Biplot of mean grain size vs. sorting, CM5	135
6.6. Comparison of χ_{lf} , $\chi_{fd}\%$ and sand content, CM5	138
6.7. Biplot of CaCO_3 content vs. shell content, P2	141
6.8. Particle size histograms for three samples from core P2	142
6.9. Pejrup ternary diagram: P2 sand/silt/clay data	143
6.10. Biplot of mean grain size vs. sorting, P2	144
6.11. Comparison of χ_{lf} , $\chi_{fd}\%$ and sand content, P2	145
6.12. Particle size histograms for four samples from core P5	148
6.13. Pejrup ternary diagram: P5 sand/silt/clay data	149
6.14. Biplot of mean grain size vs. sorting, P5	150
6.15. Comparison of χ_{lf} , $\chi_{fd}\%$ and sand content, P5	152
7.1. Pollen assemblage biozone (P.A.B.) boundaries and CONISS results	164
7.2. Summary pollen percentage diagram, CM5	183
7.3. Pollen percentage diagram, CM5	184
7.4. Concentration diagram, CM5, select taxa	189
7.5. <i>Pinus</i> morphometric analysis	190
7.6. Pollen percentage diagram, P2	191
7.7. Concentration diagram, P2, select taxa	195
7.8. Pollen percentage diagram, P5	196
7.9. Concentration diagram, P5, select taxa	200
8.1. Theoretical pollen dispersal curve	202
8.2. Transport pathways of pollen entering an estuary	205
9.1. CM5 pollen percentage data plotted against age	236

List of Tables

2.1. Classification of the thermomediterranean and mesomediterranean thermotypes .	20
2.2. Classification of ombrotypes occurring in the Algarve	20
2.3. Climate data for two Algarve climate stations	20
3.1. Malvern 2000 measurement settings	43
3.2. Pollen preparation stages	48
4.1. Sediment zone summary, core CM5	52
4.2. Sediment zone summary, core P2	58
4.3. Sediment zone summary, core P5	63
4.4. Summary of results of sediment analyses, core CM5	70
4.5. Summary of the results of sediment analyses, core P2	78
4.6. Summary of the results of sediment analyses, core P5	86
5.1 Radiocarbon dates from cores CM5, P2 and P5	95
5.2. Calibrated age ranges for shell dates using different reservoir effects	102
7.1. List of pollen and spores identified in the CM5, P2 and P5 cores by family	156
7.2. Classification of tree and shrub taxa for the purposes of summary diagrams	163
7.3. Taxa occurring at >5% of total pollen and spores and included in CONISS	166
7.4. Taxa occurring in only one sample, CM5	167
7.5. Taxa occurring in only one sample, P5	179
9.1. Summary of sedimentological and palynological findings from core CM5	235
9.2 Summary of sedimentological and palynological findings, Boina-Arade estuary ..	248

1 Introduction

The Holocene, the present interglacial period, is studied both as an analogue for understanding earlier interglacial periods, and as the unique interglacial where environments heavily modified by human pressure have come to dominate many parts of the world. For northern Europe, numerous studies of terrestrial sedimentary records of Holocene age provide evidence for relatively well-understood patterns of environmental change. During the Late-glacial and especially from the onset of the Holocene, the forest cover responded to climatic changes by expansion from refugial areas of glacial growth (Huntley, 1988; Huntley & Prentice, 1993). The thermal maximum and increasingly moist conditions of the mid-Holocene permitted the maximum northward and altitudinal extension of range for many broadleaf vegetation types (Huntley, 1988). During the last 4 thousand years, changes in forest composition increasingly reflect the influence of human activity on vegetation and soil. For southern Europe, more varied and complex patterns of Holocene environmental change are emerging (Roberts *et al.*, 2001). These patterns reflect the diversity of landscapes (structured fundamentally by the heterogeneous geology of the basin (Blondel & Aronsen, 1999)), the role of the southern European peninsulas (Iberian, Italian, Balkan) as refugia for plant and animal life during glacial periods (Bennett *et al.*, 1991; Willis, 1994), inter-regional climatic variability and the rich history of human settlement and civilisation. In addition to these conditioning factors, patterns of Holocene environmental change are

increasingly understood to be responsive to climate change on a centennial to millennial scale (Bond *et al.*, 1997). The understanding of these variables and their influence on vegetation history is limited by the relatively small number of well-dated pollen records for Mediterranean Europe, particularly as one approaches the southernmost margins of the region.

The Algarve province of southern Portugal, located at the southwestern corner of Europe, has not been the focus of extensive research in the fields of climate and vegetation history. In common with other areas of southern Europe, knowledge of palaeoenvironmental change is poorly developed, limited to a great degree by the scarcity of depositional basins providing preservation of organic material. The accumulation of sediments with organic preservation in the estuaries of the Algarve, however, provides an opportunity for sedimentological and palynological research. The situation of estuaries at the boundary of the terrestrial and marine domains means that they provide an archive of palaeoenvironmental data related to changes in both wetland and dry ground environments. With estuarine deposits in the Algarve extending to the Late-glacial period, there is the potential to develop the history of environmental changes in the region, both at the Late-glacial/Holocene transition, and over the course of the Holocene.

1.1 Aims and objectives

This study aims to develop the record of vegetation and landscape history in southern Portugal through the investigation of estuarine sediments from the Algarve.

The principal objectives, which structure the framework of the study, are:

- To develop the understanding of changes in estuarine depositional environments
- To construct a record of vegetation history in the Algarve for the Late-glacial/ Holocene transition and the Holocene through palynological investigation.
- To constrain the chronology of estuary infilling and vegetation history

- To situate the record of Holocene landscape history within the wider research context of Iberian Holocene studies.

1.2 Rationale

The primary justification for investigating the Holocene vegetation history of the Algarve is the lack of palynological data from the region, and the general scarcity of well-dated pollen records from the southern Iberian peninsula. Only two previous studies have published the results of pollen analysis from Holocene sediments in the Algarve. A pollen record for the last 1200 years has been published from the Boca do Rio marsh in the western Algarve (Allen, 2003). A localised pollen source area results in a record which reflects primarily changes in the wetland environment. At this site, a transition from saltmarsh to freshwater wetland is detected, associated with decreasing marine influence and increased fluvial sediment supply. The sequence also includes a likely hiatus of *c.* 700 years, related to erosion resulting from the tsunami of the AD 1755 Lisbon earthquake. The other published pollen study is based on archaeological cave sediments from Goldra in the eastern Algarve (Straus *et al.*, 1992). A radiocarbon date indicates a mid-Holocene age (*c.* 5000 ¹⁴C bp) for the time of deposition, with archaeological material pertaining to the Middle-Neolithic cultural period. Archaeological and botanical evidence indicate an established agricultural way of life, with domesticated animals and crops. Pollen spectra from seven sediment samples contain a small quantity of tree and shrub pollen (mostly of pine (*Pinus*), oak (*Quercus*) and heaths (Ericaceae)), but are dominated by herbaceous pollen of Asteraceae (daisy family). Although a trend across the seven samples suggests an expansion of Ericaceae and decline in *Pinus* — a possible indication of expanding human impact — the interpretation is complicated by taphonomic factors related to pollen transport and taphonomy in a cave setting. Moreover, there is no chronological control for the length of elapsed time represented by the sample sequence. It is clear, therefore, that the longer perspective on vegetation development in the Algarve during the Holocene is wholly missing.

From the botanical perspective, the imperative for palynological investigation is clear. “The primeval vegetation of the Algarve, a land peopled since antiquity, has been completely transformed by Man” (Braun-Blanquet *et al.*, 1964: 232, trans.). The swathes of *Cistus* maquis clothing the hills of the Algarve, the scattered oaks harvested for their cork, and the dry orchards of the lowlands constitute a landscape modified and maintained through human action by cutting and clearance, intentional burning, pastoralism and agriculture. Few, if any, stands of natural or climax vegetation exist to confirm the composition of the vegetation prior to human influence (Capelo, 1996). From this perspective, one objective in undertaking pollen analysis is to identify the ‘natural’ vegetation of the region. However, recognising that plants display highly individualistic responses to climatic, edaphic and biotic factors (Webb, 1987), the objective in fact must be to trace the changing composition of the vegetation over the Holocene period, and to identify and distinguish climatic and anthropogenic influences, rather than to identify a set of climax communities.

At present, inferences in the literature regarding the Holocene vegetation history of the Algarve (for example with regard to soil erosion or valley alluviation (Jahn *et al.*, 1989; Chester & James, 1991, 1999) are generally drawn from distant sites (Figure 1.1). The most detailed record of vegetation history in Portugal comes from sites in the Serra da

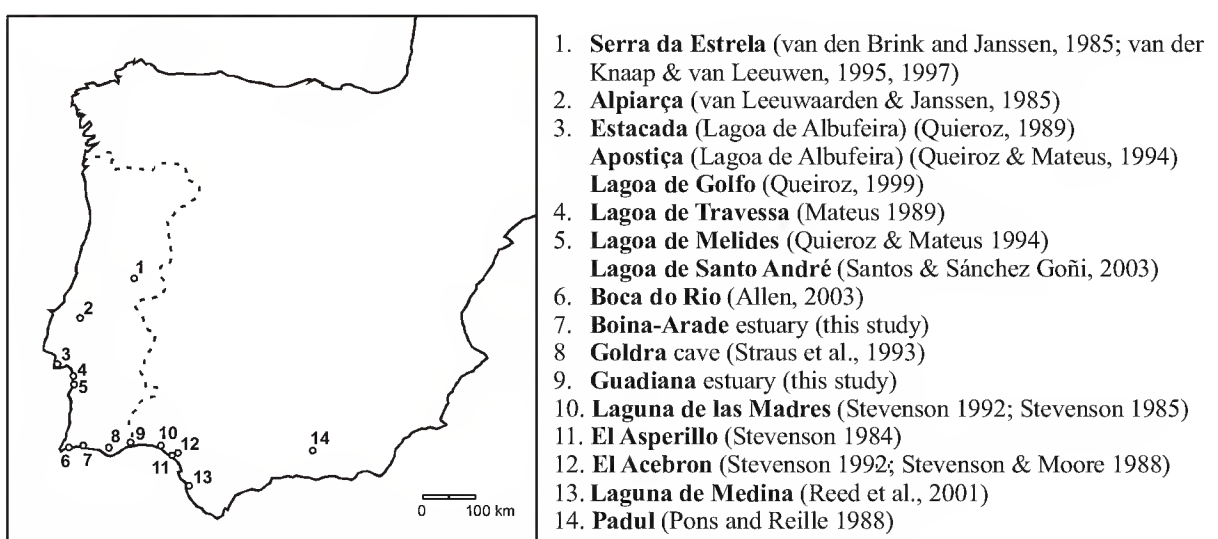


Figure 1.1. Location of Holocene pollen records from the southwestern Iberian peninsula.

Estrela, a montane region in northern Portugal (van den Brink and Janssen, 1985; van der Knaap & van Leeuwen, 1995, 1997). These pollen records show the sensitive response of the upland vegetation to climatic conditions and human activities during the Late-glacial and Holocene, and also detect indications of vegetation changes in the surrounding lowland. However, the Serra da Estrela may not necessarily provide a good model for vegetation history in southern Portugal, as the flora, climate, geology, relief and history of glaciation are quite distinct from the lowlands of southern Portugal. The other record from which inferences have been drawn for southern Portugal comes from the famous site of Padul, located at the base of the Sierra Nevada in southeastern Spain (Pons & Reille, 1988). The pollen record from Padul reveals the response of regional vegetation to climatic fluctuations during the Upper Pleistocene and Holocene, and highlights an important and early role for evergreen vegetation in the post-glacial afforestation of the region. The southern location and Mediterranean modern climate suggest that the Padul record may be more indicative of vegetation in southern Portugal. However, the Mediterranean climate at Padul is more strongly continental and arid, the region is more mountainous, and Atlantic floristic elements (such as the heaths, Ericaceae), are less important. Finally, the impact and expression of climate changes driven by North Atlantic processes may be different between the southwestern and southeastern sectors of the Iberian peninsula. Overall, the Iberian peninsula is characterised by a varied climate, topography and flora, and the reliability of inferences drawn from the distant sites of the Serra da Estrela and Padul must be confirmed through direct palynological investigation.

A number of sites, some less well known, have been investigated closer to the Algarve. In the lowlands of the Tagus valley (central Portugal), preliminary pollen analyses of two valley peat sequences covering the period *c.* 5000 to 2000 ¹⁴C bp reveal a decline in *Pinus* and *Quercus*, and an increase in NAP (non-arboreal pollen) related to human activities at a nearby archaeological settlement (van Leeuwaarden & Janssen, 1985). In southern Portugal, a cluster of sites have been investigated in the littoral zone of the Alentejo province (Mateus 1989; Queiroz 1989, 1999; Queiroz & Mateus, 1994; Santos & Sánchez Goñi, 2003). The

records from these coastal lagoons generally date from the mid- to late Holocene (after c. 6000 ^{14}C bp), although early Holocene sediments and an undated record of likely Late-glacial age are also known (Queiroz, 1999). These records show an important role for pinewoods in the early Holocene, succeeded by the mid-Holocene development of oak forest, and finally the development of evergreen shrub vegetation during the late-Holocene. The littoral character of these sites means that the records also document major changes in local environments, related to changes in coastal geomorphology and sea-level. To the east of the Algarve, radiocarbon-dated pollen records for the last c. 4500 ^{14}C years have been published from the Huelva area of southwest Spain (Stevenson, 1985b, 1988; Stevenson & Harrison 1992), as well as an undated pollen record of probable Late-glacial age (Stevenson, 1984). A record of herbaceous and aquatic pollen types has been published for the last c. 8000 ^{14}C years from a saline lake near Cadiz, and shows fluctuations in pollen content related to changing water depth and salinity associated with aridification episodes (Reed *et al.*, 2001).

These studies provide important comparative material for the southwestern Iberian sector, and identify a number of interesting phenomena which merit further investigation. In the Alentejo, these include the possible expression of a Younger Dryas (Late-glacial Stadial) type event in the vegetation, and the impact of climatic, biotic and anthropogenic factors on changing early to mid-Holocene forest composition. An important feature of the Alentejo records, identified also in the Tagus valley, is the development and expansion of shrub vegetation communities in the late-Holocene. The timing and causes of these changes need further exploration. In southwest Spain, notable features of the Huelva pollen records include evidence for early viticulture and woodland management. The extent to which these phenomena are identifiable in the Algarve, and by extension characteristic of the southwestern Iberian sector, will be explored through new palynological data in this study.

1.3 Choice of sites and methods

The principal challenge in the Algarve for palaeoecological research in general and palynology in particular is the scarcity of sites offering organic preservation. The absence of permanent lakes rules out the possibility of pollen analysis of lacustrine deposits, the type of study for which the methodology and conceptual basis for palynology is best developed (e.g. Jackson, 1994; Bennett & Willis, 2001). Fieldwork during the early phases of this study explored a number of sites in different areas of the Algarve and Alentejo, and tested a range of sediments for pollen preservation including sediments from seasonal freshwater ponds, alluvial valley-fill deposits and calcretes. On the whole, these assays proved unsuccessful, suggesting that subaerial weathering in these settings promotes high rates of organic decay under biological and chemical attack, and physical degradation of palynomorphs through wet-dry cycles associated with the strong seasonality of the Mediterranean climate regime.

In contrast with these terrestrial environments, estuaries of the Portuguese coast represent major sediment sinks and sites of organic preservation (Dias *et al.*, 2000; Boski *et al.*, 2002). Since 1999, a series of boreholes has been drilled by the Portuguese Geological Survey (IGM) in intertidal sediments of several Algarve estuaries. The cores are stored in the Universidade do Algarve, and are part of ongoing research into the impact of sea-level changes on the Algarve littoral at the Centre for Marine and Environmental Research (CIMA) under the direction of Professor T. Boski. Collaboration with CIMA provided the opportunity to extend the field of estuarine research in the Algarve to include pollen analysis. Three cores form the basis of this study, one from the Guadiana estuary on the Portugal/Spain border, and two from the Boina-Arade estuary in the western Algarve. The sediment sequences of these cores relate to the infilling of the Guadiana estuary during the Late-glacial and Holocene, and of the Boina-Arade estuary during the Holocene.

While estuaries provide valuable archives for palaeoenvironmental research, interpretation of the resulting records may be complex. Estuaries generally act as traps for sediments

from both fluvial and marine sources, and are often characterised by rapid sediment accumulation. Estuarine sedimentation is sensitive to the influence of several factors, including sea-level change and accommodation space, sediment supply from the fluvial basin and the continental shelf range, tectonic activity and anthropogenic disturbance (Colman *et al.*, 2002). This sensitivity means that sedimentation rates, sediment source areas and depositional environments may vary considerably over time. As these factors may influence the deposition, composition and preservation of pollen and spore assemblages, pollen analysis must be accompanied by critical investigation of the sediment record.

In this study, several techniques were chosen in order to characterise the sediment sequences and to evaluate changing environments of deposition at the three sites. The main techniques used in this study, in concert with core log descriptions from CIMA, are loss-on-ignition (LOI), laser particle-size analysis, and magnetic susceptibility. Shell matter content of the sediment content is also quantified. These techniques were chosen to provide several lines of information regarding the physical and magnetic properties of the sediments, namely: organic matter, carbonate and shell content, particle or grain size distribution, and the concentration of magnetic minerals. Variation in these properties is conditioned by a range of environmental variables related to hydrodynamic conditions, sediment sources and biological and geochemical conditions. The study of these properties therefore provides important information both regarding the history of the sedimentary environment and the discrimination of potential taphonomic biases affecting the pollen record.

A chronological framework is essential for comparison of sediment and pollen results between sites and for evaluation of the impact of external factors such as sea-level and climate changes on the environment. In this study, age-depth models for sedimentation at the three core locations are developed. These are based on multiple AMS radiocarbon dates which were obtained both by CIMA and as part of this project. The age-depth models are used to constrain the timing of changes in the sediment and pollen records and to provide estimates for zone boundary and sample ages.

Although the record of changes in the sedimentary environment in the studied estuaries is developed with a view to improving the interpretation of the pollen data, this record also contributes to a wider field of research, namely the study of Holocene estuarine infilling and changes in the coastal zone. It is only in recent years that detailed studies of the post-glacial history of estuarine development have been undertaken (Cearreta & Murray, 2000). In the Algarve, the first results of borehole investigations in the Guadiana estuary have been published (Boski *et al.*, 2002), presenting an outline of sedimentary infilling since the Late-glacial. This work, which focuses on estuarine sedimentary response to sea-level rise, is based on the study of four cores (CM1-4), and does not include the core studied here (CM5). Mollusc content and foraminifera abundance data presented by these authors represent the first palaeoecological data related to the impact of the Holocene transgression in the Guadiana. Other research in the Guadiana estuary has examined: 1) the sedimentary characteristics of modern estuarine surface sediments (Morales *et al.*, 1997), 2) the evolution of the Guadiana delta complex (Morales, 1997), 3) the seismic stratigraphy of the terminal segment of the valley (Lobo *et al.*, 2003), 4) the distribution of benthic foraminifera and ostracoda in modern surface sediments from the Guadiana shelf and estuary (Muñoz *et al.*, 1993; Mendes *et al.*, 2004) and 5) the characteristics of near-shore sediments of the Guadiana coastal shelf (González *et al.*, 2004; Lobo *et al.*, 2004).

The research in the Guadiana is linked in approach and subject matter to a cluster of studies from the Spanish sector of the Gulf of Cadiz coast. These have developed the knowledge of estuarine environments and their history, examining: 1) the characteristics of modern estuarine sedimentary facies and recent sedimentation (Borrego *al.*, 1995; Pendón & Morales, 1997; Pendón *et al.*, 1998; Ruiz *et al.*, 2004), 2) the Holocene sedimentation of the Guadelete, Tinto, Odiel and Piedras river estuaries (Borrego *al.*, 1993; Borrego *et al.*, 1999; Dabrio *et al.*, 2000; Lario *et al.*, 2002a) and 3) the Holocene development of spit and barrier structures (Zazo *et al.*, 1994; Rodríguez-Ramírez *et al.*, 1996). This body of previous research informs the investigation and interpretation of sediment properties undertaken in this study. In contrast

with the Guadiana and other Gulf of Cadiz estuaries, no published data relating to either sedimentological or palaeoecological research is available for the Boina-Arade estuary.

1.4 Palynology of estuarine sediments

The analysis of pollen and spores from estuarine sediments is undertaken with the goal of investigating the vegetation history of both wetland and dry ground environments. From the outset, and in light of previous research, a number of potential disadvantages are recognised in working with estuarine material. First, pollen of local wetland vegetation may be strongly over-represented in the pollen spectra, obscuring a vegetation signal from dry ground, regional or upland environments (Heyvaert, 1980; Patterson & Clark, 1985). This over-representation may not be of consequence if the wetland environment is of primary interest. A number of studies have employed pollen analysis with the main intent of exploring changes in the local setting related to salt marsh development and sea-level response (Mudie & Byrne, 1980; Jennings *et al.*, 1993; Collins *et al.*, 2001; Freund *et al.*, 2004). However, changes in dry ground vegetation communities in response to climatic and anthropogenic factors may be concealed. Second, in contrast with some depositional environments (e.g. small lake basins), pollen source areas are likely to be poorly defined, related to a multiplicity of pollen transport pathways into an estuary. Changes in local sub-environment may correspond with changes in pollen source area, influencing the composition of the pollen assemblage (Santos *et al.*, 2001). Third, in common with pollen from fluvial sediments, the contribution of reworked pollen and spores from inwashed soils and sediments may raise a question regarding the contemporaneity of the pollen assemblage. This may be compounded in the estuarine environment by the recycling and redistribution of palynomorphs by tidal currents within the estuary. Finally, pollen preservation may be variable, related to bacterial activity and oxidation, complex transport history, and wet/dry cycles at the sediment/water interface.

A number of distinct advantages, however, accompany the study of pollen from estuarine sediments. First, the diversity of pollen types is often high, providing a record of several

habitats. Second, plants with poor pollen dispersal (e.g. insect pollinated plants) may be much better represented than at sites where an atmospheric pollen contribution is dominant (Chmura *et al.*, 1999). This may result in a more complete picture of past vegetation composition. Third, and most important, estuarine palynology has the scope to identify changes in both the tidal wetland zone and the upland or dry ground environment, and to assess the synchronicity and relationships (or contrasts) between changes in the two domains. A number of successful studies illustrate this potential (e.g. Clark & Patterson, 1985; Visset, 1985, 1987; Planchais, 1987; Saa Otero & Diaz Fierros, 1990; Diot & Tastet, 1995; Sánchez Goñi, 1996; Andrieu-Ponel *et al.*, 2000).

An awareness of both the potential advantages and disadvantages of estuarine palynology, reinforced by a preliminary study of pollen surface samples from the marshes of the Beliche floodplain (Appendix A), strongly influences the approach to pollen analysis in this study. In addition to generally large pollen counts (typically >500 pollen and spores per sample) and identification to precise taxonomic levels where possible, particular attention is paid to the taxonomic and ecological significance of pollen types, and to the potential sources of pollen in terms of wetland or dry ground habitats. The impact of overrepresentation is assessed through the use of multiple pollen sums (Rybníèková & Rybníèek, 1971) and pollen concentration values.

1.5 Structure of the thesis

The first part of the thesis presents information about the research area and methodology of the study. Chapter 2 provides an overview of the geology, climate and flora of the Algarve and an introduction to the study areas of the Guadiana and Boina-Arade estuaries. Chapter 3 details the methodology of the research project, including the background and method for each technique of sediment analysis, and the methods for pollen preparation and counting. The second part of the thesis relates to the characterisation and chronology of the sediment sequences. Chapter 4 presents the description and zonation of the sediment sequences, followed by zone-by-zone description of the results of sediment analyses, including LOI,

shell content, particle size and magnetic susceptibility data. Chapter 5 presents the radiocarbon data for the sequences and develops age-depth models for the sedimentation histories at the three locations. Chapter 6 introduces the conceptual basis for interpretation of the sediment records, and discusses the interpretation of changes in sedimentary parameters for each site in relation to changes in the depositional environments. The third part of the thesis relates to the presentation and discussion of the pollen data. Chapter 7 describes the results of pollen analysis, beginning with the construction of the pollen diagrams and the delimitation of biostratigraphical zones, and followed by zone-by-zone descriptions of the pollen data for each site. Chapter 8 introduces the conceptual basis for the interpretation of pollen data, specifically with regard to estuarine pollen, and presents an interpretation of the record of vegetation changes at each site based on the pollen data. The final part of the thesis, chapter 9, integrates the results of sediment and pollen analyses to provide an interpretation of the history of depositional environments at the sites and vegetation history of the region. The conclusions of the study are presented in Chapter 10.

2 Study areas

2.1 Algarve: a general overview

The Algarve, the southernmost province of Portugal, is located between 37°35' and 36°58' N and between 7°25' and 9°00' W (Figure 2.1). The province stretches *c.* 135 km east to west and 40 km north to south, bounded by the Guadiana river to the east, the Atlantic Ocean to the south and west, and the province of Baixo Alentejo to the north. The highest point in the region is the peak of the Monchique massif (Foia, 902 m) and the mean altitude of the region is 182 m (Loureiro, 1983). The province is divided into three geographical zones which reflect the geological and geomorphological structure of the Algarve, and which influence vegetation, land-use and settlement. These are the *Serra*, an upland zone in the northern part of the province, the *Barrocal*, an intermediate zone of limestone terrain and the *Litoral*, a lowland coastal plain. Although located outside the Mediterranean hydrological basin, the Algarve is linked to the Mediterranean in terms of climate and flora. The long-term history of the Algarve also reveals the wider Mediterranean region as a source of cultural change and technological innovation both in prehistoric times (Zilhão, 2000) and during later phases of Greek, Roman and north African colonisation.

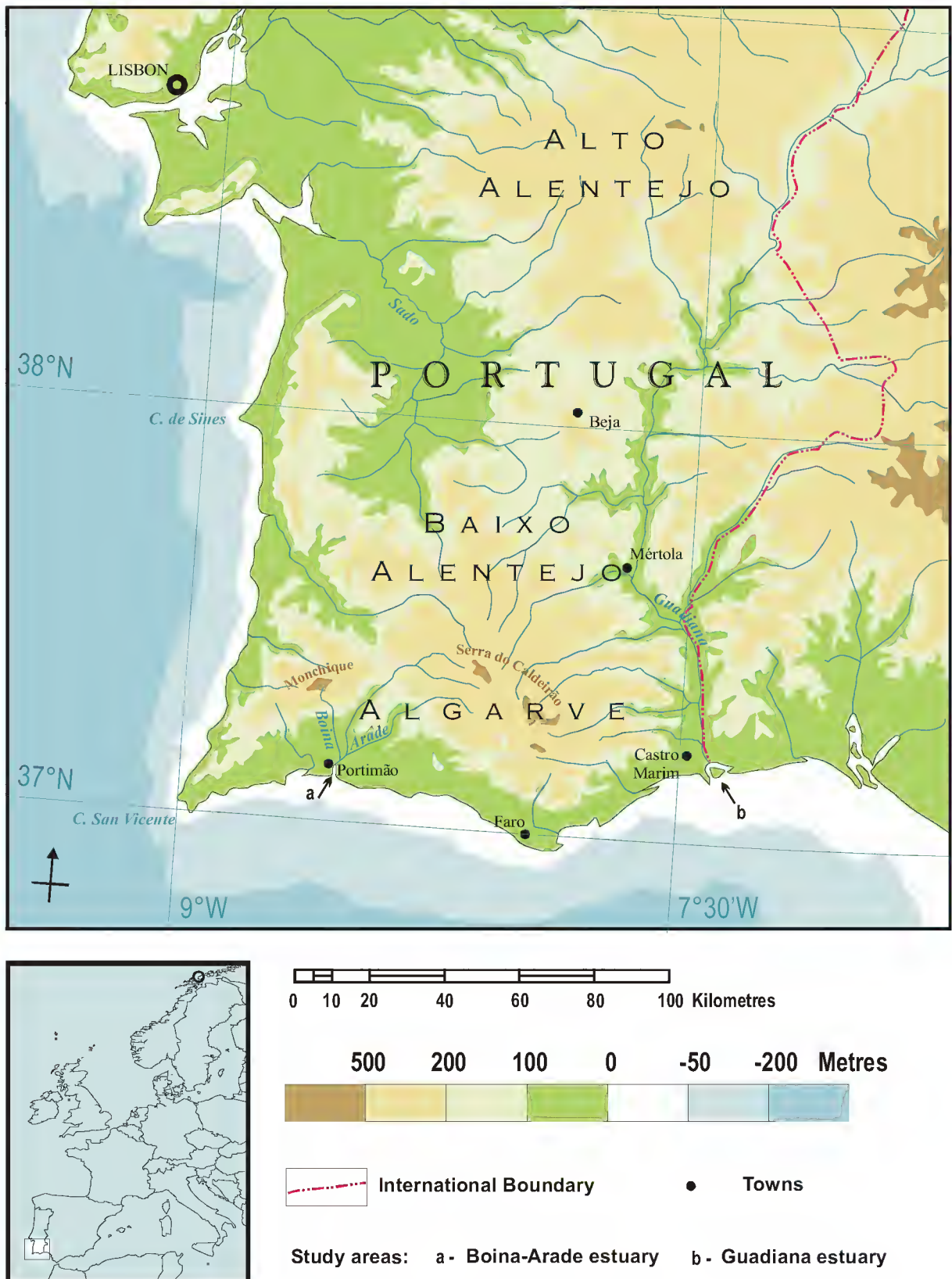


Figure 2.1. Map of southern Portugal and location of study areas.

In this section, a general overview of the geology, climate and flora of the Algarve precedes the description of the study sites.

2.1.1 Geology and landforms

The geology of the Algarve includes two distinct entities: the Palaeozoic southern Portuguese zone (Zona Sul Portuguesa), and the Mesozoic and Cenozoic Algarve basin (Figure 2.2). The area of outcropping Palaeozoic formations in the northern part of the province corresponds to the *Serra* zone, while the Algarve basin includes the *Barrocal* and *Litoral* zones to the south. A more detailed map of the geology of the Arade basin displays the major geological zones of the Algarve (Figure 2.6). The following account draws on the

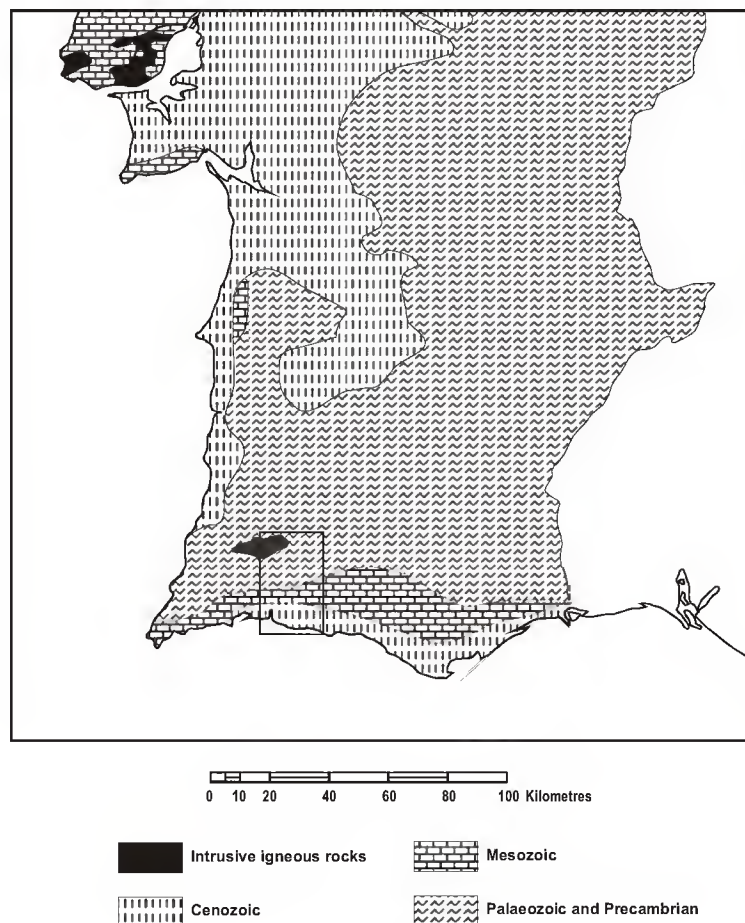


Figure 2.2. Geological sketch map of southern Portugal, redrawn from Rocha (1976). Inset box shows location of Figure 2.6.

explicative guide of Manupella (1992), information from INAG (2000), and various other sources mentioned in the text.

The Palaeozoic interior, part of the Hesperic Massif, consists principally of Carboniferous turbidites arranged in rhythmic sequences or flysch facies. These flysch facies are intensely folded and lightly metamorphosed, and have also been described as ‘metasediments’ (James & Chester, 1995). The Palaeozoic upland is characterised by polycyclic relief and intense erosion. A series of denudation surfaces are recorded at altitudes between 100 and 500 m, which are highly dissected by the deep incision of the region’s rivers. These characteristics contribute to the characteristic high relief of the *Serra* landscape and the dense drainage network. In the northwestern part of the province, a Cretaceous volcanic intrusion of syenite forms the Monchique massif. This massif forms the highest relief in southern Portugal, with the Foia peak reaching 902 m a.s.l.. The Monchique massif is characterised by steep slopes and weakly incised rivers.

Overlying the Palaeozoic formations on an angular unconformity is the Grès de Silves or Silves series, a formation of upper Triassic and lower Jurassic rocks, which outcrop along a narrow zone bordering the *Serra* across virtually the entire width of the Algarve. This formation is composed of a series of conglomerates, sandstones and pelites, culminating in a vulcano-sedimentary complex of basalts, volcanic breccias and tuffs. This series corresponds to a transition from continental terrigenous sedimentation to shallow marine sedimentation accompanied by rifting and volcanic rifting during the opening of the Algarve basin. In general, the rocks of the Silves series are poorly cemented and erodible. In many places this has produced a scarp at the boundary of the *Serra*, and a geomorphological depression in the Silves series resulting from the action of rivers such as the Arade.

Overlying the Silves series are carbonate formations of Jurassic and Cretaceous age corresponding to phases of marine sedimentation in the Algarve basin. These formations, comprising limestones with variously coralline, oolitic and dolomitic variants, display

extensive faulting, folding, and karstification. These limestones form the substrate of the *Barrocal* region of the Algarve. The relative hardness of these formations has resulted in a generally rolling terrain with broad, shallow valleys, with peaks reaching above 300 m a.s.l.

Resting unconformably above Carboniferous, Jurassic and Cretaceous formations, are Miocene deposits corresponding to a phase of carbonate sedimentation with terrigenous influence in a coastal platform setting (Lagos-Portimão formation). The Lagos-Portimão formations outcrops over large areas of the coastal zone, characterised by low relief and extensive karstification (Pais *et al.*, 2000; Dias *et al.*, 2002).

Another important feature of the coastal region are reddened siliciclastic deposits of Quaternary age, the Faro-Quarteira formation. These sand and gravel deposits represent fluvial and debris-flow transport of material derived from predominantly terrestrial sources — soils and weathered bedrock, bedrock outcrops and aeolian sediments — and corresponding to deposition in the coastal zone under a transgressive coastal regime (Chester & James, 1995; Moura & Boski, 1999).

In addition to the Faro-Quarteira formation, the Quaternary is represented by fluvial and alluvial deposits. Quaternary gravel terraces are preserved in fragmentary form in the larger valleys of the Algarve, occurring between 10 and 40 m elevation and often covering valley spurs (Chester & James, 1991; James & Chester, 1995). As recognised by Devereux (1983), many valleys contain sediment fills of Holocene age. The deposition of the fills that currently occupy the floor of the valleys generally dates from after 3000 BP, and reflects the erosion of hillslope soils, particularly in the Serra region (James & Chester, 1995). A climatic cause related to the seasonality of rain distribution has been proposed to account for erosion and valley sedimentation (Devereux, 1982, 1983). In contrast, Chester & James (1991, 1999) have argued the case for an anthropogenic cause for these sedimentation events. In particular,

these authors highlight the temporal correlation of phases of human settlement in the region and phases of valley alluviation.

2.1.2 Climate

In climatic terms, the Algarve is located at the intersection of two distinct regions: the Atlantic and Mediterranean. The climate of the Algarve, as of southern Portugal overall, is of mediterranean-type, with hot, dry summers with at least two months of drought after the summer solstice ($P < 2T$, monthly precipitation less than twice the mean monthly temperature), and mild winters during which the majority of rain falls. Mean annual air temperature is 16.3°C , with a minimum in January (9.9°C) and maximum in August (23.3°C); annual

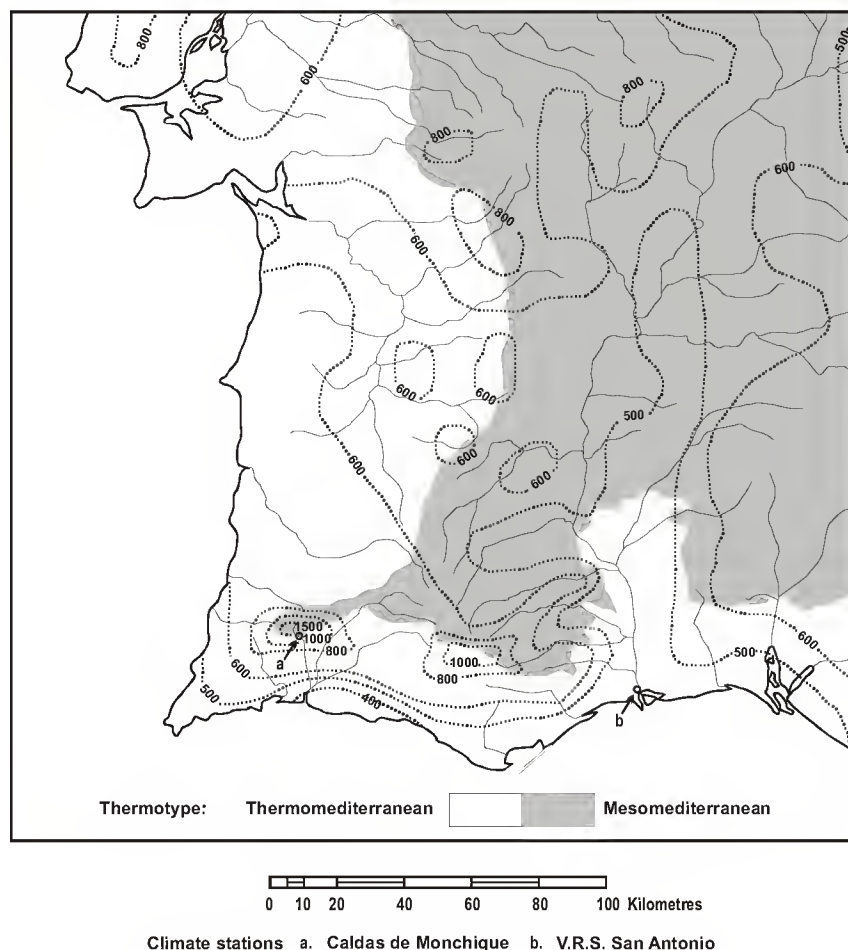


Figure 2.3. Distribution of thermotypic stages and rainfall (annual mean precipitation in mm) in southern Portugal. Thermotypes redrawn from Rivas-Martínez et al. (1990); isohyets redrawn from Maberley & Placito (1993) & Allen (2001).

rainfall varies from 500 to 1000 mm (Loureiro & Coutinho, 1995). These figures disguise major variability, both interannual and geographic.

Within the Algarve province, climatic conditions vary in terms of temperature, seasonality (oceanic vs. continental) and rainfall. In terms of thermotypic classification, most of the Algarve is categorised as thermomediterranean (oceanic influence, mild winters) while some inland areas at slightly higher altitudes in the Serras are mesomediterranean (continental influence, cold winters) (Rivas-Martínez *et al.*, 1990) (Table 2.1, Figure 2.3). Annual thermic amplitude varies considerably from the coast to the uplands, from a minimum of 6.3°C at the Cabo de S. Vicente (SW coast) to a maximum of 16.5°C in Ameixial (Serra do Caldeirão, NE Algarve) (Loureiro, 1983). The attenuation of oceanic influence away from the coastal areas results in an augmentation of winter severity (frosts) from W to E and S to N. This trend is disrupted by the basins of major rivers like the Guadiana which permit the inland extension of thermomediterranean and oceanic conditions (Capelo, 1996).

Precipitation in the Algarve varies significantly between the geographic zones (Figure 2.3). The upland regions of the Monchique massif and the Serra do Caldeirão receive high annual orographic rainfall (1000 to 2000 mm), while the southern littoral and Guadiana valley receive typically less than 500 mm. Climate data for two locations, one located near the mouth of the Guadiana (Vila Real de San Antonio) and one within the upper part of the Boina valley (Caldas de Monchique), are shown in Table 2.3, illustrating the contrast in orographic rainfall. In terms of ombrotypic classification, areas within the Algarve range from dry to hyperhumid (Table 2.2). High insolation (in excess of 2800 hours per year in the Serras, and 3000 hours in the lowlands) and high potential evapotranspiration (average, 850 mm per year) result in serious water deficits in some areas (Loureiro, 1983). In terms of plant life, the severity of drought during the dry summer season poses the main limiting factor on vegetation development (Capelo, 1996).

	T	M	m	It
Thermotype	Average annual temperature (°C)	Average maximum temperature of the coldest month in the year (°C)	Average minimum temperature of the coldest month in the year (°C)	Thermicity index 10 (T + M + m)
Thermomediterranean	(15) 16 to 18 (19)	(12) 14 to 18 (20)	(3) 5 to 9 (10)	350 to 450
Mesomediterranean	(12) 13 to 16 (17)	(7) 9 to 14 (17)	(-3) -1 to 5 (7)	210 to 350

Table 2.1. Normal values (and limits) of several climatic variables for the thermomediterranean and mesomediterranean thermotypes. From Rivas-Martínez *et al.*, 1990.

Ombrotype	Precipitation (mm)
Dry	350 to 600
Subhumid	600 to 1000
Humid	1000 to 1500
Hyperhumid	1500 to 2300

Table 2.2. Classification of ombrotypes occurring in the Algarve by annual precipitation.

Station	Alt. (m)	T	M	M	It	P	Bioclimatic stage
V.R.S. Antonio	7	17.2	15.4	6.8	394	483	Thermomediterranean, dry
Caldas de Monchique	203	17.4	15.3	7.2	399	1093	Thermomediterranean, humid

Table 2.3. Climate data for two Algarve climate stations. From Rivas-Martínez *et al.*, 1990.

2.1.3 Flora

The Portuguese flora, numbering about 2500 species of vascular plant (Mabberley & Placito, 1993) includes European, Mediterranean, Macaronesian (Atlantic island) and North African elements. Fossil evidence suggests a marked impoverishment of the Portuguese flora since the Pliocene, possibly associated with aridification during the Quaternary glacial periods (Pais, 1989). While the Algarve flora contains representatives of the various phytogeographical groups, the vegetation is Mediterranean in character, with widespread communities of evergreen trees and shrubs adapted to summer heat and drought, ephemeral herbaceous plants and a wide variety of drought-tolerant geophytes or bulbous plants. In common with much of the Mediterranean basin, much of the rural landscape is dominated by evergreen shrublands tolerant of fire and grazing, and under various degrees of pressure from human disturbance (Blondel & Aronson 1999). The following account of the main vegetation elements draws on several references (Braun-Blanquet *et al.*, 1956, 1964; Malato-Beliz, 1982; Rivas-Martínez *et al.*, 1990; Mabberley & Placito, 1993; Simonson, 1994; Capelo, 1996), and focuses on the vegetation types most critical to the interpretation of the pollen records. The rich Algarvian dune and cliff vegetation is not described.

2.1.3.1 Forests

In common with many parts of the Mediterranean basin, evidence for the composition and structure of natural forest vegetation is scarce. Across vast areas of southern Portugal, the history of agricultural and pastoral activities has produced a landscape of parkland character quite different from a forest environment. This parkland landscape, best developed in the *montados* (Spanish equivalent: *dehesas*) of the Alentejo, contains scattered oaks (mainly *Quercus suber*, the cork oak, and *Quercus rotundifolia*) above a grazed vegetation of annual plants and low shrubs. Only in inaccessible areas on steep terrain where agriculture has been restricted do relict stands and copses provide insights into the composition and structure of forests which must formerly have been of much wider extent.

The drier parts of the Algarve province (dry to sub-humid ombrotypes) are considered the domain of *Quercus rotundifolia* (a closely related species or possible subspecies of *Q. ilex*)

accompanied by the wild olive (*Olea europea* var. *sylvestris*), and the more moist areas (sub-humid to humid) the domain of *Quercus suber* (Capelo, 1996). Other species of oak occur in the Algarve, notably in the humid Serra de Monchique, where semi-evergreen *Q. canariensis* and *Q. faginea* are considered elements of the native forest (Malato-Beliz, 1982). Deciduous *Q. robur* and *Q. pyrenaica* have also been recorded from the Monchique area, far south of their main distributions (Simonson, 1994). It is not clear whether these reflect relics of a formerly more extensive distribution or historic introduction as ornamentals. In relict forest stands on deep, humus rich soils, a multi-storeyed structure is documented with broadleaf evergreen shrubs (*Viburnum*, *Myrtus*, *Phillyrea*), lianas (*Smilax*, *Clematis*, *Hedera* and *Rosa*) and shade-tolerant herbs (*Carex*, *Luzula*, *Deschampsia*, *Rubia*) (Capelo, 1996).

In the coastal zone, especially in the eastern Algarve, there are pinewoods of *Pinus pinea* and *P. pinaster*. These woods contain an understorey of shrubs including the switch-leaved *Lygos monosperma* (Fabaceae), *Cistus salvifolius*, *Erica umbellata*, *Halimium calycinum*, and a rich geophyte flora including species of *Scilla*, *Asphodelus*, *Fritillaria* and *Ornithogalum*.

The landscape and vegetation of the Algarve have been much altered by agriculture, and many of the common trees in the landscape are planted. In the Serra, there are extensive agroforestry plantations of *Pinus pinaster* and *Eucalyptus*. In the Barrocal region, traditional dry orchards of almond, olive, fig and carob are commonplace, although their commercial value has been superseded by irrigated *Citrus* agriculture.

2.1.3.2 Shrublands

Across the Algarve, extensive areas of both the lowland and upland landscape are dominated by semi-natural shrublands of variously sclerophyllous (leathery-leaved), armoured (thorny, spiny, prickly) and aromatic plants. The structure and composition of these shrublands is conditioned and maintained by grazing and browsing, burning and cutting. Shrub communities range from tall thickets (known in Portuguese as *matagais*), through dense

scrub of intermediate height less than 2 m (*matos*) to open, dwarf-shrublands lower than knee-height (*charnecas*). The density and stature of these communities decreases with the intensity of anthropic pressures.

Tall thickets up to 4m high of *Quercus coccifera*, *Juniperus* or *Pistacia lentiscus* with *Olea*, *Phillyrea*, *Rhamnus*, *Myrtus* and *Asparagus* are considered a permanent community of the xerophytic forest margins on incipient soils and also representative of the first stages of degradation (Capelo, 1996). *Erica arborea*, *Arbutus unedo* and *Viburnum* are characteristic of thickets of the *Q. suber* domain.

The most important plants of the *matos* shrublands are members of the families Cistaceae, Ericaceae, Fabaceae (Leguminosae) and Labiateae (Lamiaceae). Overall, shrub communities dominated by *Cistus* occur in the drier ombrotypes, while heath communities occur in the wetter ombrotypes. On the siliceous soils of the Serra, members of the Cistaceae family (*Cistus ladanifer*, *C. monspeliensis*, *C. salvifolius*) accompanied by *Lavandula* spp. and leguminous shrubs (*Genista*, *Astragalus* and *Ulex* spp.) dominate under a dry to subhumid regime, while heathlands with *Erica* spp. and *Calluna vulgaris* predominate under a wetter (sub-humid to humid) regime. On calcareous soils of the Barrocal, species-rich shrublands are observed with *Quercus coccifera*, *Olea europea*, *Jasminum fruticans*, *Phlomis purpurea*, *Asphodelus* and the palm *Chamaerops humilis*. A heterogeneous mix is observed, with dome shaped thickets of dense vegetation up to 2 m high (*Pistacia lentiscus*, *Q. coccifera*, *Daphne*, *Rhamnus*, *Juniperus*) surrounded by areas of low shrubs (*Cistus salvifolius*, *Lavandula* spp., *Rosmarinus*, and a rich flora of geophytes (bulbous plants) and annuals including *Asphodelus* and *Scilla*. Where anthropic pressures are most intense, particularly in the littoral zone, the shrublands take on an open character. Characteristic species of these areas include the herbaceous member of the Cistaceae family, *Tuberaria guttata*, plantains (*Plantago* spp.) and grasses.

2.1.3.3 Wetland vegetation

The Algarve is rich in riverine and estuarine wetland habitats, but poor in lacustrine habitats (Pullan, 1988). With a relatively high tidal range compared with areas within the Mediterranean basin, extensive areas of saltmarsh are developed in many of the Algarve's estuaries. The halophytic vegetation of saltmarshes is dominated by succulent plants of the family Chenopodiaceae, including shrubby species of *Arthrocnemum* (*Sarcocornia*), *Atriplex*, *Limoniastrum*, *Halimione*, *Salsola* and *Suaeda*, and annual species of *Salicornia*. Chenopodiaceae are accompanied by other plants tolerant of flooding by saltwater, including *Aster tripolium*, *Inula crithmoides*, *Artemisia* spp., *Armeria* spp., *Limonium* spp., *Spergularia* and *Frankenia laevis*. A number of grasses (Poaceae) such as *Puccinellia maritima*, *Parapholis filiformis* and *Hordeum marinum*, and sedges (Cyperaceae, e.g. *Scirpus maritimus*) are also important saltmarsh constituents.

A characteristic series of changes in the saltmarsh vegetation is observed seaward to landward and with low to high position relative to the tide. The cordgrass, *Spartina maritima*, occupies the lowest tidal position, accompanied by a flora of green algae, or Chlorophyta. This is followed by a zone with *Arthrocnemum perenne*, then of *A. fruticosum* and *Atriplex portulacoides*. Next, a zone of *Arthrocnemum macrostachyum* and *Suaeda vera*, often invaded by grasses, is interspersed with areas of bare ground or sterile marsh. Characteristic plants of the transitional, brackish areas between estuary and river floodplain include the reed *Phragmites australis*, *Juncus acutus* and *J. maritimus* and *Tamarix africana*.

The freshwater domain includes the many small rivers and streams of the Algarve. River banks are colonised by the giant reed, *Arundo donax*, and spiny brush of *Rubus ulmifolius* and *Rosa canina*. Gravel stream beds, periodically submerged by floodwaters, are colonised by the rheophytes *Tamarix africana* and *Nerium oleander*. Fragments of riverine woodlands occur in some Algarve valleys, with narrow-leaved ash (*Fraxinus angustifolia*), willow (*Salix salviifolia*), alder (*Alnus glutinosa*) and poplar (*Populus nigra*), accompanied by a herbaceous flora including *Osmunda regalis*, *Arum italicum* and *Scrophularia scorodonia*.

Water-lilies (*Nuphar* and *Nymphaea*) and *Myriophyllum alterniflorum* occur in slow-flowing rivers, while *Typha latifolia*, *Iris pseudacorus*, *Alisma plantago-aquatica* and other freshwater aquatics occur in marshes bordering waterways.

Although of minor spatial extent, seasonal freshwater wetlands occurring in shallow depressions and small basins and drying out completely during the summer months are of significant ecological and botanical interest. These temporary ponds and pools, occurring in both upland and lowland settings on acidic and basic substrates, provide habitats for distinct plant communities with species of *Isoetes*, *Juncus*, *Lythrum*, *Ranunculus* and *Callitriche* and members of the Cyperaceae family (Pinto-Gomes *et al.*, 1999).

2.2 Guadiana estuary

The Guadiana is one the largest rivers of the Iberian peninsula, and the most important river flowing through southern Portugal. As such, the Guadiana has been the focus of scientific research in a variety of fields. The following sections draw on the published literature on the geological history and modern sedimentary dynamics of the Guadiana estuary.

2.2.1 Physiographic setting

The Guadiana is one of the major rivers of the Iberian peninsula, with a total length of 730 km and a drainage catchment of *c.* 67,000 km² (Lobo *et al.*, 2003). The last 200 km forms a natural border between Portugal and Spain. The tidal segment of the Guadiana extends over 50 km inland to the vicinity of Mértola in the province of Baixo Alentejo (Ruiz *et al.*, 1996), and follows a N-S trend perpendicular to the coast defined through fluvial incision during the Quaternary (Boski *et al.*, 2002). In this section, the Guadiana is incised into the Hercynian basement consisting of Carboniferous metasediments. The resistant bedrock defines the channel morphology of the valley — narrow and deep, about 600 m wide and 70 m deep (below mean sea level) at around 7 km from the mouth of the river (Boski *et al.*, 2002: 104). Only the terminal 5 km are underlain by Cretaceous and Jurassic limestones permitting a widening of the valley. The contrast in valley form underlines the observation

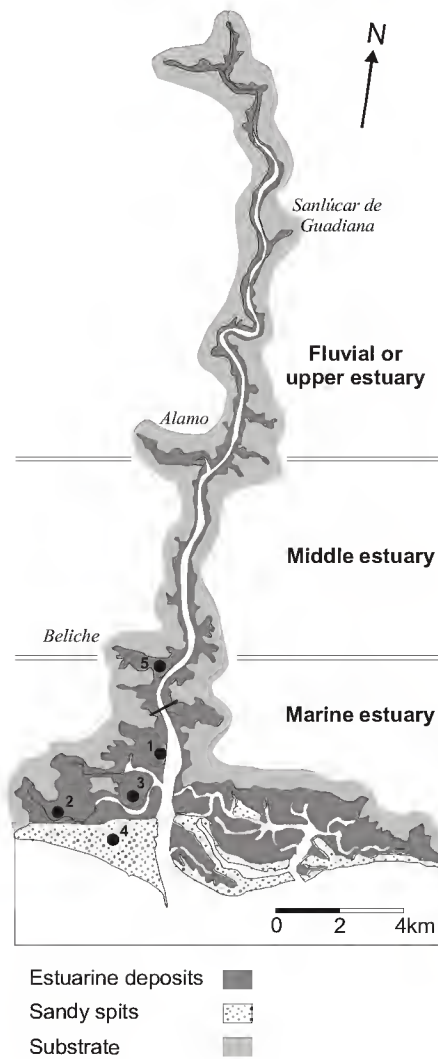


Figure 2.4. Map of the Guadiana estuary, showing hydrodynamic domains. Adapted from Borrego *et al.* (1995) and Ruiz *et al.* (1996). Numbered locations refer to Guadiana boreholes CM1-4 (Boski *et al.*, 2002) and CM5 (this study). Solid line north of CM1 shows location of international bridge and destructive drillings (Figure 2.5.).

of two distinct physiographic domains (Morales, 1997): a) the estuarine valley, characterised by the complex interaction between fluvial and marine hydrodynamic and sedimentary processes, and b) a prograding deltaic complex of barrier sands and marshes around the mouth of the main estuary channel dominated by wave activity.

2.2.2 Hydrodynamic setting

The Guadiana estuary experiences mesotidal conditions, with a mean tidal range of 2.0 m (mean neap range 1.22 m and mean spring range 2.82 m) (Morales, 1997). The tidal wave moves along the coast of the Gulf of Cadiz from east to west. Within the estuary, the width-

depth ratio of the tidal channel compensates the effects of friction and convergence, and the tidal wave propagates in synchronic manner, with the tidal range remaining constant up to 50 km from the mouth (Borrego *et al.* 1995: 153). The ebb tide is of longer duration than the flood tide, resulting in a net sediment transport toward the coast (Morales, 1997). The coastline is exposed to waves of medium and low energy, of both Atlantic swell and local origin. The prevailing waves, resulting from Atlantic swell energy and coming from the southwest, produce a strong east-to-west longshore current. In general terms (Davis & Hayes, 1984), the Gulf of Cadiz coast may be classified as a mixed-energy, tide-dominated coastline (Borrego *et al.*, 1995).

Mean fluvial discharge for the Guadiana river is $144.4 \text{ m}^3 \cdot \text{s}^{-1}$ (Borrego *et al.*, 1995). The water discharge of the Guadiana river, in common with other rivers in the region, is strongly seasonal, with winter discharge reaching in excess of $3000 \text{ m}^3 \cdot \text{s}^{-1}$ and summer discharge falling to as little as $10 \text{ m}^3 \cdot \text{s}^{-1}$ (González *et al.*, 2004). Inter annual variability is also high (Morales, 1997). The position of the fresh water/sea water interface and the extent of mixing in the estuary is conditioned by fluvial discharge. Under mean discharge conditions, the estuary becomes well stratified (Borrego *et al.*, 1995).

Three domains may be identified on the basis of hydrodynamic criteria: 1) an upper estuarine domain, extending from north of Mértola to Alamo, characterised by predominantly fresh water and the dominance of river currents; 2) a central estuarine domain, extending from Alamo to Beliche, characterised by the mixing of fresh and salt water and dominated by tidal currents; 3) a marine domain, extending from Beliche to the mouth of the river, and characterised by predominantly salt water and marine action (tides and waves) (Ruiz *et al.*, 1996) (Figure 2.4).

2.2.3 Sediment supply

The Guadiana estuary is in an advanced state of infilling and undergoing deltaic progradation. Progradation is favoured by a high sediment supply and the narrow, bedrock-controlled morphology of the estuary. Sediment supply to the Guadiana estuary is of two main sources:

fluvial and marine. The Guadiana supplies a large volume of fluvially-derived sediments to the estuary. Although there are no published data on the Guadiana sediment supply, Morales (1993, cited in Morales, 1997: 130) estimated the suspended sediment load at $57.90 \times 10^4 \text{ m}^3\cdot\text{yr}^{-1}$ and bedload at $43.96 \times 10^4 \text{ m}^3\cdot\text{yr}^{-1}$. During modal discharge conditions, the bulk of sediments brought into the estuary are reworked by the tide and carried out to the shelf. Together with the Guadalquivir, the Guadiana is the most important supplier of fluvial sediment to the Gulf of Cadiz shelf (Lobo *et al.*, 2004). However, during maximum instantaneous discharge, most of the sandy sediment remains in the estuary (Morales, 1997).

Some of the sediment contribution to the estuary derives from marine sources via longshore drift. Prevailing onshore wave conditions along the coastline produce an eastward net annual littoral drift with potential sediment transport between 100 and $300 \times 10^3 \text{ m}^3\cdot\text{yr}^{-1}$ of sediment (Morales, 1997). This current carries predominantly sandy sediments from the friable lithologies of the southern Portuguese coast towards the eastern portion of the Gulf of Cadiz. While some of these sand- and gravel-sized sediments are trapped in the Guadiana estuarine system as they pass the river mouth, most sediment bypasses the Guadiana mouth and remains within the inner shelf area (Morales, 1997).

2.2.4 Modern Sedimentary environments

The present estuary is characterised by a wide variety of sedimentary sub-environments, e.g. sub-tidal and intertidal channel, channel margin, tidal flat, saltmarsh and sand spit. The distribution of these sub-environments within the estuary and the characterisation of lithofacies from the different settings is dealt with in detail by Borrego *et al.* (1995) and Pendón & Morales (1997). Overall, sediment texture, physical sedimentary structures (e.g. desiccation cracks, ripple laminations), biological content (e.g. shells, plant debris) and the extent of bioturbation provide the criteria for discrimination of depositional facies associated with the various sub-environments.

The work of Borrego *et al.* (1995) and Pendón & Morales (1997) demonstrates that lithofacies characteristics are conditioned primarily by sediment supply and variation in the relative

influence of fluvial, tidal and wave-related processes associated with the hydrodynamic domains of the estuary. The upper estuarine domain of the Guadiana is characterised by fluvial sediments and bedforms showing only limited evidence of tidal influence. For example, channel bed and lateral bar deposits are dominated by gravels, and adjacent supra-tidal marsh deposits of silts, sands and gravels display grain-size alternations associated with energy fluctuations in the fluvial regime (Pendón & Morales, 1997). In the central estuarine domain, sediment supply is primarily fluvial but dynamic processes are dominated by the strong influence of tidal currents. This dominance is evident, for example, in the high degree of sorting of sands in deeper areas of the estuarine channel, and in characteristic tidal structures such as flaser and wavy bedding in deposits of alternating fine sands and organic rich muds occurring in shallow channel areas (Borrego *et al.*, 1995). The marine domain is characterised by a diversification of depositional facies, reflecting the interaction of river, tide and wave processes and a two-fold sediment supply, i.e. sands of fluvial and marine origin. A wide variety of bedforms and sedimentary processes, and extensive spatial variability are observed in this domain. Considering channel facies as an example, both deep and shallow channel facies consist of sandy sediment with abundant shell fragments; however dense networks of tidal channels unconnected to the main estuarine channel exhibit a range of sediment types including bioturbated muds, muddy sands and well-sorted clean sands (Borrego *et al.*, 1995).

2.2.5 Sedimentary infill

Borehole data provide evidence for the structure of the sedimentary infill of the Guadiana estuary. Destructive drillings from the construction of the Guadiana international bridge (Figure 2.5) show three main lithostratigraphical units (Boski *et al.*, 2002): 1) a pre-Holocene gravelly layer of fluvial origin overlying the Carboniferous basement, with thicknesses up to 35 m in the valley thalweg, containing frequent intercalations of finer sediments; 2) a 15–20 m thick unit of clay and silt with intercalation of fine and medium sands; and 3) a sandy unit up to 15 m thick. The location of four cores drilled near the town of Castro Marim (CM1-4, Boski *et al.*, 2002) is shown in Figure (2.4). Boreholes CM1 and CM3 (42 and 36 m deep, respectively) are located near the main estuarine channel and confirm this

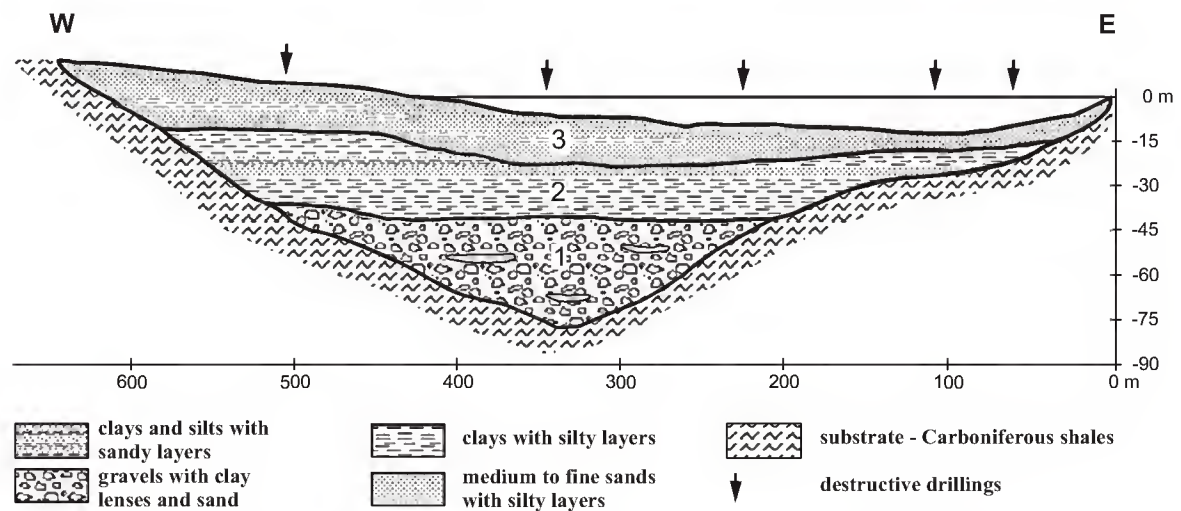


Figure 2.5. Schematic cross section of the Guadiana infill. Cross section located ca. 8km from the mouth of the principal channel, based on destructive drillings made during the construction of the Guadiana international bridge. Redrawn from Boski *et al.*, (2002).

sequence of lithostratigraphical units. Coarse sands and gravels are recorded in the lowest part of the cores, followed by thick sequences of clays and silts with shells and organic matter, followed by tidal sand deposits above *c.* 15 m depth (relative to present mean sea level). The stratigraphic units (1,2,3) show a close correlation with spatially extensive seismic units identified through high-resolution profiling of the terminal segment of the Guadiana (Lobo *et al.*, 2003).

Two other cores CM2 and CM4, contain different sediment sequences, related to their locations in the estuary. Core CM2, located in a back-barrier lagoon distant from main channel, contains a shallow (*c.* 10m) sequence of shelly clays deposited between *c.* 6000 and 3000 ^{14}C bp (*c.* 6800 and 3200 cal BP), overlying a thin layer of micaceous sands and gravels at the core base. Core CM4, located in the prograding delta area of the Guadiana, contains a complex sedimentary sequence of *c.* 36 m depth with a transition from coarse fluvial and deltaic fan deposits to sandy deposits associated with the barrier complex.

Radiocarbon dating confirms the Holocene age of the upper part of the fill (units 2 and 3), and places the main period of sedimentation in the estuary between 9800 and 3000 ^{14}C bp

(*c.* 11,200–3200 cal BP) (Boski *et al.*, 2002). The contrast between units 2 and 3 is attributed to the introduction of shelf sands to the estuary after 7500 ¹⁴C bp and to deceleration in the rate of sea-level rise after 6500 ¹⁴C bp. After 3000 ¹⁴C bp, the main area of sedimentation shifted from within the estuarine valley to the river mouth. Promoted by a number of factors, including sea-level stabilisation, moderate to high sediment supply, and infilling in the estuarine valley, a prograding delta complex developed at the river mouth (Morales, 1997).

Within the estuarine valley, a long term trend (continuing in the present estuary) of accretion on the western side of the estuary and erosion on the eastern side has resulted in the eastward migration of the axis of the principal estuarine channel; this trend accounts for the observed asymmetry in the incision of the river valley (Boski *et al.*, 2002).

2.2.6 Study site: core CM5, Beliche-Guadiana

The CM5 borehole is located on the floodplain of a small tributary of the Guadiana, the Beliche river, *c.* 500 m west of the main channel of the Guadiana (Figure 2.4). The confluence of the Beliche and Guadiana rivers is located *c.* 10 km inland of the mouth of the Guadiana. The borehole is located in a saltmarsh within the upper ranges of the intertidal zone of the Guadiana river, and is inundated during spring high tides. The general location lies at the seaward limits of the central estuarine domain of the Guadiana estuary.

The Beliche itself is a relatively small river contained entirely within the eastern part of the Algarve province. The Beliche drains an area of *c.* 116 km² of the *planalto* or upland of the Serra do Caldeirão. The drainage basin of the Beliche is located entirely on heavily-folded Palaeozoic turbidites of the Zona Sul Portuguesa (Manupella, 1992). The basin rises to *c.* 500m a.s.l., and displays the steep, intensely dissected terrain that characterises upland areas of the Algarve. The floodplain of the Beliche contains a mosaic of agricultural, pastoral and semi-natural environments. A zone of *Spartina maritima* occurs in the lowest areas of the marsh on the edge of the Guadiana. Away from the Guadiana, this zone rapidly gives way to more extensive upper marshes of shrubby halophytic plants of the Chenopodiaceae family (*Arthrocnemum* and *Limoniastrum* spp.) interspersed with areas of sterile marsh

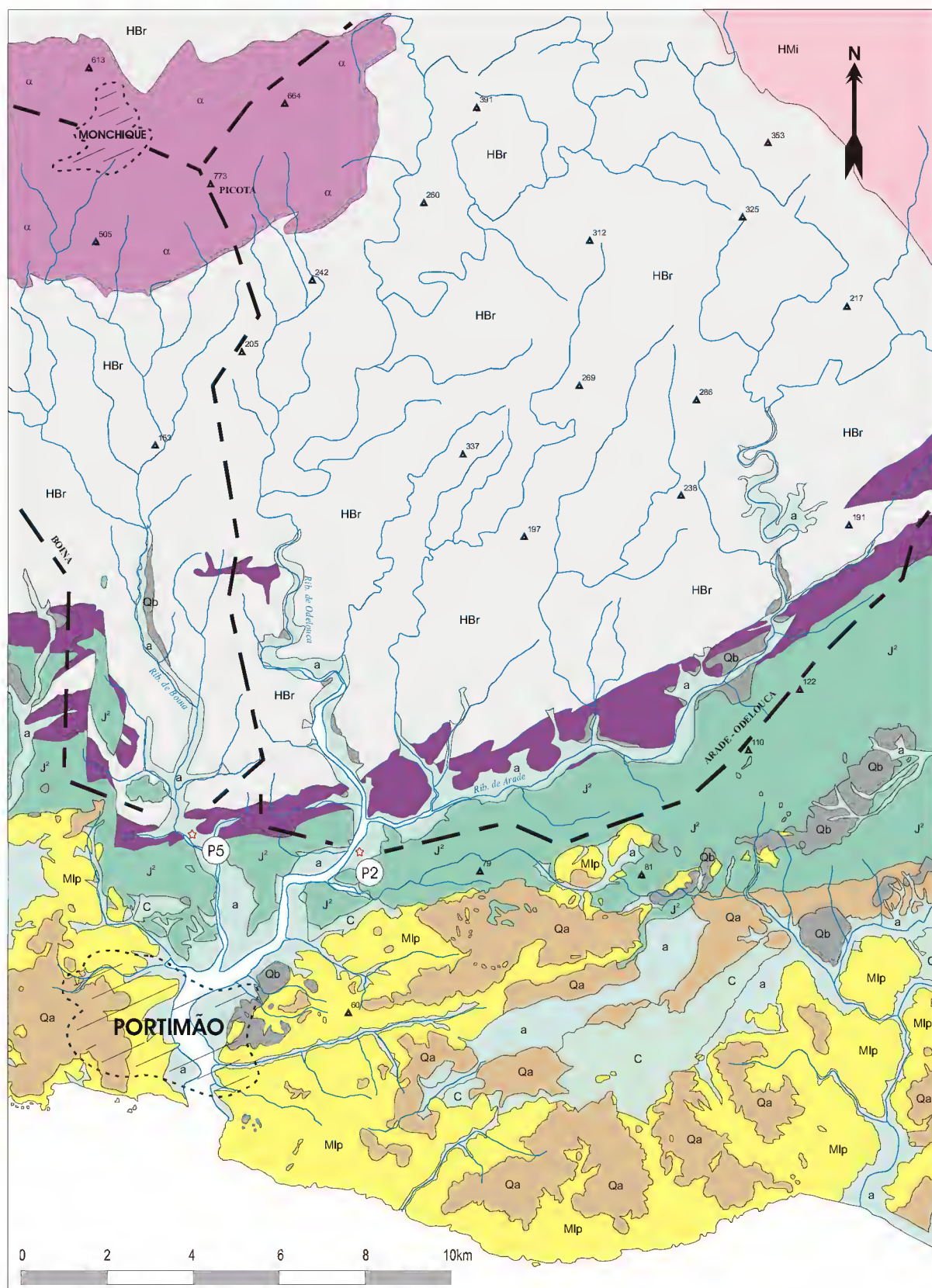
with evaporative salt crusts. Progressing inland and towards the edges of the valley, a transitional saline/freshwater zone which is subject to grazing by cattle displays a vegetation of with *Suaeda vera*, *Juncus* sp., grasses and a wide range of herbaceous plants (*Rumex*, *Plantago*, and numerous Asteraceae spp.). Patches of wet woodland with *Fraxinus angustifolia* and *Tamarix africana* occur near the fluvial channels. Vegetation in the surrounding areas is a mixture of agricultural land and maquis. To the south of the core location, the hills are covered in dry orchards of carob (*Ceratonia siliqua*) and winter arable crops with a summer flora rich in herbaceous annuals. To the north of the core location, a maquis with *Cistus ladanifer* and *C. monspeliensis*, *Phillyrea angustifolia*, *Genista* sp. and *Lavandula stoechas* occurs on the hill-slopes and encroaches on a narrow zone of former agricultural activity at the break of slope.

2.3 Boina-Arade estuary

2.3.1 Physiographic setting

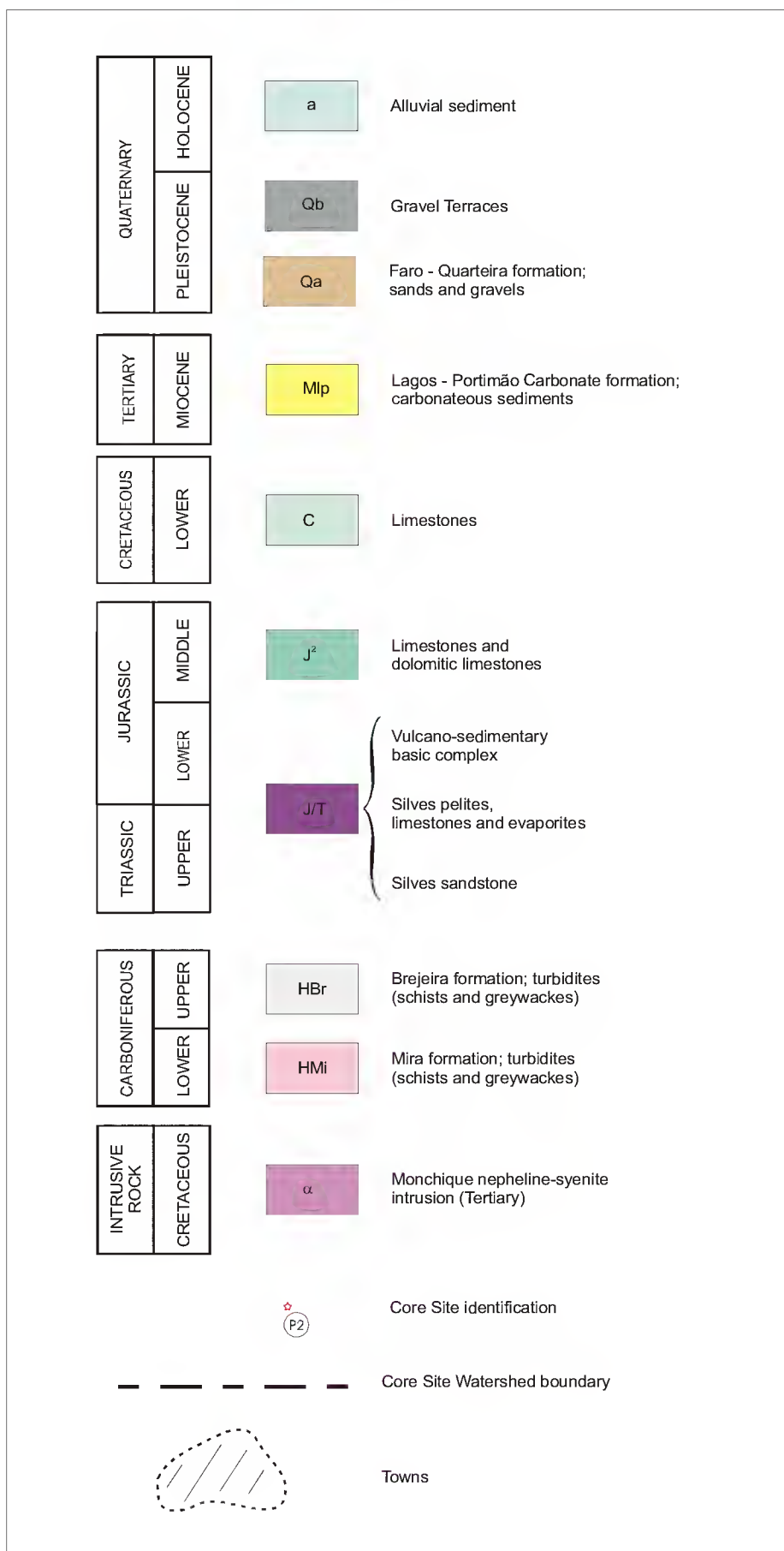
The Boina-Arade estuary is located in the western Algarve near the city of Portimão. The Y-shaped estuary represents the drowned valley of the combined Boina and Arade rivers, which meet about 4 km landward of the modern shoreline (Figure 2.6). The Arade is the largest river contained within the Algarve province, which, together with its tributary the Odelouca river, drains a basin of c. 966 km² including the western portion of the Serra do Caldeirão and the eastern slopes of the Monchique massif. The course of the Arade runs ENE-WSW, with a length of 75.1 km and a mean gradient of 0.6% (INAG, 2000). The upper reaches of the Arade cross the Carboniferous metasediments of the Serras, while in the lower reaches, in the vicinity of Silves, the river flows across the Silves series.

The Boina river is a high-gradient mountain river renowned for its flash-floods (Boski, pers. comm.) fed by high orographic rainfall in the Monchique uplands. The river rises on the southern slopes of the Foia and Picota peaks of the Monchique massif, and flows N-S, crossing the major geological boundaries of the Algarve. The drainage catchment is fairly



Legend overleaf

Figure 2.6. Geology of the Portimão Area, redrawn from Manupella (1992).



small (c. 78 km²), with a river course of 26.1 km in length and a mean gradient of 2.6 % (INAG, 2000).

The terminal segment of the combined Boina-Arade rivers is cut into calcareous rocks and reaches a maximum depth of about 30 m. The estuary experiences a mesotidal regime. The main tidal channel follows the Arade valley, where the tidal segment of the Arade river extends inland for about 16 km, above the town of Silves. Tidal marshes are well developed around the area of the Boina-Arade confluence, and flanking the valleys of the Boina and Arade. In general, these marshes show extensive modifications through activities related to drainage, agriculture and aquaculture.

2.3.2 Study site: core P2, Arade

The P2 borehole is located near the margin of the Arade estuarine channel approximately 4 km from the confluence with the Boina and approximately 8 km inland from the coast (Figure 2.6). The core site is located on the western edge of an extensive area of reclaimed cultivated land, the Tapada do Corte, which is developed on estuarine/alluvial deposits. The slopes surrounding the tapada are covered in a tall scrub vegetation with *Olea*, *Quercus coccifera*, *Juniperus*, *Cistus albidus*, *Smilax aspera* and *Daphne*.

2.3.3 Study site: core P5, Boina

The P5 borehole is located approximately 2 km upstream of the confluence of Boina and Arade rivers, in an area of saltmarsh called the Sapal do Vau, towards the inland limits of the intertidal part of the Boina valley (Figure 2.6). In this area, the western slopes of the valley are covered in settlements, gardens and agricultural plots, while the eastern slopes have a scrub vegetation with *Olea*, *Pistacia* and *Quercus coccifera*. The core site is located near the landward extent of strong tidal influence, as evidenced by the decline of halophytic marshes with *Chenopodiaceae* and their replacement by brackish and freshwater floodplain vegetation within c. 1 km upstream.

3 Methodology

3.1 Sample collection and preparation

3.1.1 *Sampling strategy*

Sampling for pollen and sedimentary analyses was undertaken in the sediment laboratories of the Universidade do Algarve, Faro, Portugal. The choice of sample depths was made with the aims of obtaining a representative sampling of the various lithological units encountered in the cores, and of maintaining a regular depth distribution of samples, where possible based on a 32cm spacing. Sampling strategy was conditioned, however, by a number of other factors, namely incomplete core recovery, access to material, and to some extent the palynological richness of the material (as determined during initial experiments during the early phases of this study).

Core recovery at the time of drilling (indicated on the core summary diagrams, Chapter 4) was not complete, placing restrictions on the availability of material for sampling. Core recovery is especially poor, for example, in the sandy upper sections of cores P2 and P5. The larger between-sample spacing at some depths reflects missing core sections. Access to the cores was also different for the three sites. For core CM5, vials of sediments had been refrigerated and set aside with a view to future pollen analysis at the time the core was

first sampled at CIMA (prior to the commencement of this study). Only a pre-selected range of sample depths was available for analysis. Sediment samples from cores P2 Arade and P5 Boina, however, were taken directly from archived core sections, in consultation with core log descriptions. Finally, a preliminary assessment of the palynological content of the cores identified both sections of particular interest and sections with poor pollen preservation. Although no sections were excluded from further sampling on this basis, some sections (e.g. uppermost metres of core CM5) were sampled more intensively.

3.1.2 Sample collection and storage

Sediment samples from core CM5 Guadiana of *c.* 20 cc were collected from refrigerated vials of moist sediment using a clean spatula, and stored in airtight bags. Sediment samples from cores P2 Arade and P5 Boina were taken directly from archived core sections, which

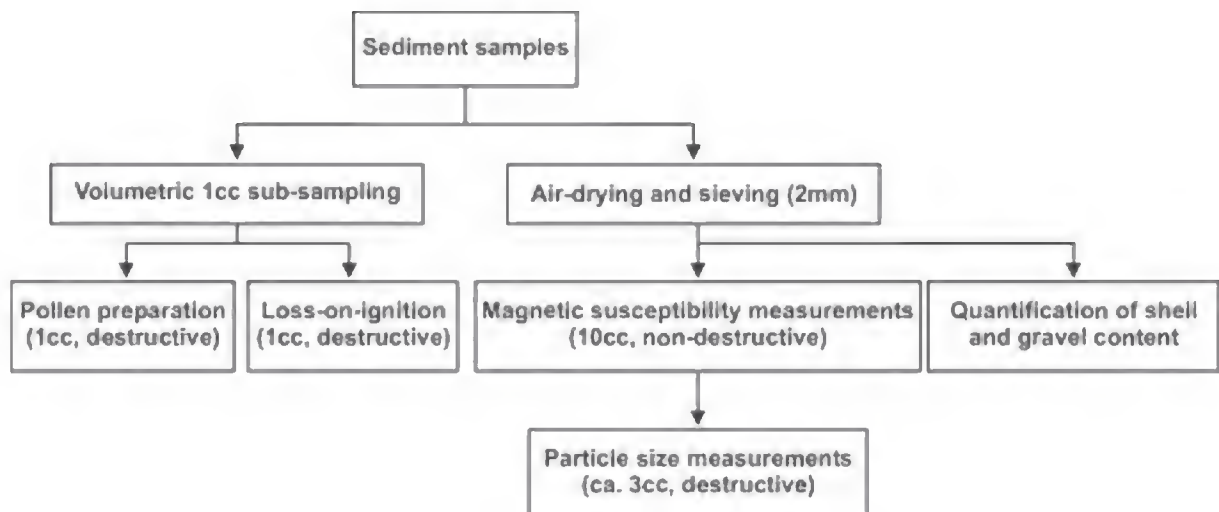


Figure 3.1. Strategic sequence of analyses for small sediment samples

had been stored in plastic guttering, wrapped in cling-film and stored at room temperature (and were, in effect, air-dried). Samples of *c.* 15cc–20cc were taken using a knife and spatula from single-centimetre bands (excluding material from the edges of the core) at selected depths. Samples were placed in airtight bags and transported to Cambridge for subsequent analysis.

3.1.3 *Subsampling and preparation for analysis*

As the overall quantity of sediment available for each sample was fairly small, a considered sequence of analyses was necessary, taking into account the sediment requirements and losses relating to the various techniques (Figure 3.1). At each stage, care was taken to avoid cross-contamination between samples, with washing and force-drying of all sampling equipment between samples.

1cc sub-samples were taken for loss-on-ignition (LOI) and pollen analysis using a calibrated volumetric sampler. In the case of unconsolidated (e.g. sandy) sediments, the 1cc chamber of the volumetric sampler was packed and gently tamped using a spatula to provide sediment plugs of comparable density. The remainder of the sediment samples, to be used for magnetic susceptibility and particle size measurements, were air dried at room temperature for 48 hours and weighed. The samples were then gently broken down using a ceramic mortar and pestle and passed through a 2mm sieve.

From cores CM5 and P2, only shell material was collected in the 2mm sieve. From core P5, however, gravel clasts were also encountered, which were then passed through a nest of sieves (16mm, 8mm, 4mm, 2mm; -4 to -1 ϕ) and the various fractions weighed. All gastropods and intact valves observed during disaggregation were collected, along with all shell fragments >2mm. This shell material was weighed to provide an estimate of the concentration of shell in each sample.

3.2 Methods for sediment analyses

3.2.1 *Loss-on-ignition*

3.2.1.1 Background

In soils and sediments, carbon is present in three basic forms: organic, elemental and inorganic (Schumacher, 2002). Organic carbon forms, derived from the decomposition of plants and animals, include a variety of organic substances including carbohydrates, proteins, waxes and organic acids. Elemental carbon forms include charcoal, graphite and coal derived

from the combustion products of organic material and geological sources. Inorganic carbon, of which carbonate minerals such as calcite (CaCO_3) and dolomite [$\text{CaMg}(\text{CO}_3)_2$] are the predominant representatives in soils and sediments, is derived from a variety of geological and biogenic sources.

As an analytical technique, loss-on-ignition (LOI) relies on the principle that different forms of carbon become volatile at different temperatures. At moderate temperatures between 200°C and 600°C, organic matter (including organic and elemental carbon forms (Ball, 1964)) is oxidised, producing carbon dioxide and ash. At high temperatures (generally >800°C), carbonate compounds become volatile, producing carbon dioxide and oxide residue (Dean, 1974). The measurement of weight loss for a sediment sample following sequential heating at controlled temperatures (ashing) can therefore provide an indication of the relative proportions of different carbon forms in the composition of a sample. Although LOI values for organic matter and carbonate content must be considered “rough determinations” (Bengtsson & Enell, 1986: 428), the correlations between LOI and organic C and CaCO_3 content as determined by other analytical techniques are generally very good (Ball, 1964; Dean, 1974; Sutherland, 1998; Konen *et al.*, 2002). Moreover, compared with other analytical techniques such as dry combustion or wet chemical oxidation, LOI is quick, inexpensive, relies on readily available equipment, and does not require dangerous chemicals.

Although LOI is a widely used technique in geological, marine and soil science investigation (Bisutti *et al.*, 2004), published methodologies vary considerably and some concern surrounds the influence of methodological choices and the comparability of results (Hieri *et al.*, 2001). It is critical, therefore, to adhere to an explicit protocol and to maintain standard combustion times and temperatures for reproducible LOI results. Concern also surrounds the interpretation of LOI values because of weight losses incurred during ashing from non-carbon sources, such as structural water in clays and volatile salts (Mook & Hoskin, 1982), and because of low temperature loss of inorganic carbon from certain carbonate minerals

(Krom & Berner, 1983; Sutherland, 1998). In light of this concern, an additional ashing stage was undertaken in this project.

3.2.1.2 Method

In this study, a modified version of the Bengtsson & Enell (1986) protocol was followed, with ashings at 400°C, 550°C and 950°C. The ashing of the organic fraction was undertaken at 400°C. The results of ashing at this temperature are considered a reliable estimate of organic matter content (Keeling, 1962; Ball, 1964; Konen *et al.*, 2002). Losses incurred during the second ashing at 550°C will reflect a residual organic fraction (possibly with certain elemental carbon forms such as graphite predominant (Blanchard, 1960)), the bulk of water loss from clay minerals (Mook & Hoskin, 1982), and possibly some early loss of carbonate minerals (Sutherland, 1998). Ashing at 950°C completes the evolution of CO₂ from carbonates and the results provide an estimate of the carbonate content of the sediment samples (Dean, 1974). In this study, we focus on the results of ashing at 400°C (LOI₄₀₀) as an indicator of organic matter content and 950°C (LOI₉₅₀) as an estimate of carbonate content.

Ashing time at each stage was 6 hours. This exposure time has been demonstrated to be sufficient to ensure complete ashing for both organic matter and carbonate content in a variety of sample types (Krom & Berner, 1983; Luczak *et al.*, 1997; Heiri *et al.*, 2001). In order to ensure comparable results, sample size, furnace temperatures and ashing times were kept constant throughout the research. Sample order within the furnace was maintained between ashings for sample batches. Crucibles were handled at all times with tongs, and samples were weighed prior to reaching room temperature to prevent weight gain through uptake of moisture from the air.

1 cc sediment samples (mean weight 1.77g, StDev 0.173g) were placed in dry, pre-weighed crucibles and weighed to determine the moist sediment weight (MW). The samples were force dried overnight at 105°C in a drying oven and weighed again to determine the sediment dry weight (W₁₀₅). For samples from core CM5 (Guadiana), the water content of the sediments was then calculated, following Bengtsson & Enell (1986):

$$\text{Water content (\%)} = 100 \times (MW - W_{105}) / MW$$

Samples from cores P2 and P5 (Boina-Arade estuary) were already air dried and their water content is not considered further.

The samples were then heated at 400°C for 6 hours in a muffle furnace. Samples were allowed to cool to 105°C, transferred to a warm drying oven to prevent rehydration from moisture in the air, and weighed again (W_{400}). The loss-on-ignition at 400°C (estimated organic content) as a proportion of the sediment dry weight was calculated:

$$LOI_{400} = 100 \times (W_{105} - W_{400}) / W_{105}$$

The procedure was repeated at 550°C and 950°C, calculating loss-on-ignition at 550°C (LOI_{550}) and 950°C (LOI_{950}) in a similar manner:

$$LOI_{550} = 100 \times (W_{400} - W_{550}) / W_{105}$$

$$LOI_{950} = 100 \times (W_{550} - W_{950}) / W_{105}$$

Assuming that carbonates are present mainly in the form of calcium carbonate, an estimated value for $CaCO_3$ content was derived, following Dean (1974:243):

$$CaCO_3 \text{ content (estimated)} = LOI_{950} * f$$

where f is a conversion factor reflecting the proportion of carbon dioxide in calcium carbonate:

$$f = (\text{molecular weight of } CaCO_3) / (\text{molecular weight for } CO_2) = 100 / 44 = 2.27$$

Finally, an estimate of the residual mineral component may be derived as follows:

$$\text{Mineral residue} = 100 - (\text{LOI}_{400} + \text{LOI}_{550} + (\text{LOI}_{950} * f))$$

This value is presented in the results as a rough estimate of the non-carbonate mineral component in the sediments.

3.2.2 Particle size analysis

3.2.2.1 Background

Granulometric or particle size investigations have proved an important tool in the environmental analysis of Holocene coastal and estuarine deposits on the Iberian margin (e.g. Borrego *et al.*, 1995, 1999; Morales, 1997; Pendón *et al.*, 1998; Bao *et al.*, 1999; Psuty & Moreira, 2000; Boski *et al.*, 2002). Although no universal model exists to distinguish past depositional environments on the basis of particle size data (McLaren, 1981; McManus 1988), the particle size characteristics of a sediment can provide indications of the energy conditions, transport mechanisms and sorting processes affecting a depositional location (Long *et al.*, 1996). This information, in concert with other sedimentological and biological proxies, can be extremely useful in characterising the depositional setting.

Estuaries are complex and varied sedimentary environments, where sedimentation is conditioned by a variety of factors, including river discharge, tidal flow, salinity and topography (Dyer, 1979). Estuarine sedimentary sequences may contain a wide range of particle sizes, from cohesive clays and silts associated with saltmarshes and mudflats to sands and gravels of channel fills and coastal barriers. Measurements of particle size are sensitive to such factors as the location of saltmarsh edges, relative water depth and sea-level rise on mudflats and saltmarshes, seasonal controls on deposition, the degree of evolution of tidal creek networks, and the impact of storm or tsunami events (Allen, 1996; Lario *et al.*, 2001; Dark & Allen, 2005). Particle-size analyses are therefore a valuable tool

in the study of past depositional environments within estuarine settings, assisting in the identification of both long-term changes related to the evolution of an estuary and in the identification of specific sub-environments.

A wide range of granulometric techniques are available to the sedimentologist (McManus, 1988). In the study of sediment samples from coastal and estuarine sequences, instruments using X-ray nephelometry or the scattering of laser or polarised light have largely replaced the older methods based on the pipette, hydrometer or Coulter Counter (Allen & Thornley, 2004). In this study, a Malvern 2000 particle-sizer employing low-angle laser light scattering technology (LALLS, or laser-diffraction technology) was used for the measurement of particle-size. The principle of laser-diffraction technology is that particles passing through a laser beam scatter the light, with smaller particles scattering the light at larger angles than bigger particles. The scattered light can be measured by a series of photodetectors placed at different angles, resulting in a diffraction pattern for the sample. The diffraction pattern is used to determine the size of the particles using light scattering theory developed in the early 20th century — Mie theory (Allen, 1997). Technological developments over the last three decades mean that this method has the virtues of rapid measurement, reproducibility, and wide particle size coverage [0.02–2000 μm] (Sperazza *et al.*, 2004).

Malvern 2000 measurement settings		
Optical properties	Reflective Index	1.5
	Absorption	0.01
	Dispersant Refractive Index (water)	1.33
Measurement parameters	Sample measurement	10 seconds or 10k 'snaps'
	Background measurement	10 seconds or 10k 'snaps'
	Stabilising period	10 seconds
	Measurement cycles	3-5
	Obscuration limits	5-20%
Machine settings	Pump speed	2250 rpm

Table 3.1. Malvern 2000 measurement settings

3.2.2.2 Method

Sub-samples of air-dried and screened (<2mm) sediments (*c.* 3g) were taken for particle size measurement on a Malvern 2000 particle-sizer. Samples were treated with 4.4% sodium pyrophosphate (incubation for 3 hours in a waterbath at 90°C, stirring periodically). This pre-treatment is to ensure complete disaggregation of the sample and deflocculation of clay particles. Small quantities of the samples were then extracted for measurement on the Malvern particle-sizer to determine the particle size distribution (PSD) of the whole sediment (i.e. including organics and carbonates). In order to ensure a representative sub-sample, this extraction was made using a pipette (2mm opening) to withdraw an agitated sediment/water slurry from an active vortex produced on a 'whirlimix' sample mixer. For each sample, results were only stored once stabilisation of the PSD curves was obtained across several (3-5) measurement cycles (measurement settings are shown in Table 3.1).

The sediment samples were subsequently treated with 7% HCl (1 hour at 90°C) and 100 volume H₂O₂ (addition of *c.* 15ml, reaction proceeding to completion in waterbath) in order to destroy the carbonate and organic fractions. Extracts of the treated samples were then re-measured on the Malvern particle-sizer to determine the PSD for the inorganic, non-carbonate components of the sediment. In this study we focus on the results of particle size analysis of the treated samples.

The Malvern sizer produces 32 channels of output data in half phi (φ) intervals, from which a number of standard summary variables are calculated. In this study, we use measures of average grain size (mean and median), a measure of sorting or spread about the average (inclusive graphic standard deviation, σ_1 (Folk & Ward, (1957))) and a measure of preferential spread (inclusive graphic skewness). The logarithmic phi (φ) scale is used in order to facilitate the presentation and description of data which includes a wide range of particle sizes. Descriptive terminology follows the Udden-Wentworth system, with the clay-silt boundary at 8 phi.

3.2.3 Magnetic Susceptibility

3.2.3.1 Background

The study of the magnetic properties of environmental materials, or environmental magnetism (Thompson & Oldfield, 1986), has a wide range of applications. Magnetic analyses provide information relating to the physiochemical status of iron minerals within soils and sediments and can provide a powerful diagnostic tool in various depositional environments for the study of sediment source areas (Oldfield *et al.*, 1985; Dearing *et al.*, 2001), weathering and pedogenetic processes (Fine *et al.*, 1992; Maher & Thompson, 1992; Pope & Millington, 2000), fire history (Rummery, 1983), and for stratigraphic correlation (Lees *et al.*, 1998). In the estuarine environment, magnetic properties of sediments may be related to sediment sources, hydrodynamic regime and post-depositional diagenesis (Rey *et al.*, 2000; Emiroglu *et al.*, 2004), and their study complements the investigation of other physical and biotic parameters.

In this study, a basic characterisation of the magnetic susceptibility of the sediment samples is undertaken. Magnetic susceptibility and frequency dependent susceptibility provide an indication of the overall concentration of magnetic minerals and may identify the presence of ultrafine magnetic particles ($< \sim 0.03 \mu m$). Magnetic susceptibility is defined as the relationship between a magnetic field and the strength of magnetisation created in a sample substance (Dearing, 1999), and is expressed as the ratio of the two:

$$\kappa = M/H$$

where κ is the volume susceptibility, M is the magnetic moment per unit volume of sample, and H is the applied magnetic field.

As κ values do not take into account the bulk density of the sample material, comparison of environmental samples which may have widely differing bulk densities is difficult. To permit comparison of samples of different densities, for example between different lithologies

or between sites, mass specific magnetic susceptibility (χ) values may be obtained by dividing κ by the bulk density of a sample. Mass specific magnetic susceptibility is expressed as:

$$\chi = \kappa/\rho$$

where κ is volume susceptibility and ρ is sample density.

Measurements made at two frequencies a decade apart (470 and 4700 Hz) may be used to detect the presence of ultrafine superparamagnetic ferrimagnetic minerals which occur as crystals produced by bacteria or by chemical processes mainly in soil (Dearing, 1999). In principle, magnetic minerals smaller than $\sim 0.03 \mu\text{m}$ residing near the domain size boundary between the superparamagnetic and stable single domains do not contribute fully to susceptibility at high frequency (Dearing, 1999). However, the precise physical basis for frequency dependence is not fully known.

By measuring the same sample twice at low and high magnetisation frequencies (0.46 and 4.6 kHz, respectively) percentage frequency dependent susceptibility ($\chi_{fd\%}$) can be calculated as follows:

$$\chi_{fd\%} = \{(\chi_{lf} - \chi_{hf}) / \chi_{lf}\} * 100$$

where χ_{lf} is the mass specific susceptibility measurement at low frequency and χ_{hf} is the mass specific susceptibility measurement at high frequency.

3.2.3.2 Method

Sub-samples of air-dried and screened ($< 2\text{mm}$) sediments were packed into standard 10cc plastic pots. Susceptibility measurements were taken on a Bartington Instruments MS2 meter with dual-frequency sensor. Results for each sample are the average of at least 3 measurement cycles; for samples with weak susceptibility, averages of 6–8 measurement cycles were recorded. As recommended in Dearing (1999: 46), samples with values for κ

<150 were measured with the range multiplier at the high resolution (0.1) setting; samples with values for κ >150 were measured on the low resolution (1.0) setting. The same sample orientation within the sensor was maintained between measurements for each sample.

The results presented in this thesis do not include corrections for the diamagnetic effects of organic matter and calcium carbonate. Although corrections were calculated on the basis of LOI estimates for organic and carbonate content, they were insignificant, reflecting the overall low organic and carbonate content of the sediments.

3.3 Methods for pollen analysis

3.3.1 Pollen preparation

The process of extracting pollen from sediments is well established, and is described in detail in several sources, e.g. Faegri *et al.* (1989), Moore *et al.* (1991), Bennett & Willis (2001). From a more or less standard suite of processes, modifications or alternative stages may be required depending on the nature and composition of the sediment samples. The stages of the preparation routine followed in this study are detailed in Table 3.2. In addition to standard procedures, the high silicate content of the sediment samples necessitated a second phase of HF treatment for all samples, and the presence of iron sulphide particles (pyrite) in many samples demanded treatment with nitric acid.

Silicone oil was used as the mounting medium because it does not set, permitting pollen grains to be rotated during observation through the application of gentle pressure on the coverslip using a toothpick. This mobility is highly advantageous in the identification of difficult specimens, particularly those with complex morphologies or present in a crumpled state.

3.3.2 Pollen counting and identification

Pollen slides were counted on a Leica DMLB transmitted-light microscope at $\times 400$ magnification, with regular use of the $\times 1000$ objective and immersion oil for the observation of critical morphological features and difficult determinations. Slides were counted in

complete, evenly spaced traverses. Total counts were large (typically >500 pollen and spores; average count 1460 pollen and spores) to ensure that both wetland and dry ground taxa were well represented. In particular, a minimum of 200 grains representing forest, scrub (*matos*) and heath communities (e.g. *Pinus*, *Quercus*, Cistaceae and Ericaceae types) were counted in each sample. In addition to pollen and spores, a number of other microfossils observed during counts were recorded. These include dinoflagellates and algal forms such as *Pediastrum*, *Spirogyra* and Zygnemataceae.

Pollen and spore identifications were made to the narrowest taxonomic category possible with the aid of: a) the reference pollen collection of the Quaternary Palaeoenvironments

Stage	Rationale
Sediment (1cm ³)	Sediment sample of known volume
Lycopodium tablets	Addition of known quantity of marker spore permits estimation of pollen and spore concentration
7% HCl, hot ¹ , 20 min+	Removes carbonates
H ₂ O, wash+	Removes waste products of HCl treatment, neutralise sample
10% NaOH, hot, 3½ min	Removes humic acids
Sieve (180µm)	Removes coarse mineral and organic particles
H ₂ O, multiple washes (~8-10)+	Removes clays
7% HCl, wash+	Acidifies sample prior to HF
48% HF, hot, 2 hrs+	Removes silica and silicates
48% HF, hot, 2 hrs+	Stage repeated
7% HCl, hot, 1 hr 15 min+	Removes colloidal silica and silicofluorides resulting from HF treatment
10% HNO ₃ , hot, 4-6 min+	Removes pyrite
H ₂ O, wash+	Removes waste products of HNO ₃ treatment
CH ₃ COOH (glacial acetic acid), wash+	Removes H ₂ O prior to acetolysis
Acetolysis ² , hot, 3½ min	Removes polysaccharides (cellulose)
CH ₃ COOH, wash+	Ends acetolysis reaction, permits rehydration
H ₂ O, wash+	Removes waste products of acetolysis
~1% NaOH, wash+	Neutralises residual acid prior to staining
0.2% aqueous Safranin, 2 drops + H ₂ O+	Staining; increases contrast of pollen and spore surface structure under light microscopy
TBA (tertiary-butyl alcohol), wash+	Dehydrates sample residue; miscible with silicone oil
Silicone oil	Mounting medium
Slides	Residue mounted on microscope slides under glass coverslips for counting pollen and spores

¹ 'hot' indicates sample incubation in waterbath at ~90°C for specified time

⁺ balance samples, centrifuge, decant (discarding supernatant), whirlimix

² acetolysis mixture = 9 parts acetic anhydride, (CH₃CO)₂O: 1 part concentrated sulphuric acid, H₂SO₄

Table 3.2. Pollen preparation stages

Group, b) new reference pollen slides made as part of this project for *c.* 35 additional species collected in the field and sourced from botanical gardens in the UK, c) published images contained in the pollen atlas and supplement of Reille (1992; 1995) and d) detailed pollen morphological studies and identification keys from numerous sources, including sections of the *Northwest European Pollen Flora* (Punt, 1976; Punt & Neinhuis, 1976; Punt *et al.*, 1976a, 1976b; Clarke, 1980; Clarke & Jones, 1980; Engel, 1980; Kalis, 1980; Clarke & Jones, 1981; Jones & Clarke, 1981; Punt. & den Breejen, 1981; Blackmore, 1984; van Benthem *et al.*, 1984; van Leeuwen *et al.*, 1988; Clarke *et al.*, 1991; Stafford & Blackmore, 1991; Punt *et al.*, 1991; Stafford, 1991) and studies on Mediterranean and/or southwest European pollen and spore groups (Sáenz de Rivas, 1973; Berthet & Lecocq, 1977; Saad, 1986; Mateus, 1989; Queiroz, 1999). The dichotomous key contained in Moore *et al.*, (1991) was used as a general guide for pollen and spore identification. Dinoflagellates were identified with the aid of Rochon *et al.* (1999).

Pollen type nomenclature follows the various sources listed in the previous paragraph, with the chief aims of producing pollen records that are accurate, repeatable, and botanically meaningful. The changes to pollen nomenclature arising from revisions to the British flora of Stace (1991) described in Bennett *et al.* (1994) are observed here, as they are becoming widely used in many places beyond Britain both in botany and palynology. Conventions used to indicate the accuracy and certainty of identifications as described in Berglund & Ralska-Jasiewiczowa (1986) are observed here. The pollen and spores types identified in this study, literature references for their description, and likely botanical and ecological significance accompany the results of pollen analysis. The construction of pollen diagrams is also discussed in the results chapter.

Morphometric studies on Iberian *Pinus* pollen has shown that grain diameters may help to discriminate between different species (Roure, 1985 (data presented in Carrion *et al.*, (2000)); Queiroz, 1999). During the course of pollen counts in the CM5 core, measurements of the equatorial diameter of *Pinus* pollen grains were taken using a calibrated eyepiece graticule.

Measurements were made at the widest point of the grain body, excluding the sacci (as illustrated in Moore *et al.*, 1991: 90). Measurements were only taken on grains that were not crumpled or broken and where the sacci were not folded in such a way as to conceal the grain body.

3.3.3 Calculation of pollen concentrations

Lycopodium marker spore tablets (Stockmarr, 1971) were added in known quantities to the sediment samples at the beginning of the preparation procedure and were counted during analysis of the pollen slides. The ratio of fossil pollen to marker spores permits the determination of pollen concentration, calculated as follows:

$$C = (T \cdot X_{\text{TAB}} \cdot P) / (X \cdot S)$$

where C is the concentration of fossil pollen in grains/cm³; T, the number of tablets added; X_{tab}, the number of marker spores per tablet; P, the number of fossil pollen grains counted; X, the number of marker spores counted; and S, the volume of sediment in cm³.

3.4 Radiocarbon data

The bulk of radiocarbon data used in this study for the construction of age-depth models was obtained by T. Boski of the Universidade do Algarve. Four additional dates for the CM5 core were obtained in a collaborative manner. Small bulk samples of organic detritus or shell material were sent to Cambridge from Faro. These samples were washed in deionised water, dried overnight at 50°C, and material for dating was weighed and packed in foil. Species identifications were obtained for shell samples, but the small size prohibited identification of wood fragments. Necessary precautions for the handling of AMS samples were undertaken at each stage to avoid contamination with modern carbon (Polach & Golson, 1966). These samples were pre-processed for AMS dating at the Waikato Radiocarbon Laboratory in New Zealand, with AMS measurements undertaken at the NSF facility in Arizona, USA. The details of all radiocarbon data are presented in Chapter 5.

4 Core lithology and results of sediment analyses

Lithostratigraphical zones are delimited on the basis of the information content of core log descriptions received from CIMA, Universidade do Algarve and (for cores P2 and P5) on direct observations of archived core sections. Lithostratigraphical or sediment zones are prefixed with the site code and the letter 's' (e.g. CM5s-) to distinguish them from independent biostratigraphical zones defined on the basis of pollen data. Zones are numbered from the base upwards. Sediment zone summaries are presented in Tables 4.1, 4.2 and 4.3. The results of sediment analyses (loss-on-ignition, particle size, magnetic susceptibility and shell content) follow the description of sediment zonation. The results are displayed in diagrams at the end of the chapter, and summarised for each site in Tables 4.4, 4.5 and 4.6.

4.1 CM5 Guadiana

4.1.1 Core lithology (CM5)

The CM5 borehole, located *c.* 500 m from the right bank of the Guadiana in the infilled tributary valley of the Beliche River, reached bedrock at a depth of *c.* 51 m (Figure 4.1). The following lithological zones are distinguished from the base to the top:

CM5s-1: 5080–4856 cm

At the base of the CM5 sequence is a unit of sand and gravel. The unit is most coarse at the base (5080–5032 cm) with large pebbles and cobbles of rounded greywacke, small to medium

Zone	Depth range		General description
CM5s-6	252 cm	- 0 cm	Oxidised silts and soil
CM5s-5	2102 cm	- 252 cm	Shelly silts with fine sand
CM5s-4	4080 cm	- 2102 cm	Silts
CM5s-3	4570 cm	- 4080 cm	Fine sands, flaser-bedding
CM5s-2	4856 cm	- 4570 cm	Laminated silts
CM5s-1	5080 cm	- 4856 cm	Gravel
Bedrock		- 5080 cm	Palaeozoic (Culmian)

Table 4.1 Sediment zone summary, core CM5.

platy pebbles of schist, and rare clasts of angular, fractured quartzite. The clasts are contained within a matrix of coarse sand. Above 5032 cm, the fill comprises medium to coarse sands with small to medium pebbles, predominantly of schist, and also with rare clasts of fractured quartzite. At depth 5060 cm, small lenses of charcoal and plant detritus are present.

CM5s-2: 4856–4570 cm

This zone contains predominantly fine-grained sediments (silts) with sand and carbonised plant fragments. Small fragments of schist are present at the base of the zone. In the lower part (depth 4856–4635 cm), laminations of silt and fine sand occur, in some parts with loading structures, pockets of clay and small charcoal lenses. A thin layer of medium sand (not sampled) is noted at depth 4740 cm, resting on a very abrupt contact with the underlying layer. The upper part of the zone (4635–4570 cm) is predominantly fine-grained, enriched in parts with organic material.

CM5s-3: 4570–4080 cm

This zone contains fine sands, interlaminated with silt and clay. At the base of the zone, the sands contain millimetre-scale flame-structures and sedimentary dyke structures. In large sections (4520–4450 cm and 4216–4360 cm) the sediments display flaser-type bedding with drapes or fine layers of clay within fine sand.

CM5s-4: 4080–2102 cm

A thick zone of compact, silty-argillaceous sediment with dispersed fragments of carbonised plant material overlies the flaser-bedded sands. Towards the base of the zone (4080–3784 cm) small lenses of charcoal and fine, centimetre-scale peaty layers of organic material are recorded. In the lower part of the zone (below 3512 cm depth), small lenses of chestnut-coloured clay are dispersed within the silts. Traces of bioturbation are noted, with pockets of greenish clay (2.5Y 6/2).

CM5s-5: 2102–252 cm

This zone contains compact silts and sandy silts with shell and dispersed organic material. Shell fragments and intact shells (bivalves and gastropods) are present from the base of the zone, varying in abundance and preservation state across the zone. Below 1730 cm, shell fragments are poorly preserved and very dispersed. Above 1730 cm, the sediments are rich in shell fragments and intact shells. At some depths (1652–1730 cm, 635–730cm), the shell material shows signs of carbonate dissolution, with only shell-moulded sediment casts preserved. Small, dispersed fragments of carbonised plant material are noted at several depths.

CM5s-6: 252 cm –0 cm

The uppermost zone contains compact silts with nodular zones of chestnut-coloured oxidation. Shells are absent. A clay-rich soil with live roots and signs of anthropogenic disturbance is recorded above 90cm.

Sampling with respect to lithostratigraphy

Sediment samples subjected to further investigation of sedimentary characteristics span zones CM5s-2 to CM5s-5, and part of zone CM5s-6. Sample locations are shown in Figure 4.1.

4.1.2 Loss-on-ignition (CM5)

Values for water content, organic matter content (LOI_{400}), estimated CaCO_3 content, and mineral residue are presented in Figure 4.2.

Water content of the sediment samples ranges between 16.7 and 37.8%. Values are generally low in the lower zones (CM5s-2, CM5s-3), intermediate in zone CM5s-4, and high in zone CM5s-5. Intermediate, declining values are recorded from the uppermost zone (CM5s-6).

LOI values for organic matter content range between 1.5 and 5.9% (mean value 3.2%). Values for organic matter are generally low in the lower part of the core (zones CM5s-2, CM5s-3, CM5s-4), with minimum values occurring in zone CM5s-3. Elevated values are recorded in zone CM5s-5, with consistent high values around 4%. Towards the top of the core (zone CM5s-6) values for organic matter decline sharply.

Values for CaCO_3 content, estimated from LOI_{950} , range between 1.7 and 8.6% (mean value 4.0%). Intermediate to high values for CaCO_3 content are recorded in zone CM5s-2. Minimum values occur in zone CM5s-3. Intermediate values are recorded in the lower part of Zone CM5s-4, and low values in the upper part. High values are recorded from zone CM5s-5, before declining sharply towards the top of the core in zone CM5s-6.

Values for estimated silicate mineral residue range between 84.6 and 94.3%, with high values occurring in zone CM5s-3, and low values occurring in zone CM5s-5.

Biplots of the LOI data are presented (Figure 4.3). Water content shows a broad positive correlation with organic content (Pearson correlation coefficient = 0.765). Samples from zone CM5s-5 occupy a region of the biplot corresponding to relative high values for water and organic content, while the area corresponding to relative low values is occupied by samples from zone CM5s-3. The other samples, representing zones CM5s-2, CM5s-4 and CM5s-6 occupy a central area corresponding to intermediate values for water and organic content.

Zone CM5s-5 is also differentiated in terms of relatively high values for organic matter and CaCO_3 content, as shown in the biplot (Figure 4.3b). The other zones, with low and

intermediate values are not clearly differentiated, although the lowest values for organic matter and CaCO_3 content occur in zone CM5s-3. Overall, organic and CaCO_3 content show a slight positive correlation (Pearson correlation coefficient = 0.505).

4.1.3 Particle size analysis (CM5)

The results of particle size measurements are presented in ϕ units for the non-organic, non-carbonate fraction (treated with H_2O_2 and HCl) (Figure 4.4), and summarised in Figure 4.5. The salient features of the PSD discussed here apply to both the whole and treated sediment samples.

It should be noted that a stratified sampling with respect to drapes, laminae or other sedimentary structures was not undertaken, so: a) individual sample depths represent to some extent ‘averaged’ conditions, b) recorded values for sedimentary parameters do not provide an indication of fine-scale variability within the zone, and c) no estimate is made of the density or number of fine-scale sedimentary changes.

The PSD for zone CM5s-2 reveals a fining-upward trend across the zone, with decreasing values for very fine to medium sand (4–1 ϕ), and increasing values for very fine and fine silt (8–6 ϕ). These changes are recorded in decreasing (fining) median and mean grain size. Decreases in overall grain size are accompanied by a trend towards better sorting (low ϕ_1). Zone CM5s-3 is distinguished by an overall elevated sand content and reduced silt content compared with other zones, although considerable between sample variation is recorded. Peak values occur for very fine, fine and medium sand (4–1 ϕ). Reduced values occur for the coarser clay fraction (9–8 ϕ) and very fine to medium silt fractions (8–5 ϕ). The increased sand component recorded in several of the samples is reflected in increased (coarser) median and mean grain size. The sediment samples are very poorly sorted (peak values for ϕ_1) and are, in part, very positively skewed.

Zone CM5s-4 is characterised by the dominance of clay and silt fractions (9–4 ϕ), with a minor component of very fine sand (4–3 ϕ). The sediments display the best sorting (reduced

values for ϕ_1) compared with other zones and display fairly symmetrical (skewness ~ 0) grain-size distributions. Zone CM5s-5 is distinguished by the characteristics of the sand fraction. Relative to underlying zone CM5s-4, values for very fine and fine sand (4–2 ϕ) increase, and a minor presence of medium sand (2–1 ϕ), which is largely absent in zone CM5s-4, is recorded. Towards the top of the zone, two local peaks (depths 550cm and 300cm) are recorded in coarse silt and very fine sand content (5–3 ϕ). Median and mean grain sizes are slightly coarser than in the underlying zone, and show local peak values towards the top of the zone. The sediment samples are more poorly sorted and are symmetrical to negatively skewed. Zone CM5s-6 shows a fining upward trend, with decreasing content of coarse silt and sand (5–1 ϕ) and increasing content of finer silt and clay (9–5 ϕ). Median and mean grain sizes decrease; sorting improves.

On the whole, silt-sized particles in the size range 8–5 ϕ dominate the PSD. The sediment zones are distinguished by variation in the sand content. The greatest variation between sample depths is recorded in the fine sand content (3–2 ϕ) for both whole (StDev = 4.55%) and treated (StDev = 5.03%) sediment samples.

4.1.4 Magnetic susceptibility (CM5)

Values for low frequency mass specific magnetic susceptibility (χ_{lf}) and percent frequency dependent magnetic susceptibility ($\chi_{fd\%}$) are plotted in Figure 4.6.

Values for χ_{lf} range between *c.* 9 and $90 \times 10^{-8} \text{ m}^3 \text{ kg}^{-1}$ (mean value $24 \times 10^{-8} \text{ m}^3 \text{ kg}^{-1}$). Intermediate to high values occur in the lower part of the core, with moderate values for zone CM5s-2 (*c.* $30\text{--}50 \times 10^{-8} \text{ m}^3 \text{ kg}^{-1}$) and peak values for χ_{lf} in the lower part of zone CM5s-3 ($>80 \times 10^{-8} \text{ m}^3 \text{ kg}^{-1}$). Zone CM5s-4 displays low to moderate values for χ_{lf} (*c.* $15\text{--}50 \times 10^{-8} \text{ m}^3 \text{ kg}^{-1}$), with a distinct peak in χ_{lf} at the top of the zone between depths 2100 cm and 2200 cm. In zone CM5s-5, overall values for χ_{lf} are low, with the bulk of observations less than $20 \times 10^{-8} \text{ m}^3 \text{ kg}^{-1}$. A local peak in χ_{lf} with values up to $27 \times 10^{-8} \text{ m}^3 \text{ kg}^{-1}$ occurs towards the top of the zone around 550cm depth. Towards the top of the core (CM5s-6), values for χ_{lf} are low.

A strong contrast is observed in values for $\chi_{fd\%}$ between the lower and upper parts of the core. In the lower zones (CM5s-2, CM5s-3), values for $\chi_{fd\%}$ are predominantly greater than 2%, reaching peak values (>5%) toward the base of the core and in the upper part of zone CM5s-3. In the overlying zones (CM5s-4, CM5s-5, CM5s-6), values for $\chi_{fd\%}$ do not exceed 2%.

The magnetic susceptibility data is shown in biplot form (Figure 4.7). A broad positive correlation is observed between χ_{lf} and $\chi_{fd\%}$ (Pearson correlation coefficient = 0.643). An overall contrast is identified between the samples of zones CM5s-2 and CM5s-3, and zones CM5s-4, CM5s-5 and CM5s-6. The stratigraphically lower samples of CM5s-2 and CM5s-3 generally display moderate to high values for χ_{lf} (greater than $\sim 30 \times 10^{-8} \text{ m}^3 \text{ kg}^{-1}$) and elevated values for $\chi_{fd\%}$ (>2%). The overlying samples display moderate to low values for both χ_{lf} and for $\chi_{fd\%}$ ($< 30 \times 10^{-8} \text{ m}^3 \text{ kg}^{-1}$, <2%). The exception to this pattern are samples displaying relatively high χ_{lf} and low $\chi_{fd\%}$ related to the peak in χ_{lf} which occurs at the boundary between zones CM5s-4 and CM5s-5.

4.1.5 Shell content (CM5)

The content of recovered shell material is shown in Figure 4.8. Shell material was only present in sediment samples of zone CM5s-5, reaching peak values between 3 and 4 % of the total sediment dry weight. The recovered shell material includes fragmented bivalves, intact juvenile specimens of *Cerastoderma glauca* and *Corbula gibba*, and intact small gastropods of *Hydrobia ulvae*.

4.2 P2 Arade

4.2.1 Core lithology (P2)

The P2 borehole from the estuary of the Arade River reached bedrock at *c.* 22 m depth (Figure 4.9). The following lithological zones are described:

Zone	Depth range		General description
P2s-5	184 cm	- 0 cm	Sandy-clay and soil
P2s-4	956 cm	- 184 cm	Sands and sandy shell-beds
P2s-3	1785 cm	- 956 cm	Silt
P2s-2	1925 cm	- 1785 cm	Silts and sands
P2s-1	2220 cm	- 1925 cm	Gravel
Bedrock		- 2220 cm	Limestone

Table 4.2. Sediment zone summary, core P2.

P2s-1: 2202–1925 cm

The lowest zone of the P2 sedimentary fill is composed of gravel with very coarse sand. The fill contains predominantly pebbles and cobbles up to 10 cm in diameter of quartz and greywacke, of low sphericity and angular shape.

P2s-2: 1925–1785 cm

Overlying the gravel is a series of alternating layers of fines and sands, ranging in thickness between 10 cm and 20 cm. Finer laminations of sand and clay, and accumulations of organic detritus, are contained within some layers. Between depths 1876 and 1896 cm, a layer of fine and medium sands contains reddened, oxidised layers. An irregular contact is noted at 1832 cm. Between depths 1820 and 1808 cm, an organic-rich clayey-sand contains branching cracks filled with more consolidated material.

P2s-3: 1785–956 cm

Zone P2s-3 contains predominantly fine-grained sediments (silts) with plant fragments and shells. Undulating laminations of fine sand occur at several depths (1270–1286 cm, 1132–1136 cm, 1064–1085 cm). Dispersed mud-balls are noted between 1286 and 1335 cm. In the lower part of the zone (below 1286 cm), shell fragments are rare and poorly preserved, while in the upper part (above 1286 cm) shell fragments and intact shells occur in greater abundance and in a better state of preservation.

P2s-4: 956–184 cm

This zone comprises the thick deposits of sand of the upper part of the P2 sequence. A sub-zone boundary is placed at 445 cm depth based on the abundance of shell material, separating sub-zone P2s-4a (sands with dispersed shell material) from P2s-4b (shell-beds).

–P2s-4a: 956–445 cm

Sub-zone P2s-4a contains sands with dispersed shell fragments, occasional intact valves and gastropods, and pockets of organic material. Between 854 and 776 cm, variations in colour reveal intercalation of different sands, and laminations of sand and silt occur between 652 and 600 cm depth. A shell-rich layer of bedded shells, principally *Ostrea* sp. (oysters), occurs around 670 cm depth. At the top of the sub-zone (above 584 cm), a finer layer of silty-sand with laminations of black, shelly sand is observed.

–P2s-4b: 455–184 cm

Sub-zone P2s-4b contains shell-bed layers in a sandy-clay matrix. Towards the base of the sub-zone, the shells are highly fragmented, while in the upper part (above 355 cm), the shells are generally well-preserved with abundant remains of *Ostrea* and other bivalves.

P2s-5: 184–0 cm

The lower 40 cm of this zone is a layer of sandy-clay containing shells. Above 142 cm, reddening and the presence of fresh root material is observed.

Sampling with respect to lithostratigraphy

Samples for further analysis span sediment zones P2s-2, P2s-3 and P2s-4a. Sample locations are shown in Figure (Figure 4.9).

4.2.2 Loss-on-ignition (P2)

Values for organic matter content (LOI_{400}), estimated CaCO_3 content, and estimated silicate residue are presented (Figure 4.10). Although dried at 105°C following the described methodology, values for water content are not presented, as the samples were already air dry when collected.

Organic matter content of the P2 samples range between 1.0 and 6.4% (mean value 2.7%).

Values are high for zones P2s-2 and P2s-3, and low in zone P2s-4.

Values for estimated CaCO_3 content range between 2.0 and 23.2% (mean value 5.9%). Values are low in zone P2s-2 and increase steadily across zone P2s-3. Values for zone P2s-4 display considerable variability, being generally moderate or middle-of-the-range, but including a strong peak at 786 cm depth.

Values for estimated silicate mineral residue range between 73.3 and 94.1% (mean value 88.8%). Values are high in zone P2s-2 and decrease across zone P2s-3. Values are generally high in zone P2s-4, with the exception of one carbonate rich sample which displays a corresponding low value for estimated mineral residue.

Overall, the sample zones are distinguished by relative differences in estimated organic matter and CaCO_3 content, as shown in a biplot (Figure 4.11). Samples from zone P2s-2 are characterised by high organic content, low CaCO_3 content; samples from P2s-3 by high organic and high CaCO_3 content; and samples from P2s-4 by low organic content and varied CaCO_3 content. Organic and CaCO_3 content do not show a significant correlation.

4.2.3 Particle size analysis (P2)

The results of particle size measurements are presented in 1 phi units for the non-organic, non-carbonate fraction (treated with H_2O_2 and HCl) (Figure 4.12) and summarised in Figure 4.13. Overall, the results for treated and untreated samples are similar and the major features of the PSD discussed here apply to both the whole and treated sediment samples.

In the lowermost sampled zone (P2s-2) silts predominate, accompanied by clays in the size range 11–8 ϕ and finer sands (4–2 ϕ). In zone P2s-3, silts again form the major constituent part of the sediment fill, accompanied by clay and with a fluctuating component of very fine to medium sand (4–1 ϕ). The sand content shows two local peaks at about depths 1750 and 1450 cm and then increases towards the top of the zone. Overall, the samples from zones P2s-2 and P2s-3 have fine median and mean grain sizes, are relatively well sorted (low σ_1 values) and symmetrical to negatively skewed. The local peaks in sand content are

reflected (particularly for the inorganic/treated samples) in small increases (coarsening) in median and mean grain size, and positive skew. Between 1000 and 900 cm, a transition from silty to sandy grain sizes is recorded. Silt content decreases, and the content of fine, medium and coarse sands (3–0Ö) increases. Sands predominate in zone P2s-4, with corresponding increases (coarsening) of median and mean grain size. Sorting is relatively poor (increased ϕ_1 values) and the grain size distributions are very positively skewed. The uppermost samples from zone P2s-4 contain a slightly reduced sand content, with a corresponding fining of median and mean grain size.

Overall, silt-sized particles predominate in the lower part of the sampled sequence, and sands in the upper. The lower sediment zones are readily distinguished from the upper zone by changes in median and mean grain size and in the relative proportions of silt and sand. The greatest variation between sample depths is recorded in the medium sand content (2–1Ö) for the whole sediment samples (StDev = 9.65%) and in the fine sand content (3–2Ö) for the treated sediment samples (StDev = 11.61%).

4.2.4 Magnetic susceptibility (P2)

Values for low frequency mass specific magnetic susceptibility (χ_{lf}) and percent frequency dependent magnetic susceptibility ($\chi_{fd\%}$) are presented (Figure 4.14).

Values for χ_{lf} range between *c.* 5 and $225 \times 10^{-8} \text{ m}^3 \text{ kg}^{-1}$ (mean value $71 \times 10^{-8} \text{ m}^3 \text{ kg}^{-1}$). Towards the base of the sequence at 1800 cm (zone P2s-2), a local peak in χ_{lf} occurs. Values for χ_{lf} are low in zone P2s-3 ($\sim 40 \times 10^{-8} \text{ m}^3 \text{ kg}^{-1}$ and below) and decrease steadily to very low values ($< 10 \times 10^{-8} \text{ m}^3 \text{ kg}^{-1}$) at the top of the zone. In zone P2s-4, values for χ_{lf} are high ($> 100 \times 10^{-8} \text{ m}^3 \text{ kg}^{-1}$).

Values for $\chi_{fd\%}$ range between 0 and 5.4% (mean value 2.3%). Values above 2% are recorded in zone P2s-2. In zone P2s-3, $\chi_{fd\%}$ is generally low ($< 2\%$), but contains a local peak reaching 3.9% towards the top of the zone. In zone P2s-4, $\chi_{fd\%}$ is consistently higher than in lower zones, with values typically in the range 4–5%.

A biplot of the magnetic susceptibility results (Figure 4.15) clearly discriminates between zones P2s-3 (low χ_{fr} , low $\chi_{fd\%}$) and P2s-4 (high χ_{fr} , high $\chi_{fd\%}$). Samples from zone P2s-2 are not differentiated by magnetic properties, with two samples showing similar properties to the samples from zone P2s-3, and one sample more similar to zone P2s-4.

4.2.5 Shell content (P2)

The content of shell material is shown in Figure 4.16. Shell material was not recovered from sediment zone P2s-2. Shell material is present in zone P2s-3, sporadically in the lower part of the zone, and consistently in the upper part. Shell content reaches high values (> 5 % sediment dry weight) towards the top of the zone. Shell material is consistently present in zone P2s-4a, fluctuating between low and high values. A number of intact gastropods and bivalves of small size (typically <10 mm) were recovered from the P2 samples. Increased shell content in the upper part of zone P2s-3 and in P2s-4a is associated with a relatively large number of recovered taxa. Some changes in species presence/absence are recorded at or immediately below the zone boundary P2s-3/P2s-4a; for example, *Turritella communis* is common in samples from zone P2s-4a but absent from all but the uppermost sample in zone P2s-3.

4.3 P5 Boina

4.3.1 Core lithology

The P5 borehole from the estuary of the Boina river reached bedrock at *c.* 20 m depth (Figure 4.17). The following lithological units are distinguished in the P5 core:

P5s-1: 2054–1590 cm

The basal deposits of the P5 sedimentary fill are composed of layers of pebbles, cobbles and coarse sand, generally clast-supported, and containing a number of fining-upward units. The clasts are polished, of low sphericity, and include primarily schists, greywackes, and to a lesser extent, quartzites. Also present are occasional pebbles of lamprophyre and Silves sandstone, and rare degraded clasts of nepheline syenite (Monchiquite). The matrix is of chestnut-coloured clayey-silt or silt and sand.

Zone	Depth range		General description
P5s-5	72 cm	- 0 cm	Soil
P5s-4	645 cm	- 72 cm	Sand
P5s-3	1185 cm	- 645 cm	Shelly silts
P5s-2	1590 cm	- 1185 cm	Silts, sands and gravels
P5s-1	2054 cm	- 1590 cm	Gravel
Bedrock	-	2054 cm	Plutonic, altered

Table 4.3. Sediment zone summary, core P5.

Above 1674 cm, a fining-upward trend is observed with a transition from clast-supported cobbles and pebbles to matrix-supported fine gravels and coarse sands, contained within an increasingly clay-rich and reddened matrix.

P5s-2: 1590–1185 cm

Zone P5s-2 contains layers of compact silts and clays separated by gravel beds and sands. A sharp contact at 1590 cm separates this zone from the underlying basal deposits. The zone is generally rich in fine organic material, charcoal, and contains wood and shell fragments. Sub-zone boundaries are placed at 1546, 1430 and 1325 cm, distinguishing the fine-grained silty layers (sub-zones P5s-2a, P5s-2c) from the coarse grained sandy layers (sub-zones P5s2-b, P5s2-d).

–P5s-2a: 1590–1546 cm

The lower fine-grained sub-zone contains layers of compact silts with small pockets of fine sand, dispersed shell fragments and fine charcoal.

–P5s-2b: 1546–1430 cm

This sub-zone contains sands and gravels. The lower part (below 1510 cm) is composed of medium to coarse sands within a silty matrix, containing layers rich in shell fragments and gravel. The upper part contains rounded gravels in a silty matrix. The uppermost 10 cm is

a positive-graded sequence from large pebbles to small pebbles, contained within a silty matrix.

–P5s-2c: 1430–1325 cm

This sub-zone is composed of compact, silty-argillaceous sediments, rich in organic material, wood fragments and dispersed charcoal. Occasional small pockets of fine sand occur near the base. Shell fragments are recorded, increasing in abundance above 1346 cm depth.

–P5s-2d: 1325–1185 cm

The upper subzone contains a complex of sand layers, enriched in parts with shell debris and organic matter, and interspersed with charcoal-rich clay bands. Signs of oxidation are recorded near the base. Silt-sand-ball sedimentary structures are noted at between 1200 and 1300 cm. A thin (2cm) shell-bed is recorded at 1232 cm depth.

P5s-3: 1185–645 cm:

Zone P5s-3 contains compact silts, rich in shell material, including intact valves and gastropods, and with fine charcoal throughout. Localised pockets or fine layers of silty-sand or sand occur at several depths, occasionally including rare gravel clasts. Unconformities are noted at 1090 cm and 1080cm.

P5s4: 645–72 cm:

This zone contains a series of sandy layers in an overall coarsening upward sequence. Below 525 cm, silty-sands predominate, with shell fragments, pockets of organic material, and occasional dispersed gravels. Between 525 and 420 cm, fine and medium sands are present, in parts rich in shell fragments and with occasional gravels. Above 420 cm, layers of medium to very coarse sand with polished gravels of greywacke, schist and quartzite. The gravels increase in size towards the top of the zone, and include small to large pebbles. The upper contact of the zone is marked by a fine oxidised layer.

P5s5: 72–0 cm:

The uppermost zone is a chestnut-coloured, clay-rich soil with abundant plant fragments.

Sampling with respect to lithostratigraphy

Samples from the P5 core for further investigation span the uppermost part of zone P5s-1, zones P5s-2 and P5s-3, and part of P5s-4. Sample locations are shown in Figure 4.17.

4.3.2 Loss-on-ignition (P5)

Values for organic matter content (LOI_{400}), estimated CaCO_3 content, and estimated silicate residue are presented (Figure 4.18). Values for water content are not presented, as the samples were already air dry when collected.

Organic matter content in the P5 sequence ranges between 1.0 and 4.6% (mean value 2.0%). Values are low at the base of the sampled sequence, increasing towards the top of zone P5s-1. Zone P5s-2 displays alternating high and low values for the sequence, with a high value in sub-zone P5s-2a, low values in sub-zone P5s-2b, peak high values in sub-zone P5s-2c and low to intermediate values in sub-zone P5s-2d. Recorded values from zones P5s-3 and P5s-4 are intermediate, typically within the range 1.5–2.5%.

Values for estimated CaCO_3 content range between 1.6 and 13.6% (mean value 5.7%). CaCO_3 content is low at the base of the sequence, increasing towards the top of zone P5s-1. Zone P5s-2 displays contrasting values for CaCO_3 content, with an intermediate value in sub-zone P5s-2a, low values in sub-zone P5s-2b, high values in sub-zone P5s-2c and low values in sub-zone P5s-2d. High values occur in zone P5s-3, reaching peak values in the upper part of this zone. Low values are recorded from zone P5s-4.

Values for estimated mineral residue range between 81.5 and 95.3% (mean value 90.0%). Mineral residue values are high in zone P5s-1. From zone P5s-2, an intermediate value is recorded in sub-zone P5s-2a, high values in P5s-2b, low values in P5s-2c and high values in P5s-2d. Zone P5s-3 displays reduced values for mineral residue, particularly in the upper part of the zone. High values for mineral residue are recorded in zone P5s-4.

A biplot for LOI values (Figure 4.19) shows that the sediment zones are poorly discriminated on the basis of organic content. However, on the basis of CaCO_3 content, zones P5s-2c and P5s-3 are distinguished from the other zones, displaying high values for CaCO_3 content (>6%). This distinction is clearly displayed by plotting CaCO_3 content against the content of residual mineral matter (Figure 4.19b).

4.3.3 Particle size analysis (P5)

The results of particle size measurements are presented in 1 phi units for the non-organic, non-carbonate fraction (treated with H_2O_2 and HCl) (Figure 4.20) and summarised in Figure 4.21. Sieve data for the gravel fraction is presented in 1 phi units (Figure 4.22), accompanied by a composite diagram showing the arithmetic integration of the sieve data (% weight) with the laser particle size results for the non-organic, non-carbonate fraction (% volume). Overall, the results for treated and untreated samples are similar and the main features of the PSD discussed here apply to both the whole and treated sediment samples.

Zone P5s-1 contains particle sizes ranging from fine clays to gravels (14 to -4 ϕ). The samples contain a significant clay component, including very fine clay particles (14–12 ϕ). The sediments are very poorly sorted (ϕ_1 up to 3.5). A fining upward trend in median and mean grain sizes is observed, accompanied by a trend from positive to symmetrical grain size distribution (skewness).

Textural contrasts between the sub-zones of zone P5s-2 are clearly recorded in the PSD, with an overall fine-coarse-fine-coarse sequence. In sub-zone P5s2-a, silts predominate. A minor component of the finer sand classes is present, and a small component of fine gravel. Sub-zone P5s-2b displays increased sand content with increased representation of medium to very coarse sand (2 to -1 ϕ) and also gravel clasts up to -4 ϕ . Sub-zone P5s2-c contains mainly clay and silt in the range 9–4 ϕ accompanied by very fine and fine sand (4-2 ϕ). Sub-zone P5s2-d is predominantly coarse-grained, with elevated content of medium and coarse sand (2–0 ϕ); gravel is not present.

Clay and silt (9–4Ö) are predominant in zone P5s-3. Sand content is reduced overall, although a local peak in sand content is identified between 880 cm and 980 cm. Gravel is absent in most of the zone, but occurs in the upper part of the zone.

Particle size measurements for zone P5s-4 distinguish between a predominantly silty lower part (below 525 cm) and a coarser fill above. Below 525 cm, the samples are similar to the underlying zone, with small increases in coarse sand (1–0Ö) and fine gravel clasts (-1 to -2Ö). Above 525 cm, the base of a fining-upward unit is observed, with peaks in coarse sand, very coarse sand and gravel clasts (1 to -4Ö), giving way to fine sands and silt.

The series of fluctuations between fine and coarse grained deposition observed in the particle size distributions can be traced in the median and mean grain size parameters. Coarse median and mean grain size values occur in zone P5s-1, P5s-2 (sub-zones 2b and 2d), the middle of zone P5s-3 and the upper part of zone P5s-4. Coarse median and mean grain size corresponds with elevated values for ϕ_1 (very poor sorting) and generally with positive skewness in the grain size distribution.

Overall, the P5 particle-size data records contrasting sediment types; on the one hand, sandy sediments characterised by elevated mean/median grain size, poor sorting and positive skewness, and on the other clayey-silts characterised by reduced mean/median grain size, relatively better sorting, and weak negative skewness. The greatest variation between sample depths is recorded in the coarse sand content (1–0Ö) for the whole sediment data set (StDev = 9.38%) and in the very coarse sand content (0 to -1Ö) for the treated sediment data set (StDev = 5.73%).

4.3.4 Magnetic susceptibility (P5)

Values for low frequency mass specific magnetic susceptibility (χ_{lf}) and percent frequency dependent magnetic susceptibility ($\chi_{fd\%}$) are presented (Figure 4.23).

Values for χ_{lf} range between $c.30$ and $620 \times 10^{-8} \text{ m}^3 \text{ kg}^{-1}$ (mean value $220 \times 10^{-8} \text{ m}^3 \text{ kg}^{-1}$). Very high values for χ_{lf} ($>400 \times 10^{-8} \text{ m}^3 \text{ kg}^{-1}$) are recorded at the base of the sequence (zone

P5s-1). In zones P5s-2 and P5s-3, a series of local peaks and troughs are recorded, with peak χ_{f} values between 200 and $300 \times 10^{-8} \text{ m}^3 \text{ kg}^{-1}$ occurring in sub-zones P5s-2b, P5s-2d, and in the middle and upper part of zone P5s-3. In zone P5s-4, values for χ_{f} are consistently high, typically in the range $300\text{--}400 \times 10^{-8} \text{ m}^3 \text{ kg}^{-1}$.

Values for $c_{\text{fd}\%}$ range between 1.0 and 6.2% (mean value 3.3%). The curve for $\chi_{\text{fd}\%}$ displays a complex pattern of peaks and troughs that is not clearly related to the sediment zones. Peak values for $\chi_{\text{fd}\%}$ (4.2–6.2%) are recorded at the base of the sequence (zone P5s-1). For the overlying samples, moderate values for $\chi_{\text{fd}\%}$ (c. 2–4%) are recorded.

The contrast in χ_{f} between zones P5s-1 and P5s-4 on the one hand, and P5s-2 and P5s-3 on the other is illustrated in a biplot of the magnetic susceptibility results (Figure 4.24).

4.3.5 Shell content (P5)

The content of shell material, shown in Figure (4.25), varies along the sediment sequence. Shell material was not recovered from sediment zone P5s-1, or from sub-zone P5s-2a. Shell material is present in some samples from sub-zones P5s-2b and P5s-2c, and is present in all samples from sub-zone P5s-2d, P5s-3 and P5s-4. Shell content reaches peak values between 3 and 4 % of the sediment dry weight. Small gastropods (*Hydrobia ulvae*, *Bittium* sp. and *Rissoa membranacea*) predominate among the intact shell material.

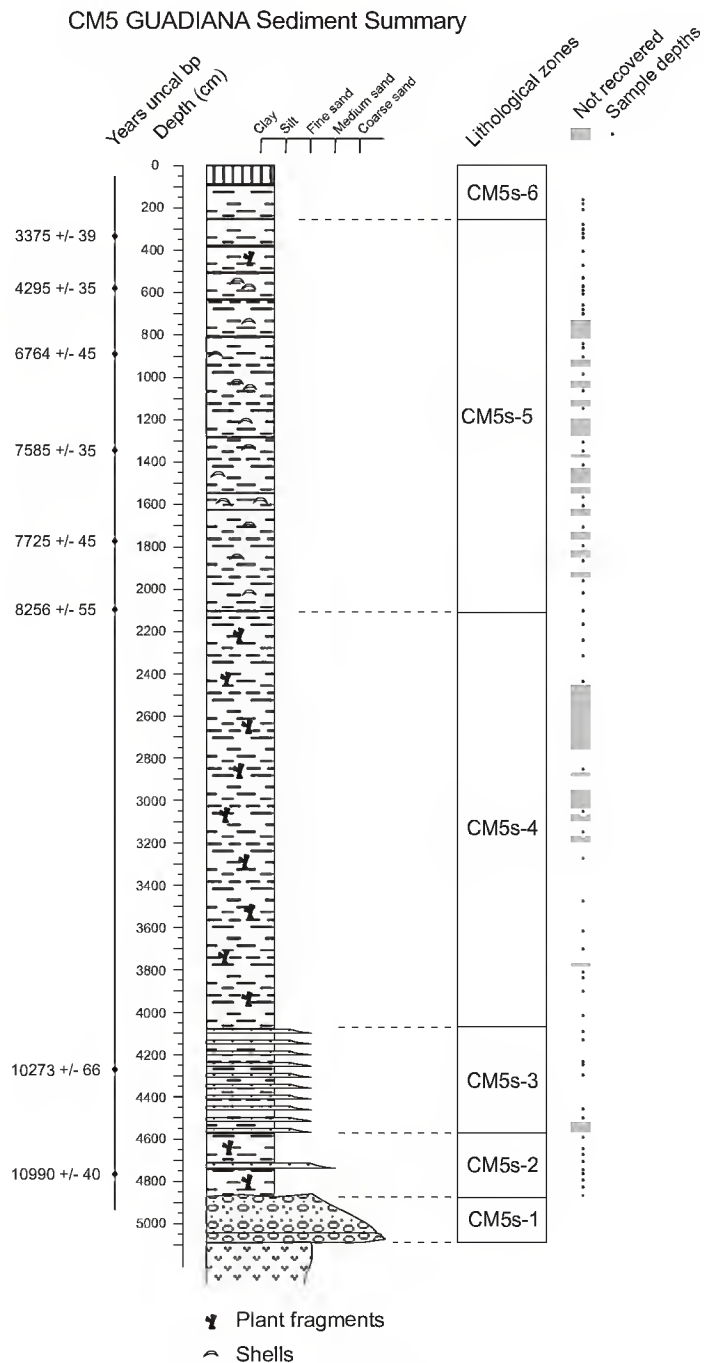


Figure 4.1. Core lithology and sample depths, CM5. Depth below surface, approx. 1 m above sea level.

Technique Parameter Range	Loss-on-ignition				Particle size			Magnetic susceptibility		Shell
	Water 16.7 - 37.8 %	Organic 1.5 - 5.9 %	CaCO ₃ 1.7 - 8.6 %	Mineral residue 84.6 - 94.3 %	Description	Sand content 2.0 - 69.9 %	Skewness and sorting	χ_{lf} 9 - 90 x 10 ⁻⁸ m ³ kg ⁻¹	$\chi_{fd}\%$ 0 - 5.4 %	
CM5s-6	Intermediate	High to low, decreasing	High to low, decreasing	Intermediate to high, increasing	Silts	Decreasing, intermediate to low	Symmetrical, poorly sorted	Low	<2%	No
CM5s-5	High	High	High	Low	Silts and sandy silts	Intermediate	Symmetrical to negatively skewed, poorly sorted	Low	<2%	Yes
CM5s-4	Intermediate	Low	Low to intermediate	Intermediate	Silts	Low	Symmetrical, poorly sorted	Intermediate	<2%	No
CM5s-3	Low	Low	Low	High	Silty sands	High	Symmetrical to very positively skewed, very poorly sorted	Intermediate to high	>2%	No
CM5s-2	Low	Low	Intermediate to high	Intermediate	Silts	Intermediate to low, decreasing	Symmetrical, poorly sorted	Intermediate	>2%	No

Table 4.4. General characterisation of sediment samples based on the results of sediment analyses, core CM5

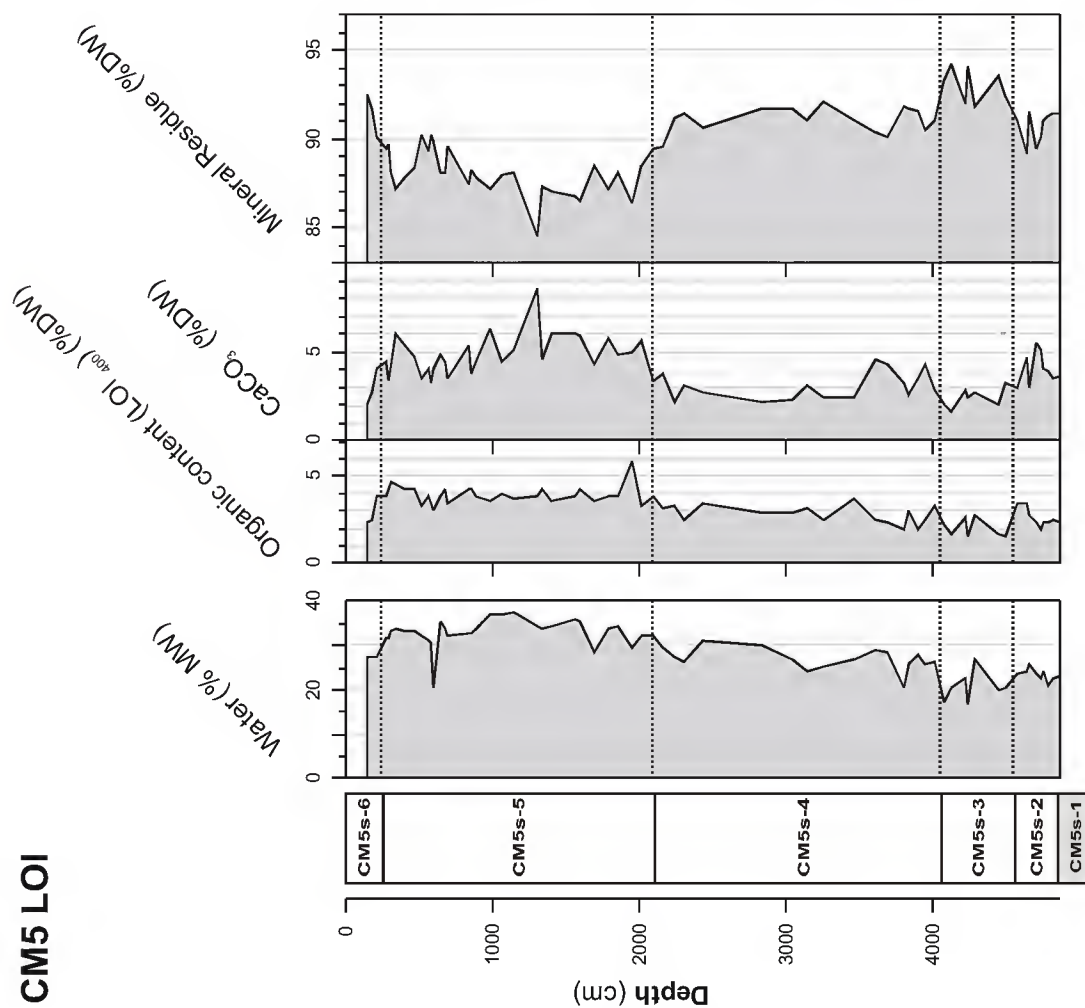


Figure 4.2. Loss-on-ignition results, CM5.

CM5 LOI

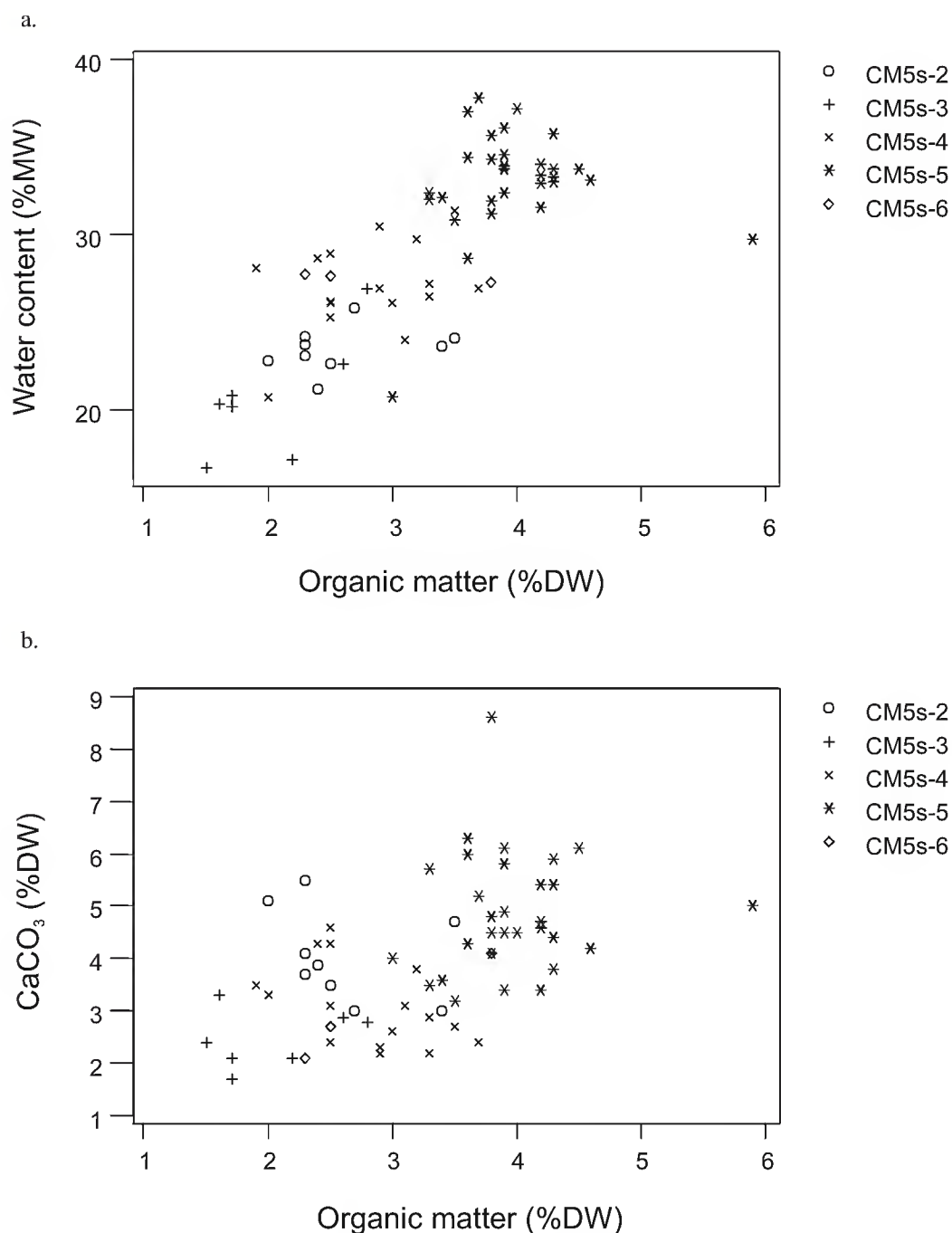


Figure 4.3. Biplots of loss-on-ignition results, CM5.
a. Organic matter vs. water content.
b. Organic matter vs. CaCO₃ content.

CM5 PSD, organics and carbonates removed

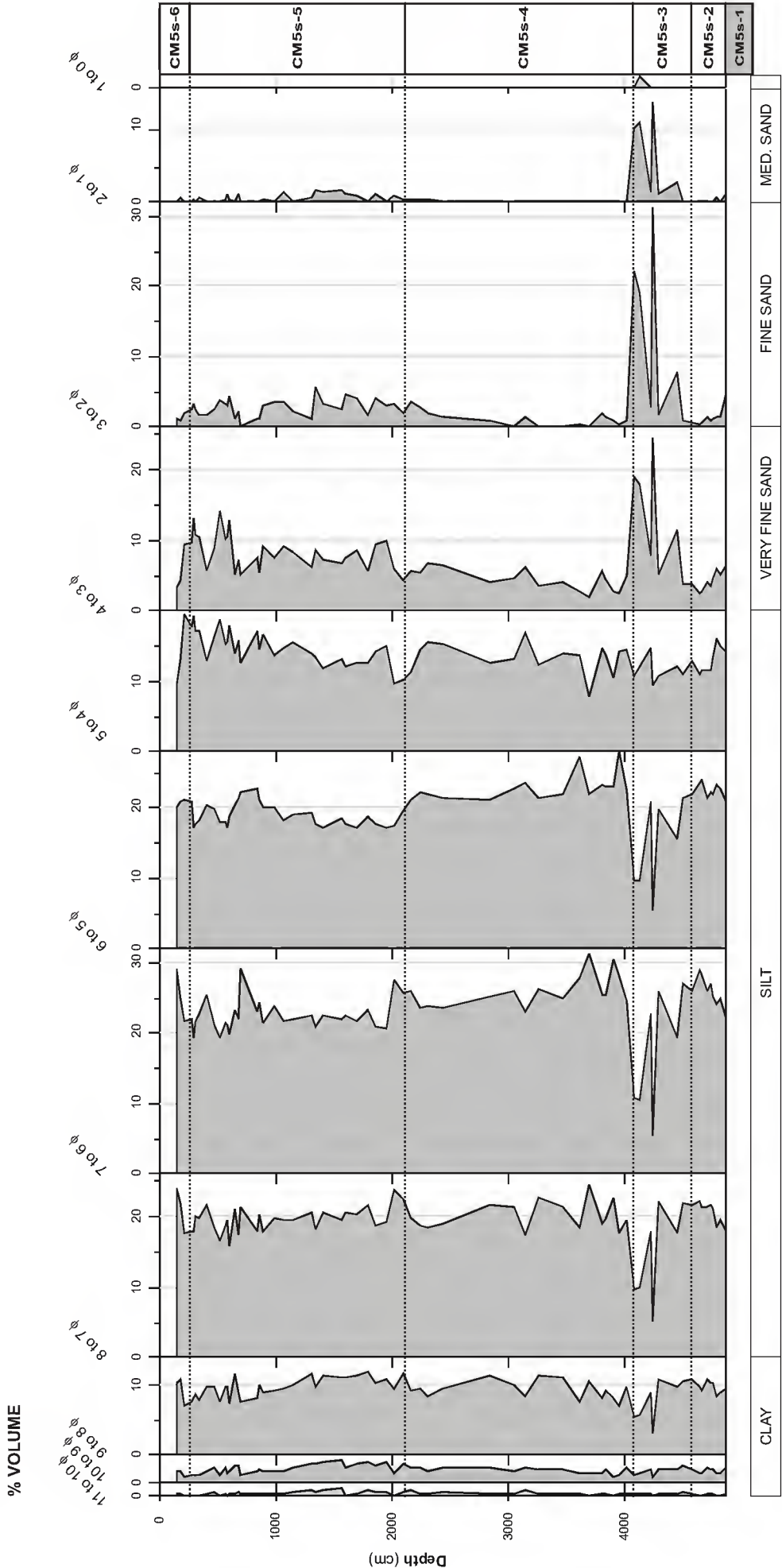


Figure 4.4. Particle size distribution, organics and carbonates removed, CM5.

CM5 PSD, organic and carbonates removed

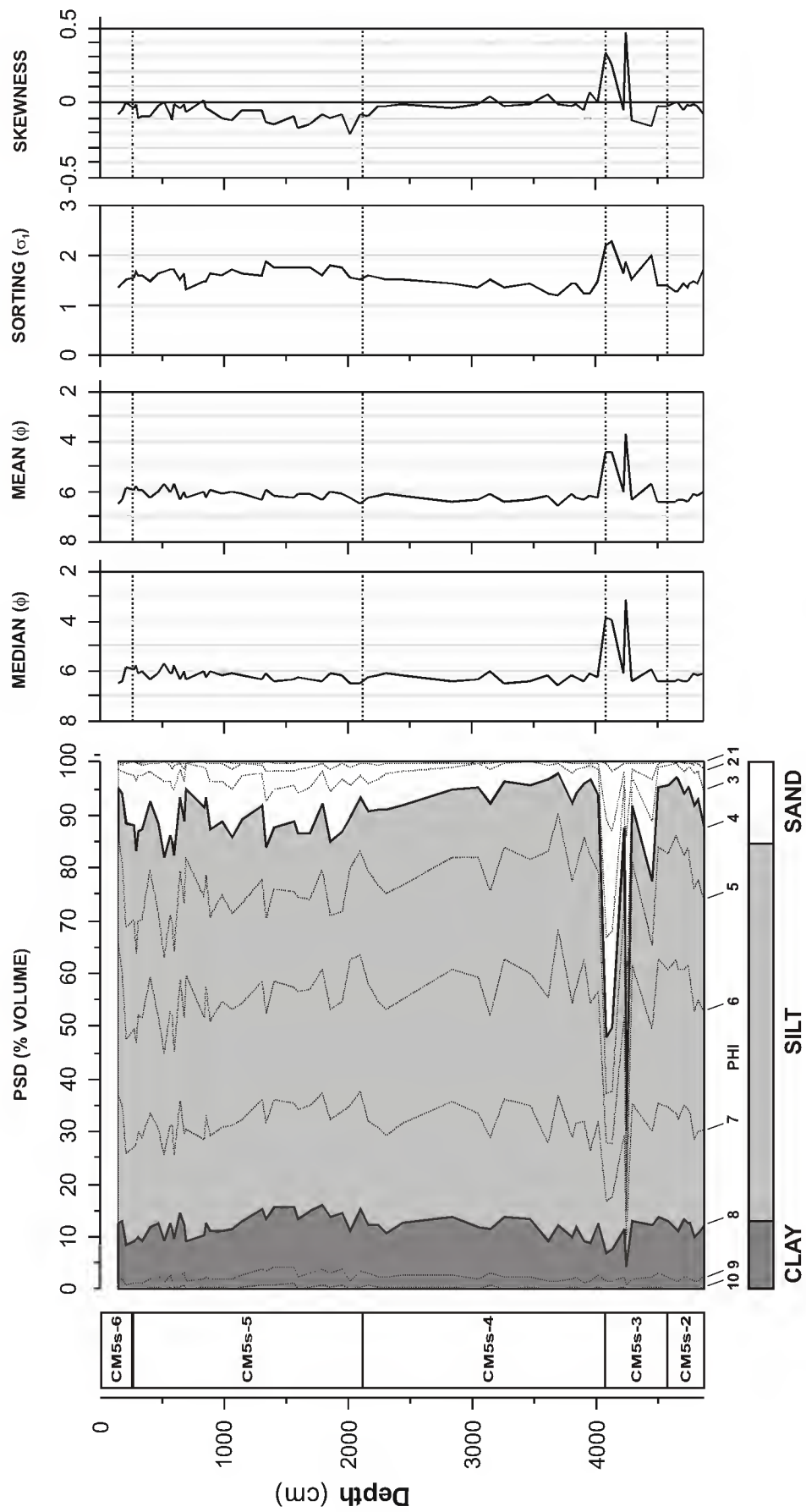


Figure 4.5. Particle size summary, organics and carbonates removed, CM5.

CM5 Magnetic Susceptibility

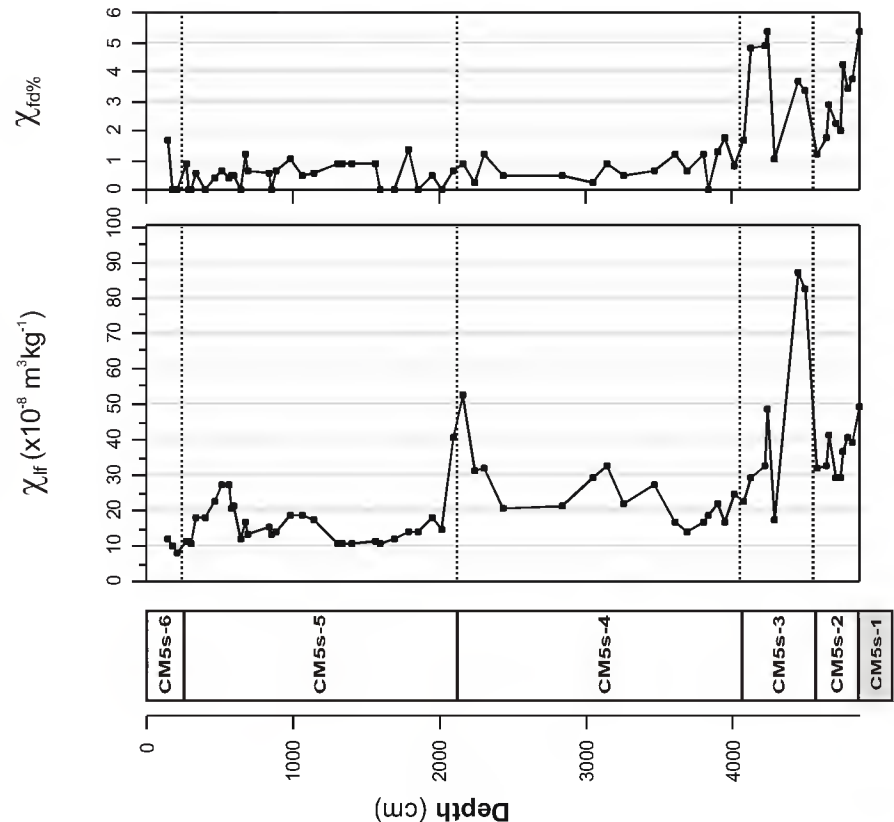


Figure 4.6. Magnetic susceptibility results, CM5

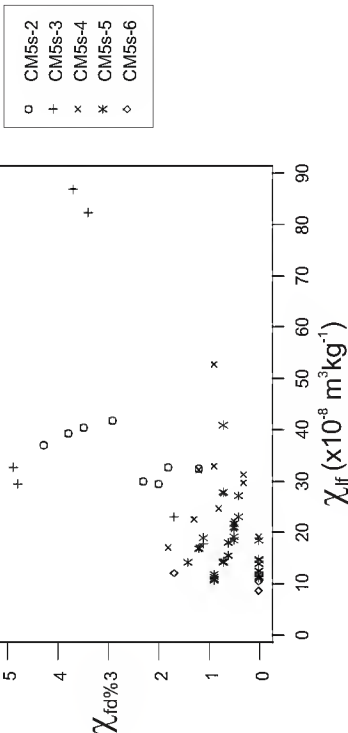


Figure 4.7. Biplot of χ_{lf} vs. $\chi_{fd}\%$, CM5.

CM5 Shell content

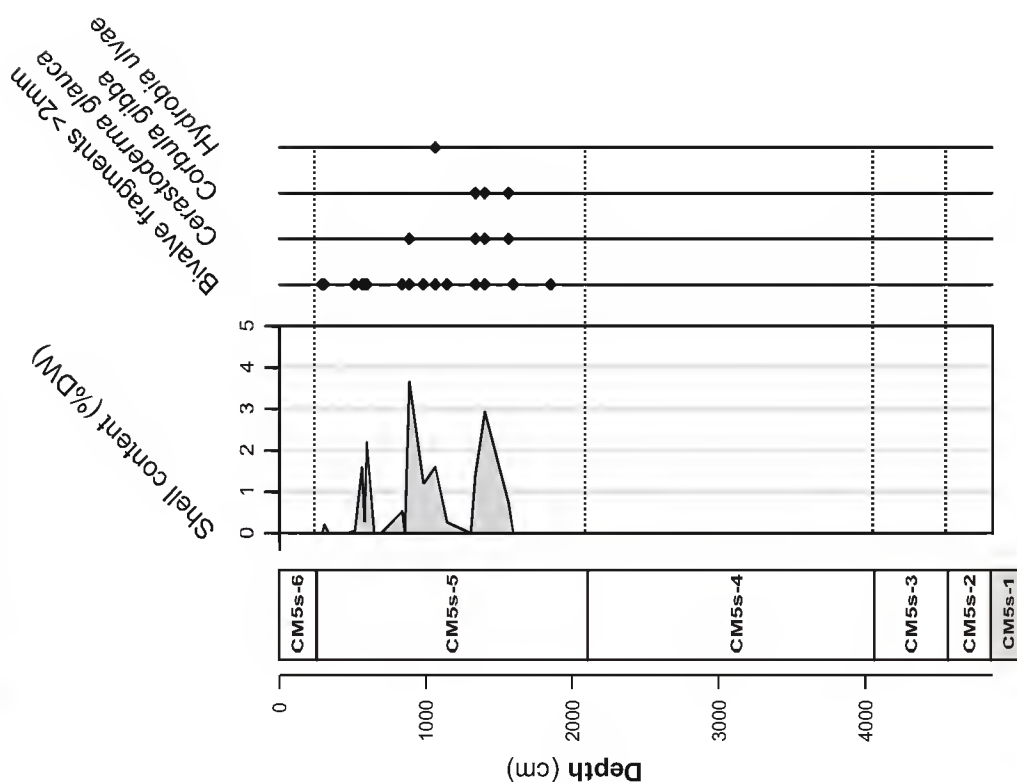


Figure 4.8. Shell content of sediment samples, CM5. Curve shows content of all shell material; black dots indicate presence of bivalve fragments and identifiable intact shells.

P2 ARADE Sediment Summary

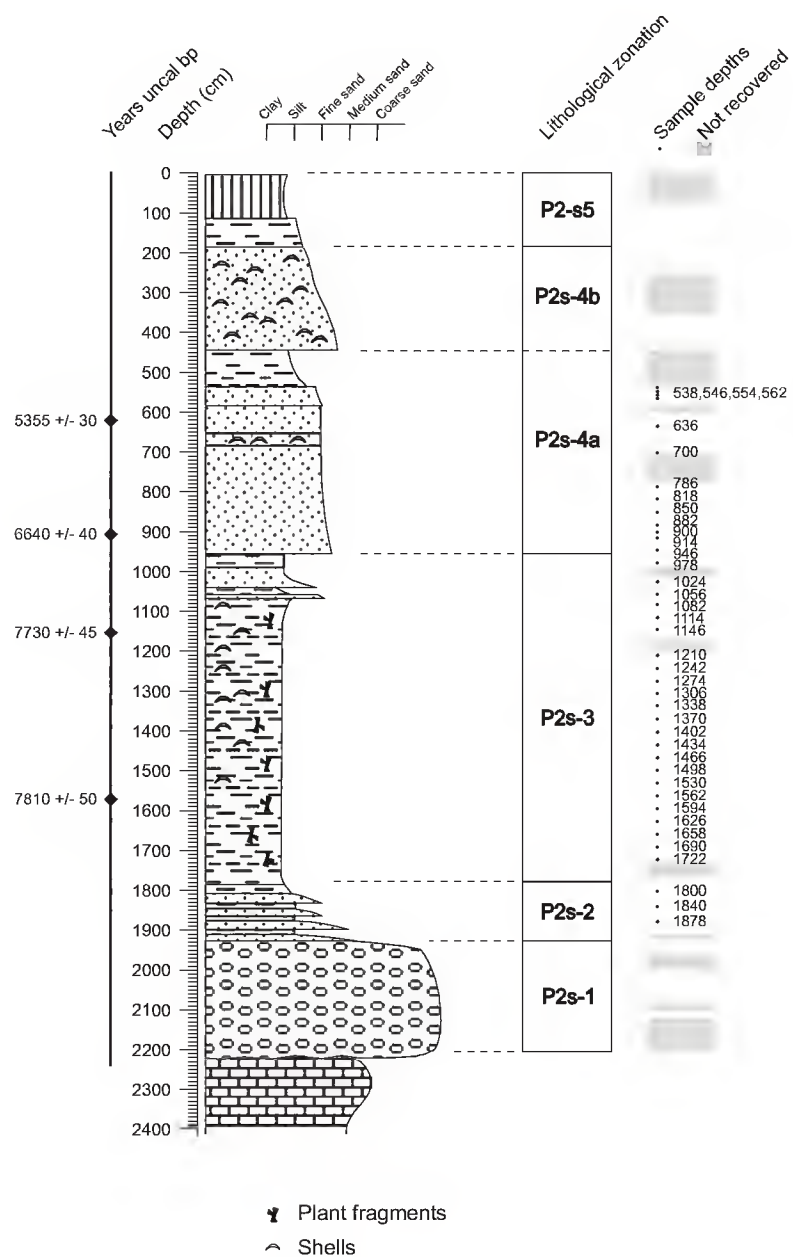


Figure 4.9. Core lithology and sample depths, P2. Depth below surface, approx. 1 m above sea level.

Technique Parameter Range	Loss-on-ignition			Particle size		Magnetic susceptibility	
	Water	Organic 1.0 - 6.4 %	CaCO ₃ 2.0 - 23.2 %	Mineral residue 73.3 - 94.1 %	Description Sand content 3.9 - 81.9 %	χ_{if} 5 - 225x10 ⁻⁸ m ³ kg ⁻¹ $\chi_{fd}\%$ 0 - 5.4 %	Shell
P2s-4a	n/a	Low	Fluctuating, low to high	High	Silty sands and sands	High	Yes
P2s-3	n/a	High	Low to high, increasing	High to low, decreasing	Sandy silts and silts	Low, decreasing	Yes
P2s-2	n/a	High	Low	High	Sandy silts	Low to intermediate	No

Table 4.5. General characterisation of sediment samples based on the results of sediment analyses, core P2

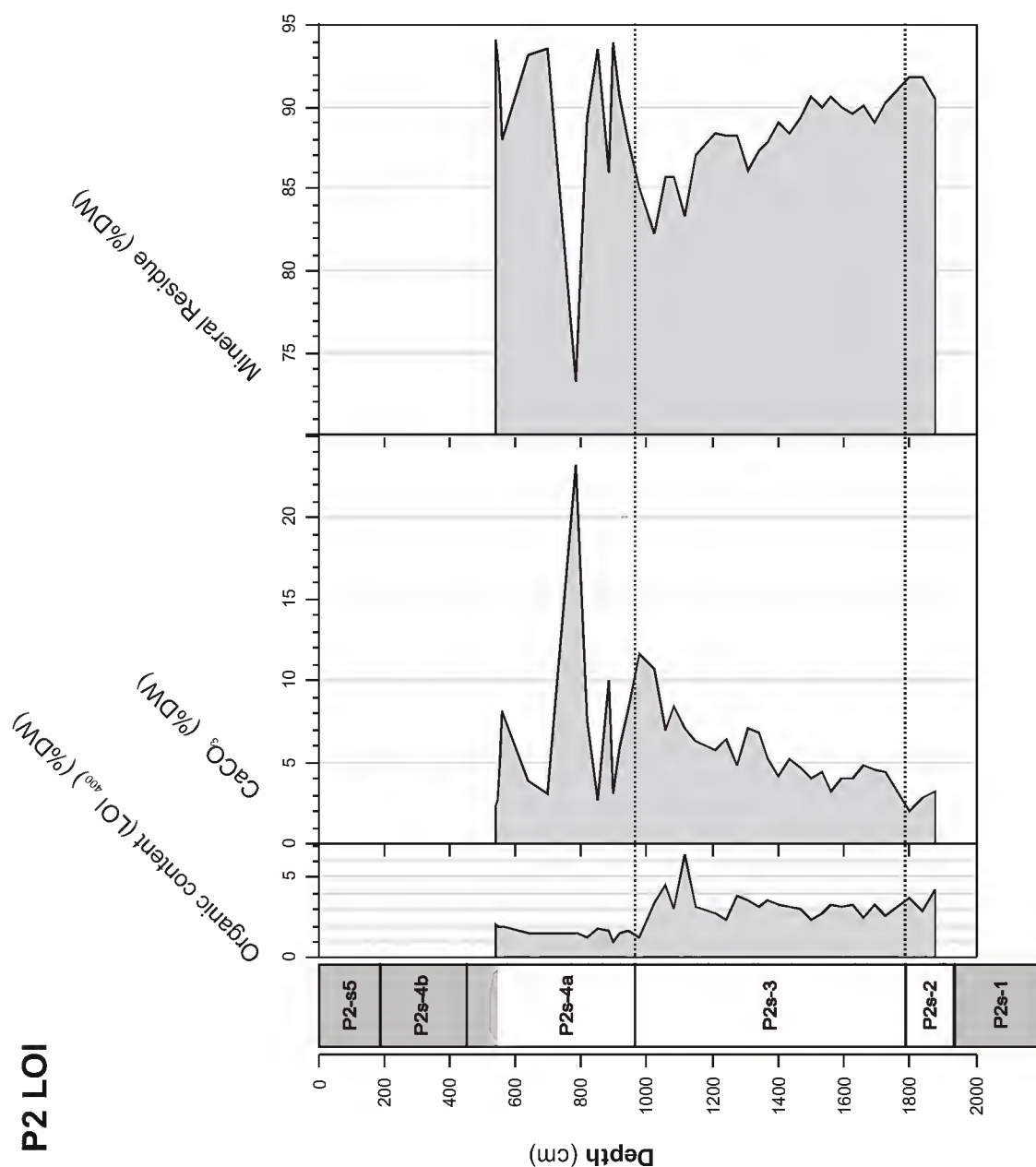


Figure 4.10. Loss-on-ignition results, P2.

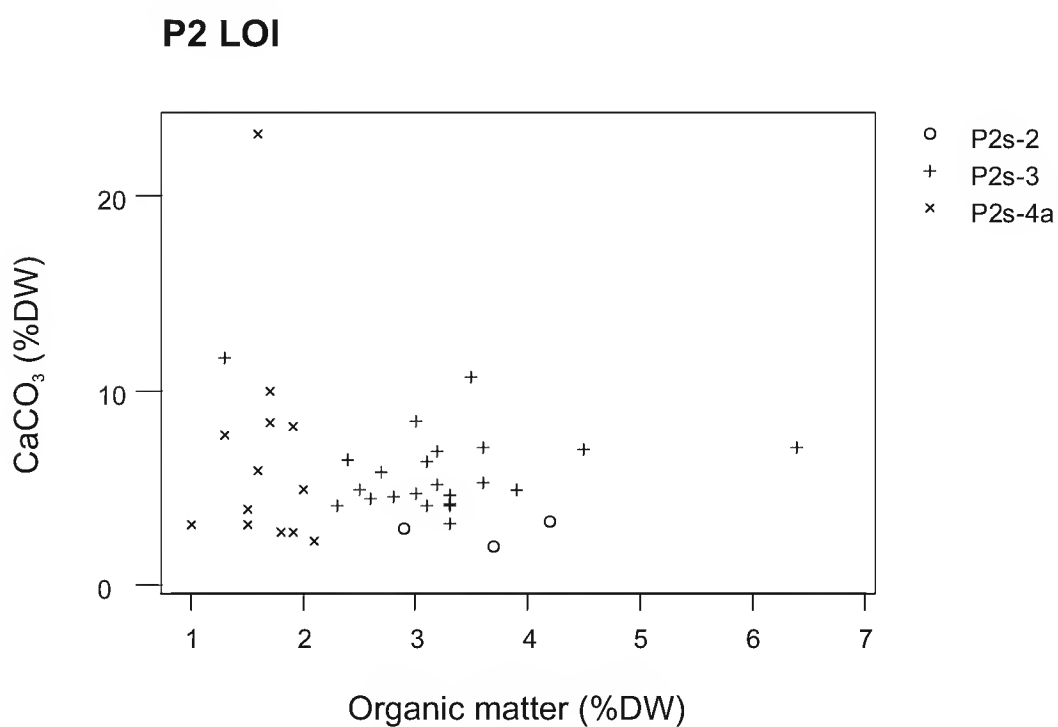


Figure 4.11. Biplot of organic matter vs. CaCO₃ content, P2.

P2 PSD, organics and carbonates removed

% VOLUME

12 to 14 ϕ
10 to 11 ϕ
9 to 10 ϕ
8 to 9 ϕ

7 to 8 ϕ

6 to 7 ϕ

5 to 6 ϕ

4 to 5 ϕ

3 to 4 ϕ

2 to 3 ϕ

1 to 2 ϕ

0 to 1 ϕ

1 to 0 ϕ

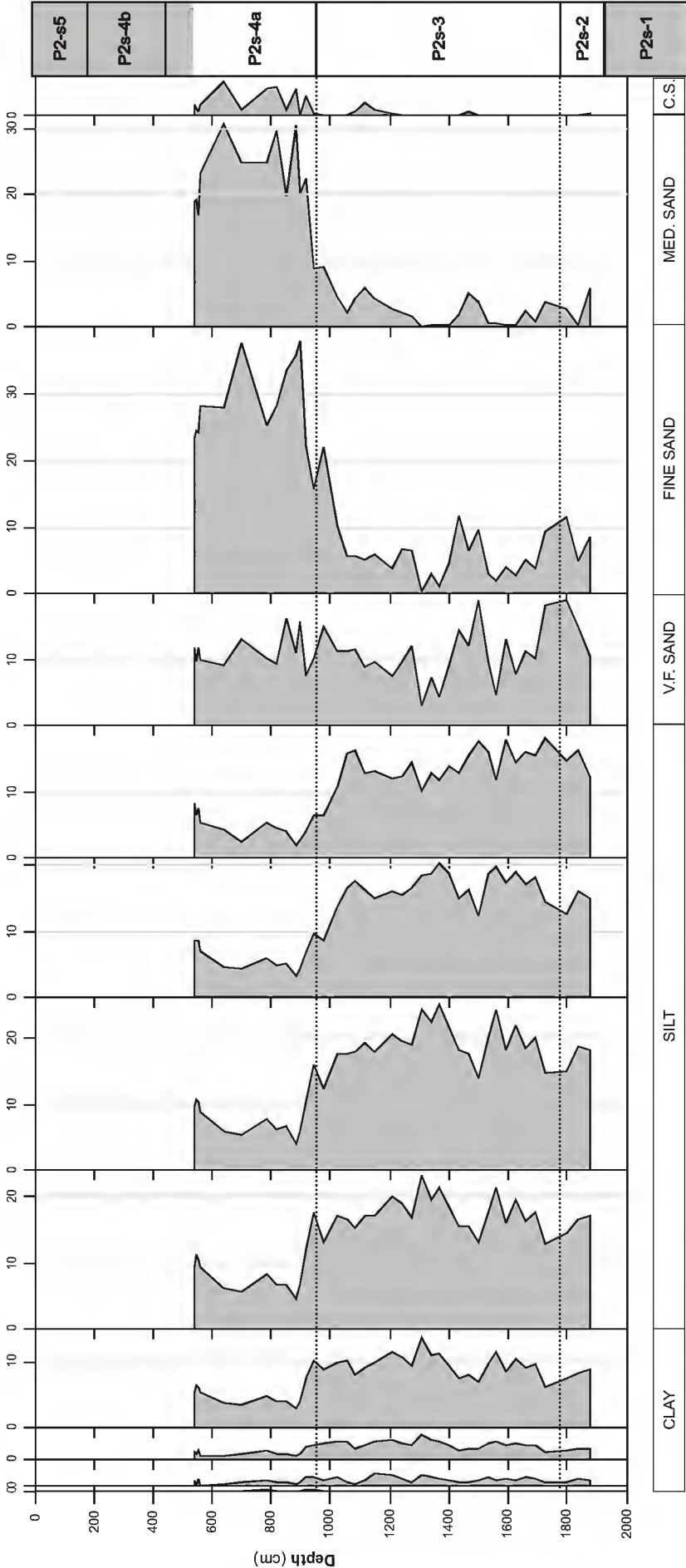


Figure 4.12. Particle size distribution, organics and carbonates removed, P2.

P2 PSD, organic and carbonates removed

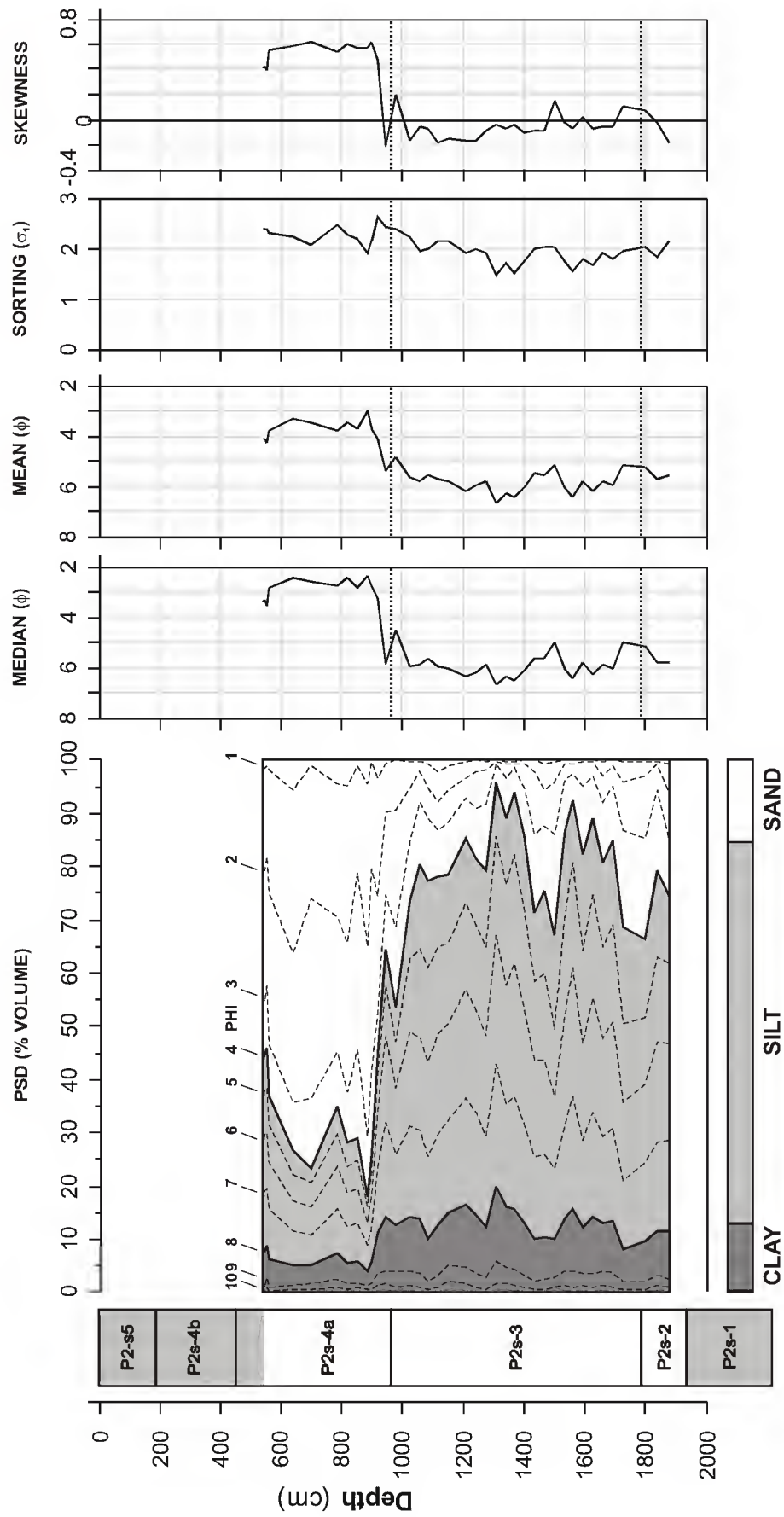


Figure 4.13. Particle size summary, organics and carbonates removed, P2.

P2 Magnetic Susceptibility

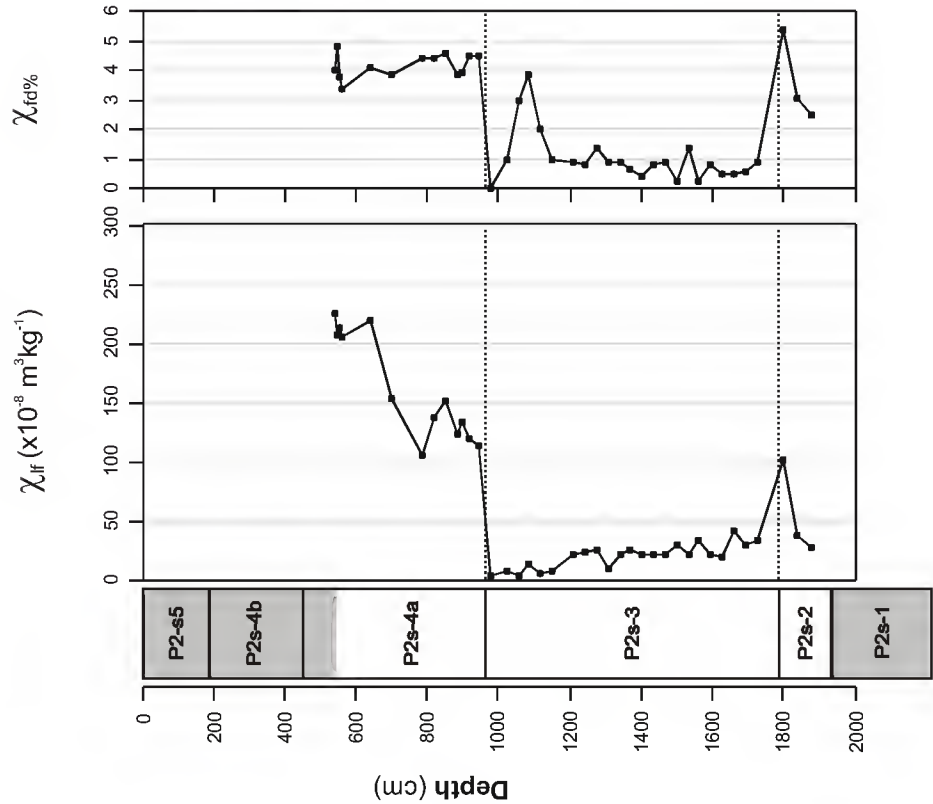


Figure 4.14. Magnetic susceptibility results, P2.

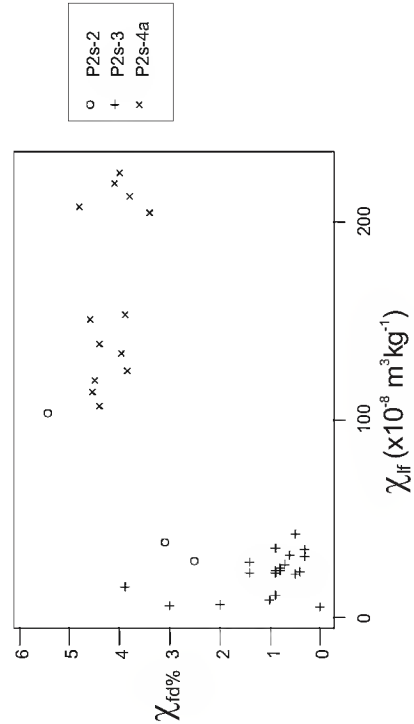


Figure 4.15. Biplot of χ_{lf} vs. $\chi_{fd}\%$, P2.

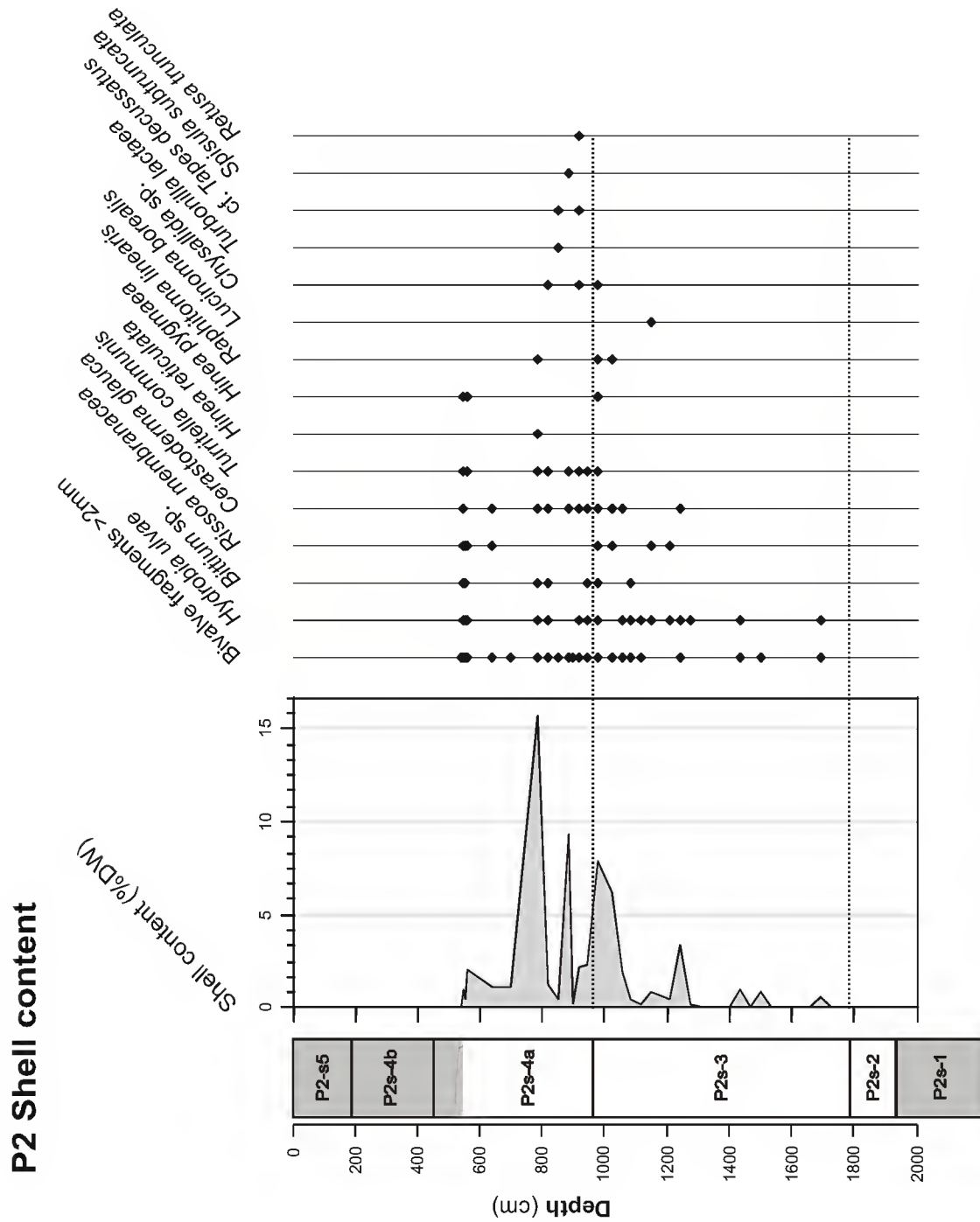


Figure 4.16. Shell content of sediment samples, P2. Curve shows content of all shell material; black dots indicate presence of bivalve fragments and identifiable intact shells.

P5 BOINA Sediment Summary

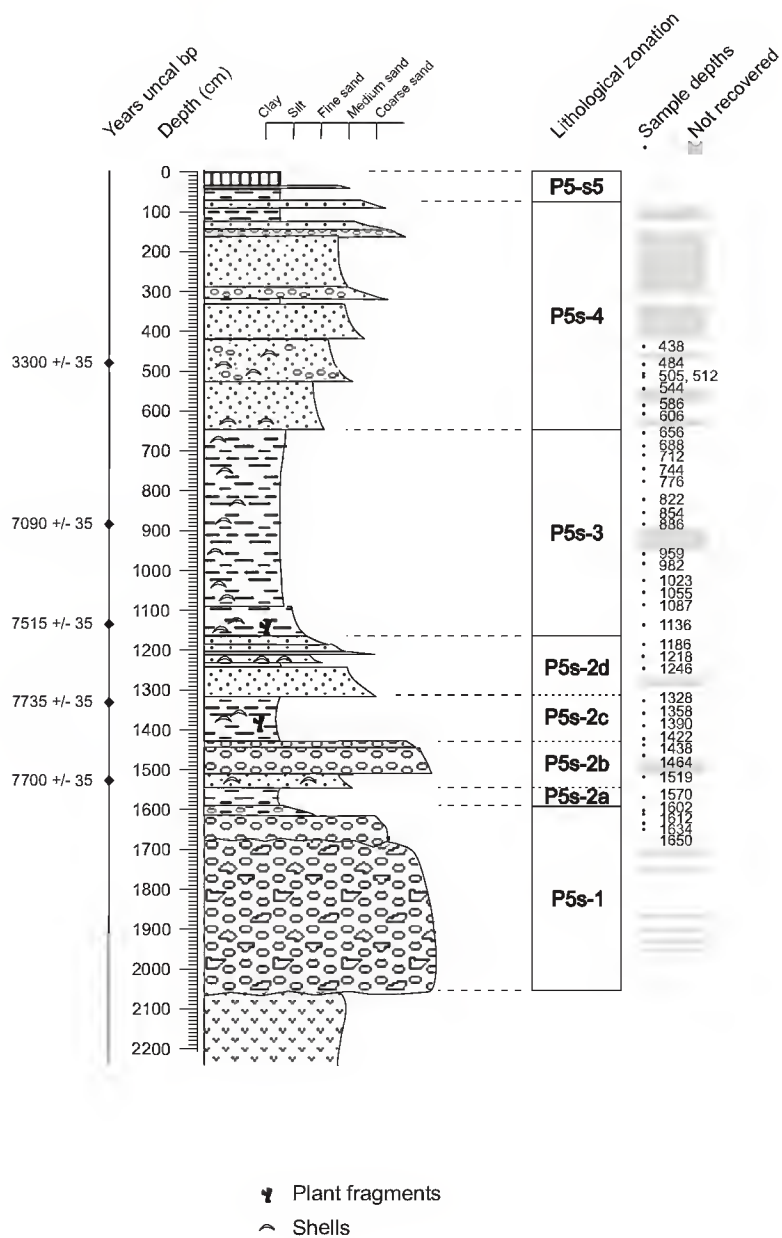


Figure 4.17. Core lithology and sample depths, P5. Depth below surface, approx. 1 m above sea level.

Technique Parameter Range	Loss-on-ignition				Particle size		Magnetic susceptibility		Shell
	Water	Organic 1.0 - 4.6 %	CaCO ₃ 1.6 - 13.8%	Mineral residue 81.5 - 95.3 %	Description	Sand content 2.0 - 69.9 %	Skewness and sorting	χ_{lf} 30 - 620 x 10 ⁻⁸ m ³ kg ⁻¹ χ_{fd} % 1.0 - 6.2 %	
P5s-4	n/a	Intermediate	Low	High	Silty sand, sandy silt, [clayey silt]	Intermediate to high	Very positively to very negatively skewed, very poorly sorted	High >2%	Yes
P5s-3	n/a	Intermediate	High	Low	Clayey silt and sandy silt	Fluctuating low to intermediate	Symmetrical to negatively skewed, poorly to very poorly sorted	Fluctuating, low to intermediate >2%	Yes
P5s-2d	n/a	Low to intermediate	Low	High	Silty sand	High	Negatively to very positively skewed, very poorly sorted	Intermediate >2%	Yes
P5s-2c	n/a	High	High	Low	Sandy silt	Low	Symmetrical to negatively skewed, poorly to very poorly sorted	Intermediate to low, decreasing >2%	Yes
P5s-2b	n/a	Low	Low	High	Sandy silt	High	Symmetrical to negatively skewed, very poorly sorted	Intermediate >2%	Yes
P5s-2a	n/a	Intermediate	Intermediate	Intermediate	Clayey silt	Low	Symmetrical, poorly sorted	High to low decreasing >2%	No
P5s-1	n/a	Low to intermediate	Low to intermediate	High	Sandy silty clay	High	Symmetrical to positively skewed, very poorly sorted	High >2%	No

Table 4.6. General characterisation of sediment samples based on the results of sediment analyses, core P5

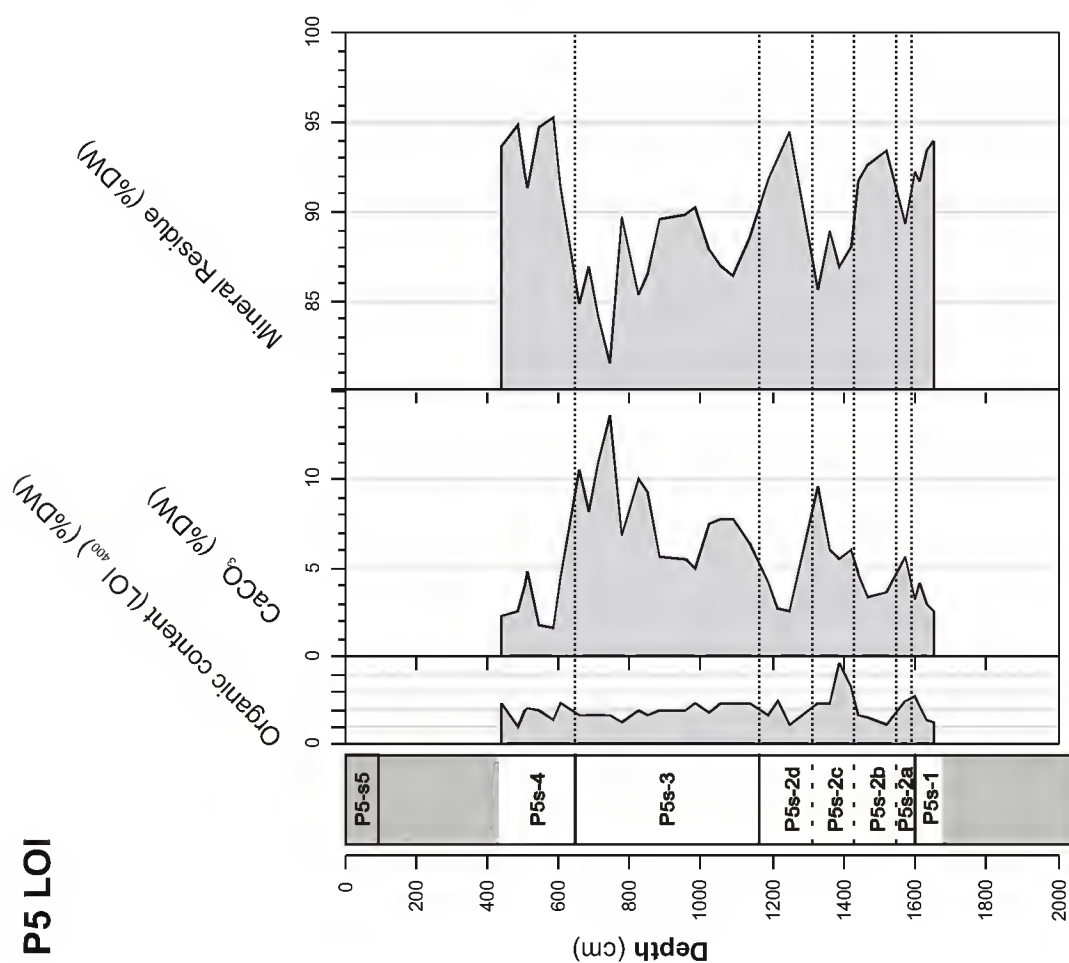


Figure 4.18. Loss-on-ignition results, P5.

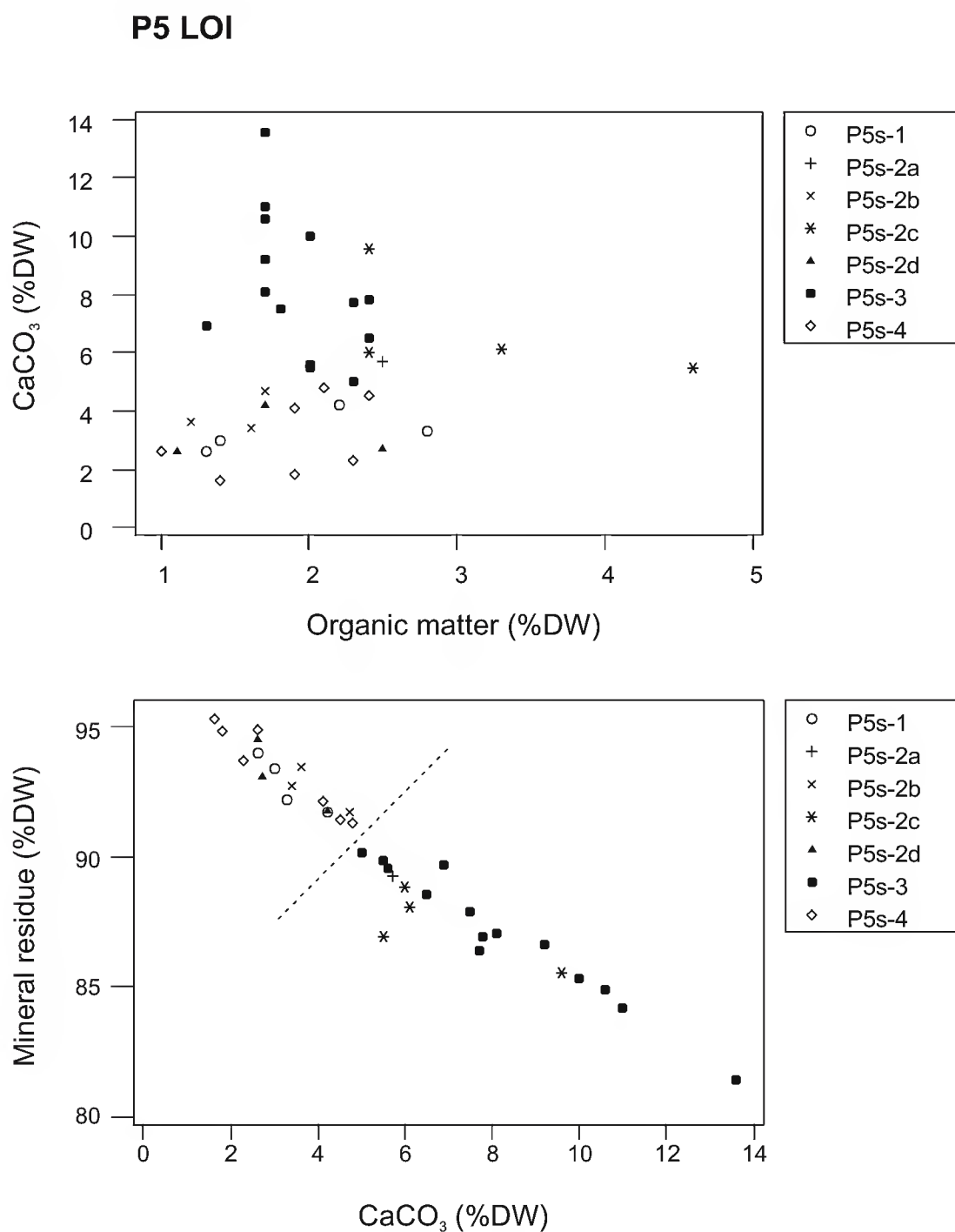


Figure 4.19. Biplots of loss-on-ignition results, P5.
a. Organic matter vs. CaCO₃ content.
b. CaCO₃ content vs. mineral residue.

P5 PSD, organics and carbonates removed

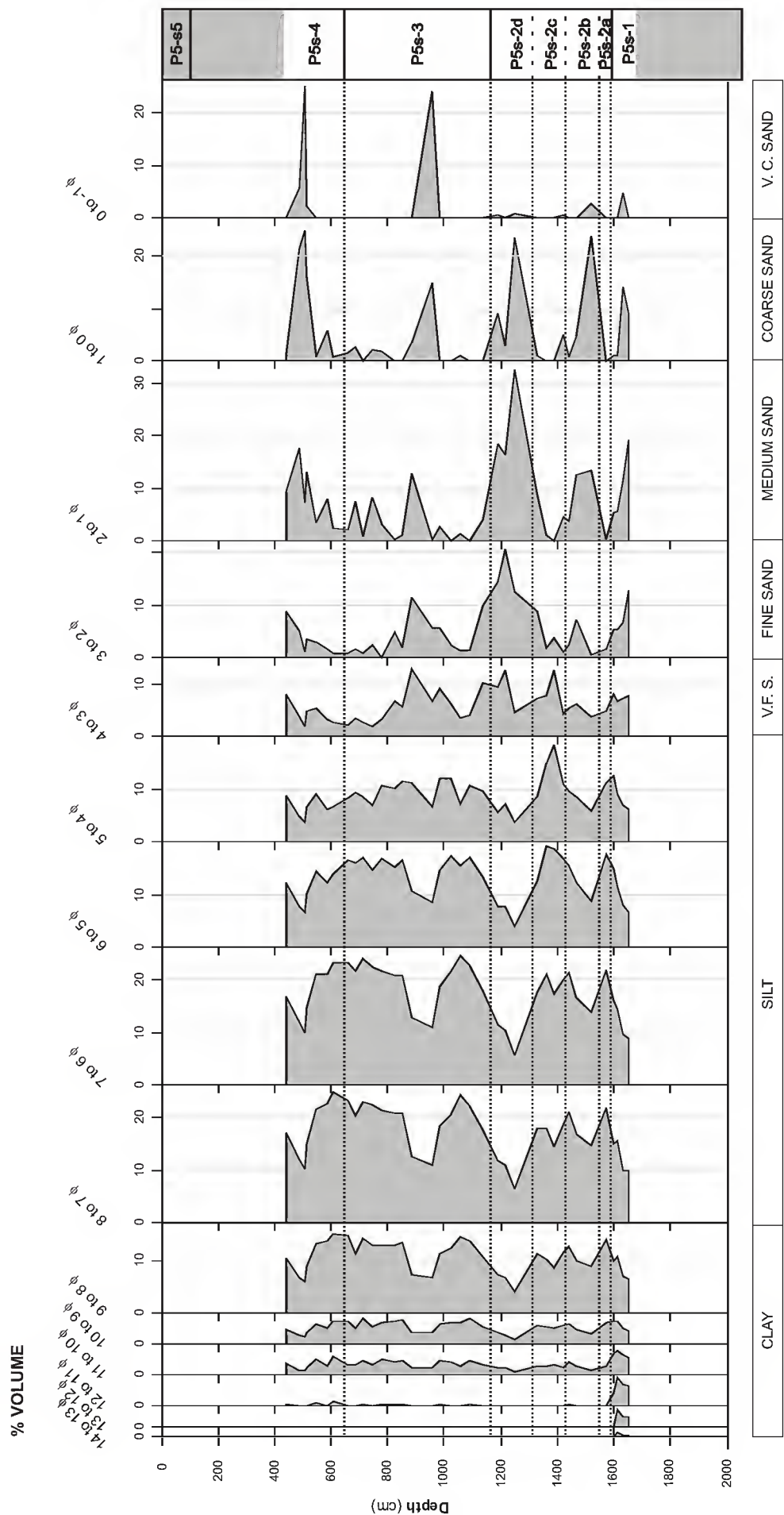


Figure 4.20. Particle size distribution, organics and carbonates removed, P5.

P5 PSD, organic and carbonates removed

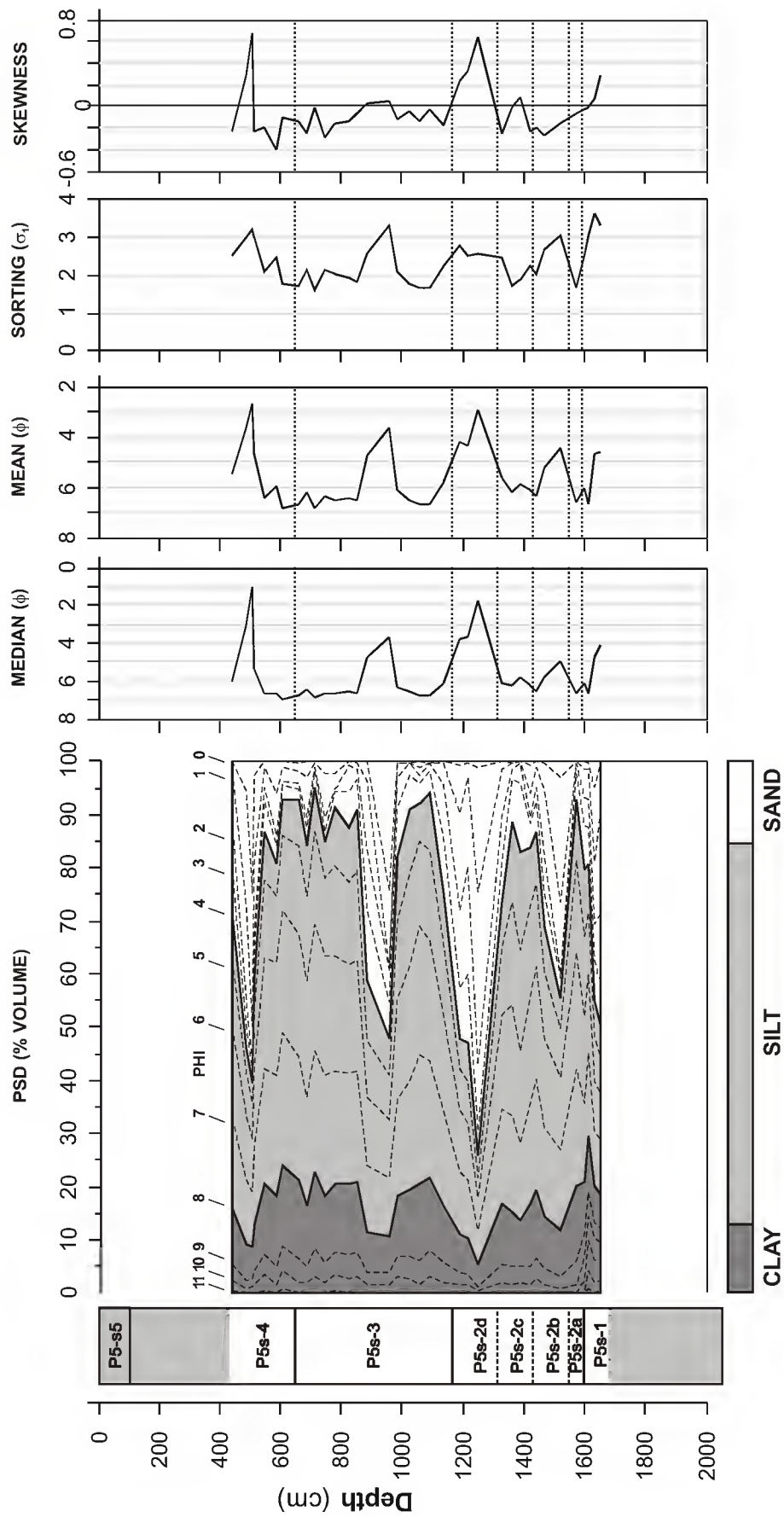


Figure 4.21. Particle size summary, organics and carbonates removed, P5.

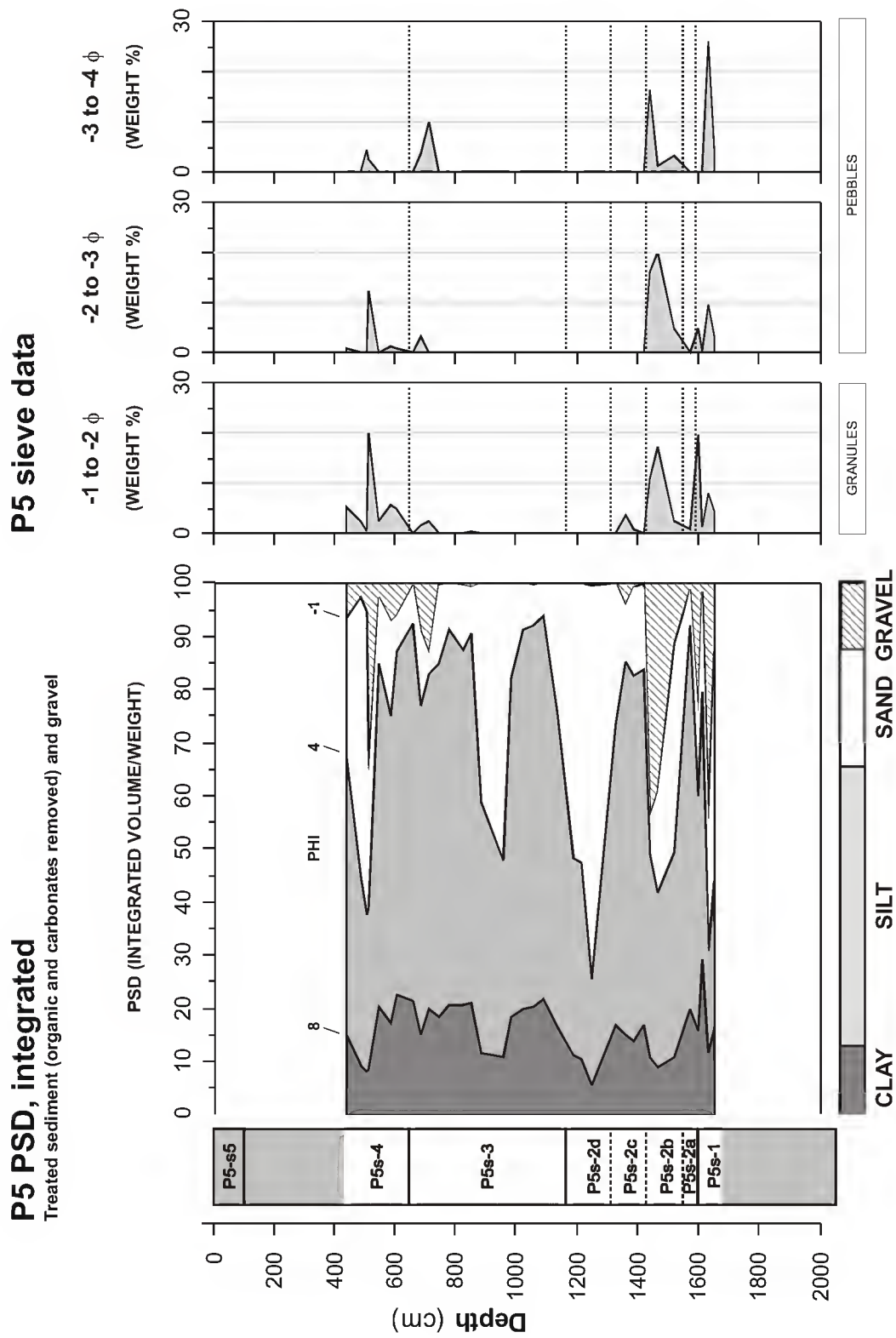


Figure 4.22. Gravel content and integrated particle size data, P5.

P5 Magnetic Susceptibility

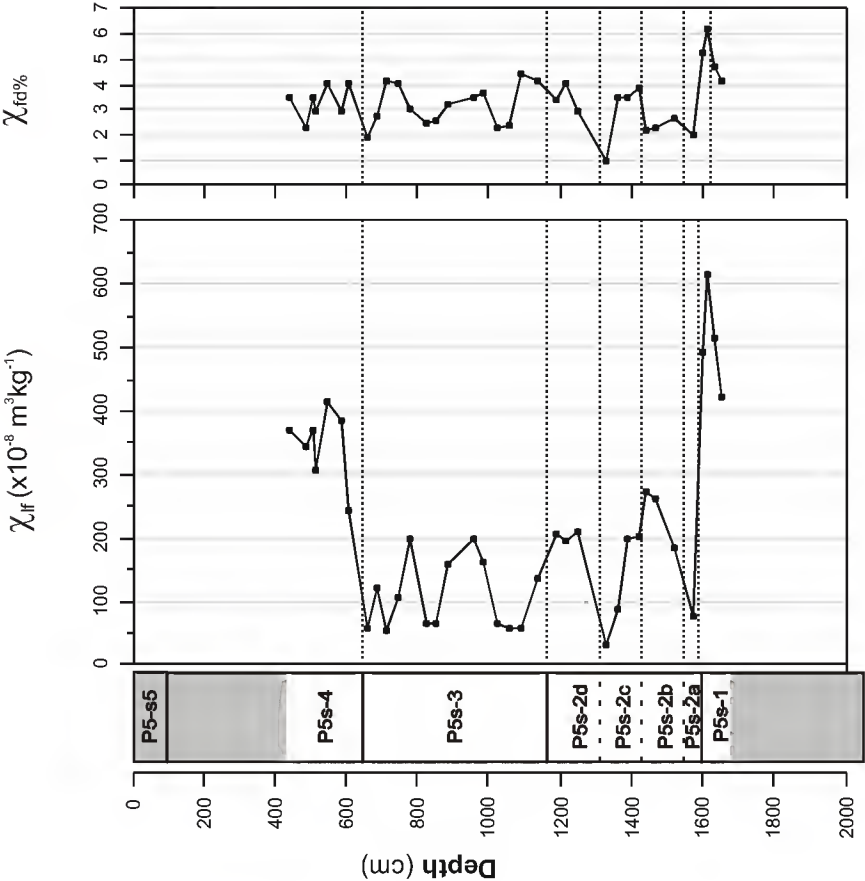


Figure 4.23. Magnetic susceptibility results, P5.

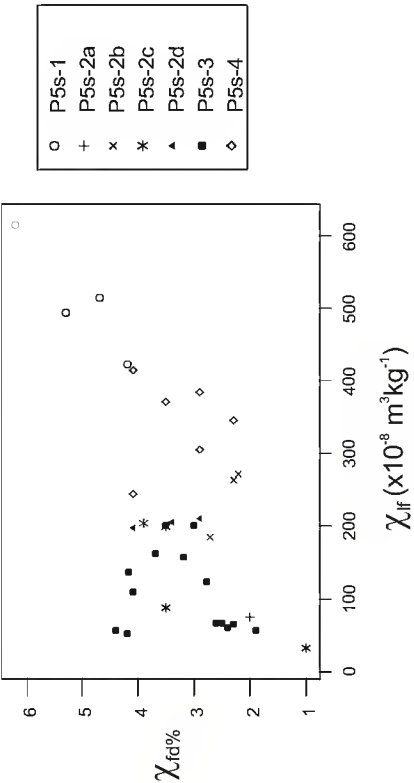


Figure 4.24. Biplot of χ_{lf} vs. χ_{fd} %, P5.

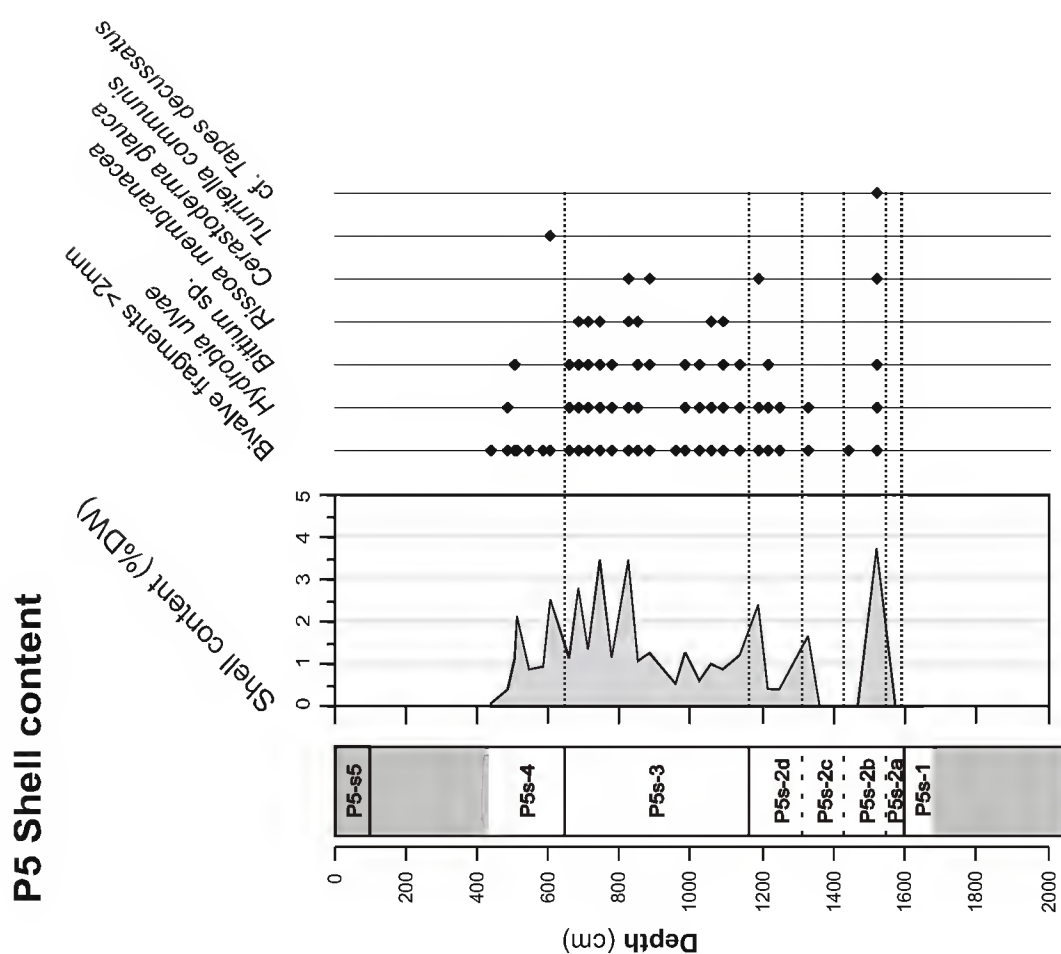


Figure 4.25. Shell content of sediment samples, P5. Curve shows content of all shell material; black dots indicate presence of bivalve fragments and identifiable intact shells.

5 Radiocarbon chronology and age-depth models

5.1 Introduction

Radiocarbon dates provide the means for the development of calibrated age-depth models for sites. From the outset it is noted that the development of radiocarbon chronologies for Holocene estuarine sequences is not straightforward, principally because of the presence of multiple sources of carbon, only some of which provide carbon of the same age as the sediment in which it was deposited (Colman *et al.*, 2002). The sample materials and potential sources of error for the radiocarbon dates are therefore discussed in detail. Age-depth models are proposed, and estimates for sedimentation rate (SR) considered.

Throughout the text, uncalibrated radiocarbon dates are quoted in radiocarbon years before present (^{14}C bp). Calibrated dates are quoted in calibrated years before present (cal BP). In both cases, present refers to 1950 AD.

5.2 Radiocarbon dates

In total, 18 AMS radiocarbon dates are available from the CM5, P2 and P5 sequences (Table 5.1). Four dates were obtained as part of this study to improve the chronology of the CM5 sequence (lab codes IGNS[NZA-]), while the others were obtained by T. Boski of the

Core	Depth (cm)	Material ¹	Laboratory number	$\delta^{13}\text{C}$ (‰, PDB)	^{14}C Age (yr bp)	Cal age, 2σ (yr BP) ²	Median Age ³	Calibration Method ⁴
CM5	333	Shell (<i>Sp</i>)	IGNS[NZA-21412]	-2.9±0.2	3375±39	3130 – 3350	3250	M
CM5	579	Shell (<i>V</i>)	KIA 15211	n/a	4295±35	4300 – 4520	4420	M
CM5	890	Shell (<i>Cg</i>)	IGNS[NZA-21413]	0.2±0.2	6764±45	7200 – 7400	7300	M
CM5	1085	Shell (<i>C</i>)	KIA 15213	n/a	4095±30	4020 – 4260	4140	M
CM5	1345	Shell (<i>V</i>)	KIA 15212	n/a	7585±35	7960 – 8140	8040	M
CM5	1775	Shell (<i>C</i>)	KIA 15210	n/a	7725±45	8060 – 8310	8200	M
CM5	2095	Wood	IGNS[NZA-21414]	-25.3±0.2	8256±55	9030 – 9420	9240	T
CM5	4270	Wood	IGNS[NZA-21415]	-25.5±0.2	10273±66	11770 – 12370	12050	T
CM5	4767	Wood	Beta-137110	-25.7	10990±40	12860 – 13030	12920	T
P2	615	Shell (x)	IRPA-13237	n/a	5355±30	5630 – 5840	5710	M
P2	903	Shell (x)	IRPA-13239	-3.12	6640±40	7050 – 7260	7180	M
P2	1150	Shell (x)	IRPA-13238	-2.22	7730±45	8070 – 8320	8210	M
P2	1570	Shell (x)	IRPA-13236	n/a	7810±50	8170 – 8370	8280	M
P5	481	Shell (x)	IRPA-13234	-2.4	3300±35	3010 – 3270	3150	M
P5	885	Shell (x)	IRPA-13233	-1.21	7090±35	7490 – 7650	7570	M
P5	1135	Shell (x)	IRPA-13232	-0.97	7515±35	7900 – 8080	7970	M
P5	1330	Shell (x)	IRPA-13235	-1.83	7735±35	8110 – 8310	8210	M
P5	1528	Shell (x)	IRPA-13231	-2.48	7700±35	8050 – 8280	8170	M

Shell i.d. = *Sp*, *Scrobicularia plana*; *V*, *Venerupis* sp.; *Cg*, *Cerastoderma glaucum*; *C*, *Cerastoderma* sp.; x, unidentified.

² Calibrated ages for the 95.4% confidence interval, rounded to the nearest 10 years

³ Calendar age estimate based on the median probability of the probability distribution

⁴ Calibration using CALIB 5.0 (Stuiver *et al.*, 1993), using:

M = Marine04 (Hughen *et al.*, 2004), $\Delta R = 0$

Table 5.1. Radiocarbon dates from cores CM5, P2 and P5.

Universidade do Algarve prior to this study. The radiocarbon dates provide the basis for the construction of age-depth relationships and sedimentation histories for the three sites.

5.2.1 Sample material and sources of error

Two distinct sample materials have been used for dating the sequences studied here — wood and estuarine shell — which present different characteristics in terms of carbon sources and pose different problems in terms of potential sources of error and accurate calibration.

5.2.1.1 Wood

In common with other estuarine infill sequences where the deeper sections tend to have more material of fluvial and terrestrial origin (e.g. Chesapeake Bay (Colman *et al.*, 2002)), wood fragments provide dating material for the lower part of the CM5 core. The carbon content of wood is derived from atmospheric carbon dioxide through photosynthesis. The initial radiocarbon (^{14}C) content will reflect atmospheric levels at the time of death of the organism. The terrestrial, atmospheric carbon source is also clearly reflected in stable carbon isotope ($^{12}\text{C}/^{13}\text{C}$) composition. Photosynthesis produces a strong fractionation of stable carbon isotopes (^{12}C and ^{13}C), resulting in depleted ^{13}C isotope values relative to atmospheric CO_2 (Libes, 1992: 579). Values for $\delta^{13}\text{C}$ around -25 ‰ are typical of terrestrial C_4 plants, and are observed in the wood samples on which radiocarbon determinations were made (Table 5.1). As organic material of terrestrial origin, wood is not subject to reservoir effects associated with marine or lacustrine environments.

While wood may provide an unambiguous source of terrestrial organic matter, taphonomic factors related to transport, storage and reworking may constitute a significant source of error. The radiocarbon age of a wood fragment will reflect the time of death or separation from the plant. An unknown period of time will have elapsed between organism death and final deposition within the estuarine setting, during which storage in catchment soils, hillslope colluvium or floodplains may have occurred. Therefore, radiocarbon dates on wood may be older than the time of sediment deposition. Erroneously old dates may also result from the “old-wood” effect, arising from the relative age of heartwood in long-lived trees. This effect has been noted, for example, to be important in the dating of charcoal from archaeological sites in Portugal (Zilhão, 2001). For these reasons, the moderate or “intermediate” level of confidence in the reliability of wood dates noted for floodplain delta environments (Brown & Pasternack, 2004) is shared here. Nevertheless, wood dates provide a maximum age of sediment deposition.

Further information on regarding the species identification or source of the wood is not available. Bearing in mind the requirements of wood identification, namely the exposure of multiple sections (Barefoot & Hankins, 1982), the small size of the wood fragments submitted for radiocarbon dating precluded identification.

5.2.1.2 Shell

The bulk of dates available from the three sites are from shell. Shell identifications, where obtained, indicate typical estuarine species, such as *Scrobicularia plana* and *Cerastoderma glaucum*; however, identifications are not available for all samples. Radiocarbon dates on shell often underpin estuarine chronologies and the dating of coastal morphological features, e.g. Dabrio *et al.* (2000). Shells have a number of advantages in terms of dating, being macroscopic, easy to handle, often abundant in many types of estuarine sediment, and identifiable. In an evaluation of dating materials available from Holocene sedimentary sequences of the Chesapeake Bay (Colman *et al.*, 2002), biogenic carbonates (including shells and foraminifer tests) were considered the most reliable material for radiocarbon dating. However, a number of attendant problems must be recognised in the dating of marine shells, particularly from estuarine settings. These may be divided broadly into reservoir effects and factors influencing sample integrity, such as burrowing and reworking.

Reservoir effects derive from the different effective ages of different carbon sources due to relative deficits or enrichment in ^{14}C . Biogenic carbonate in calcareous shells and tests is derived primarily from the ambient pool of dissolved inorganic carbon (DIC) at the growth site, notably through the precipitation of bicarbonate ions in marine water (HCO_3^-) (Libes, 1992). The initial radiocarbon content of marine shells should therefore be determined by seawater values during the period of shell growth. Open ocean water typically has a ^{14}C deficit compared with the atmosphere, constituting a global reservoir effect of around 400 years (Stuiver *et al.*, 1998). The global reservoir effect can easily be compensated for by subtracting the reservoir age from the measured radiocarbon age; this process is incorporated, for example, in marine calibration datasets. However, the marine reservoir effect is known to vary both geographically and temporally due to variation in the locations and rates of

coastal upwelling of ^{14}C -depleted, deep ocean water, with serious consequences for the precision of radiocarbon chronologies based on the dating of marine fossils (Lowe & Walker, 2000). In the estuarine environment, these complications are compounded by the mixing of marine and river water, which can result in localised reservoir effects which vary significantly from regional averages (Stuiver & Braziunas, 1993; Heier-Nielsen *et al.*, 1995).

The regional offset (ΔR) in ^{14}C ages from the global average may be determined by the radiocarbon dating of samples of known age, for example museum specimens. Ideally, regional correction factors will have been determined close to the study site, and paired dates on marine and terrestrial samples obtained from within the sedimentary sequence. These observations permit the identification of both geographic deviation from the global reservoir effect and temporal in ^{14}C offsets at that location. In the estuarine setting, however, decisions regarding the appropriate correction factors are not straightforward; these are discussed in the following section.

The apparent age of biogenic carbonates may be influenced by the contribution of carbon from sources other than marine water. On the one hand, the pool of DIC in ambient waters may include older carbon from decaying organic matter diffusing from sediment pore water (Colman *et al.*, 2002). In this situation, the radiocarbon content of shell may be older than the ambient water. On the other hand, a proportion of shell carbonate, at least for some species, may be derived not from ambient DIC, but from metabolic carbon from food sources, which may include organic matter of both terrestrial and marine origin (Tanaka *et al.*, 1986). Terrestrial carbon could affect the apparent age of the carbonate. Stable carbon isotope ratios may provide indications of the likelihood of errors derived from carbon inputs from these sources. Stable carbon isotope values for marine shell typically reflect ^{13}C -enriched or isotopically heavy seawater values. As significant fractionation of carbon isotopes does not occur during the precipitation of biogenic carbonates, $\delta^{13}\text{C}$ values should be close to those of marine water (+2 ‰) (Libes, 1992: 575). Where shells derive a significant carbonate component from pore water DIC or from metabolic carbon of terrestrial origin,

this should be reflected in distinctively light $\delta^{13}\text{C}$ values (Colman *et al.*, 2002). For those samples where $\delta^{13}\text{C}$ has been measured in this study, isotopically heavy, near zero values for $\delta^{13}\text{C}$ for the samples indicate a predominantly marine source of carbon.

A further potential source of error are “hard water effects,” resulting from the ambient presence of dissolved carbonates of lithological origin. Radiocarbon dates on shell may be erroneously old due to incorporation of lithological carbonates containing no ^{14}C (infinite apparent age), either during shell growth or through post-depositional contamination. These effects may be of considerable importance when dating lacustrine molluscs in limestone regions (e.g. Ioannina, northwest Greece (Lawson *et al.*, 2004)) or marine molluscs from calcareous coastlines (Anderson *et al.*, 2001). Hard water errors are considered relatively unlikely in this study due to the low carbonate content of the sediments and the dominance of non-calcareous upstream catchment lithologies for the sites.

In addition to the described reservoir effects, other potential sources of error relate to sample integrity, namely burrowing and reworking. Some species of shell fauna burrow beneath the sediment surface. Burrowing on the order of centimetres to tens of centimetres is especially typical of many species inhabiting tidal mudflats and marshes, such as *Cerastoderma*. Dating a deeply burrowed shell would produce a radiocarbon date younger than the age of deposition of the surrounding sediment. However, where sedimentary sequences are characterised by rapid sedimentation, burrowing is unlikely to produce distinctly anomalous results; rather burrowing might result in a slight increase in the scatter of radiocarbon results. The extent of burrowing and other types of bioturbation — best detected through the study of X-ray radiograph images (e.g. Borrego *et al.*, 1995) — should be taken into account during sample selection.

Reworking presents an opposite problem, bringing older material into contact with younger sediments, and may be responsible for anomalously old ages. In general, shells are fairly robust and many types may survive multiple phases of transport and redeposition. This

problem is likely to be most serious in dynamic sedimentary settings, for example near fluvial or estuarine channels or where wave energy is high.

To some extent, reworking may be guarded against during sample selection. Intact, well preserved shells showing minimal abrasion should be dated in preference to scattered shell fragments or highly degraded specimens. The type of deposit should also be considered; detrital shell material in channel fills, for example, is likely to be less reliable than *in situ* shells from marsh or tidal flat deposits. Within radiocarbon dated sequences, anomalously old ages due to reworking should be identifiable in age-depth plots. Where samples present a systematic, monotonic series of increasing age with depth, reworking is usually not considered significant. However, reworking may be responsible for scatter in radiocarbon ages, which may or may not be detectable.

5.2.2 Calibration

5.2.2.1 Rationale

Radiocarbon dates and age-depth models are presented in calibrated years before present. The use of calibrated ages is preferred, partly for the general reason that they permit inter-study comparison between palaeoenvironmental records based on a variety of chronological methods (e.g., varve-counts, dendrochronology), but also for the specific reason that time-dependent age differentials between radiocarbon and calendar ages can produce misleading impressions of the duration of episodes and rates of change even when working solely within a radiocarbon-based chronology (Bartlein *et al.*, 1995). For example, one of the main points of interest arising from the dating of estuarine infill sequences is the estimation of sedimentation rates. Sedimentation rates based on uncalibrated radiocarbon-ages can be misleading, producing over-estimates for the timespan under investigation here due to the effectively shorter duration of a radiocarbon year compared with a calendar year.

5.2.2.2 Calibration methods

Radiocarbon dates were calibrated using the software program CALIB (Stuiver & Reimer, 1993; version 5.01). Dates on wood fragments were calibrated using the IntCal04 dataset (Reimer *et al.*, 2004). For dates on biogenic carbonate from shells, the Marine04 calibration

dataset (Hughen *et al.*, 2004), incorporating a time-dependent global marine reservoir correction of ~ 400 years, was used. The use of the marine calibration for the shell dates is supported by near-zero $\delta^{13}\text{C}$ values (at least for those samples where this variable is recorded).

The choice of regional offset (ΔR) for the samples is not straightforward. Through the radiocarbon dating of museum specimens, Soares (1993) identified the influence of the upwelling of ^{14}C -depleted ocean water on the Portuguese coast, with an average ΔR value for the entire Portuguese margin of 256 ± 29 ^{14}C yr, or 235 ± 35 ^{14}C yr for the southern coast (37°N). Considerable variability was observed between geographic locations; for example, a ΔR value of 345 ± 90 ^{14}C yr was obtained at Portimão, and a ΔR value of 5 ± 70 ^{14}C yr at Vila Real de San Antonio at the mouth of the Guadiana. Soares also identified temporal variation in ΔR values during the Holocene, observing a *c.* 250 ^{14}C yr reduction in ΔR value for the earlier part of the Holocene (prior to 2000 ^{14}C bp). This reduction which would indicate a reservoir age close to the global average. For this reason, calibration with $\Delta R=0$ (global average reservoir correction) is considered the best choice in light of regional information.

Nevertheless, some uncertainty surrounds the choice of appropriate reservoir correction for carbonate materials from an environment where the mixing of marine and river water occurred, and where complex hydrological changes will have occurred over time, related to the Holocene process of estuarine expansion and subsequent infill. In order to gain an impression of the age uncertainty associated with reservoir correction choice, the shell dates were also calibrated with the marine dataset using ΔR values of 235 ± 35 ^{14}C yr and with the mixed Northern hemisphere terrestrial/marine dataset with a 50/50 terrestrial/marine proportion. These different options are used to model the approximate endpoints of a range of possible reservoir effects, from an open ocean offset with strong upwelling effects to a modest reservoir effect occurring in a mixed marine/freshwater environment. Table 5.2 shows the results of calibration with different reservoir effects.

As shown, the range between the extreme endpoints of the 2 sigma calibrated age ranges based on a strong reservoir effect (Marine04, $\Delta R=235\pm35$ ^{14}C yr) and a weak reservoir effect (mixed 50/50 marine/terrestrial) is generally in excess of 600 calendar years. Therefore, in addition to the 2 sigma calendar age range based on the standard marine reservoir correction (which is considered the best choice for the shell samples in light of regional evidence), the endpoints of the alternative calibrations are plotted with dotted lines on the age depth models, and are considered a more conservative estimate of the true confidence intervals for the shell dates than that based solely on the laboratory supplied analytical error.

Core	Depth (cm)	Laboratory number	^{14}C Age (yr bp)	Cal age, 2 σ (yr BP)			Range (Cal yr)
				Marine04 $\Delta R=235\pm35$	Marine04 $\Delta R=0$	Mixed NH/Marine 50/50	
CM5	333	IGNS [NZA-21412]	3375 \pm 39	2770 - 3080	3130 - 3350	3350 - 3550	780
CM5	579	KIA 15211	4295 \pm 35	3930 - 4250	4300 - 4520	4530 - 4800	870
CM5	890	IGNS [NZA-21413]	6764 \pm 45	6890 - 7180	7200 - 7400	7410 - 7560	670
CM5	1085	KIA 15213	4095 \pm 30	3680 - 3960	4020 - 4260	4250 - 4490	810
CM5	1345	KIA15212	7585 \pm 35	7690 - 7920	7960 - 8140	8170 - 8330	640
CM5	1775	KIA15210	7725 \pm 45	7830 - 8090	8060 - 8310	8220 - 8450	620
P2	615	IRPA-13237	5355 \pm 30	5330 - 5580	5630 - 5840	5880 - 5990	660
P2	903	IRPA-13239	6640 \pm 40	6730 - 7030	7050 - 7260	7280 - 7430	700
P2	1150	IRPA-13238	7730 \pm 45	7830 - 8100	8070 - 8320	8220 - 8450	620
P2	1570	IRPA-13236	7810 \pm 50	7920 - 8170	8170 - 8370	8360 - 8540	620
P5	481	IRPA-13234	3300 \pm 35	2730 - 2960	3010 - 3270	3260 - 3440	710
P5	885	IRPA-13233	7090 \pm 35	7270 - 7460	7490 - 7650	7670 - 7830	560
P5	1135	IRPA-13232	7515 \pm 35	7630 - 7860	7900 - 8080	8030 - 8280	650
P5	1330	IRPA-13235	7735 \pm 35	7850 - 8090	8110 - 8310	8310 - 8430	580
P5	1528	IRPA-13231	7700 \pm 35	7810 - 8030	8050 - 8280	8220 - 8410	600
Mean 670							
StDev 90							

Table 5.2. Calibrated age ranges for shell dates from cores CM5, P2 and P5 using different reservoir effects.

5.2.2.3 Central point calendar age estimates

As the models proposed for the sites are based either on techniques of linear regression of age onto depth (CM5) or linear interpolation between radiocarbon dates (P2, P5), it is convenient to use single, central-point estimates for the calibrated ages. As the probability fields for errors in calibrated ages are generally non-normal and frequently multimodal, single point estimates of the calibrated age range do not always provide a robust indicator of the most likely calibrated age. However, central point estimates may be derived by a number of methods, some of which are more robust than others (Telford *et al.*, 2004). Weighted average or median probability methods are more stable than methods based on the location of intercepts on the calibration curve (Telford *et al.*, 2004: 297). Here, the median probability (calculated in the software program CALIB) is used.

5.3 Age-depth models

Age-depth models based on the available radiocarbon data provide a means for estimating sample ages and sedimentation rates for the sequences. In this section, plots of calibrated dates against depth are presented for each site, and age-depth models are proposed. The age-depth models are based on linear regression (CM5) and linear interpolation (P2, P5). The data points that constrain the age-models are presented for each site, accompanied by the derived gradient for each segment of the age-depth models. The segment gradient provides an estimate of sedimentation rate (SR) or net vertical accumulation of sediment per unit time.

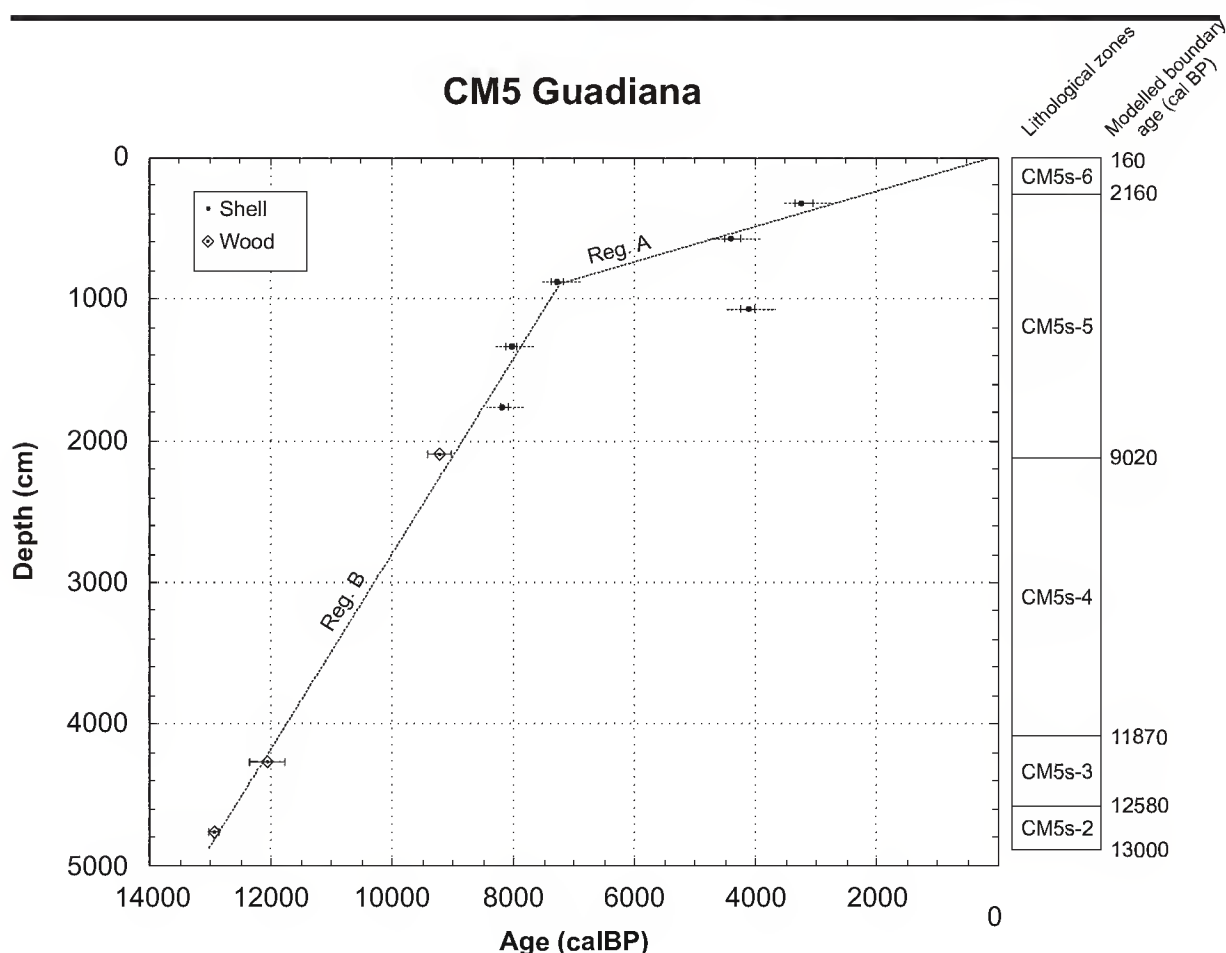
No dates have been obtained from the basal gravel fills of the sequences (sediment zones CM5s-1, P2s-1, P5s-1). Radiocarbon dates from other estuaries in the Gulf of Cadiz region (Dabrio *et al.*, 2000) and investigations of the seismic stratigraphy of the Guadiana valley infill (Lobo *et al.*, 2003) place the period of gravel accumulation during marine isotope stage 3, and suggest that the upper boundary of the gravels is an erosional surface representing a considerable period of time prior to the initiation of predominantly fine-grained sedimentation. The basal gravel fills therefore cannot be included in the age-depth modelling.

In general, the estuarine environment is characterised by complex patterns of sedimentation and highly variable deposition rates (Colman *et al.*, 1992). It is therefore recognised that the proposed age-depth models are only approximations of actual patterns of sedimentation. SR estimates based on the linear segment gradients represent long-term averages only, and represent the sum of deposition, resuspension, erosion, and compaction effects occurring at the sites. These estimates may conceal (a) short-term (i.e. annual time-scale) fluctuations in SR or (b) rapid changes occurring at lithological boundaries. The extent of short-term fluctuations is considered here essentially unknowable, as is generally true except where annually laminated sediments are preserved (Bennett, 1994). The extent of rapid changes occurring at lithological boundaries may be evaluated given a sufficient resolution of the age-depth curves (i.e. number of dates) and depending on the location of dated samples within the sequence. Where a high chronological resolution is not achieved, the likely influence of changes in SR at lithological boundaries must be evaluated in light of the characteristics of the sedimentary record. Overall, both factors (a and b) will introduce error into the estimation of ages for sample depths and zone boundaries.

5.3.1 CM5 Guadiana

Calibrated radiocarbon dates from core CM5 are plotted against depth (Figure 5.1). One date (depth 1085cm, KIA 15213) falls considerably outside the general age-depth trend of the other dates and is excluded from the age model. The date appears anomalously young for the depth. This anomaly is too great to be the result of burrowing, and must be attributed either to sample contamination with modern carbon or to sample displacement within the borehole during drilling. The other dates present a systematic series of increasing age with depth, and are included in the construction of the age-depth model.

The plotted CM5 dates suggest an age-depth profile with two distinct parts: a steeply inclined (i.e. high SR) lower part and a less steeply inclined (i.e. reduced SR) upper part. In order to model this age-depth relationship, lines of best fit were obtained by least squares regression analysis (regressing age onto depth) independently for the lower and upper parts of the age-depth profile. These regression lines display a good measure of fit with the data



Segment	Data points	Regression equation	R ²	Segment slope (mm/yr)
A	0 cm, 0 cal BP 333 cm, 3250 cal BP 579 cm, 4420 cal BP 890 cm, 7300 cal BP	$\text{Age} = 7.96 \text{ Depth} + 156.446$	98.7 %	1.2
B	890 cm, 7300 cal BP 1345 cm, 8040 cal BP 1775 cm, 8200 cal BP 2095 cm, 9240 cal BP 4270 cm, 12050 cal BP 4767 cm, 12920 cal BP	$\text{Age} = 1.44 \text{ Depth} + 5996.57$	99.3 %	6.9

Figure 5.1. Age-depth model, CM5, based on two linear regressions. Solid dots show median calibrated ages based on the IntCal04 calibration dataset (Reimer *et al.*, 2004) for wood dates and the Marine04 calibration dataset (DR = 0) (Hughen *et al.*, 2004) for shell dates. Solid error bars show the 2 sigma confidence interval based on the analytical error term. Shell dates also plotted with extended confidence ranges (dashed lines) based on multiple calibrations accounting for a range of possible estuarine reservoir effects, ranging from open ocean with strong upwelling effect (Marine04, DR = 235 ± 35 ^{14}C yr) to weak reservoir effect (mixed Northern Hemisphere 50/50 marine terrestrial).

points (high coefficients of determination, R^2), and pass through or very close to the confidence ranges of all the dates. The data points included in each regression, the regression equations and coefficients of determination are shown in Figure 5.1. The intersection point of the two segments is 896 cm, 7286 cal BP.

This age-depth model based on two linear regressions was selected in preference to a model based on linear interpolation between the age-depth data. While a linear interpolation model closely resembles the chosen linear regression model for some sections of the core, linear interpolation introduces some rather abrupt changes in gradient in some sections. Most pronounced is a segment implying reduced SR between the uppermost wood date (depth 2095 cm) and the lowermost shell date (depth 1775 cm), and a subsequent segment implying peak SR between the two lowermost shell dates (depths 1775 and 1345 cm). It is possible, of course, that these abrupt changes in gradient may reflect actual patterns of sediment accumulation at the site, possibly associated with the boundary between sediment zones CM5s-4 and CM5s-5. However, bearing in mind the possibility for dates on wood to be older than the time of deposition, and the fairly wide confidence interval associated with the shell dates, it is also considered possible that the gradient changes implied in this section may be an artefact of scatter in the radiocarbon dates. In this case, it is considered appropriate to proceed with the more simple model based on linear regressions. However, the question of changes in SR in the middle part of the core must be considered unanswered, requiring additional dating of preferably short-lived organic material from the upper part of sediment zone CM5s-4 and the lower part of CM5s-5.

Finally, other age-depth models were considered, including polynomial (quadratic and cubic forms) and cubic spline models. The polynomial forms (including all data points from both the lower and upper part of the core) produce a smoothed curve without the abrupt change in gradient at depth 890 cm associated with the two-line regression model. As a result, however, the modelled age-depth curves diverge from the data points in the regions above and below 890 cm. These models are characterised by lower coefficients of determination

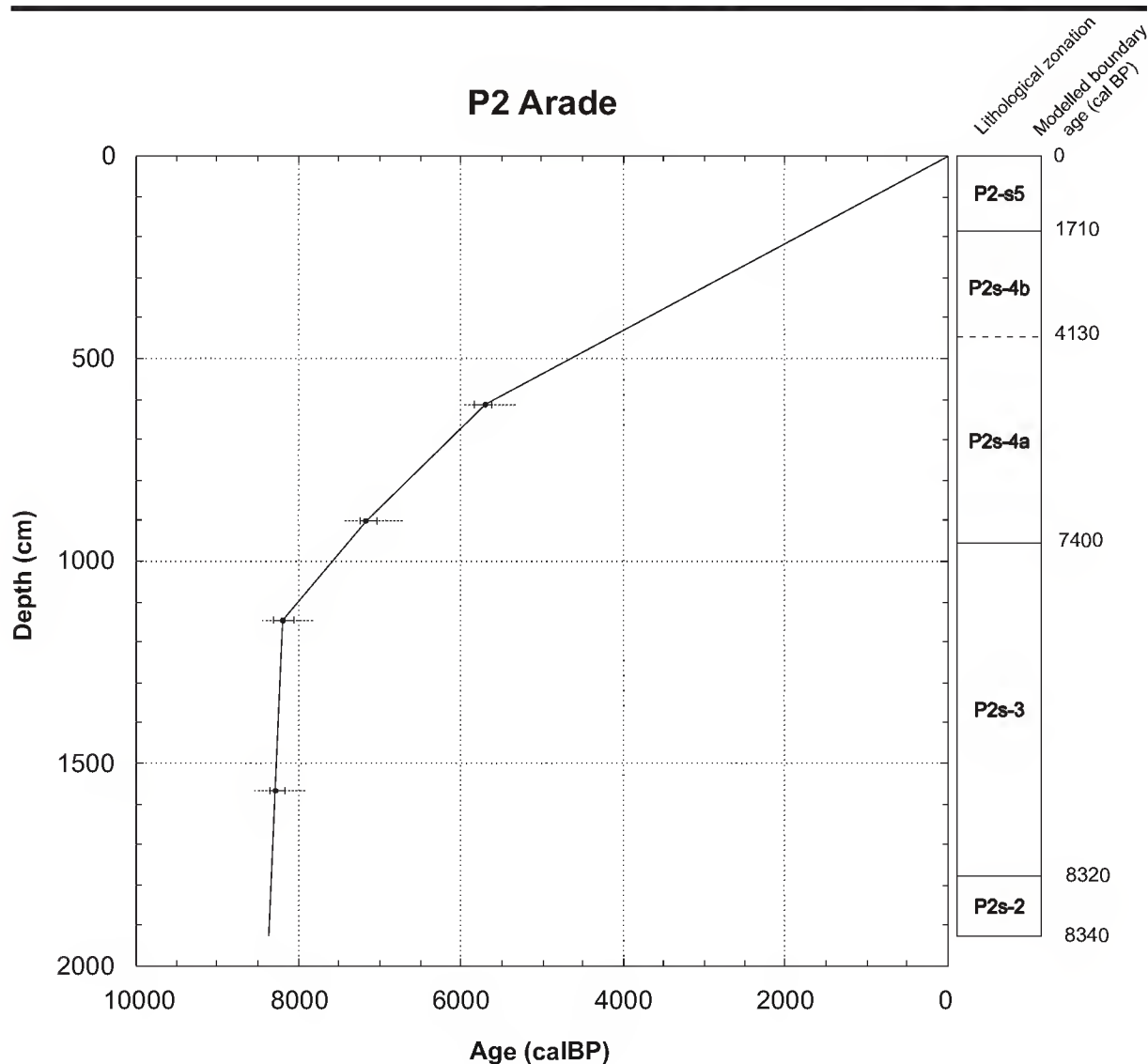
and higher residuals than the linear regressions. Moreover, there is no *a priori* reason to favour the curved age-depth relationship resulting from higher order polynomial regressions over a linear model, especially where the former suggests structure to the age-depth profile for which the radiocarbon data provide no evidence. The cubic spline method, which fits a polynomial between each pair of points for which the coefficients are determined slightly non-locally (Bennett, 1994), introduces dramatic swings including sections with negative SR, and is clearly unacceptable.

Based on the selected age-depth model, age estimates for sample depths and zone boundaries can be produced. Lithostratigraphical zones, as defined in the previous chapter, are plotted alongside the age-depth model in Figure 5.1. Based on the model, the initiation of sedimentation at the site (excluding gravels of CM5s-1) occurred at 13,000 cal BP. The age-model places the Pleistocene/Holocene boundary (assuming a calibrated age for the onset of the Holocene of 11,500 cal BP (Björck *et al.*, 1998)) at a depth of 3820cm. This suggests that the lithostratigraphical sequence may be broadly classified as Late-glacial (sediment zones CM5s-2,3) and Holocene (zones CM5s-4, 5, 6).

Overall, the age-depth curve for core CM5 indicates rapid long-term sediment accumulation during the Late-glacial and early to mid-Holocene (prior to *c.* 7300 cal BP). Long-term average SR for this period is estimated at 6.9 mm/yr, with vertical accumulation of around 40 m thickness over a period of *c.* 5700 yrs. After *c.* 7300 cal BP, sediment accumulation rates are reduced. Long-term average SR is estimated at 1.2 mm/yr, with an accumulation of 9 m thickness over 7300 yrs. Short term variation in SR, although not quantifiable, is likely to have been greater in sediment zones CM5s-2 and CM5s-3, which are characterised by laminated sediments indicating an episodic deposition regime, than the more homogenous sediments of CM5s-4, CM5s-5 and CM5s-6.

5.3.2 P2 Arade

Calibrated radiocarbon dates from the P2 core are plotted (Figure 5.2). The dates form a coherent series of increasing age with depth, and all are included in the age model. Although



Control point, upper		Control point, lower		Segment slope (mm/yr)
Depth (cm)	Age (cal BP)	Depth (cm)	Age (cal BP)	
0	0	615	5710	1.1
615	5710	903	7180	2.0
903	7180	1150	8210	2.4
1150	8210	1570	8280	60.0
1570	8280	1925	8339	60.0

Figure 5.2. Age-depth model, P2, based on linear interpolation. Solid dots show median calibrated ages based on the the Marine04 calibration dataset (DR = 0) (Hughen *et al.*, 2004). Solid error bars show the 2 sigma confidence interval based on the analytical error term. Extended confidence ranges (dashed lines) are shown, based on multiple calibrations accounting for a range of possible estuarine reservoir effects, ranging from open ocean with strong upwelling effect (Marine04, DR = 235 ± 35 ^{14}C yr) to weak reservoir effect (mixed Northern Hemisphere 50/50 marine terrestrial).

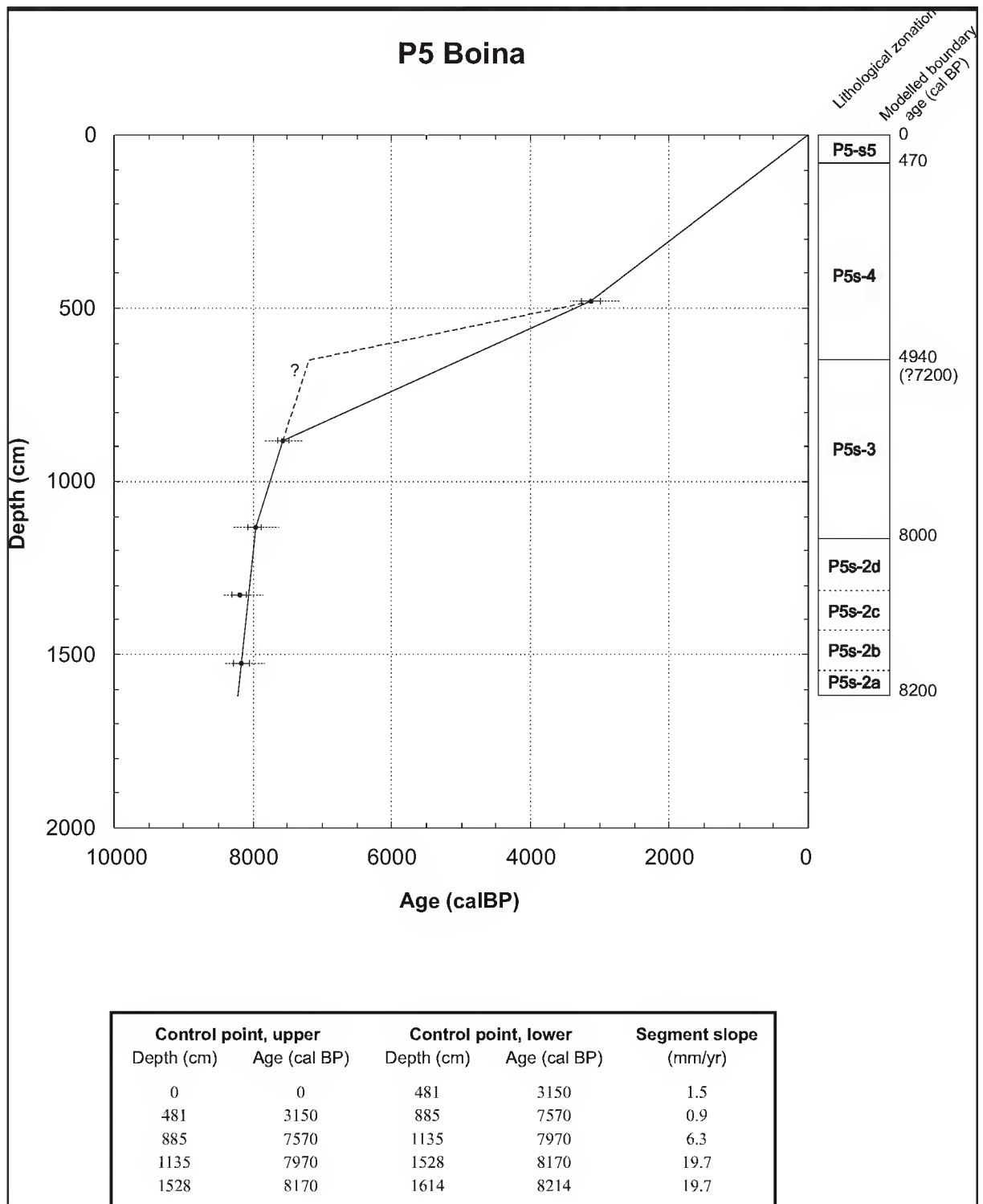


Figure 5.3. Age-depth model, P5, based on linear interpolation. Solid dots show median calibrated ages based on the the Marine04 calibration dataset (DR = 0) (Hughen *et al.*, 2004). Solid error bars show the 2 sigma confidence interval based on the analytical error term. Extended confidence ranges (dashed lines) are shown, based on multiple calibrations accounting for a range of possible estuarine reservoir effects, ranging from open ocean with strong upwelling effect (Marine04, DR = 235 ± 35 ^{14}C yr) to weak reservoir effect (mixed Northern Hemisphere 50/50 marine terrestrial). The dashed line marked (?) shows an alternative segment of the age-model which is suspected on the basis of core lithology and requires validation with further dates.

a number of methods for fitting curves to the age-depth data are available, linear interpolation is considered the most appropriate choice for the P2 age-depth model given the small number of available dates. Linear interpolation provides a straightforward and commonly used basis for age-depth models. The method is “superficially crude, but does provide reasonable estimates for both ages and gradients” (Bennett, 1994: 339). Using linear interpolation, the age models are constrained to pass directly through the available age-depth control points provided by the radiocarbon dates. The disadvantages of linear interpolation, however, are that it takes no account of the associated errors or confidence ranges of dates, and that the gradient changes sharply at each age point, which may not be realistic.

The age-model is constructed by linking the chronological control points with linear segments, on which basis age estimates for sample depths can be made. The control points and gradients of the segments of the age-model are shown in Figure 5.2. Modelled ages for the sediment zone boundaries are also shown. The lowermost segment is extrapolated on the basis of the lowermost two dates. This extrapolation provides an estimated date for the initiation of fine-grained sedimentation at depth 1925 cm (base of sediment zone P2s-2) of 8340 cal BP. This date is tentative because there are no control points in the lowermost sediment zone, and probably represents a minimum age for the onset of sedimentation.

Estimated SR for the initial phases of infilling prior to *c.* 8200 cal BP is extremely high (*~*60 mm/yr). After *c.* 8200 cal BP, estimated SR decreases to *c.* 2 mm/yr, and finally to 1.1 mm/yr for the period from *c.* 5700 cal BP until present. As the radiocarbon ages fall some distance from the sediment zone boundaries, changes in SR occurring at zone boundaries cannot be determined. However, a broad contrast in SR is demonstrated between sediment zone P2s-3 (high long-term average SR) and P2s-4 (reduced long-term average SR).

5.3.3 P5 Boina

Calibrated radiocarbon dates from the P5 core are plotted (Figure 5.3). As with core P2, a simple age-depth model based on linear interpolation between radiocarbon-based control points is used. The lowermost two dates are reversed in terms of the expected age-depth

sequence. The dates are very close in age, and display considerable overlap in confidence intervals. As the dates are very close, neither is considered anomalous. If one of the dates were erroneous, it is considered more likely to that the upper date would be too old (as a result of reworking) than the lower date too young. For this reason, the lower date is used a control point in the age model and the upper is not. Nevertheless, the plotted age-depth curve passes very close to the 2 sigma confidence interval of the upper date. The control points used in the construction of the age-depth model and the gradients for each section are shown in Figure 5.3.

Linear extrapolation from the lower dates provides an estimated age for the initiation of fine-grained sedimentation (base of sediment zone P5s-2) of 8210 cal BP. Estimated SR for the first phase of infilling prior to *c.* 8000 cal BP is very high (19.7 mm/yr). For the period between *c.* 8000 and 7600 cal BP, estimated SR falls to 6.3 mm/yr. After 7600 ka, estimated SR is further reduced, suggesting long term average SR until present around 1–1.5 mm/yr.

Lithostratigraphical zones are plotted next to the age-model (Figure 5.3). Zone P5s-2 is characterised overall by high average SR of around 20 mm/yr. However, given that changes in lithological characteristics are likely to be allied with changes in deposition time, and hence sedimentation rate, sedimentation rate across the heterogeneous sub-zones of P5s-2 is unlikely to have been uniform. Rather, sedimentation is likely to have been episodic, alternating between periods of relatively slow accumulation of silty sediments (P5s-2a/2c) and rapid to instantaneous deposition of sands and gravels (P5s-2b/2d). Nevertheless the total deposition time for P5s-2 overall appears to have been short, on the order of 200 years.

The lower part of zone P5s-3 is characterised by high average SR. On the basis of the available radiocarbon dates, the age-depth model displays a decline in SR during the deposition of zone P5s-3. However, the lack of control points in the upper part of zone P5s-3 may mean that reduced SR for the upper part of zone P5s-3 is unrealistic. It is possible,

and perhaps more likely, that sedimentation rates were more uniform during P5s-3, and that a change in SR accompanied the change in the sediment type at the P5s-3/4 boundary. This has a major implication for the modelled age of samples from the uppermost part of P5s-3. If a uniform sedimentation rate for the upper part of P5s-3 is posited, the top of P5s-3 would date to *c.* 7200 cal BP, as shown by the dashed line in Figure 5.3. This alternative is used for the estimation of ages for pollen samples. However, this question cannot currently be resolved, and the P5 age-model would be significantly more robust with, at the least, an additional date at the top of zone P5s-3.

Zone P5s-4 is characterised by reduced long-term SR. As with P5s-2, the nature of the sediments suggests an episodic depositional pattern, possibly accompanied by erosional events.

5.4 Sedimentation trends and sea-level history

The sedimentary infilling of estuaries is controlled by several factors, including sea-level rise, sediment budget, the morphology of the pre-existing landscape, the influence of wave- and tide- related processes, tectonic activity and human interference (Davis & Clifton, 1987; Fletcher *et al.*, 1993). Sedimentation in estuaries is neither homogeneous nor necessarily synchronous either between estuaries or within individual basins (Lario *et al.*, 2002a). Sedimentation rates may be spatially variable, relating to factors such as water depth, depositional environment, current strength and so on. For example, Colman *et al.* (2002) note that the main axial palaeochannel of the Chesapeake Bay, which might be expected to demonstrate low variability in sedimentation history and accumulation rates, varies from nearly empty to completely full of Holocene sediment. While a highly individualistic sedimentary response to local factors might not be unexpected, the age-depth relationships for the three sites reveal a broadly parallel development. Moreover, regional trends in sedimentation histories are emerging for southwest Iberia (Moura *et al.*, 2000; Lario *et al.*, 2002a), and it is in this context that a direct comparison of the three sites is considered.

Inter-site comparison of the calibrated radiocarbon dates against depth suggest a general sedimentation trend with two distinct phases recognised at all three sites (Figure 5.4). A first phase, beginning around 13,000 cal BP at the CM5 site and around 8500 cal BP in the Boina-Arade estuary, and continuing until *c.* 6500 cal BP, was characterised by rapid sediment accumulation. At the CM5 site, a long-term sediment accumulation rate around 7mm/yr is observed. In the Boina-Arade estuary, sedimentation rates in excess of 20 mm/yr are recorded. During the period from 7500 to 6500 cal BP, sedimentation rates declined and a second phase, beginning around 6500 cal BP, was characterised by reduced rates of sediment accumulation. Long-term average sedimentation rates around 1–2 mm/yr are recorded at all sites.

This two-fold infill pattern is not unique to these sites; similar patterns have been documented at other sites within the Guadiana estuary and at other southwest Iberian locations. Boski *et al.* (2002) document a two-fold pattern of sedimentation for other sites in the Guadiana estuary, with an early phase of rapid sedimentation prior to 6200 ¹⁴C bp (*c.* 7000 cal BP) with sedimentation rates around 8.5 mm/yr and a subsequent phase with sedimentation rates reduced to around 3 mm/yr. (These values are based on radiocarbon years and are not directly equivalent with the results presented here based on calibrated dates). On the Spanish coast of the Gulf of Cadiz, Dabrio *et al.* (2000) and Lario *et al.* (2002a) identify two phases with contrasting sedimentation rates for Holocene infill sequences of the Tinto-Odiel, Guadalquivir and Guadalete estuaries. Across these sites a two-fold infill pattern is recognised, with a first phase between *c.* 10,000 and 6500 cal BP with sedimentation rates higher than 5mm/yr, and a second phase between 6500 cal BP and present with rates lower than 1.5 mm/yr.

The agreement between the CM5, P2 and P5 age-depth relations for the last 8500 years and the similarity in general age-depth trends with other sequences in the Gulf of Cadiz support the view that a common external factor is primarily responsible for controlling sedimentation

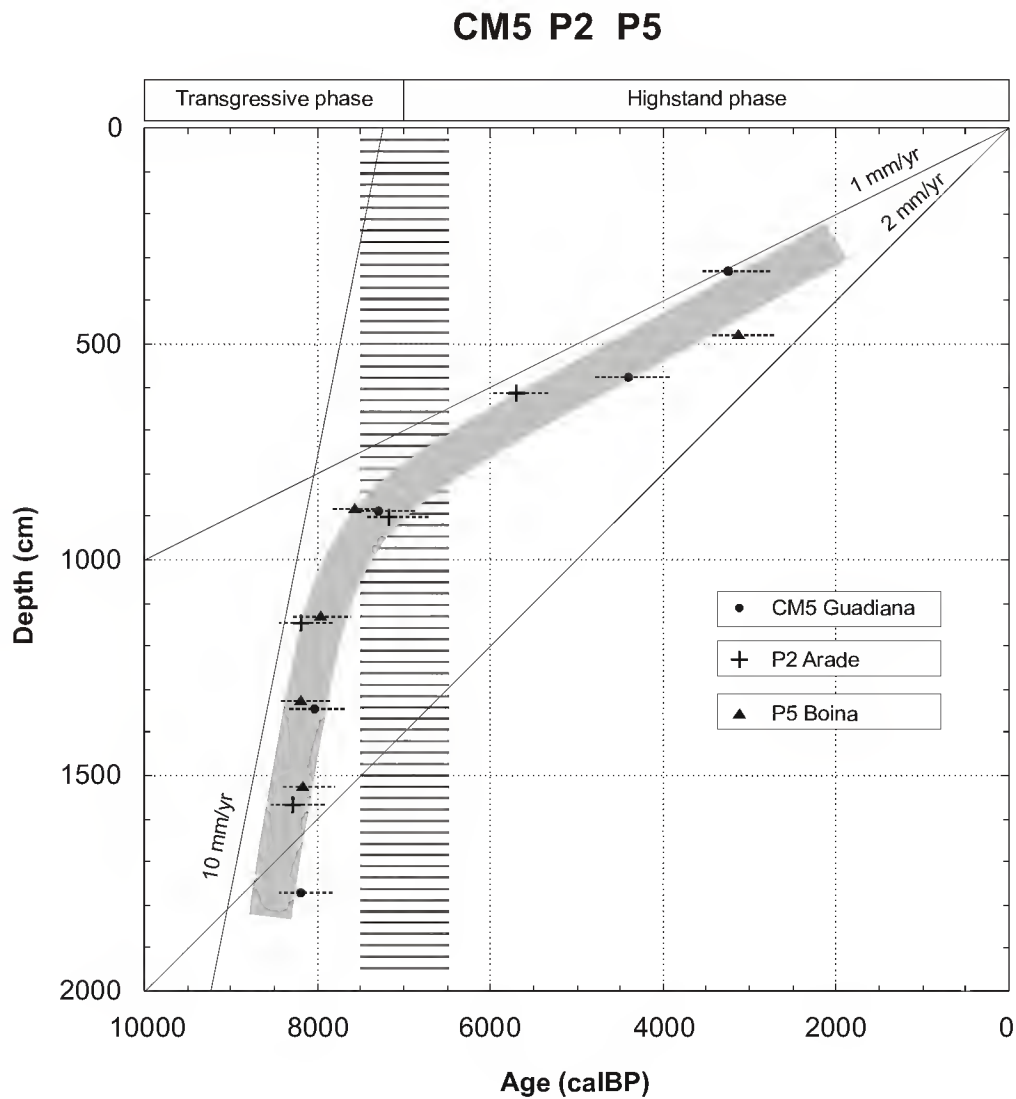


Figure 5.4. General sedimentation trend in the CM5, P2 and P5 cores, shown by a shaded line. Median calibrated ages and extended confidence ranges as shown in figures 5.1, 5.2 and 5.3. Transition from Holocene transgressive to highstand eustatic sea-level phases marked by hash lines between 7500 and 6500 cal BP, corresponding to deceleration in sedimentation rates in the CM5, P2 and P5 cores. Lines showing sedimentation rates of 10, 2 and 1 mm/yr plotted for reference.

rates at these sites during this period. Overall, the curvature of the age-depth profiles are consistent with the proposed history of post-glacial sea-level rise for the entire Portuguese coast (Dias *et al.*, 2000) and with eustatic sea-level curves derived from non-glaciated areas (Fairbanks, 1989; Bard *et al.*, 1996; Camoin *et al.*, 2004). These eustatic curves show a deceleration in sea-level rise around 7000 cal BP. This deceleration across the shift from the Holocene transgressive to highstand sea-level phases is considered the most likely explanation for the sedimentation trend observed at the sites. The first phase of rapid sedimentation prior to *c.* 6500 cal BP occurred under a regime of rapid sea-level rise and coastline retreat, with major increases in accommodation space in the drowned valleys promoting sediment trapping and rapid sediment accumulation. The subsequent deceleration and phase of reduced sedimentation rates corresponds with the onset of the sea-level highstand phase.

For a number of reasons, sedimentation trends do not represent sea-level curves (Haslett *et al.*, 1998). Estimated sedimentation rates do not take into account *in situ* sediment compaction (autocompaction), changes in the depositional altitude within the tidal frame, nor long term tectonic subsidence. A recent best-fit model for sea-level data from the Caribbean and South America estimates a relatively rapid rise of 7–8 mm/yr in the early Holocene with a marked reduction in this rate around 7000 cal BP (Milne *et al.*, 2005). The long-term average sedimentation rate at the CM5 site (~7mm/yr) presents a good match for this eustatic estimate. However, during the transgressive phase in the Boina-Arade estuary, sediment accumulation exceeded the rate of sea-level rise. This suggests a high sediment delivery and/or influence of basin morphology on sedimentation during this phase.

It is recognised that tectonic activity may present a complicating factor in the study of sedimentation trends, in that changes in the relationship between land and sea may be due to tectonic displacements (Allen, 2001). Southern Portugal is a tectonically active region, and Portuguese coastal deposits record evidence of sedimentary impacts of the 1755 AD and earlier tsunamis related to powerful earthquakes (Dawson *et al.*, 1995; Scheffers &

Kelletat, 2005). However, the maximum tectonically controlled vertical displacements during the Quaternary are several orders of magnitude less than eustatic sea level changes (Dias *et al.*, 2000) and, for the Guadiana valley at least, seismic stratigraphy does not reveal evidence for significant neotectonic activity during the Holocene (Lobo *et al.*, 2003).

At a low temporal resolution, these observations support the view that sea-level movements are the dominant influence on sedimentation in the Guadiana and Boina-Arade estuaries. Sedimentation in the CM5 core appears to have kept pace with sea-level rise, and long-term average sedimentation rates reflect the decrease in sea-level rise after 7000 cal BP. In the P2 and P5 cores, rapid infilling took place during the final part of the Holocene transgression. Long-term average sedimentation rates are also reduced for the upper part of the cores, associated with a transition from fine to coarse-grained sedimentation.

6 Discussion: sediment properties

6.1 On the interpretation of sedimentary parameters

6.1.1 Organic content

Organic content, estimated by LOI_{400} , represents the contribution of organic matter from a wide range of sources. For tidal sediments these include: 1) detrital organic material of terrestrial origin (allogenic), e.g. pollen, charcoal, wood, cuticles and other plant detritus; 2) organic material of local (endogenic) origin within the tidal water body, such as phytoplankton, faecal material from zooplankton and filter-feeding organisms (e.g. mussels), and benthic animals; 3) *in situ* (authigenic) organic matter resulting from microalgal and bacterial populations within the sediment column (Volkman *et al.*, 2000). In vegetated saltmarsh settings, halophytic plants provide a further important source of organic matter, including both above ground litter and below ground biomass, e.g. roots, rhizomes and tubers (Allen, 2000).

Variation in sediment organic content will reflect factors such as biological productivity and trapping potential of the depositional environment, and the ratio of mineral to organic input at the site. Where the mineral component is derived from the tidal water body and organic material is derived predominantly from detrital or *in situ* plant material, organic

matter content may show structured variation according to gradients of inundation frequency and altitude. For example, Fletcher *et al.* (1993) characterise marsh sub-environments in the Wolfe Glade wetland on the Delaware coast on the basis of LOI values. Values for organic content increase from low to high position with respect to the tidal frame, and with distance from tidal creeks and channels. In terms of percentage values, Fletcher *et al.* (1993) encounter LOI values > 50% for peats forming in waterlogged settings with low tidal influence (palustrine marsh), between 23 and 47 % for low to high marsh sub-environments, and between 9 and 14% for tidal flat samples. These last values are quite high, as the organic content of tidal flats, although variable, is generally much lower. Dyer (1998) suggests a rough division between high and low organic content in mudflat sediments at about 5% organic content as determined by LOI.

In the present day Guadiana estuary, organic matter content has been shown to vary between estuarine sub-environments (Morales *et al.*, 1997). Organic content is generally higher in channel margin samples than channel samples, and highest of all in saltmarsh samples. However, organic content also varies across the hydrodynamic zones of the estuary, being highest in the central estuarine domain and lowest in the fluvial estuarine domain. The authors attribute the elevated organic content of sediments of the central estuarine domain to the greater influence of settling and flocculation processes in this domain, and to the reworking of organic material from the fluvial domain.

While organic content will reflect a range of sources and environmental variables, it must be recognised that variation in sediment organic content, particularly down-core variation, may also be strongly conditioned by diagenesis. A considerable proportion of deposited organic matter will decay as a result of bacterial and fungal processes, the activities of invertebrate grazers, and the presence of moisture and oxygen (hydrolysis and oxidation processes) (Allen, 2000; Volkman *et al.*, 2000). Therefore, measured organic content will reflect preservation factors associated with chemical and biological conditions at the sediment-water interface and within the sediment column. For example, the commonly

observed trend in marine and intertidal sediments, of increasing organic content with decreasing grain size, results from increased preservation potential through ‘sorptive protection’ or adsorption, whereby organic compounds adhere to the surface of clastic material (Mayer, 1994).

6.1.2 Carbonate content

Calcium carbonate content, estimated from values for LOI_{950} , represents the contribution of CaCO_3 and possibly other carbonate minerals from several sources, including: 1) fluvially-sourced detrital carbonates from geological sources within the drainage catchment of the rivers, 2) detrital carbonates eroded from the coastal zone of the Algarve, or 3) biogenic CaCO_3 from microscopic marine fauna such as calcareous foraminifera, and macroscopic mollusc fauna. For the sediment sequences studied here, the latter two sources are considered the most important. The upstream areas of the drainage basins of the Boina, Arade and Beliche rivers are dominated by non-calcareous lithologies. A small contribution of detrital carbonates may be present for the P5 and P2 cores, derived from at both sites from local runoff and for P2 from limestone outcrops in the southern part of the Arade drainage basin. Although the Beliche basin does not include carbonate lithologies, a small contribution may derive from detrital material from the Guadiana river. However, calcareous bedrock only forms a significant part of the Guadiana basin in the uppermost reaches of the river in the central part of the Iberian peninsula, and this contribution is considered minor. In contrast, biogenic sources are considered much more important for all sites, as it is in other estuaries where fluvial sediment input is low in CaCO_3 , such as the Rías Bajas of Galicia (Nombela *et al.*, 1995). These sources include calcareous foraminifera, calcareous dinoflagellates and molluscs. A possible detrital contribution eroded from coastal rocks and sediments of the Algarve littoral and carried into the estuaries by tidal currents is also recognised. As both the contribution of mineral matter of coastal origin and biogenic material derived predominantly from salt or brackish water fauna is likely to increase with more open connection with marine waters, CaCO_3 content is considered a crude proxy for general marine influence at the sites.

As with organic content, carbonate content may be significantly influenced by diagenetic processes. Although more commonly discussed with respect to deep marine deposits, carbonate dissolution cannot be discounted in nearshore terrigenous sediments and shallow water conditions (Aller, 1985). Carbonate dissolution occurs primarily near the sediment-water interface due to the release of carbonic acid during the decomposition of organic matter and sulphuric acid during the oxidation of ferrous sulphide minerals. Carbonate dissolution is exacerbated by irrigation of the sediment surface by burrowing fauna and particle reworking by deposit feeders (Aller, 1982), and conditioned by the supply of metabolizable organic matter (Reaves, 1985).

6.1.3 Particle Size

Particle size analysis is undertaken with a view to the characterisation of the hydrodynamic environment of deposition. The interpretation of particle size data is only possible within the framework of a general understanding of the nature of sedimentation in the estuarine environment. Sediment transport within an estuary depends on several factors, including river discharge, tidal circulation patterns and salinity (Dyer, 1979). Coarse-grained sediments (sand and gravel) are supplied from fluvial and shelf sources, and tend to travel as bedload material. Deposition occurs where the velocity of fluvial and tidal currents fall below the sediment transport threshold. In the river dominated reaches of the estuary, bedload material is transported downstream until the point where flood and ebb currents are equal; in the seaward areas of the estuary coarse-grained sediments are transported landward until the point where flood current energy is low enough to permit deposition (Dyer, 1979). These processes result in an idealised picture for the main axis of the estuary, of decreasing grain size in a seaward direction in the river dominated reaches of the estuarine channel, and decreasing grain size in a landward direction in marine estuarine domain (Dyer, 1979). However, the distribution of tidal currents is usually more complicated and deposition shows considerable lateral variability. In the estuarine setting, coarse grained deposits are generally associated with high-energy sub-environments such as tidal channels (channel fill and lag deposits), sand flats, and tidal bars (Dalrymple, 1992).

Fine-grained material (silt and clay) is supplied to the estuary from river and marine sources, local runoff and organic production, and is carried in suspension within the tidal water body. The highest concentrations of suspended sediment occur near the maximum landward intrusion of the saline water body. Here, at the turbidity maximum, the circulation pattern of well- or partially-mixed estuaries maintains a higher concentration of suspended particles than either further upstream or further towards the seas (Dyer, 1979). Fine-grained sediment of fluvial origin enters the estuary where vigorous mixing exchanges sediment to the upper layer where the residual flow is downstream. In the middle estuary, the sediment settles into the lower layer where the residual flow is transported upstream. This cycle forms an effective sorting mechanism, and there are often considerable areas of mud-flat and tidal marshes in the area of the turbidity maximum (Stevenson *et al.*, 1986).

A highly characteristic feature of the suspended sediment content of tidal and near coastal waters is its incorporation into aggregate particles, both organic-mineral floccules and bioaggregates (Eisma, 1986; Eisma *et al.*, 1991a,b). Flocculation results from the collision of fine particles (predominantly clays) in the presence of an electrolyte (saline water) and is a function of sediment concentration, shear stress, salinity, organic coatings on the surface of particles and mineralogy (Mikkelsen & Pejrup, 1998). Organic matter, notably mucopolysaccharides produced by bacteria, algae and higher plants, plays an important role in maintaining flocculated particles (Eisma, 1986). Processes of coagulation by organisms, or bioaggregation, are also very important for the formation of aggregate particles in estuaries (Carson *et al.*, 1988). Flocs are structurally delicate and subject to breakage by turbulence (Eisma, 1986; Wolanski & Gibbs; 1995). These include the production of faecal pellets and pseudofaeces by zooplankton and benthic invertebrates during filtering of estuarine water. Deposition of fine-grained material therefore generally occurs in the form not of single grains but of flocs or bioaggregates with higher settling velocities than the constituent particles (Carson *et al.*, 1988; Gibbs *et al.*, 1989). During the tidal cycle, as currents diminish, aggregate particles adhere to the bed, and consolidate during the slack-water period. As the current strengthens during the subsequent stage of the tide, some of

the deposited material may remain on the bed, as erosion may not be sufficient to remove all the deposited sediment (Dyer, 1979). In general, fine grained deposits (silts and clays, or muds) are associated with the central portion of an estuary, and with low energy sub-environments fringing the estuary such as mudflats, marshes and lagoons.

The important role of aggregation of fine particles has ramifications for particle size analysis, as the size of constituent particles within aggregates may vary widely making interpretation of the hydrodynamic characteristics of a sediment sample difficult. The detailed investigation of aggregate particles in suspended sediments from the New Jersey shore (Carson *et al.*, 1988), provides an example of the range of sizes of constituent particles. Faecal pellets measuring between 50 and 3000 μm (4.3 to -1.6 phi) in length contain particles in the range 1–50 μm (10 to 4.3 phi) and display settling velocities equivalent to quartz grains in the range 25–160 μm (5.3 to 2.6 phi). Organic-mineral aggregates (flocs) measuring up to about 150 μm (2.7 phi) are composed dominantly of inorganic grains smaller than 6 μm (7.4 phi), and displaying settling velocities equivalent to quartz grains smaller than 25 μm (5.3 phi). As discussed by Allen (2000), mixtures of aggregate particles in the tidal water column tend to be unimodal in terms of overall dimensions or settling velocity, but may be perceived as polymodal assemblages once dispersed for the purposes of analysis. Aggregation is likely to extend the range of particle sizes included in a sample, with impact on grain size parameters such as sorting and skewness.

6.1.3.1 The Pejrup ternary diagram

While flocculation effects may be important for the very fine (clay and fine silt) fraction, and bioaggregation for the fine fractions in general, the sand fraction is likely to have been deposited as single grains. The distinction between an aggregated fine fraction and non-aggregated coarse fraction provides the basis for one of the interpretive tools employed in the discussion of the particle size results, the Pejrup ternary diagram (Figure 6.1). While a range of classification schemes exists for the description of non-gravelly sediments using clay-silt-sand ternary diagrams (reviewed, for example, in Flemming, 2000), the Pejrup

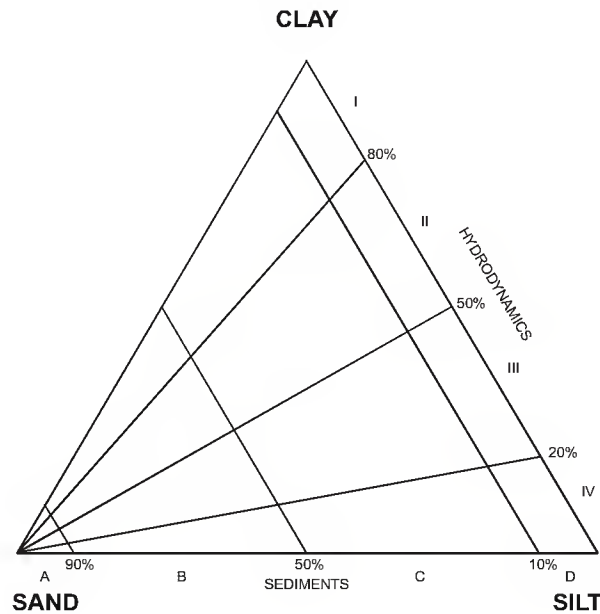


Figure 6.1. The Pejrup ternary diagram for estuarine sediments, redrawn from Pejrup (1988). Lines indicating 90%, 50% and 10% sand divide the diagram into sections A to D, corresponding to textural changes related to decreasing sand content. Lines of constant clay/silt ratio divide the diagram into sections I to IV, corresponding to decreasing clay content within the mud (silt and clay) fraction. Decreasing clay content is considered to reflect increased turbulence and breakage of flocs.

scheme (1988) is unusual in that it attempts to add a genetic aspect related to hydrodynamic considerations and specifically for estuarine sediments.

Pejrup (1988) notes that the composition of the fine fraction less than about 6 ϕ ($16 \mu\text{m}$) in estuarine sediments tends to vary only within rather narrow limits. This lack of variability suggests that composition of this fine fraction does not reflect internal hydraulic sorting, but instead the deposition of flocculated particles. As flocs are susceptible to breakage by turbulence (e.g. Wolanski & Gibbs, 1995), hydrodynamic conditions influence the extent to which flocculated particles contribute to sedimentation and hence the proportion of clay within the sediments. On the basis of this reasoning, clay content is taken to represent the contribution of a fine flocculated fraction, which in turn is considered to reflect the degree of turbulence in the hydrodynamic environment. Lines of constant clay content (within the fine fraction) delineate four sections on the ternary diagram corresponding to increasing hydrodynamic energy (zones I to IV on the diagram). Hydrodynamic section I, corresponding

to clay content of >80%, indicates very calm conditions, rarely found in estuaries, and sections II to IV indicate increasingly higher levels of turbulence.

Lines at 10, 50 and 90% sand content further divide the diagram into four sections, A to D — a textural classification corresponding to decreasing sand content. As described by Pejrup, the sand content is not necessarily a clear indicator of the depositional environment, because the sand group covers a range of grain sizes including particles transported both in suspension and along the bed. Also, sand content in estuarine sediments is usually dependent on distance from the source, which is likely to be the tidal channel. The major control imposed on sand content by distance from channels for tidal sediments is illustrated in the research of Pendón *et al.* (1998) on the tidal sediments of the Domingo-Rubio estuarine system near Huelva. Using the Pejrup diagram, channel samples plotted in sections A and B, channel margin samples in section C, and saltmarsh samples in section D.

6.1.3.2 Biplots of mean grain size vs. sorting

A second interpretive tool used in the discussion of the particle size data is a biplot of mean grain size versus sorting (phi standard deviation). The use of bivariate plots (biplots) in the interpretation of particle size data extends back over several decades (e.g. Stewart, 1958; others). A number of researchers have attempted to define graphic envelopes related to different depositional environments, e.g. beach, dune and river. Attempts to make environmental sense of biplots have not been entirely successful, possibly due to oversimplified outcome options (e.g. river vs. beach) or confusion arising from inherited, source-related grain size characteristics (Socci & Tanner, 1980; Tanner, 1991a). For these and other reasons, it is apparent that universal diagnostic models do not exist (McManus, 1988). In this study, the use of biplots as an interpretive tool is undertaken not with the aim of establishing new graphic envelopes or predicting a variety of environmental settings, but as an aid to the discrimination of changes in hydrodynamic conditions within the estuarine setting and a means for inter-site comparison.

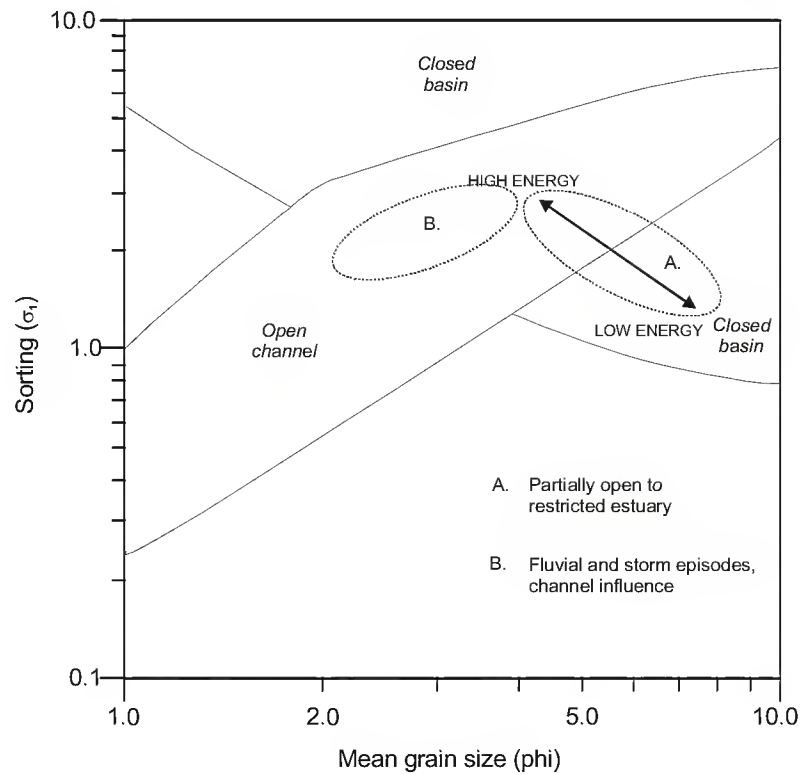


Figure 6.2. Template for biplot of mean grain size vs. sorting. Graphic regions (Closed basin, open channel) redrawn from Spencer *et al.* (1998) following the work of Tanner (1991a, b). Fields A and B (redrawn from Lario *et al.* (2000)) show the common envelopes for estuarine sediments, and their interpretation in terms of increasing energy of the depositional environment.

Recently, biplots of sorting versus mean grain size, parameters generally accepted to reflect hydrodynamic controls (Griffiths, 1967), have been shown to be useful in illustrating changes in the energy of the depositional environment and the degree of sediment processing in estuarine and back-barrier sediments (Spencer *et al.*, 1998; Lario *et al.*, 2000; Lario *et al.*, 2002b). The biplot diagrams used in these studies adopt graphic interpretive regions derived from the research of Tanner (1991a,b). The diagram represents a “close-up” of one section of Tanner’s tail-of-fines diagram, which aims to distinguish ‘new supply’ (river or closed-basin) environments from winnowing environments subject to strong sorting processes (beach and dune). New supply environments are those where abundant supply of new sediments means that winnowing cannot be very effective (Tanner, 1991a). The biplot used here (Figure 6.2), adopted from Spencer *et al.* (1998) focuses on the part of the diagram

related to new supply environments, and attempts to distinguish between river and closed-basin or settling environments. The distinction relates primarily to current energies of the depositional setting, and has been shown to distinguish, for example, between calm, settling conditions and fluvial flood or storm episodes (Lario *et al.*, 2000) or between closed and open conditions related to barrier development (Spencer *et al.*, 1998). Although the interpretive regions are derived from Tanner's research into suite statistic properties, the approach is, in fact, more traditional (and falls foul of some of Tanner's criticisms of bivariate plotting), employing measures of average size (mean phi) and spread about the average (standard deviation or sorting) for the entire grain size distribution of individual samples, rather than measures of mean and standard deviations for the fine tail only (<4 phi) and for suites of samples.

Previous use of the Tanner-derived biplot shows that estuarine samples tend to fall within an elliptical envelope spanning the boundary between the closed basin and channel graphic regions (Figure 6.2). The relative position of samples within this envelope has been suggested to relate primarily to energy conditions, with samples from higher energy settings plotting towards the channel region (Lario *et al.*, 2000). Samples which are strongly influenced by the input of coarse material tend to plot within the channel region of the diagram. For marsh samples of the Guadalquivir and Guadelete estuaries (Lario *et al.*, 2000; 2002b) samples falling within the channel region have been correlated with high-energy conditions occurring in storm, flood and possibly tsunami events. As noted with regard to samples from Scotney Marsh, in the southeast England, samples falling within the channel region of the diagram may relate not only to fluvial influence but to tidal channel influence (Lario *et al.*, 2002b).

6.1.4 Magnetic susceptibility

A brief review of the basis for the interpretation of magnetic susceptibility is presented, drawing on Smith (1999) and Dearing (1999). Different substances exhibit different behaviour when placed in a magnetic field, and fall into different generalised categories of magnetic behaviour. In order of strongest to weakest influence on magnetic susceptibility,

these categories are: ferromagnetism, ferrimagnetism, canted antiferromagnetism, paramagnetism and diamagnetism. Ferromagnetic substances, such as pure iron, cobalt, and nickel, have very high magnetism but are not normally found in the natural environment in this form. Ferrimagnetism is the most important category of magnetic behaviour in natural materials. Ferrimagnetic minerals include magnetite and other iron minerals such as maghaemite and greigite which have high magnetic susceptibility values. Canted antiferromagnetic minerals, such as haematite and goethite, and paramagnetic minerals, which include a wide range of generally iron-bearing minerals common in rocks and soils, such as pyrite and dolomite, have weaker magnetic susceptibility. Diamagnetic substances oppose an external magnetic field and include non-iron bearing minerals such as quartz and calcite, and non-mineral substances including water and organic matter. Diamagnetic substances have very weak or negative magnetic susceptibility values.

For soils and sediments, low frequency magnetic susceptibility (χ_{lf}) chiefly gives information about the total concentration of ferrimagnetic minerals, or, where ferrimagnetic mineral concentration is extremely low, about the total concentration of canted antiferromagnetic and paramagnetic minerals. Samples of rocks and soils showing purely paramagnetic behaviour rarely show χ_{lf} values exceeding $10 \times 10^{-8} \text{ m}^3 \text{ kg}^{-1}$; higher magnetic susceptibility values are typically controlled by the concentration of ferrimagnetic minerals (Dearing, 1999). Several sources of ferrimagnetic minerals in estuarine sediment are recognised, including: 1) detrital particles derived from rocks and soils and transported by river or tidal currents, 2) biogenic particles derived from bacterial activity (e.g. production of intracellular magnetosomes), and 3) authigenic particles formed within the sediment. With respect to sediments, soil-derived particles are considered detrital, although their mode of production may be related to both chemical and biogenic processes (Oldfield, 1992). Although authigenic minerals are regarded as the products of inorganic chemical processes, the activity of bacteria is generally involved in the formation processes (Dekkers, 1997). For example, bacterial reduction of sulphate is critical in the formation of pyrite and other iron sulphides such as pyrrhotite and greigite (Berner, 1984). The mineral

magnetic assemblage may represent several different sources; for example, in Irish saltmarsh sediments, Oldfield & Yu (1994) identify a coarse magnetic mineral fraction of detrital origin and a fine mineral fraction of likely biogenic, bacterial origin.

While χ_{f} provides an indication of the total concentration of ferrimagnetic minerals in a sample, it does not discriminate well between magnetic mineral grain sizes. Frequency dependent susceptibility exploits the behaviour of superparamagnetic grains (SP) and permits the identification of ultrafine grains within the magnetic mineral assemblage. The basis for frequency dependent behaviour is complex and the precise range of contributing grains sizes is not fully known (cf. Dearing *et al.*, 1996a; Eyre 1997). An outline is presented here. Magnetic minerals may be classified according to the organisation of magnetic domains, or regions of parallel atomic magnetic moment (Smith, 1999), with a basic division between grains with more than one domain (multi-domain (MD)) and single domain (SD) grains. The existence and behaviour of magnetic domains is strongly influenced by grain size. Below a critical size (less than $\sim 0.03 \mu\text{m}$), SD grains exhibit a behaviour termed superparamagnetism whereby the induced magnetisation arising from placement in a magnetic field is lost (relaxation) in a very short period of time (around 1/10,000 of a second) (Dearing, 1999). This behaviour relates to the high natural thermal energy of ultrafine crystals. For a narrow range of grain volumes at the boundary between the SP and stable single domains, the relaxation time is measurable. Susceptibility measurements at two frequencies a decade apart exploits the relationship between grain size and relaxation time, identifying grains that have relaxation frequencies (inverse of relaxation time) that lie between the two measuring frequencies (Dearing *et al.*, 1996a; Eyre, 1997). At low frequencies, grains near the superparamagnetic/ stable single domain (SP/SSD) boundary are able to contribute fully to susceptibility; at high frequencies, these grains do not contribute fully to susceptibility.

Maximum values for percentage frequency dependent susceptibility ($\chi_{\text{fd}\%}$) are similar in theoretical calculations and empirical observations (around 14%) (Dearing *et al.*, 1996b)

Plots of $\chi_{fd\%}$ versus χ_f and χ_{fd} can be helpful for the identification of different types of magnetic assemblage. Three types of assemblage can be identified on the basis of $\chi_{fd\%}$: dominance of frequency independent grains ($\chi_{fd\%} < 2\%$), mixture of frequency-dependent and independent grains ($\chi_{fd\%} 2-6\%$), and dominance of frequency-dependent grains ($\chi_{fd\%} > 6\%$) (Dearing *et al.*, 1996a). The identification of a frequency-dependent assemblage is of interest in soil studies where frequency-dependent grains are indicative of the presence of secondary ferrimagnetic minerals (SFMs) derived from biologically active organic-rich topsoil horizons, particularly where burning processes have been effective (Le Borgne 1955; Dearing *et al.*, 1996a; Dearing *et al.*, 1997). In sediment sequences, the record of SFMs is of interest for the identification of soil formation (pedogenic) processes, inwash episodes of eroded soil material, and as a signal of burning in the catchment (Rummary *et al.*, 1979).

In the estuarine environment, the detection of a terrestrial, detrital magnetic signature is of interest for the evaluation of sediment sources (e.g. fluvial versus marine) and for the identification of catchment-scale erosion events. However, the interpretation of the magnetic susceptibility record in these terms may be severely hindered by the extent of post-depositional alteration of the iron mineral assemblage. Of particular importance are processes of iron mineral diagenesis involving the formation of iron sulphides in reducing geochemical environments. Post-depositional changes may influence mineral magnetic properties in contrasting ways. First, reductive diagenesis of detrital ferrimagnetic grains can reduce the magnetic concentration and alter concentration-independent magnetic parameters (Karlin & Levi, 1985; Canfield & Berner, 1987). Detrital iron minerals, including magnetite and other iron oxides, provide a source of reactive iron for the formation of pyrite under anaerobic and reducing conditions in the presence of organic matter (Berner, 1984). As pyrite is a paramagnetic mineral, a consequent reduction in magnetic susceptibility may occur. Reductive diagenesis has been shown to occur in a range of hydric settings including hemipelagic marine sediments (Karlin & Levi, 1983; 1985), lake sediments (Anderson & Rippey, 1988), waterlogged soils (Grimley *et al.*, 2004) and peats (Williams, 1992). In estuarine samples, loss of magnetic susceptibility due to rapid iron mineral diagenesis has

been shown in down-core magnetic profiles for near-surface estuarine muds of the Galician Rías Bajas by Rey *et al.* (2000; 2005). These studies show that a reducing geochemical environment, rapid sedimentation and anoxic conditions promote reductive diagenesis.

Second, the production of authigenic iron minerals can *increase* the ferrimagnetic mineral concentration. Certain iron sulphides, possibly occurring as intermediate forms in the production of pyrite (Roberts & Turner, 1993; Dekkers, 1997), are ferrimagnetic, notably pyrrhotite and greigite. Greigite, which was formerly considered rather rare in environmental samples (Thompson & Oldfield, 1980), is now recognised as an important component of natural magnetic assemblages in a number of sedimentary environments (Hilton *et al.*, 1986; Snowball & Thompson, 1990), often occurring in discrete, well-defined zones (Snowball, 1991). Other authigenic minerals may occur, such as paramagnetic and canted antiferromagnetic oxyhydroxides, such as ferrihydrite and goethite (Dearing *et al.*, 1998), although the impact on magnetic susceptibility will not be as significant. Finally, the *in situ* formation of ultrafine-grained magnetite and possibly greigite in the form of intracellular magnetosomes may alter the magnetic mineral assemblage (Snowball, 1994).

In samples taken for pollen analysis from the fine-grained sediments of cores P2, P5 and CM5, high levels of authigenic iron sulphides were observed to have formed within and around small organic particles such as pollen grains. This observation indicates that the iron mineral assemblage cannot be considered purely detrital. In the subsequent discussion, the possible role of detrital magnetic minerals is evaluated in light of other sedimentary evidence from the cores. However, it is recognised that precise discrimination of detrital and authigenic/biogenic components would require a full suite of magnetic measurements (notably remanence measurements (e.g. Oldfield, 1994)) allied with geochemical and microscopic mineral investigation.

6.2 CM5 Guadiana

6.2.1 *Organic and carbonate content*

Two main patterns emerge from the LOI results of the CM5 samples: the correlation of water and organic content, and inter-zone differences in organic and carbonate content. The correlation of water and organic content in the CM5 core may be explained in part by water retention by organic particles, or by a common relationship with grain size variables favouring both increased moisture and organic preservation in the finer grained sediments. Down-core compaction and diagenetic effects probably also explain in part the overall trend towards lower values for water content and organic content in the lower half of the core. However, the influence of sedimentary characteristics is clearly superimposed on top of any long-term progressive effects, for example with characteristic changes in LOI variables associated with zone CM5s-3.

In the lower part of the core (CM5s-2/3/4) organic content is low, suggesting a relatively high ratio of minerogenic to biogenic input. In part, a progressive increase in the influence of organic matter decay may account for this overall trend towards lower values for organic content. However, values for these parameters are clearly also related to lithological characteristics because the curves show distinct changes associated with lithological boundaries, and may therefore relate to changing depositional or environmental conditions. Carbonate content is observed to vary between sediment zones.

CM5s-2, with low organic content and moderate CaCO₃ content suggests a sedimentary setting with low organic productivity and some marine influence. CM5s-3, which is clearly distinguished in terms of grain size parameters, is distinct in terms of low organic and carbonate content. While this may in part relate to reduced preservation potential for organic material in sandy sediments, some of the samples from this zone are indistinguishable from silts of zone CM5s-5, for example, on the basis of grain size parameters alone. Nevertheless, all the samples are distinct in terms of LOI values, suggesting a possible environmental control on organic and carbonate matter content independent of grain size effects. These

include low biological productivity of the depositional setting, and low calcareous biogenic input suggesting limited marine influence. In the overlying sediment zone, CM5s-4, low to intermediate values for organic and carbonate content suggest a low biogenic input. Slight elevation of carbonate suggests a slightly more open marine influence.

Elevated values for organic and carbonate content occur in zone CM5s-5. Core high values for organic content suggest relatively high levels of biological productivity. The peak values for carbonate content suggest the strongest marine influence of any depositional phase at the site. High levels of carbonate minerals are associated with the presence of shells and shell detritus in this zone. This association may be a direct result of the inclusion of fine fragments of shell material in the LOI samples. However, high values for shell content may be indicative of environmental and taphonomic factors favouring the deposition and preservation of carbonates from a range of sources. A preliminary assessment of foraminifer content indicates that this section of the core is rich in calcareous forms (Boski, pers. com.). Dissolution effects are recognised in the CM5 core, both in the variable preservation state of shell material and, the extreme case, in the form of sediment casts moulded to the form of dissolved shells. An active mollusc fauna and increased supply of organic matter may underline evidence for significant carbonate dissolution noted in this zone. It is recognised that dissolution is most prevalent in biologically active sediments where the sediment surface is disturbed through bioturbation and where decaying organic matter is present (Aller, 1982).

The decline in organic content in the uppermost section of the core (CM5s-6) — in light of the reddened colour of the sediment in this zone — is probably related to increased oxidation at the sediment surface and increased rates of decay of organic matter. Parallel decline in values for carbonate content suggest a reduced influence of marine water, possibly associated with decreased frequency of inundation.

6.2.2 Particle Size

The sediment samples from the CM5 sequence are characterised by a high silt content, a variable but overall low sand content, and poor sorting. Figure (Figure 6.3) shows the

particle size distributions for three characteristic samples from the core, which serve to illustrate some of the important changes observed in the sequence, and to explain the variation in sorting and skewness which characterise the sediment zones.

Overall, the CM5 samples are dominated by fine sediments in the range 9 to 4 phi. Sediments in this range represent a near symmetrical unimodal distribution, as illustrated by sample 2850cm. This distribution is considered the background grain size population for all the CM5 samples, and probably represents particles deposited through settling processes and in the form of aggregates, either organic-mineral flocculates or bioaggregates. Increased sand content, which characterises the lower part of CM5s-2 and zones CM5s-3 and CM5s-5, is considered to reflect the variable contribution of a distinct population of fine sands in

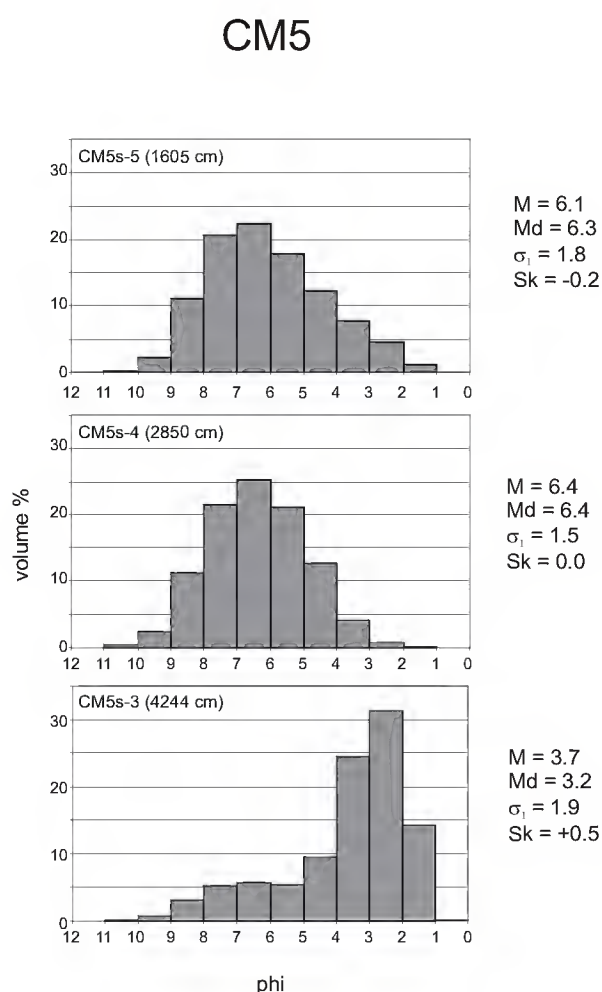


Figure 6.3. Histograms of particle size data for three samples from core CM5. Summary statistics: M (mean grain size), Md (median grain size), σ_1 (inclusive graphic standard deviation, or sorting), Sk (inclusive graphic skewness).

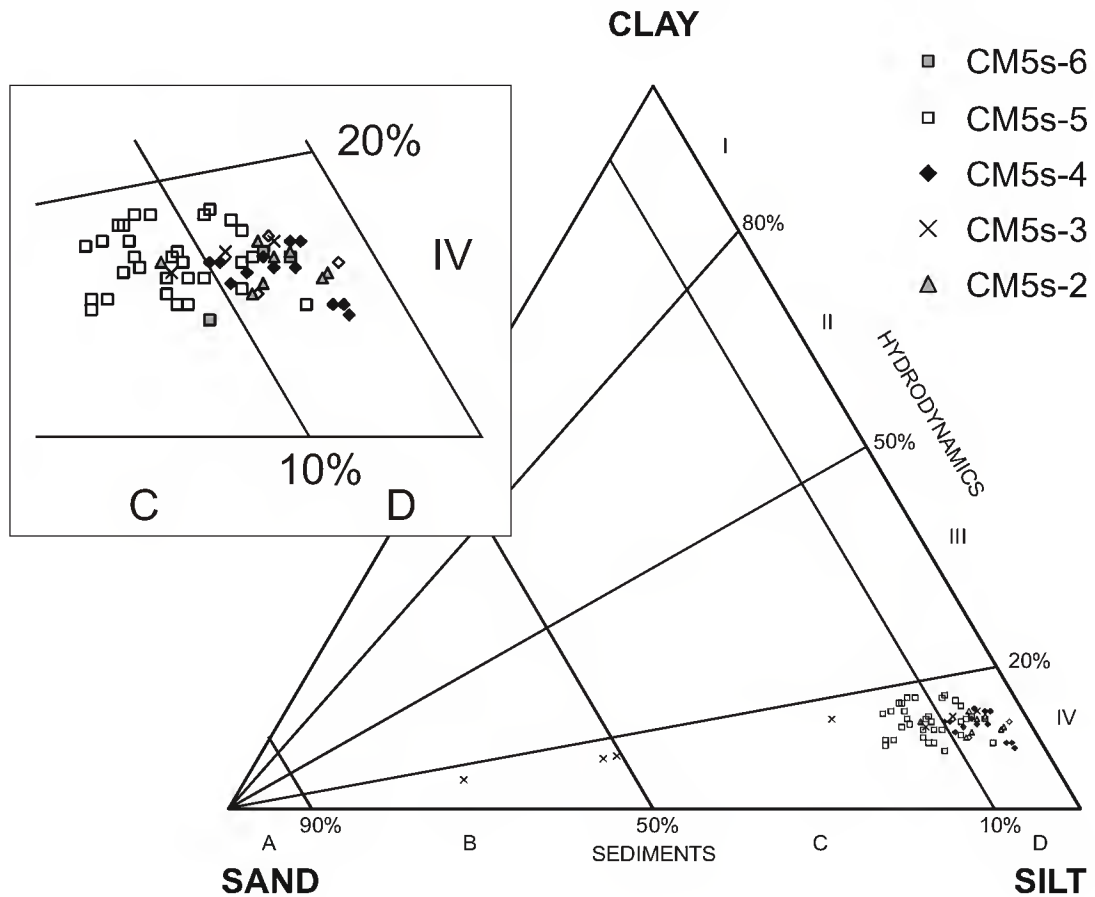


Figure 6.4. Pejrup ternary diagram: CM5 sand/silt/clay data.

the range 4 to 1 phi. This population probably represents particles deposited as single grains and transported under increased current velocities in suspension or saltation. In sample 4244cm, it is observed that although sands are dominant, the overall particle size distribution is bimodal and the background population can still be identified with a secondary mode between 7 and 6 phi. In sample 1605 cm (characteristic of the slightly sandy silts of zone CM5s-5), the background population is much more strongly represented, with a small addition of extra sandy material resulting from increased representation of the size classes in the coarse tail. This grain size distribution is recognised from all three sites studied, and is considered to be representative of a low-energy tidal setting, where a settling regime predominates except for the deposition of small quantities of fine sands during flood tides.

The addition of sands to the background population of fines has the effect of increasing the coefficient of sorting (i.e. more poorly sorted), although this may be considered the result of a combination of modes of sedimentation (aggregate and single grain) rather than a change in sorting processes acting on one mode. The relative proportions of two modal populations (fine aggregated population and coarse sandy) also determine the skewness of the distribution curves. Both positive, symmetrical and negative skewness is variously recognised in the sediment samples of the CM5 (and P2 and P5) sequences. Where only the fine modal population is present (e.g. 2850 cm), the distribution is symmetrical, reflecting a more or less normal distribution. As small quantities of the coarse modal population are added (e.g. 1605 cm), the distribution initially becomes negatively skewed, because the distribution now contains excess material in the coarse size classes relative to the dominant mode. Once the quantity of sand increases to the point where the coarse mode becomes

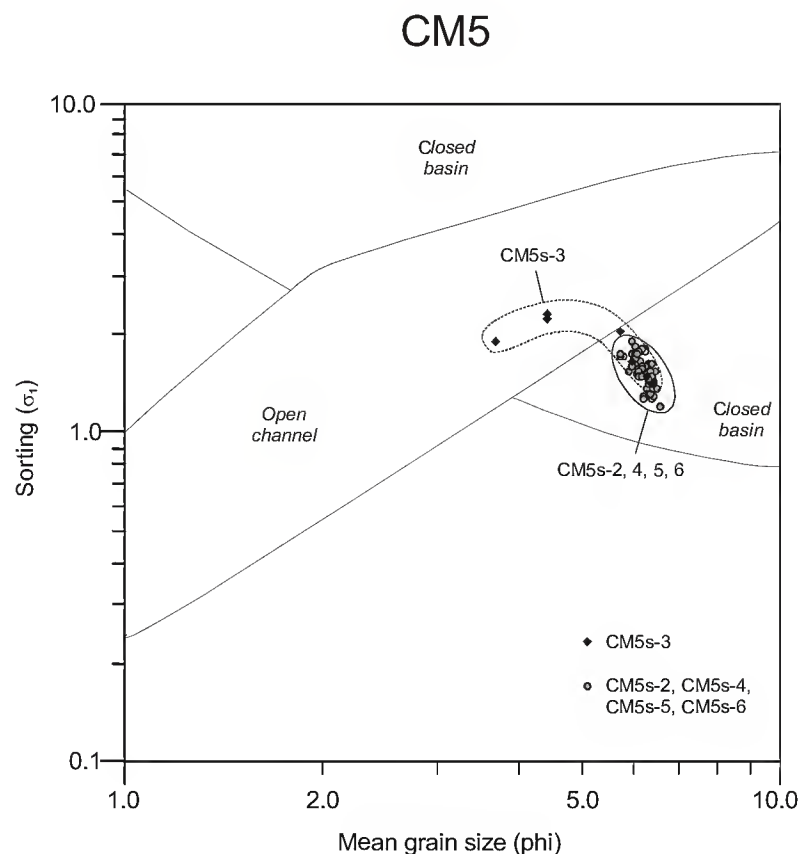


Figure 6.5. Biplot of mean grain size vs. sorting, CM5. Graphic regions redrawn from Spencer et al. (1998).

dominant, the distribution becomes positively skewed, because the distribution now contains excess material in the fine size classes relative to the dominant mode. Therefore, it is observed that the both positive and negative skewness (seemingly opposite conditions) can be explained by one factor, i.e. increasing sand content. This pattern of relationships between skewness and grain size populations was identified by Folk & Ward (1957) in a fluvial setting where sediments were composed of two distinct grain size populations.

Plotted on the Pejrup ternary diagram (Figure 6.4), the majority of samples are tightly clustered in sections IV, C and IV, D. The boundary line marking sand content of 10% (diagram zones C/D) is considered the value below which sand content in muddy sediments becomes insignificant (Pejrup, 1988). This line discriminates fairly effectively between the sandier samples of CM5s-5 (section C) and the majority of samples from CM5s-2, CM5s-4, and CM5s-6 (section D). This discrimination, related to a greater supply of sandy material in zone CM5s-5, suggests increased current activity or proximity to the estuarine channel in this zone. Only the samples from zone CM5s-3 occupy diagram zone B, suggesting stronger current action and/or proximity to channel sand sources than in any other zone. These interpretations are consistent with the view that variation in sand content reflects the changing sand contribution to a background fine-grained population. This view is also supported by observation that despite strong textural contrasts in terms of sand content between zone CM5s-3 and the other zones, the proportion of clay and silt within the fine (non-sand) fraction remains fairly constant. All samples from core CM5 contain less than 20% clay in the fine fraction and fall within region IV on the diagram. The region is considered by Pejrup to indicate moderate to high energy conditions with respect to turbulence and the breakage of flocs, although source-related features might also be important in determining the relative composition of the fine fraction (Flemming, 2000).

Figure 6.5 shows the position of the CM5 samples on a biplot of mean grain size vs. sorting. The bulk of samples from all stratigraphic levels in core CM5 fall within a tight cluster within the “closed basin” region. This observation supports the view that low-energy settling

processes dominated in the depositional environment. Only samples from CM5s-3 plot in the “open channel” region, suggesting increased influence of fluvial or tidal currents.

6.2.3 Magnetic susceptibility

The range of values for low-frequency susceptibility ($9\text{--}90 \times 10^{-8} \text{ m}^3 \text{ kg}^{-1}$) for the CM5 core suggests that χ_{lf} is controlled by the concentration of ferrimagnetic minerals, although the lowest values border on the range in which paramagnetic behaviour becomes more important (Dearing, 1999). A strong contrast in the magnetic signature of the lower part of the core (zones CM5s-2 and CM5s-3) and the upper part is recorded. In the lower part, the association of relatively high values for χ_{lf} and $\chi_{\text{fd}\%}$ and coarse grain sizes (sand content) suggest that the contribution of terrigenous detrital ferrimagnetic minerals may have a strong influence on the susceptibility signal (Figure 6.6). The relatively high $\chi_{\text{fd}\%}$ values, indicating a mineral assemblage containing a mixture of frequency dependent and independent grains (Dearing et al., 1996), may suggest a more significant contribution of soil-derived detrital minerals. Frequency dependent susceptibility is an effective means for the detection of superparamagnetic (SP) grains in the size range $0.01\text{--}0.025 \mu\text{m}$ (Dearing et al., 1997). Secondary ferrimagnetic minerals (SFMs), which are often identified as SP grains of magnetite or maghaemite, are produced in most topsoils and result in detectable concentrations of SP grains ($\chi_{\text{fd}\%} > 2\%$) (Dearing et al., 1996b). Although $\chi_{\text{fd}\%}$ reflects a superfine mineral magnetic component, high $\chi_{\text{fd}\%}$ values are associated with peaks in sand content in CM5s-2 and CM5s-3. This association suggests that the SP magnetic mineral component may occur as coatings on sand grains (Oldfield & Yu, 1994).

The contrast between the lower and upper parts of the sequence is considered to reflect the evolution of the estuary and a general transition from conditions of strong to reduced fluvial influence. However, the actual controlling factors underlying reduced susceptibility values in the upper part of the core are difficult to determine. Two scenarios may be considered. In the first, susceptibility values unambiguously reflect the concentration of detrital terrigenous material. In this scenario, the susceptibility record indicates reduced input of terrigenous material relative to the lower core sections, with a further reduction between zones CM5s-

5 and CM5s-4. A series of notable peaks, however, also occur within and at the boundary between zones CM5s-4 and CM5s-5, which may relate to episodes of inwash of detrital material. A minor effect on the general reduction in χ_{lf} will also derive from dilution by diamagnetic substances including organic matter and CaCO_3 which are more abundant in zone CM5s-5.

One problem with this scenario is that variation in χ_{lf} and $\chi_{fd\%}$ in the upper part of the core does not show strong associations with grain size parameters. A second scenario must be considered, namely that diagenetic effects related to redox changes in the geochemical

CM5 Magnetic susceptibility and sand content

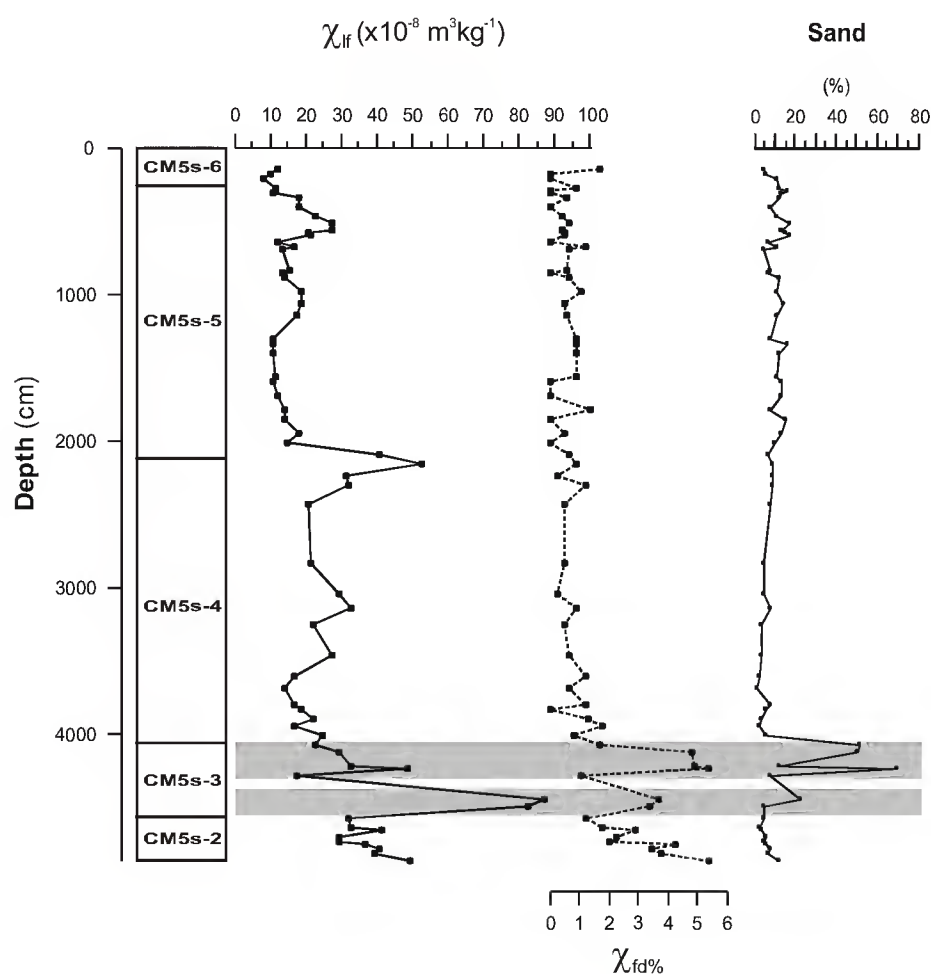


Figure 6.6. Comparison of χ_{lf} , $\chi_{fd\%}$ and sand content, CM5. Shaded bands highlight sections of the core displaying an association of peaks in magnetic susceptibility and coarse grain sizes in the particle size distribution.

environment underline the overall reduced values in the upper part of the core and variation within that core section. The CM5 sediment sequence contains evidence for complex patterns of iron mineral diagenesis involving pyrite, siderite and goethite (Boski, pers. comm.). The abundance of these non-ferrimagnetic minerals may be diagnostic of the diagenetic alteration of ferrimagnetic iron oxides, and could indicate post-depositional loss of magnetic susceptibility. Karlin & Levi (1985), investigating hemipelagic marine sediments, clearly demonstrate that down-core loss of magnetic signal can be related to iron reduction in organic-rich rapidly deposited sediment. They argue that the most likely cause of down-core decreases in magnetic properties is the reduction of magnetite and the subsequent formation of pyrite occurring as a result of anaerobic microbial decomposition of organic matter utilising the ferric/ferrous transition as a source of metabolic energy. Progressive dissolution of magnetite with depth has also been demonstrated for estuarine sediments of the Ría de Arousa in northern Spain by Emiroglu *et al.* (2004). Given that indications of the appropriate environment for reductive diagenesis are present in the fine-grained sediments from CM5 (rapid sedimentation rates, presence of organic detritus, high sulphide content) it seems very likely that the lowest values for χ_{lf} in the CM5 core may be associated with iron mineral diagenesis occurring within a poorly aerated, reducing environment.

The possibility of *in situ* enhancement of the magnetic signal is also recognised, notably in the distinct peak in χ_{lf} around the boundary between CM5s-4 and CM5s-5. This peak is not associated with an increase in coarse grain size fractions, and an authigenic source of magnetic minerals is suspected. Two contrasting explanations are recognised. On the one hand, the formation of authigenic greigite, a ferrimagnetic mineral associated with reducing conditions, may be responsible. Alternatively, the association of this peak with high levels of manganese at this depth (Boski, pers. comm.) may indicate the formation of oxidised minerals (for example, Mn-Fe hydroxides). In this case, the conditions underlining this localised peak in χ_{lf} may relate to an abatement of suboxic or reducing condition, possibly reflecting a phase of decreased sedimentation rate and a stabilisation of the oxidation front (Reitz *et al.*, 2004).

In summary, the Late-glacial sediments (CM5s-2, CM5s-3) show stronger evidence for a terrigenous, detrital mineral magnetic assemblage associated with the input of coarse grain sizes than the overlying Holocene sequence. In the overlying part (CM5s-4, CM5s-5, CM5s-6), $\chi_{fd\%}$ is insignificant, but χ_{fr} displays a number of localised peaks. Two scenarios, detrital and diagenetic, are presented for the interpretation of variability in this part of the core, a detrital scenario and a diagenetic scenario.

6.3 P2 Arade

6.3.1 Organic and carbonate content

Values for organic content (LOI_{400}) are higher in the lower part of the sampled sequence (zones P2s-2 and P2s-3) than the upper (P2s-4). Organic content shows a strong negative correlation with sand content (Pearson correlation coefficient, $R = -0.716$). This correlation is considered to reflect a combination of hydrodynamic, biotic and taphonomic factors. First, fine-grained sediments are indicative of low-energy settling conditions conducive to the deposition of detrital organic matter either as aggregate or individual particles. Second, the transition from a muddy to sandy substrates is likely to have an impact on the nature and extent of biological activity in the upper layers of the sediment. Third, differential preservation of organic matter in fine versus coarse grained sediments may be significant, either related to the role of fine-grained particles as carriers of organic coatings, or in terms of changes in the geochemical environment at the sediment/water interface between two contrasting sedimentation regimes.

$CaCO_3$ content (LOI_{950}) displays a trend of increasing values across zones P2s-2 and P2s-3. An important component of biogenic carbonate is identified, with a strong positive correlation between $CaCO_3$ content and shell content ($R = 0.886$) (Figure 6.7). The changes in $CaCO_3$ and shell content are considered to reflect a transition from predominantly fluvial to open estuarine conditions. $CaCO_3$ content in zone P2s-4a fluctuates between low and very high values which is partly related to fluctuations in shell content. This variability

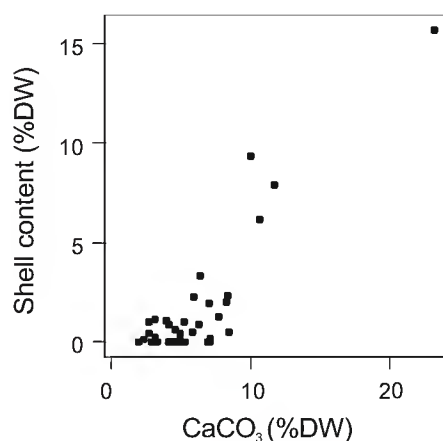


Figure 6.7. Biplot of CaCO_3 content vs. shell content, P2.

reflects the heterogeneous sediment composition with varying proportions of shell and non-carbonate mineral content.

6.3.2 Particle Size

The sediment samples from core P2 display contrasting particle size distributions, in particular associated with the transition from fine to coarse grained sediments across the P2s-3 to P2s-4a boundary. Figure 6.8 shows three particle size distributions for individual samples, which highlight some of the important characteristics of the P2 sequence. Two samples are shown from the lower part of the core (P2s-2 and P2s-3). In one sample (1800 cm), a bimodal distribution is observed, with mean and median values falling between the peaks. This distribution is characteristic of the sandier levels of zones P2s-2 and P2s-3. The primary mode occurs in the very fine sand class (4 to 3 phi), and probably represents a population of particles transported in suspension by current activity and deposited as single grains. The secondary mode occurs in the fine silts, 8 to 6 phi, and is probably associated with the settling of aggregated particles under low current velocities. In the fine-grained sediments of P2s-3 (e.g. sample 1210 cm), this latter mode becomes dominant, and the coarse mode is not apparent, although the coarse tail is well represented. This distribution is considered a typical low-energy tidal ‘mud’, as identified in the CM5 core. In the coarse grained sediments of P2s-4a (e.g. sample 636 cm), the fine grained mode is apparent,

P2

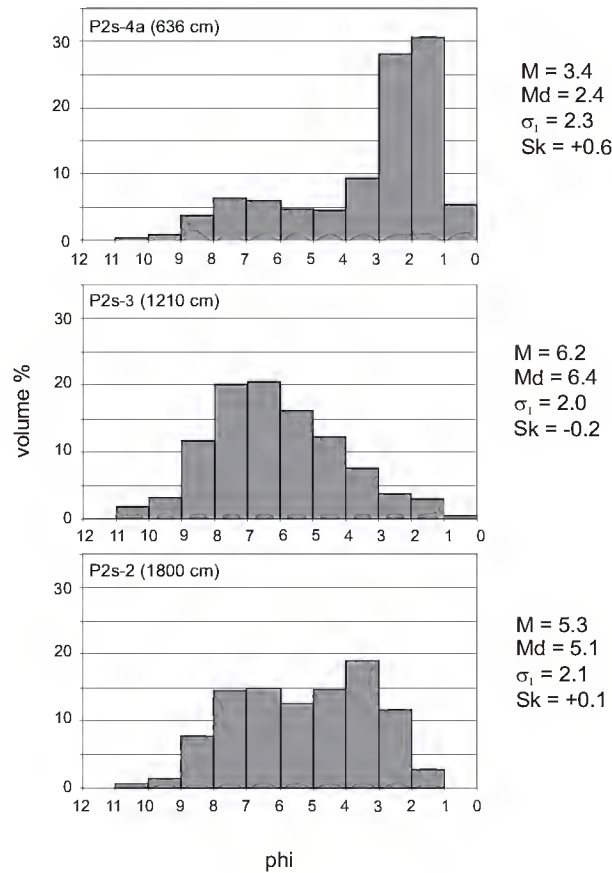


Figure 6.8. Histograms of particle size data for three samples from core P2.
Summary statistics: M (mean grain size), Md (median grain size), σ_1 (inclusive graphic standard deviation, or sorting), Sk (inclusive graphic skewness).

although poorly represented. As in the sandy sediments of the lower part of the core, a coarse grained mode is dominant; however, the mode occurs in the medium sands (2 to 1 phi). This coarsening of the sand population suggests either the deposition of suspended particles under strongly fluctuating current velocities, e.g. storm-related events, or increased proximity to the main estuarine channel associated with the supply of bedload material.

The Pejrup diagram (Figure 6.9), illustrates that the P2 samples display a fairly constant clay/silt ratio, with clay forming around 20% of the fine fraction. Samples fall on the boundary between regions III and IV, suggesting moderate hydrodynamic energies associated with some breakage of flocs. The zones are strongly discriminated on the basis of sand

content, with samples from P2s-2 falling in region C, samples from P2s-3 in regions C and D, and samples from P2s-4 primarily in region B. This textural distinction between the zones relates not to changes in the range of represented particle sizes, but to the relative contribution of sand, as observed in the distribution histograms (Figure 6.8), and is considered to reflect changing proximity/influence of the channel activity.

The biplot of mean grain size versus sorting for the P2 samples is shown Figure 6.10. Samples from P2s-2 and P2s-3 plot mainly within the ‘closed basin’ region of the diagram, with some samples falling in to the ‘open channel’ category. This straddling of the closed basin/ open channel boundary is rather typical of estuarine sediments (Lario *et al.*, 2002b). Samples from P2s-4a plot entirely within the ‘open channel’ region of the diagram, illustrating the overall stratigraphic progression from closed basin settling conditions to

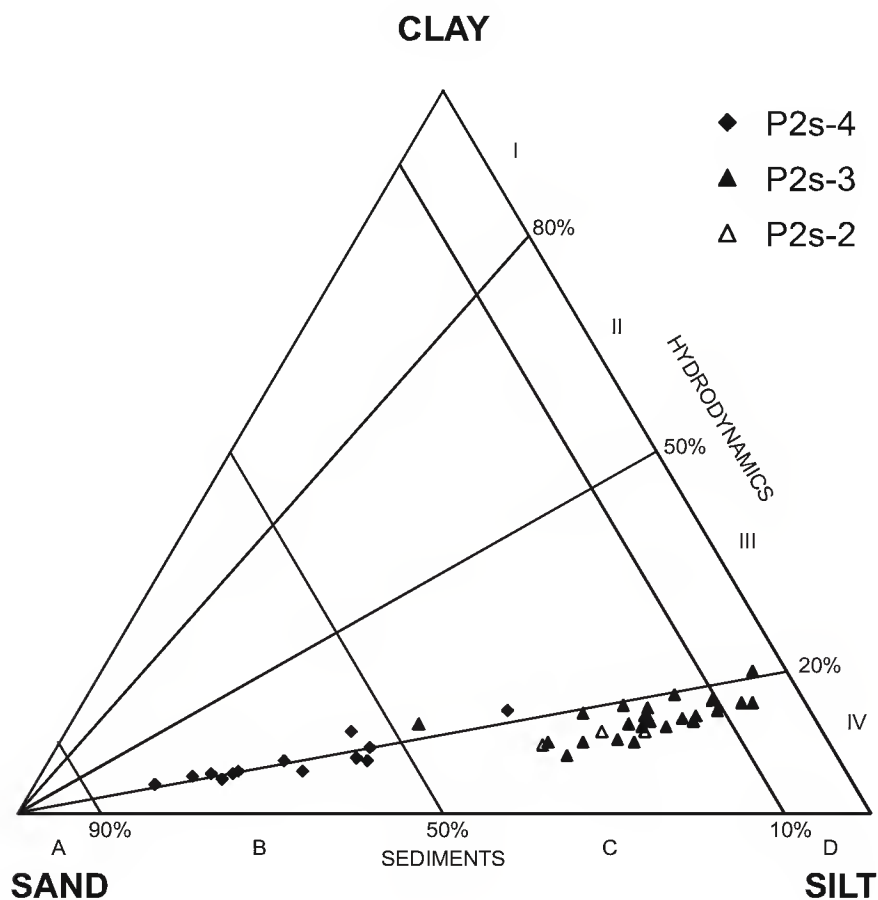


Figure 6.9. Pejrup ternary diagram: P2 sand/silt/clay data.

more strongly current dominated channel conditions. The P2s-4a samples plot within a graphical envelope which shows a different alignment to the other sample envelopes. This change of alignment results in an overall curvature to the envelope of all plotted samples. A reason for this graphical curvature may be posited, related to the different sources of sediment and corresponding modes of deposition occurring in the estuarine environment. In the most calm settings (e.g. saltmarsh, closed lagoon), particles are derived virtually exclusively from the settling of fine particles or aggregates out of suspension in the tidal water body. Mean grain size is small, and sediments are relatively well sorted (low coefficient of sorting). In transitional sub-environments (e.g. tidal flats, channel margin), sediments comprise a mixture of fine suspended particles and coarse grained bedload material; mean grain size is intermediate and sorting is relatively poor (increased coefficient of sorting). In the more dynamic settings under the influence of fluvial or tidal currents, the contribution of fine

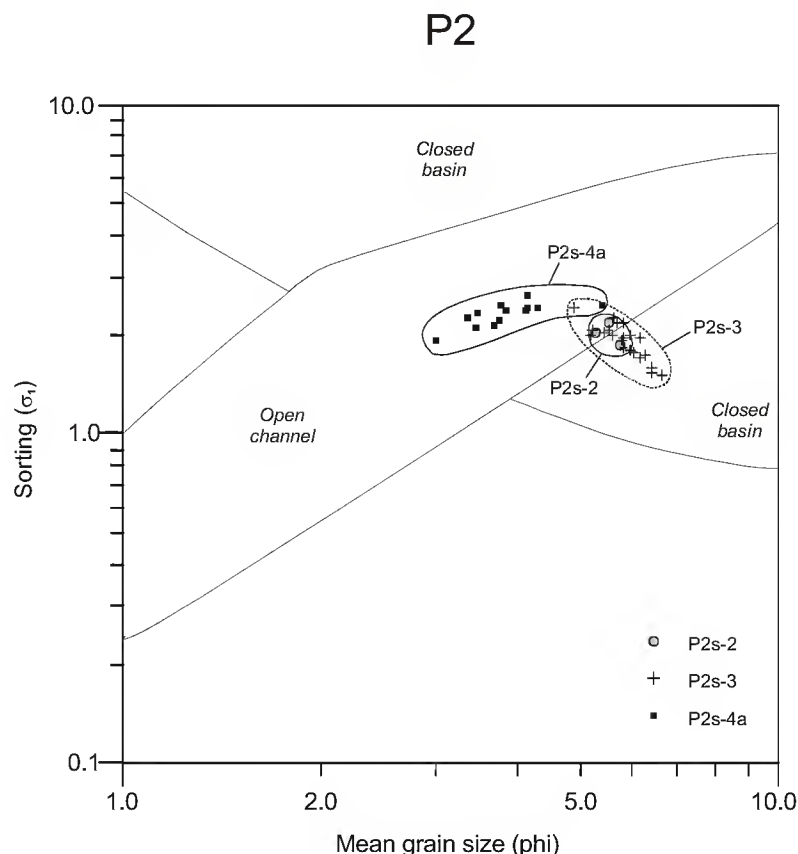


Figure 6.10. Biplot of mean grain size vs. sorting, P2. Graphic regions redrawn from Spencer et al. (1998).

grained particles is reduced, and current action may exert a slight winnowing effect on the finest particles; mean grain size is large and sorting may improve (decreased coefficient of sorting). These observations are an example of a widely recognised and robust set of relationships between sorting or dispersion and average (mean or median) grain size in natural environments (Griffiths, 1967).

6.3.3 Magnetic Susceptibility

Values for magnetic susceptibility in the range $5\text{--}225 \times 10^{-8} \text{ m}^3 \text{ kg}^{-1}$ indicate a magnetic mineral assemblage controlled by the varying concentration of ferrimagnetic minerals. Values for $\chi_{fd\%}$ indicate the presence of a mixture of frequency dependent and frequency independent

P2 Magnetic susceptibility and sand content

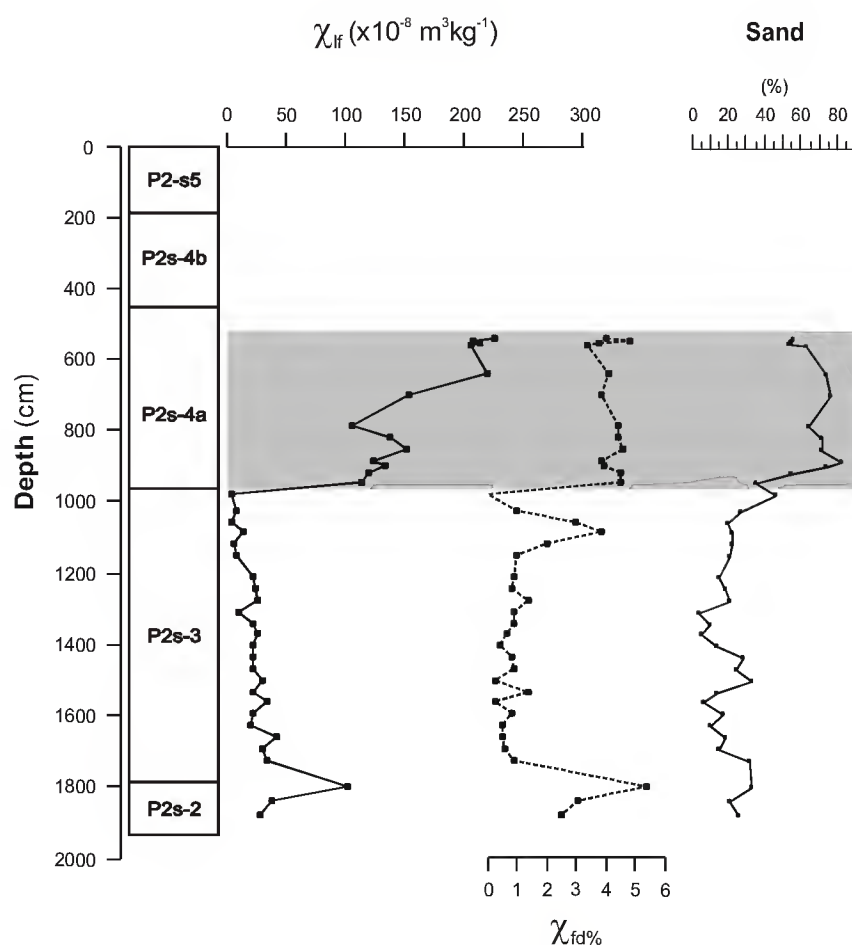


Figure 6.11. Comparison of χ_{lf} , $\chi_{fd\%}$ and sand content, P2. Shaded bands highlight sections of the core displaying an association of peaks in magnetic susceptibility and coarse grain

grains in P2s-2 and P2s-4, but of virtually no frequency dependent grains in P2s-3. The general association of higher values for χ_{lf} and $\chi_{fd\%}$ with the sandier core sections (laminated silty-sands in P2s-2, shelly sands in P2s-4a) suggests that the concentration of ferrimagnetic minerals may relate primarily to the input of terrestrial detrital material of fluvial origin. However, a diagenetic pattern may be superimposed onto the detrital record, reflecting major changes in the sedimentary geochemical environment between sandy and muddy bed settings.

The significant values for $\chi_{fd\%}$ towards the base of the core (P2s-2) and the peak in χ_{lf} below the P2s-2/3 boundary occur in a zone of laminated silty/sandy sediments and may relate to flood episodes bearing detrital magnetic minerals of terrestrial origin. In P2s-3, low values for χ_{lf} and $\chi_{fd\%}$ may be associated with a reduced fluvial input of terrestrial ferrimagnetic minerals (related to the transition to a low energy tidal environment). However, diagenetic effects may be of greater impact. The observation of iron sulphide particles in sediment samples from this zone indicates a reducing geochemical environment, consistent with radiocarbon evidence for high sedimentation rates. The dissolution of ferrimagnetic minerals such as magnetite and the formation of paramagnetic pyrite may account for the very low values of χ_{lf} observed in this zone, which border on the range in which paramagnetic minerals may control susceptibility values ($\sim 10 \times 10^{-8} \text{ m}^3$). At the top of P2s-3, a peak in $\chi_{fd\%}$ occurs which does not correspond with an increase in χ_{lf} . This peak may derive from a number of causes, and is not readily explained. The concentration of this peak within a narrow stratigraphic zone is suggestive of a localised authigenic or biogenic contribution (Snowball, 1991).

The contrast in χ_{lf} and $\chi_{fd\%}$ values between P2s-3 and P2s-4a corresponds with a shift from silty to sandy sediments in the upper part of the core (Figure 6.11). The association of the strongest susceptibility values and elevated sand content suggests that a detrital ferrimagnetic component associated with the coarse sediment fraction is detected in P2s-4a. However, the contrast between zones may be exaggerated by a shift from anoxic, reducing conditions

occurring at a muddy sediment/water interface under conditions of rapid sedimentation to oxidising conditions in an aerated substrate at a sandy sediment/water interface under reduced sedimentation rates. This shift would probably be associated with reduced diagenesis and better preservation of a ferrimagnetic mineral assemblage.

6.4 P5 Boina

6.4.1 Organic and carbonate content

The P5 sequence is characterised by a series of fluctuations in organic (LOI_{400}) and CaCO_3 (LOI_{950}) content. In the lower part of the sampled sequence (zones P5s-1, P5s-2), broadly parallel fluctuations in organic and carbonate content are observed, which relate to the contrasting lithological layers observed in this section of the core. In the samples from the basal fill (P5s-1), both organic and CaCO_3 content are very low. This is considered to reflect both long term diagenetic factors associated with exposure and weathering of the basal fill during the last Glacial cycle and a fluvial origin for the sediments. In zone P5s-2, variation in both organic and CaCO_3 content is closely related to lithological characteristics, notably grain size. Values for both parameters are high in the fine-grained layers of P5s-2a and P5s-2c, and reduced in the sandy deposits of P5s-2b and P5s-2d. Peak values for organic content in P5s-2c are associated with the observation of wood fragments in this sub-zone. The relation between LOI values and grain size may be conditioned by taphonomic factors related to the diagenesis of organic matter and carbonates in coarse grained deposits. However, the patterns are also likely to reflect changes in the local environment related to the biological activity in different substrates (sandy vs. muddy) and increased carbonate deposition during periods of enhanced tidal vs. fluvial influence.

In zone P5s-3, organic content is fairly stable, while CaCO_3 content increases. Increased CaCO_3 content in this zone is accompanied by the presence of an estuarine shell fauna and is considered to reflect an influence of open tidal/marine conditions. In P5s-4, CaCO_3 content is reduced, reflecting a decline in tidal influence. Organic content shows little change at the P5s-3/4 boundary.

6.4.2 P5 Particle Size

Particle size data from the P5 sequence suggest a dynamic sedimentary environment. Overall, the sequence displays a number of fluctuations between fine and coarse grained sedimentation. A wider range of particle sizes are encountered in the P5 core than the other sites, with a fine clay component towards the base of the core and gravel both in the lower and upper sections of the core. Distribution histograms for a selection of individual samples including the gravel fractions are shown in Figure 6.12, illustrating the complex and

P5

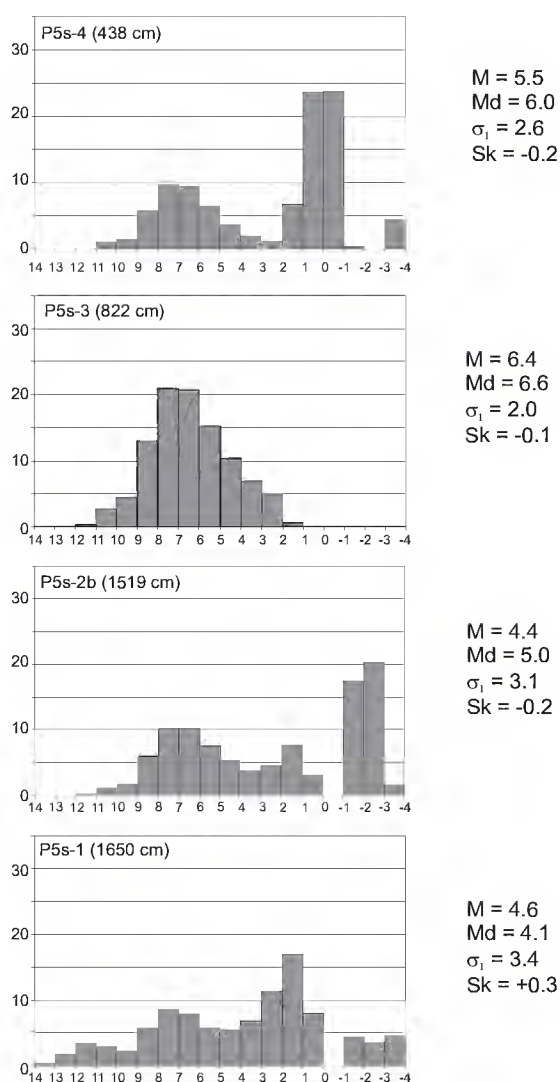


Figure 6.12. Histograms of particle size data for four samples from core P5. Summary statistics: M (mean grain size), Md (median grain size), σ_1 (inclusive graphic standard deviation, or sorting), Sk (inclusive graphic skewness).

frequently polymodal nature of the particle size distributions. A minor mode in the finer clay fractions (12 to 11 phi) is detected in the samples from the uppermost layers of the basal fill (P5s-1; e.g. 1650 cm). This fine clay component is not detected in any other zone, and is considered to reflect weathering processes. A consistent mode is observed in the fine silts (8 to 7 phi); this is the dominant mode in fine-grained samples from P5s-3 (e.g. sample 822 cm), P5s-2a and P5s-2c. This mode is considered to represent the central value for a population of clays and silts in the range 9 to 5 phi, probably representing fine particles deposited as part of aggregates. Superimposed on this population are inputs of sands and gravels of different sizes. Gravels occur towards the base of the core (P5s-2) and in the upper sections (part of P5s-3 and P5s-4), and provide evidence for high energy transport of bedload material of fluvial origin. Sands occur at several depths, and with peaks in different size classes. For example, sample 1519 cm (P5s-2b) displays a small population of grains

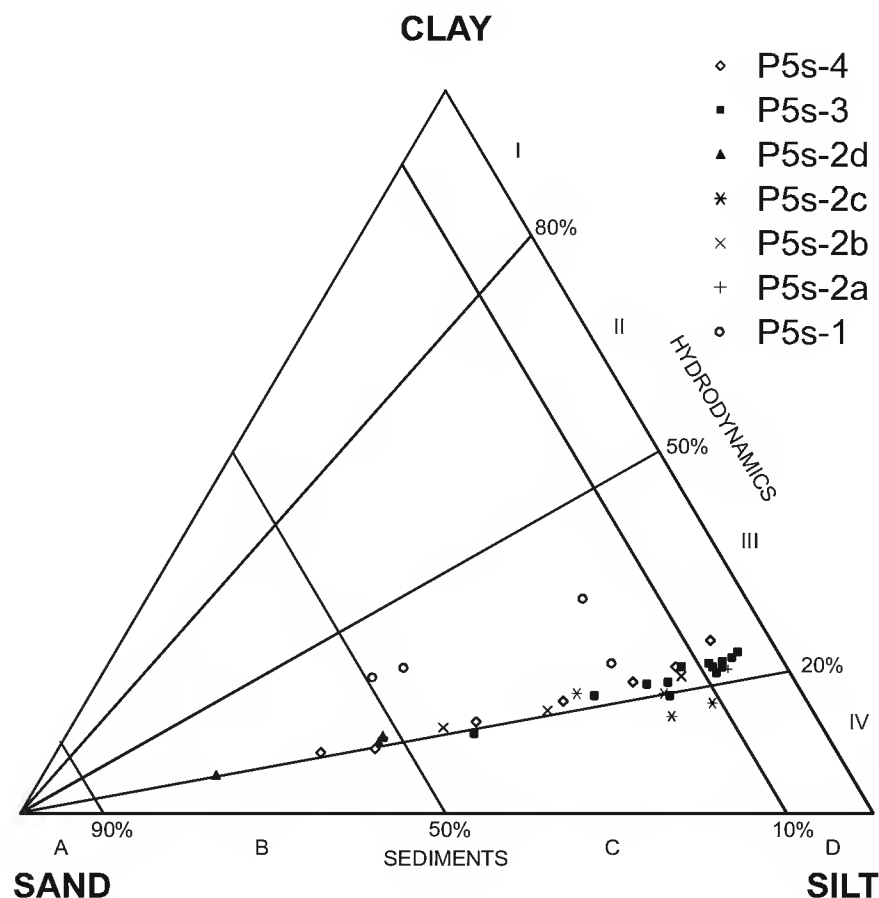


Figure 6.13. Pejrup ternary diagram: P5 sand/silt/clay data.

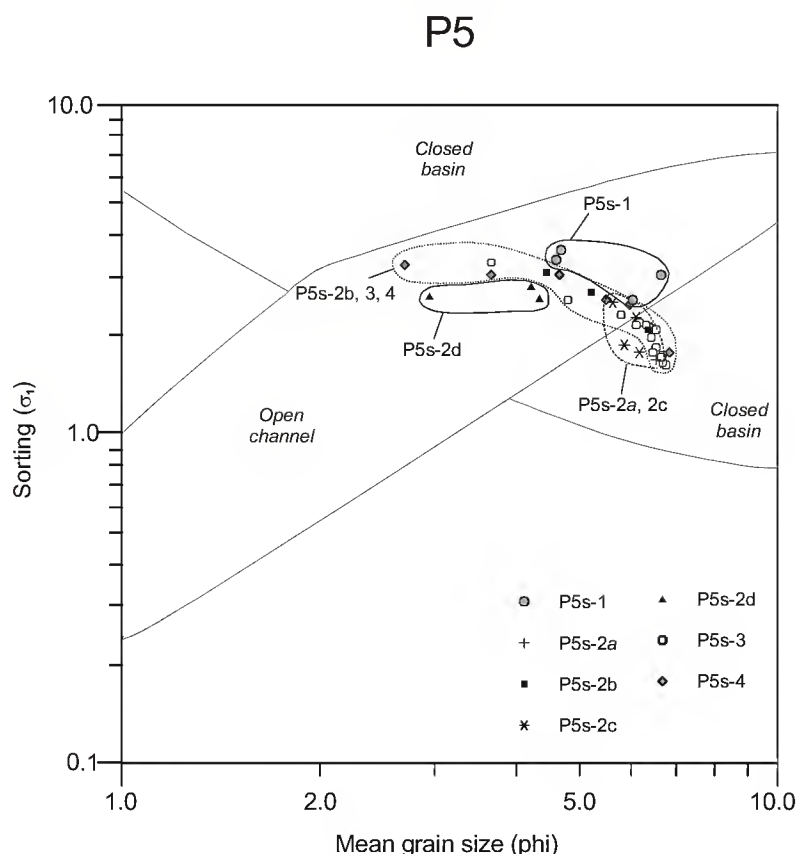


Figure 6.14. Biplot of mean grain size vs. sorting, P5. Graphic regions redrawn from Spencer et al. (1998).

with a mode in the medium sands (2 to 1 ϕ) in addition to a strong representation of fine gravel (-1 to -3 ϕ). Sample 438 cm (P5s-4) displays a well represented population of coarse to very coarse sands (1 to -1 ϕ). The variability in sand content and the presence of a significant gravel fraction at some depths is considered to reflect the periodic influence of fluvial events of varying energy.

The Pejrup diagram (Figure 6.13), illustrates that the majority of P5 samples display a fairly constant clay/silt ratio, with clay forming around 20–25% of the fine (silt and clay) fraction. This consistency supports the view that the particles in the cluster of grain size around the modal value of 8 to 7 ϕ represent an aggregated sedimentary component which is not subject to internal hydraulic sorting. Overall, the majority of samples fall on the

boundary of regions III and IV, suggesting moderate hydrodynamic energies associated with some breakage of flocs. Samples from P5s-1 fall outside the trend presented by the other samples. This highlights the distinct grain size distribution displayed by uppermost part of the basal fill (e.g. sample 1650 cm (Figure 6.12)) and is due to the high clay content of these samples. Variation in sand content is marked, even within zones.

The P5 biplot for mean grain size versus sorting (Figure 6.14) displays the most scattered distribution of data points compared with the other sites. Samples from zone P5s-1 plot within the ‘open channel’ region. Samples from subzones P5s-2a and P5s-2c fall within or close to the ‘closed basin’ region. Samples from zones P5s-2b, P5s-3 and P5s-4 plot across the boundary between closed basin and open channel, although the bulk of samples from P5s-3 fall within the closed basin region. These contrasts reflect a dynamic sedimentary environment with alternation of high- and low- energy sedimentary conditions.

6.4.3 P5 Magnetic susceptibility

High values for magnetic susceptibility are recorded in the P5 sequence, in the range 30–620 $\times 10^{-8} \text{ m}^3 \text{ kg}^{-1}$, indicating that ferrimagnetic minerals control the magnetic assemblage. Values for $\chi_{\text{fd}\%}$ are also significant, indicating a mineral assemblage containing a mixture of frequency dependent and frequency independent grains.

Peak values for χ_{lf} and $\chi_{\text{fd}\%}$ at the base of the core are associated with clay rich samples from the top of the basal gravel fill. The strong magnetic susceptibility of these sediments may be associated with weathering or pedogenetic processes, as these values are comparable with those reported from soils developed on terraces and colluvium in the Serra region of the Algarve (James & Chester, 1995).

For the overlying zones, the broad association of high values for χ_{lf} and elevated sand content (Figure 6.15) suggests a detrital source of magnetic minerals derived from catchment soils and sediments via the fluvial system. Peaks in χ_{lf} are associated with increases in sand content in zones P5s-2b, P5s-2d, P5s-3 and P5s-4. Following this interpretation, reduced values for χ_{lf} in the generally fine grained (silty) sections may be related to reduced input of

P5 Magnetic susceptibility and sand content

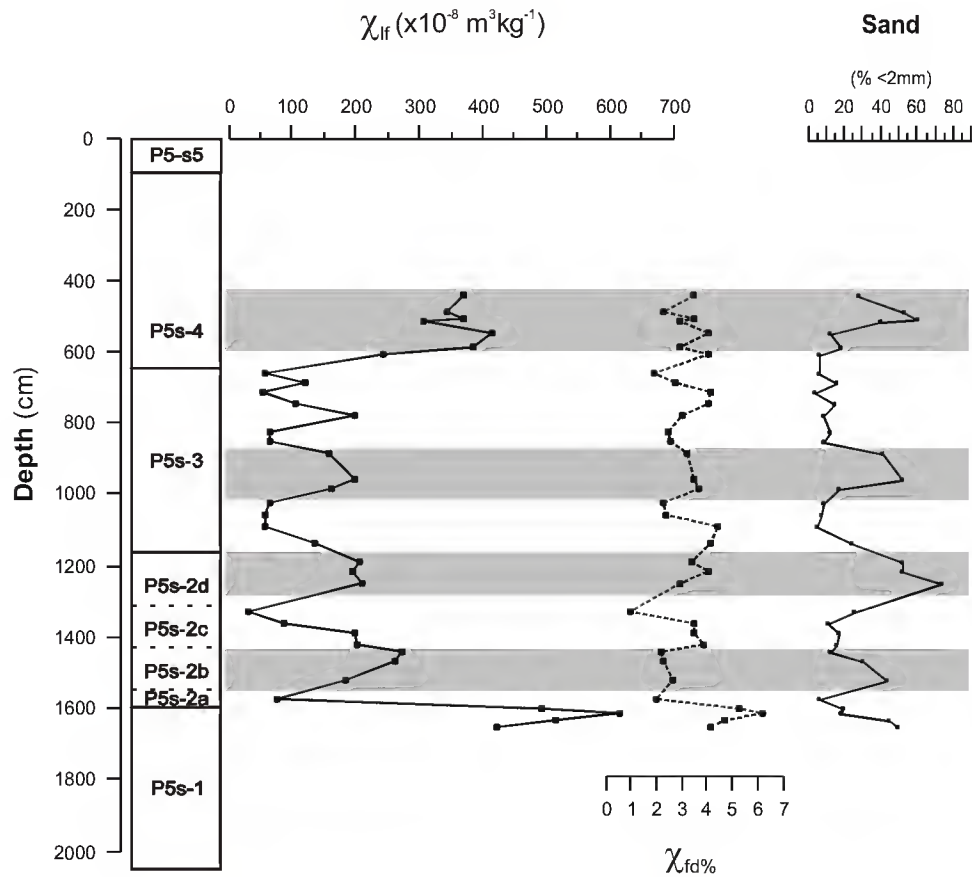


Figure 6.15. Comparison of χ_{lf} , $\chi_{fd\%}$ and sand content, P5. Shaded bands highlight sections of the core displaying an association of peaks in magnetic susceptibility and coarse grain sizes in the particle size distribution.

fluvially derived terrigenous material, combined with dilution of the magnetic signal through higher levels of diamagnetic organic matter and CaCO_3 . Peaks in $\chi_{fd\%}$ are not clearly associated with sand content, and this suggests that a population of superfine frequency dependent grains is present in concentrations independent of the influx of detrital ferrimagnetic minerals, possibly associated with biogenic sources (Oldfield & Yu, 1994).

Although the evidence for a detrital magnetic signature is fairly strong for the P5 sequence, diagenetic influences are probably also involved. The presence of authigenic iron sulphides in sediment samples from P5s-3 (observed during pollen preparations) means that the

ferrimagnetic mineral assemblage may have undergone dissolution and/or enhancement through the processes of magnetite diagenesis and greigite formation. As in each of the studied sites, the likelihood that changes in the sedimentary environment associated with broad changes from coarse to fine deposits were accompanied by changes in redox potential means that it may be difficult to fully distinguish detrital and diagenetic effects.

6.5 Characterisation of the infill sequences: summary

Loss-on-ignition data helps to characterise the composition of sediments. Overall, the infill sediments are highly minerogenic, with low organic matter and CaCO_3 content. Variations in sediment composition as determined by LOI are related to lithological characteristics of the sediment zones at each site. In general, fine-grained silty sediments show higher values for organic matter and CaCO_3 content. This pattern is partly related to hydrodynamic and taphonomic factors influencing the deposition and preservation of biogenic particles. However, the patterns are also considered to reflect changes in the biotic environment associated with changing substrate (sandy vs. muddy) and varying degrees of marine influence. These changes are assessed in light of pollen and other microfossil evidence in Chapter 9.

Particle size analyses help to identify changes in the energy conditions of the depositional environments. As shown by the examination of representative grain size histograms and Pejrup ternary diagrams, the entire range of grain sizes does not appear to be subject to hydraulic sorting. Instead, inter-sample differences relate to changing proportions of a population of fine grains with a mode in the silt classes (8–6 phi) and sands of different sizes. This is considered highly representative of a tidal environment, where the fines and sands are deposited during different parts of the tidal cycle (Dalrymple, 1992) and represent different modes of deposition (settling from suspension in aggregate particles vs. instantaneous deposition of single grains). Slight differences between the sites in the modal values of the fines population (7–6 phi for CM5 and P2, 8–7 phi for P5 Boina) may relate, as suggested by Pejrup (1988), to hydrodynamic influence on the stability of floccules, or

alternatively, to inherited characteristics related to sediment sources. The population of sands is more variable across the sites, and does suggest hydraulic sorting related to current strength and channel proximity. In the CM5 core, the sand content is predominantly very fine to fine (4–2 phi), and in general represents a small proportion of the sediment. This observation is consistent with a marginal location some distance from the main estuarine channel in a tributary valley. In the P2 core, the sand content is higher overall, and in the upper parts contains a large component of fine to medium sands (3–1 phi). In contrast with CM5, the P2 core site is located in a more central location within the Arade valley and must have been close to the main fluvial/estuarine channel throughout the period of infilling. In core P5, a range of coarse sediments, including both sands and gravels, are recorded. These provide evidence for much more direct fluvial sediment supply than at the other sites, and suggest the influence of a flashier fluvial regime within the catchment.

The sediment sequences show significant variability in magnetic susceptibility parameters. In general, a broad trend of higher susceptibility in coarse grained sediments and lower susceptibility in fine-grained sediments is observed at the sites. The discussion of the individual records has focussed on two explanations for this trend: first, that the concentration of ferrimagnetic minerals is dependent of the supply via fluvial sources of detrital minerals originating from rocks and soils in the drainage basin, and second, that the concentration of ferrimagnetic minerals is selectively and profoundly altered by reductive diagenesis in fine-grained transgressive sediments. The presence of iron sulphides in the fine-grained deposits supports the latter explanation. However, a combination of the two factors (high fluvial/terrigenous supply, sandy sedimentation, oxidising environment, high susceptibility vs. reduced fluvial/terrigenous supply, silty sedimentation, reducing environment, low susceptibility) is considered the best explanation. The factors which underlie the alternations between these two contrasting sedimentary/magnetic states are related to the development of the estuaries. This development is discussed in Chapter 9, drawing on the observations presented in this chapter, and insights from pollen analysis.

7 Pollen analysis results

7.1 Presentation of the pollen data

7.1.1 *Pollen types and nomenclature*

The pollen types observed in the course of analysis are listed in Table 7.1 by plant families in botanical order according to Flora Europea (Tutin *et al.*, 1964-1980). Although Flora Europea has been used as the reference for plant nomenclature, name changes in some plant families proposed for the British flora by Stace (1991) have become increasingly standard in much pollen analytical work and are increasingly being adopted more widely in other European floras. For these reasons, the following alternative family names are therefore used (in preference to their Flora Europea counterparts): Asteraceae (for Compositae); Brassicaceae (Cruciferae); Poaceae (Gramineae); Lamiaceae (Labiatae); Fabaceae (Leguminosae); and Apiaceae (Umbelliferae).

The pollen types encountered are also presented in alphabetical order in Appendix B, accompanied by sources for the definition and description of pollen types, notes on likely species which may be represented by the pollen types and their general ecological habitat. Plant nomenclature for generic and specific names follows Flora Europea. The notes on habitat preferences of the likely contributory species are based on a wide range of sources

Chapter 7 - Pollen Analysis Results

Family	Taxon	Family	Taxon
Selaginellaceae	<i>Selaginella denticulata</i>		<i>Helianthemum salicifolium</i> type
Isoetaceae	<i>Isoetes histrix</i>		<i>Tuberaria guttata</i> type
	<i>Isoetes</i> undiff.		Cistaceae undiff.
Ophioglossaceae	<i>Ophioglossum lusitanicum</i>		<i>Halimium/Tuberaria</i>
Osmundaceae	<i>Osmunda regalis</i>	Tamaricaceae	<i>Tamarix</i>
Sinopteridaceae	<i>Cheilanthes catanensis</i>	Frankeniaceae	cf. <i>Frankenia laevis</i> type
Gymnogrammeaceae	<i>Anogramma leptophylla</i>	Lythraceae	<i>Lythrum salicaria</i> type
Polypodiaceae	<i>Polypodium vulgare</i> type	Myrtaceae	<i>Myrtus</i>
Marsileaceae	<i>Pilularia globulifera</i>		<i>Eucalyptus</i>
Class Pteropsida	monolete undiff.	Haloragaceae	<i>Myriophyllum alterniflorum</i>
	trilete undiff.		<i>Myriophyllum spicatum</i>
Pinaceae	<i>Pinus</i> (Diploxylon type)	Araliaceae	<i>Hedera helix</i>
Cupressaceae	<i>Juniperus</i>	Apiaceae	<i>Apium inundatum</i> type
Ephedraceae	<i>Ephedra distachya</i> type		<i>Eryngium</i>
	<i>Ephedra fragilis</i> type		Apiaceae undiff.
Salicaceae	<i>Salix</i>	Ericaceae	<i>Erica arborea</i> type
Myricaceae	<i>Myrica</i>		<i>Erica australis</i> type
Betulaceae	<i>Betula</i>		<i>Erica scoparia</i> type
	<i>Alnus</i>		<i>Erica umbellata</i> type
Corylaceae	<i>Corylus</i>		<i>Erica erigena</i> type
Fagaceae	<i>Castanea</i>		<i>Arbutus unedo</i>
	<i>Quercus coccifera</i> type		<i>Calluna vulgaris</i>
	<i>Quercus suber</i> type		<i>Rhododendron ponticum</i>
	<i>Quercus deciduous</i> type		Ericaceae undiff.
	<i>Quercus</i> undiff.	Primulaceae	<i>Anagallis arvensis</i> type
Ulmaceae	<i>Ulmus</i>		<i>Anagallis tenella</i> type
Polygonaceae	<i>Rumex acetosa</i> type		<i>Samolus</i>
	<i>Rumex acetosella</i> type	Plumbaginaceae	<i>Ameria/Limonium</i>
	<i>Rumex</i> undiff.	Oleaceae	<i>Fraxinus</i>
	<i>Polygonum aviculare</i> type		<i>Olea</i>
	<i>Polygonum persicaria</i> type		<i>Phillyrea</i>
Chenopodiaceae	Chenopodiaceae	Gentianaceae	<i>Cicendia filiformis</i>
Caryophyllaceae	<i>Spergula</i> type		<i>Centaureum</i>
	<i>Illecebrum verticillatum</i> type	Rubiaceae	<i>Galium</i> type
	<i>Herniaria</i> type	Convolvulaceae	<i>Convolvulus</i>
	Caryophyllaceae undiff.	Boraginaceae	<i>Echium</i>
	Caryophyllaceae trizonocolpate indet.		<i>Cynoglossum</i>
Nymphaeaceae	<i>Nymphaea</i>		Boraginaceae undiff.
	<i>Nuphar</i>	Callitrichaceae	<i>Callitriche</i>
Ranunculaceae	<i>Ranunculus</i> type	Lamiaceae	<i>Stachys sylvatica</i> type
Papaveraceae	<i>Fumaria officinalis</i> type		<i>Teucrium</i>
	<i>Hypecoum</i>		Lamiaceae (6-colpate)
	<i>Papaver rhoeas</i> type	Scrophulariaceae	<i>Linaria</i>
Brassicaceae	Brassicaceae		<i>Scrophularia</i> type
Crassulaceae	Crassulaceae	Plantaginaceae	<i>Plantago albicans</i> type
Rosaceae	<i>Sanguisorba minor</i>		<i>Plantago coronopus</i> type
	<i>Alchemilla</i> type		<i>Plantago lanceolata</i> type
	Rosaceae undiff.		<i>Plantago major</i> type
Fabaceae	<i>Coronilla</i> type		<i>Plantago</i> undiff.
	<i>Ulex</i> type	Caprifoliaceae	<i>Sambucus ebulus</i>
	<i>Lotus</i> type		<i>Viburnum linus</i> type
	<i>Trifolium</i> type	Valerianaceae	<i>Valerianella</i>
	<i>Ononis</i> type	Dipsacaceae	<i>Scabiosa colombaria</i> type
	<i>Onobrychis</i> type	Campanulaceae	<i>Jasione montana</i> type
	Fabaceae undiff.	Asteraceae	<i>Artemisia</i>
Oxalidaceae	<i>Oxalis pes caprae</i>		<i>Aster</i> type
Geraniaceae	<i>Geranium</i>		<i>Anthemis</i> type
	<i>Erodium</i>		<i>Cirsium</i> type
Linaceae	<i>Linum bienne</i> type		<i>Centaurea nigra</i> type
	<i>Linum catharticum</i> type		<i>Centaurea</i> , type unknown
	<i>Linum</i> undiff.		<i>Serratula</i> type
	<i>Radiola</i>		Asteraceae (Asteroideae/Cardueae) undiff.
Euphorbiaceae	<i>Euphorbia</i>		<i>Amoseris minima</i> type
	<i>Mercurialis</i> cf. <i>annua</i>		Asteraceae (Lactucaceae)
	<i>Mercurialis</i> cf. <i>tomentosa</i>		
Anacardiaceae	<i>Rhus</i>	Alismataceae	<i>Alisma</i>
	<i>Pistacia</i>	Potamogetonaceae	<i>Potamogeton</i> subg. <i>Potamogeton</i>
Aceraceae	<i>Acer campestre</i> type	Liliaceae	<i>Asphodelus</i>
Aquifoliaceae	<i>Ilex aquifolium</i>		<i>Colchicum</i>
Rhamnaceae	<i>Rhamnus</i>		Liliaceae undiff.
Vitaceae	<i>Vitis vinifera</i>	Iridaceae	<i>Gynandris sisyrinchium</i>
Malvaceae	Malvaceae	Poaceae	Poaceae
Thymelaeaceae	<i>Daphne</i>		Poaceae D>38 P>8
Cistaceae	<i>Cistus albidus</i> type	Palmae	<i>Chamaerops</i>
	<i>Cistus ladanifer/populifolius</i> types	Lemnaceae	<i>Lemna</i>
	<i>Cistus monspeliensis</i> type	Typhaceae/Sparganiaceae	<i>Typha/Sparganium</i>
	<i>Halimium halimifolium</i> type	Typhaceae	<i>Typha latifolia</i> type
	<i>Helianthemum croceum</i> type	Cyperaceae	Cyperaceae

Table 7.1. List of pollen and spores identified in the CM5, P2 and P5 cores by family.

(including Coutinho, 1939; Tutin *et al.*, 1963-1980; Polunin & Smythies, 1973; Malato Beliz, 1982; Rivas-Martínez, *et al.*, 1990; Mabberley & Placito, 1993) and from observations in the study areas. The information in Appendix B underlines the decisions made regarding the construction of the pollen diagrams and the interpretation of the pollen records.

7.1.2 Construction of the pollen diagrams

The pollen sum is the basis for the calculation of pollen percentages. “The establishment of the pollen sum is a very important step in any percentage analysis, as it defines the question asked in the investigation and consequently the framework for the possible answers” (Faegri & Iversen, 1989: 4). As a general rule, only those taxa relevant to the research question should be included in the pollen sum, which means that different research questions presume different pollen sums. In this study, three research questions are posed of the pollen data. First, what changes occurred in the regional vegetation and landscape during the period of estuarine infilling? Second, what changes in the vegetation of wetland environments were occasioned during the evolution of the estuaries? Third, does the composition of the total assemblage of pollen and spores reflect changes in pollen transport and pollen source areas? In most pollen analysis, the first (and to a lesser extent the second) question generally dominates the research focus. However, in the study of pollen from a complex, dynamic sedimentary environment, the third question is also critical. The aim of answering these questions provides the rationale behind the construction of the diagrams.

In order to answer the first research question, it is necessary to calculate pollen percentages on the basis of a pollen sum which excludes taxa which are constituents of a local flora occurring within the depositional environment. In current lacustrine studies, the most frequently used basis for modern percentage pollen diagrams is a main sum including all pollen and spores and excluding aquatics (Moore *et al.*, 1991). This basis, however, may be unsuitable for estuarine and tidal sites where the abundance of pollen derived from a wider range of local plants may be very great and may fluctuate widely. Pollen types such as Poaceae (grasses), Cyperaceae (sedges), Chenopodiaceae (goosefoot family) and Asteraceae (daisy family) are typically abundant in pollen records from marshes, mudflats and other

tidal wetlands, reflecting a pollen input from local vegetation. This over-representation has been documented in a number of studies (e.g. Andrieu-Ponel *et al.*, 2000; Freund *et al.*, 2004) and was noted in a preliminary assay of the pollen content of surface samples from the Beliche floodplain near the location of core CM5 (Appendix A). The inclusion of local taxa in the pollen sum may preclude the identification of a regional signal of pollen from dry ground environments. At best, percentage values for dry ground or upland taxa will be suppressed; at worst, important changes may be concealed, and artefacts in the pollen percentage curves may arise from the varying input of local types resulting from changes in the local environment (Clark & Patterson, 1985; Santos *et al.*, 2001). A method for dealing with the problem of local overrepresentation is to define a more restricted pollen sum which includes only taxa of dry land environments. Percentage values for taxa within this restricted pollen sum are then isolated from the effects of overrepresentation of wetland pollen types. This approach has been employed in a range of settings, including tidal marshes (Clark & Patterson, 1985) and coastal lagoons (Mateus, 1992), as well as lake basins (Van den Brink & Janssen, 1985; Van der Knaap & van Leeuwen, 1995).

In order to answer the second research question, taxa excluded from a restricted main sum of dry ground taxa are generally presented either in a separate pollen diagram of local taxa or as an extension of the main diagram, with percentage values calculated relative to the restricted main sum. These percentages may be calculated in slightly different ways, of which the most common is either relative to the main sum of dry land pollen plus the individual taxon sum or relative to the main sum plus the sum of a group of excluded taxa (e.g. marsh aquatics) (Bennett & Willis, 2001). Changes in the proportions of local or wetland taxa relative to the restricted main sum may then be assessed in terms of changes in the environment within the depositional basin.

Certain problems are attendant in the construction of diagrams based on a main sum where many taxa are excluded. The basis for inclusion or exclusion may not be straightforward, especially with regard to taxonomically broad pollen types. Also, the robustness of the

restricted sum depends on the complexity of pollen transport pathways into the basin. Where dry ground taxa chiefly reflect an airborne pollen rain deposited uniformly and more or less continuously across the basin, a restricted sum of these types provides a useful benchmark for the calculation of all percentage values. However, in the estuarine setting, where pollen may derive chiefly from fluvial sources and where pollen of both local and regional vegetation may be redistributed within the tidal water body, a restricted sum of dry ground types may not provide as robust a basis for the calculation of all percentages. This leads to the third research question, which is more securely addressed by inspection of the proportions of pollen taxa with respect to the entire pollen assemblage (and also by inspection of pollen concentration values).

A dual calculation of pollen percentages on the basis of both the total sum of pollen and spores and separate partial sums, as described by Rybníèková & Rybníèek (1971), provides an elegant and intuitive way of addressing all three research questions. Percentage values are calculated for each taxon in two ways, on the basis of 1) the total sum of all pollen and spores, and 2) separate sums totalling 100% for dry ground and wetland taxa (partial sums). The two percentage values for each taxon can then be shown as a dual curve on the pollen diagrams, permitting the proportion of any taxon with respect to both the entire assemblage and the appropriate ecological group to be viewed easily. The percentage values for dry ground taxa based on the partial sum (of dry ground taxa only) are comparable to those shown in diagrams based on restricted main sums of regional pollen types (e.g. Mateus, 1992). These values should provide the best indication of vegetation composition in the wider landscape. The percentage values for wetland taxa based on the partial sum (of wetland taxa only) should provide the best indication of changes in wetland habitats, especially those in the vicinity of the coring site. The percentage values for all taxa based on the total sum provide a straightforward description of the proportional composition of the entire pollen assemblage, and as such, are comparable with those presented by researchers who regard the exclusion of any taxa from the sum with suspicion (e.g. Pons & Reille, 1988). Finally, the relation between the two percentage values as observed in the dual curves

illustrates certain features of the pollen which would otherwise be difficult to explain. This method was used by Rybnièková & Rybnièek to deal with the overrepresentation of local pollen elements in organogenic peat deposits. A similar approach was taken by Heyvaert (1980), who demonstrated the value of using multiple pollen sums in the study of pollen samples from surface muds of the Somme and Pas-de-Calais estuaries.

In this study, a basic division of the pollen and spore taxa into two groups has been made. The first group, “dry ground taxa”, includes only pollen types derived from plants that in all likelihood inhabited dry land environments above the tidal frame and above the level of ground-water. This group includes upland forest taxa and associated understorey shrubs, shrub taxa of heath, moor and scrub communities, and herbaceous taxa of dry ground habitats. The second group, loosely defined as “wetland taxa”, includes those pollen types which may be derived from plants growing in wetland habitats within the estuary and the fluvial domain. In addition to the aquatic taxa which are commonly excluded from the main pollen sum in most pollen studies (e.g. *Nymphaea*, *Potamogeton*), this group includes many other damp ground taxa and ambiguous pollen types. The pollen and spore taxa included in this group fall into three general categories, namely: 1) pollen and spore types representing a single or limited number of contributory species and derived with certainty from wetland habitats, e.g. *Alnus*, *Myriophyllum alterniflorum*; 2) pollen types representing numerous contributory species derived chiefly, though not uniquely from wetland sources, e.g. Chenopodiaceae, Cyperaceae, Poaceae; 3) ecologically ambiguous pollen types representing numerous contributory species from both wetland and dry ground habitats, e.g. Apiaceae undiff.. The main emphasis in the definition of the two groups is on the ecology of the pollen types (dry ground vs. wetland) rather than on distance from the pollen source (i.e. local vs. regional *sensu* Janssen (1966)). This is because the definition of source areas and transport pathways for estuarine pollen is complex. These issues are discussed in detail with regard to the interpretation of the pollen data in Chapter 8.

Percentage values for all pollen and spore types are calculated in two ways. First, percentages for all taxa are calculated on the basis of the total sum of all pollen and spores. Second, percentages are calculated for dry ground taxa on the basis of the partial sum of dry ground taxa, and for wetland taxa on the basis of the partial sum of wetland taxa. On the pollen diagrams a dual curve is presented for each taxon, with the percentage of the total sum shown in a solid (shaded) curve, and the percentage of the partial sum shown in an open (not shaded) curve. Taxa which occur only in low frequencies and which do not exceed 1% of the partial sum are indicated only by a symbol (+). This method has the advantage that both the composition of the overall pollen assemblage and the abundance of taxa with regard to the appropriate dry ground or wetland group are readily observed. Percentage values for reworked trilete spores, indeterminate pollen grains, and non-pollen microfossils such as dinoflagellates and algae are calculated relative to the total sum of pollen and spores plus the individual sum for that taxon.

7.1.2.1 A note on *Isoetes* undiff.

Spores of *Isoetes* (recorded under the pollen type *Isoetes* undiff.) were recorded in great abundance in core CM5. During the sieving stage of pollen preparation, *Isoetes* megaspores were encountered at several depths. It is not known whether the breakdown of fossil megaspores during pollen preparation can liberate additional microspores, although this might partly account for the tremendous abundance of microspores in some of the pollen samples, reaching up to 6 times the total pollen and spore count. Certainly, the presence of megaspores and the abundance of microspores reflects a local presence (*sensu* Janssen 1966) of *Isoetes* plants. In order to prevent the total depression of percentage values for other wetland taxa, *Isoetes* undiff. is excluded from the sum of wetland taxa for the CM5 samples. A pseudo-percentage value (i.e. a percentage value of a total sum of which *Isoetes* undiff. is not actually part) is calculated relative to the total sum of pollen and spores and the partial sum of wetland taxa. These “percentages” shows the abundance of *Isoetes* undiff. relative to other pollen and spores (e.g. 200% equals twice as abundant). Although this practice is generally not recommended (Faegri & Iversen, 1989: 125), it works well in this

case for an extremely abundant taxon which would dominate any sum of which it were a part.

7.1.3 Order of taxa in the diagrams

In the pollen diagrams, dry ground taxa are shown first, followed by wetland taxa. In order to assist the interpretation of the pollen records, taxa are arranged within the diagrams in floristic groups according to likely habitat or vegetation type. Dry land taxa are arranged with forest taxa first, followed by taxa of thickets, scrub and heath, followed by dry ground herbaceous taxa. Two family groups, the Cistaceae and Ericaceae, are grouped together for easy comparison of the types. It should be noted that *Tuberaria guttata* type, which represents herbaceous annual species of the Cistaceae family, is included with shrub taxa. In practice, this overall order approximates the traditional approach where pollen types are arranged according to life-form (i.e., trees, shrubs and herbs). The wetland taxa are arranged in floristic groups reflecting different wetland habitats. Ecologically ambiguous taxa of possible wetland origin are shown first, followed by groups representing saltmarsh, aquatic, riparian and flooded ground vegetation.

7.1.4 Summary diagrams

It is customary to present a summary diagram showing the proportions of arboreal pollen (AP) vs. non-arboreal pollen (NAP) or the proportions of trees, shrubs and herbs to accompany the detailed or resolved diagram of individual pollen curves. However, these divisions are not straightforward for a Mediterranean-type flora where many plants may occur in different growth forms (i.e. tree or shrub) under different edaphic and anthropic pressures. The shrub category is especially very varied, including plants ranging in size from small trees 4-6 m in height to prostrate and dwarf shrubs less than 0.5 m in height. A slightly modified version of the traditional summary diagram is presented, with four categories: trees, tall shrubs / small trees, shrubs and herbs. The taxa included in each summary category are shown in Table 7.2, except for herbs, which simply include all the taxa grouped as dry ground herbs in the pollen diagram. The intermediate category (tall shrubs / small trees) includes certain taxa which do not clearly belong to a tree or shrub

Chapter 7 - Pollen Analysis Results

Summary group	Taxa	Summary group	Taxa
Trees	<i>Acer campestre</i> type	Shrubs, cont.	<i>Coronilla</i> type
	<i>Betula</i>		<i>Onobrychis</i> type
	<i>Castanea</i>		<i>Ononis</i> type
	<i>Ilex aquifolium</i>		<i>Ulex</i> type
	<i>Pinus</i>		Lamiaceae (6-colpate)
	<i>Quercus deciduous</i> type		Cistaceae undiff.
	<i>Quercus suber</i> type		<i>Cistus albidus</i> type
	<i>Quercus undiff.</i>		<i>Cistus ladanifer/populifolius</i> types
Tall shrubs/ small trees	<i>Arbutus unedo</i>		<i>Cistus monspeliensis</i> type
	<i>Corylus</i>		<i>Halimium halimifolium</i> type
	<i>Juniperus</i>		<i>Halimium/Tuberaria</i>
	<i>Myrtus</i>		<i>Helianthemum croceum</i> type
	<i>Olea</i>		<i>Helianthemum salicifolium</i> type
	<i>Phillyrea</i>		Ericaceae undiff.
	<i>Pistacia</i>		<i>Erica arborea</i> type
	<i>Quercus coccifera</i> type		<i>Erica australis</i> type
	<i>Viburnum tinus</i>		<i>Erica scoparia</i> type
Shrubs	<i>Hedera helix</i>		<i>Erica umbellata</i> type
	<i>Rhamnus</i>		<i>Rhododendron ponticum</i>
	<i>Chamaerops</i>		<i>Calluna vulgaris</i>
	<i>Rhus</i>		<i>Ephedra distachya</i> type
	<i>Daphne</i>		<i>Ephedra fragilis</i> type

Table 7.2. Classification of tree and shrub taxa for the purposes of summary diagrams.

category, taking on a tree-like stature as part of woodland understorey but also occurring as shrubs. Although a great emphasis is not placed on the interpretive value of the summary diagrams, distinctive behaviour of the separate categories is noted at the three sites.

7.1.5 Pollen zonation

To aid description of the pollen diagrams, clusters of similar pollen spectra are grouped together into site-specific pollen assemblage biozones. These zones, based purely on the pollen data and defined without reference to timescale or sediment stratigraphy, are considered biostratigraphical units, and are referred to here as biozones. Biozones are labelled with the core prefix (CM5-, P2-, P5-) and numbered in Roman numerals from the base upwards.

RESULTS OF CONISS ZONATION

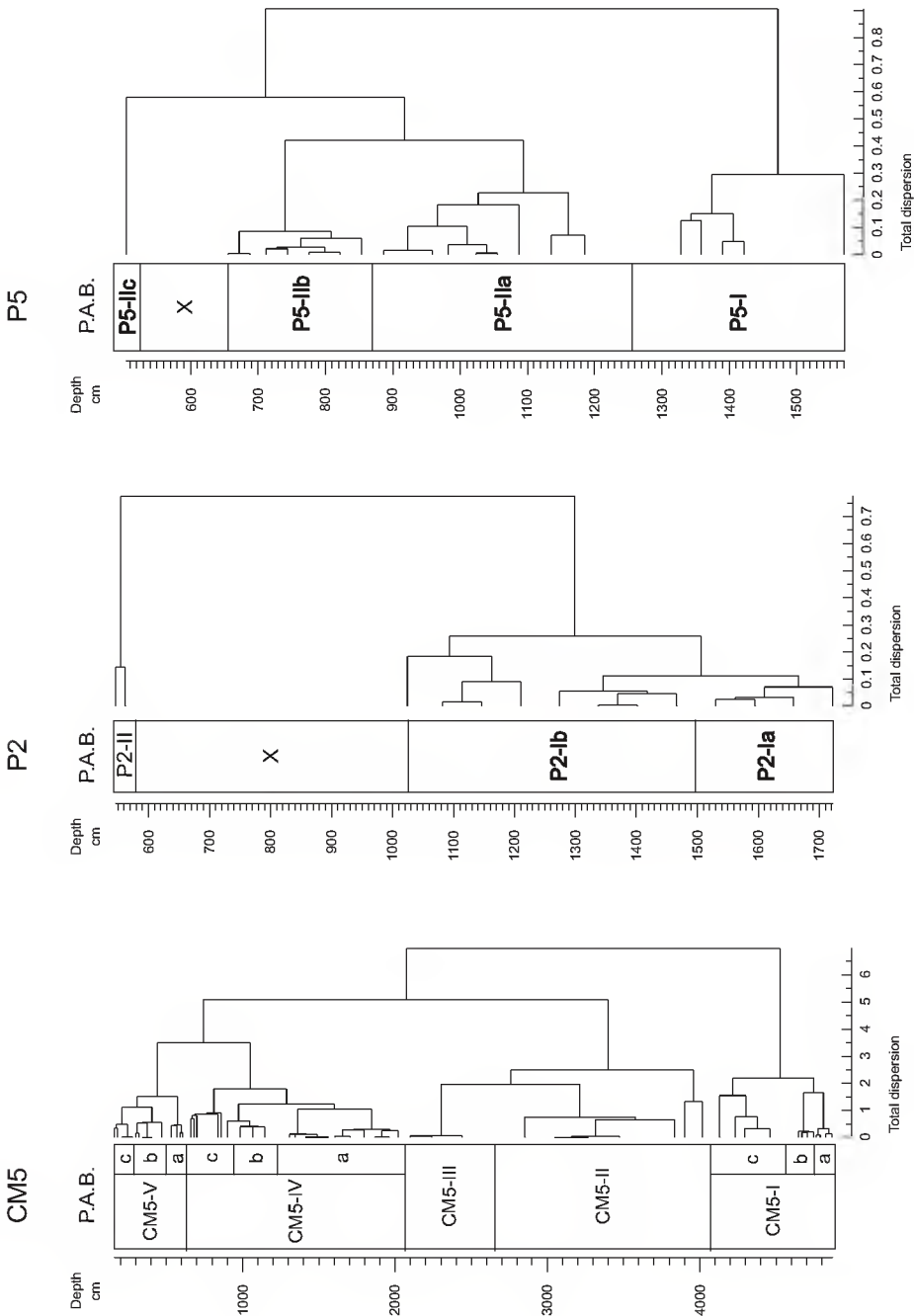


Figure 7.1. The placement of pollen assemblage biozone (P.A.B.) boundaries based on CONISS cluster analysis.

The construction of biozones was aided by stratigraphically constrained incremental sum-of-squares cluster analysis, or CONISS (Grimm, 1987), implemented in the software program Psimpoll (Bennett, 1994; version 4.10). Zonation was conducted on percentage values for all taxa based on the total sum of pollen and spores. (Experimentation with separate zonation of the dry ground and wetland data showed that most zone boundaries fell at or near the same depths for both data sets, and that a separate zonation scheme would create a confusing and redundant set of zone labels.) Only taxa occurring at values >5 % were included, with percentage values recalculated as proportions of the new sum. The included taxa are shown in Table 7.3. Cluster analysis was performed based on Edwards and Cavalli-Sforza's chord distance and square-root transformation of the data. Experimentation with setting a lower percentage value for inclusion of taxa (3%) resulted in no significant changes in the main clusters. Experimentation with transformations suggested that without upweighting of the less abundant taxa by square-root transform some clusters reflected only one or two dominant taxa. The results of CONISS clustering are shown in Figure 7.1. In general, zone boundaries correspond to the midpoints between clusters identified as statistically significant by the broken-stick method (described in Bennett, 1996), and sub-zone boundaries correspond to clusters observed in the CONISS output which may not be statistically significant. This rule has not been followed absolutely strictly; the final placement of zone and sub-zone boundaries was decided in light of the nature and possible ecological significance of changes in the pollen record, and also by the aim to avoid zones with only one or two samples. In the P2 and P5 cores, this last aim could not be fulfilled due to intermittent pollen preservation; the need for further sampling in some core sections is stressed in the description of the results.

7.2 Description of the pollen results

The following section presents a zone by zone description of the pollen results to accompany the pollen percentage diagrams and concentration summaries (Figures 7.2 to 7.9, located at the end of the chapter). Percentage values mentioned in the description of pollen frequencies refer to the open curves on the diagrams (percentages of the partial sums of dry ground/

Taxon
<i>Pinus</i> ^{1,2,3}
<i>Quercus suber</i> type ¹
<i>Quercus deciduous</i> type ^{1,2}
<i>Quercus</i> undiff. ^{1,3}
<i>Quercus coccifera</i> type ^{1,2,3}
<i>Myrtus</i> ^{1,3}
<i>Cistus ladanifer/populifolius</i> types ¹
Ericaceae undiff. ^{1,2}
<i>Calluna</i> ²
<i>Plantago coronopus</i> type ¹
Asteraceae (Lactucaee) ^{1,2,3}
<i>Artemisia</i> ¹
<i>Aster</i> type ¹
Poaceae ^{1,2,3}
<i>Alnus</i> ^{2,3}
Cyperaceae ^{1,2,3}
<i>Isoetes</i> undiff. ^{2,3}
<i>Isoetes hystrix</i> type ¹
<i>Ophioglossum lusitanicum</i> ¹

¹ CM5 Guadiana, ² P2 Arade, ³ P5 Boina

Table 7.3. Taxa occurring at >5% of total pollen and spores and included in CONISS.

wetland taxa). Where necessary, specific attention is drawn to the percentages of the total sum.

7.2.1 CM5 Guadiana

The pollen contained within the CM5 core is characterised by variable preservation states. In general, the condition of pollen and spores at the base of the core, (corresponding to sediment zone CM5s-2) and in the upper part (corresponding to sediment zones CM5s-5/6)

Depth (cm)	Taxon
160	<i>Frankenia laevis</i> type
210	<i>Ilex aquifolium</i>
320	<i>Herniaria</i> type
320	<i>Valerianella</i>
590	<i>Gynandriris sisyrinchium</i>
660	<i>Jasione montana</i> type
700	<i>Sambucus ebulus</i>
1305	<i>Rhus</i>
1565	<i>Scrophularia</i> type
2100	<i>Corylus</i>
2240	<i>Teucrium</i>
4706	<i>Convolvulus</i>
4745	<i>Viburnum tinus</i>
4762	<i>Halimium/Tuberaria</i>

Table 7.4. Taxa occurring in only one sample, CM5.

is good. However, in the middle part (corresponding to CM5s-3 and CM5s-4), the condition of pollen is much poorer. This contrast is reflected in less diverse pollen spectra for the middle section. Also, in some layers, the combination of low concentration and poor preservation meant that counts reaching the desired sum of 200 dry ground pollen were not possible.

The pollen diagrams (Figure 7.3 percentage data, Figure 7.4 concentration data) shows the results of analysis of 54 samples. Taxa occurring in only one sample are not shown in the diagram and are listed in Table 7.4

Five biozones and 9 sub-zones are distinguished in the CM5 pollen record:

CM5-I: 4865–4073 cm (13000–11860 cal BP)

In terms of the dry ground taxa, CM5-I is characterised by generally high values for *Pinus* (>25 %) and fluctuating frequencies of *Quercus* pollen types. Moderate to high values for Sum Cistaceae (chiefly pollen of *Cistus ladanifer/populifolius* types, *Helianthemum croceum* type, and Cistaceae undiff.), and low values for Sum Ericaceae are recorded. The biozone is characterised by elevated values for *Juniperus* pollen (~5 %), and the presence of *Ephedra distachya* and *Centaurea nigra* types. Among the wetland taxa, *Artemisia*, Chenopodiaceae, *Aster* type and Poaceae are dominant.

On the basis of changes in both the dry ground and wetland taxa, three subzones are defined:

–CM5-Ia: 4865–4754 cm (13000–12840 cal BP)

CM5-Ia is characterised by high frequencies of *Pinus* pollen between 30 and 40 %, and high frequencies for Sum *Quercus* (up to 40 %), reflecting high values for *Quercus* deciduous type and *Quercus* undiff. *Quercus coccifera* type is recorded in moderate to high frequencies, reaching local peak values of nearly 15 %.

In terms of the wetland taxa, CM5-Ia is characterised by high frequencies of *Aster* type (>10 %) and low frequencies of *Isoetes* undiff. Rising curves for *Artemisia* and Chenopodiaceae are noted, while frequencies of Apiaceae undiff., Asteraceae (Lactucaceae), and Cyperaceae pollen decline across the sub-zone. Frequencies of Poaceae are high (>20 %).

Dinoflagellates are rare, with low frequencies of *Spiniferites* sp.

–CM5-Ib: 4754–4553 cm (12840–12550 cal BP)

CM5-Ib displays peak values for *Pinus* reaching between 50 and 60 %. Values for Sum *Quercus* are sharply reduced relative to CM5-Ia, with frequencies falling below 20 %. *Quercus coccifera* type shows a similar decline, with values falling below 5 %. Associated with decreased values for *Quercus* are elevated values for *Juniperus*, Caryophyllaceae undiff. and *Plantago lanceolata* type. An occurrence of *Olea* is noted. In the wetland group,

peaks in *Artemisia* and *Chenopodiaceae* pollen are recorded, accompanied by high frequencies of *Aster* type. Frequencies of *Poaceae* pollen decrease across the sub-zone. Spores of *Isoetes* undiff. are rare. CM5-Ib is also marked by a peak in dinoflagellate content, reflecting core high values for *Spiniferites* sp.

–CM5-Ic: 4553–4073 cm (12550–11860 cal BP)

This sub-zone is characterised by rather poor pollen preservation, reflected in very high frequencies of indeterminate grains (~40 %). In terms of the dry ground taxa, CM5-Ic is characterised by fluctuating frequencies of *Pinus*, with moderate to high values (~25–45 %). Sum *Quercus* increases from low values in CM5-Ib to intermediate values (~20–30 %). *Quercus coccifera* also regains moderate to high values. In terms of wetland taxa, CM5-Ic is distinguished by high frequencies of *Artemisia* and *Chenopodiaceae* pollen (>25 %). Recorded in this biozone are peak abundances for *Spergula* type (~5%), *Aster* type (~20 %) and *Armeria/Limonium* (~4 %). Low frequencies for *Cyperaceae* (generally <10 %) are recorded. Rising curves for *Asteraceae* (*Lactuca*) and *Isoetes* undiff. are noted, while frequencies of *Poaceae* pollen decrease. Intermediate values for dinoflagellates, comprising chiefly *Spiniferites* sp., are recorded.

Significant changes in pollen concentration values are observed across the sub-zones of CM5-I. In CM5-Ia, pollen concentration for dry ground taxa is at peak levels $>40 \times 10^3$ grains·cm⁻³. Concentration of wetland pollen and spores is also high $>30 \times 10^3$ grains·cm⁻³. In CM5-Ib, pollen concentrations for both dry ground and wetland types are slightly reduced. In the dry ground taxa, this reduction reflects in part a significant decrease in concentration values for the *Quercus* pollen types. In contrast, pollen concentration for *Pinus* and for Sum *Cistaceae* are comparable with the CM5-Ia. In sub-zone CM5-Ic pollen concentration is greatly reduced for all taxa, with concentrations of dry ground taxa less than 5×10^3 grains·cm⁻³ and wetland taxa less than 6×10^3 grains·cm⁻³.

CM5-II: 4073–2643 cm (11860–9800 cal BP)

CM5-II is characterised by poor pollen preservation, and a strong disparity between the abundance of dry ground and wetland taxa. Overall, the total pollen and spore assemblage

is dominated by a small number of abundant types (Asteraceae (Lactucae), Cyperaceae, and *Ophioglossum lusitanicum*) and characterised by elevated values for *Isoetes* undiff. Dry ground pollen types represent a minor proportion of the pollen and spore assemblage, as illustrated by the depressed values relative to the total sum. As in CM5-Ic, the partial sum of dry ground taxa is low, so that percentage values for dry ground taxa with respect to this sum are not robust. However, these values provide an indication of the composition of dry ground group, which is considered below.

The dry ground group in CM5-II is characterised by moderate to high frequencies of *Pinus* pollen (generally >30 %). Values for Sum *Quercus* are moderate, (20 – 30 %), and moderate to high for *Quercus coccifera* (~10 %). The biozone is characterised by high values for Sum Cistaceae (reflecting chiefly *Cistus monspeliensis* type and Cistaceae undiff.) and increased values for Sum Ericaceae. Pollen preservation in both Cistaceae and Ericaceae is poor in this biozone, with a relatively large proportion occurring in the undifferentiated categories. Relative high frequencies are also noted among some of the minor taxa, notably *Coronilla* type, Lamiaceae, and open ground herbaceous taxa Caryophyllaceae undiff., *Centaurea*, *Erodium* and *Serratula* type. *Juniperus* declines in importance in this zone. At the top of the biozone, the continuous curve for *Phillyrea* begins.

The wetland group is dominated by peak frequencies of Asteraceae (Lactic.) pollen (up to 60 %). High frequencies of *Isoetes* undiff. are recorded, accompanied by increased frequencies *Ophioglossum lusitanicum* spores (~10 %) and modest peak values (~1 %) for spores of *Pilularia globulifera*. Lowest core frequencies of *Artemisia*, Chenopodiaceae, *Aster* type and Poaceae are recorded. Frequencies of Cyperaceae pollen decline from a peak at the base of the biozone but maintain moderate values (~10 %). Spores of *Isoetes* undiff. are abundant. Frequencies of rebedded trilete sporomorphs are high, and increase across the biozone

Moderate frequencies of dinoflagellates are recorded in this biozone, and the green algae *Spirogyra* and Zygnemataceae are well represented.

A major disparity between the concentration of dry ground and wetland taxa is recorded. The zone is characterised by very low pollen concentration for dry ground taxa (generally $<2 \times 10^3$ grains·cm⁻³). Concentration of wetland pollen and spores (excluding *Isoetes* undiff.) is moderate ($\sim 20 \times 10^3$ grains·cm⁻³).

CM5-III: 2643–2060 cm (9800–8960 cal BP)

CM5-III displays high values for *Pinus* (>40%), moderate values for Sum *Quercus* (~25 – 30 %) and moderate to high values for *Quercus coccifera* type (~10 %). The biozone is characterised by the start of the continuous curve for *Olea* and the first significant occurrence of *Pistacia*. Low values are recorded for Sum Cistaceae and Sum Ericaceae. High values are noted for *Serratula* type.

In terms of wetland taxa, CM5-III is similar to CM5-II, with high frequencies of Asteraceae (Lactucaee), Cyperaceae, *Isoetes* undiff., *Ophioglossum lusitanicum* and rebedded trilete spores. Frequencies of Asteraceae (Lactucaee) display a slight decline in frequencies to ~40 %. Spores of *Isoetes* undiff. reach peak frequencies, representing more than 6 times the contribution of all other pollen and spores. . Frequencies of pollen of Chenopodiaceae, *Aster* type and Poaceae are slightly increased relative to the underlying biozone.

Very low frequencies of dinoflagellates are recorded in this biozone. Increased frequencies of *Pediastrum* are recorded.

A disparity between the concentration of dry ground and wetland taxa is recorded in this biozone, although it is not as marked as in CM5-II. Values for pollen concentration for dry ground taxa are moderate ($\sim 10 \times 10^3$ grains·cm⁻³). Concentration of wetland pollen and spores (excluding *Isoetes* undiff.) is high (up to 40×10^3 grains·cm⁻³).

CM5-IV: 2060–633 cm (8960–5200 cal BP)

CM5-IV Shows an increased diversity of recorded types across the range of ecological groups in both the dry ground and wetland groups.

CM5-IV is characterised by high values for Sum *Quercus* (>30 %), reflecting increased frequencies of *Quercus suber* type as well as *Quercus* deciduous type and *Quercus* undiff. The abundance of *Pinus* with respect to other dry ground taxa declines to moderate values (~20 – 30 %). Values for *Q. coccifera* type are moderate to high (~10 %). *Olea*, *Phillyrea* and *Pistacia* are well represented in this biozone. Low values for Sum Cistaceae, and low to moderate values for Sum Ericaceae are recorded. Frequencies of *Plantago coronopus* type and *Rumex acetosella* type are increased relative to the preceding biozones.

For the wetland taxa, CM5-IV is characterised by high frequencies of *Aster* type (~10 %), Poaceae (~20 %) and Cyperaceae (up to 20 %). Frequencies of *Isoetes* undiff. are high, but show a decrease relative to the previous biozone, and values for *Ophioglossum lusitanicum* are low. Frequencies of Asteraceae (Lactucaceae) pollen (~20 %) are reduced from CM5-III. Fluctuating curves for *Artemisia* and Chenopodiaceae are observed. Apiaceae undiff., Brassicaceae and *Ranunculus* type show increased values relative to the previous zone. Riparian taxa are well represented in this biozone, with increased frequencies of *Alnus*, *Fraxinus* and *Salix* pollen, accompanied by frequent occurrences of *Lythrum salicaria* type and *Osmunda regalis* spores. Aquatic types are fairly well represented in this zone, with the common occurrence at low frequencies of *Typha/Sparganium*, *Myriophyllum* types, *Nymphaea* and *Potamogeton*.

Among non-pollen micro-fossils, increased frequencies of dinoflagellates are noted in the lower part of the biozone, resulting from peaks in the abundance of *Lingulodinium machaerophorum*. Increased frequencies for *Lingulodinium machaerophorum* are accompanied by a modest increase in diversity of dinoflagellate types. *Pediastrum* colonies are abundant in this biozone.

Three subzones are defined for this biozone:

–CM5-IVa: 2060–1225cm (8960–7760 cal BP)

CM5-IVa is characterised by high frequencies of Sum *Quercus*, including peak values for *Quercus* deciduous type. Peak values for *Olea*, *Phillyrea* and *Pistacia* are observed. Low frequencies of Cistaceae and Ericaceae pollen are recorded. In the wetland group, CM5-IVa is characterised by low frequencies of Chenopodiaceae pollen, and a good representation of freshwater aquatic types including *Typha/Sparganium* and *Nymphaea*.

–CM5-IVb: 1225–943cm (7760–7350 cal BP)

CM5-IVb is characterised by a decline in frequencies of Sum *Quercus* (from around 40 to 30 %), and a slight decline in *Pinus*. In this subzone, the first significant occurrence of *Myrtus* is observed. An increased representation of Sum Cistaceae is noted, reflecting increased frequencies of *Cistus ladanifer/populifolius* types and *Cistus monspeliensis* type. Sum Ericaceae also displays increased frequencies, with increases in *Erica arborea* type and *Erica umbellata* type, and the first appearance of *Erica scoparia* type. The subzone also displays increased values for both *Plantago coronopus* and *Plantago lanceolata* types. Among the wetland taxa, a distinct peak in Chenopodiaceae (20 %) is recorded in this subzone, accompanied by a minor peak in *Artemisia*. These increases correspond with a reduced representation of freshwater aquatics.

–CM5-IVc: 943–633 cm (7350–5200 cal BP)

CM5-IVc is similar to CM5-IVa, with high frequencies of Sum *Quercus* pollen, the absence of *Myrtus*, and low values for Sum Cistaceae and Ericaceae. High frequencies of *Pinus* pollen (~30 %) are also recorded. Frequencies of *Plantago coronopus* type are reduced and *Plantago lanceolata* type is absent. In the wetland group, frequencies of Chenopodiaceae are reduced, and freshwater aquatics are more abundant, with occurrences of *Typha/Sparganium*, *Alisma* and *Nuphar*. This sub-zone also records an input of *Isoetes histrix* spores.

The concentration of dry ground taxa in CM5-IV is increased relative to CM5-III to moderate to high values ($15 - 25 \times 10^3$ grains·cm⁻³). Concentration for wetland taxa is similar to CM5-III, with high pollen and spore concentration ($25 - 40 \times 10^3$ grains·cm⁻³, excluding *Isoetes* undiff.).

CM5-V: 633–160 cm (5200–1430 cal BP)

The transition to biozone CM5-V is marked by sharp declines in *Pinus* and Sum *Quercus*. The biozone is characterised by reduced frequencies of *Pinus* (<10 %) and Sum *Quercus* (<20 %) pollen, and high frequencies for pollen of *Quercus coccifera* type and *Myrtus*. High values are recorded for Sum Cistaceae and Sum Ericaceae (reflecting *Erica arborea* type, *Erica umbellata* type and *Calluna vulgaris*). Across the biozone, increased frequencies of *Plantago coronopus* and *Plantago lanceolata* are recorded. The biozone is also characterised by the presence of *Anthemis* and *Galium* type. CM5-V contains the first appearance of *Castanea*.

Among the wetland taxa, CM5-V is distinguished by high, fluctuating values for Chenopodiaceae (~10 – 40 %), and high frequencies of Poaceae pollen (up to 25 %). *Artemisia* and *Aster* type are well represented. Frequencies of *Isoetes* undiff. decline across the biozone. Low values for Cyperaceae (~10 %) and *Ophioglossum lusitanicum* are recorded. Riparian taxa (*Alnus*, *Fraxinus*, *Salix*) decline in importance towards the top of the biozone, while frequencies of *Tamarix* increases slightly. The biozone contains a peak in the curve for the dinoflagellate type *Lingulodinium machaerophorum*. Values for *Pediastrum* decline across the biozone. Rebedded trilete sporomorphs occur in reduced frequencies.

Based on a series of declines in *Pinus* and *Quercus* types and accompanying changes in other taxa, three subzones are defined:

–CM5-Va: 633–500cm (5200–4140 cal BP)

Subzone CM5-Va is distinguished by the highest recorded frequencies of *Quercus coccifera* type (~15 – 20 %). These elevated values contrast with an overall reduction in other *Quercus*

types, with frequencies for Sum *Quercus* decreasing from around 30 to 15 % over the course of the subzone. Rising curves for *Myrtus*, Sum Cistaceae and Sum Ericaceae are observed.

–CM5-Vb: 500–290 cm (4140–2490 cal BP)

Peak values for Sum Cistaceae are attained in this subzone, reflecting elevated frequencies of the shrub taxa *Cistus ladanifer/populifolius* types, *Cistus monspeliensis* type, *Halimium halimifolium* type, and herbaceous *Tuberaria guttata* type. Peak values for *Myrtus* are also recorded.

–CM5-Vc: 290–160 cm (2490–1430 cal BP)

The transition to subzone CM5-Vc is marked by a decline in *Pinus* frequencies from around 5 to 2 %. Core low values are recorded for Sum *Quercus*, and reduced values for *Quercus coccifera* type, *Olea* and *Phillyrea*. Sum Ericaceae reaches peak values, with peak values for *Erica arborea* and *Erica umbellata* types. Peak frequencies of *C. monspeliensis* type occur, although values for Sum Cistaceae are slightly reduced overall from the preceding subzone. Peak values for *Plantago coronopus* and *Plantago lanceolata* types and *Rumex acetosella* type are observed.

Pollen and spore concentration for dry land taxa reaches peak values ($20 - 40 \times 10^3$ grains·cm⁻³), reflecting increases in the concentration of *Q. coccifera* type, *Myrtus*, Cistaceae and Ericaceae pollen. Concentration of *Pinus* pollen is greatly reduced from CM5-IV, while Sum *Quercus* (excl. *coccifera* type) is slightly reduced. Pollen and spore concentration for wetland taxa (excluding *Isoetes* undiff.) is high overall ($30 - 40 \times 10^3$ grains·cm⁻³), with peak values ($>60 \times 10^3$ grains·cm⁻³) towards the top of the zone, reflecting increased concentration of Asteraceae (Lactucaee) and Poaceae pollen.

***Pinus* grain measurements**

Measurements of the equatorial diameter of *Pinus* pollen grains were made during the pollen counts. Measurements were taken at the widest point of the grain body, excluding the sacci. Measurements were only taken on grains that were not crumpled or broken and

where the sacci were not folded in such a way as to conceal the grain body. A total of 1312 measurements were obtained out of 2802 counted grains of *Pinus*. Measured diameters range between 25 and 85 μm . As illustrated in Figure 7.5a, some changes are observed in the distribution of grain sizes between biozones. In the lower part of the core (CM5-I/II/III), a roughly bimodal distribution is displayed, suggesting more than one source population. A mode around 40 μm is well developed in CM5-I and is the primary mode in CM5-II. In the upper part of the core (CM5-IV/V), the distribution tends more towards a unimodal shape, with the mode around 55 μm . The mode around 40 μm is diminished, with decreased frequencies of the smallest grain sizes.

Previous morphometric research on pollen grains from Iberian pine species (Roure, 1985 (cited in Carrion *et al.*, 2000); Queiroz, 1999) has demonstrated that of the four pines occurring in the modern Portuguese flora (*P. pinaster*, *P. pinea*, *P. halepensis* and *P. sylvestris*), *P. sylvestris* is distinguished by its overall small size. The remaining three species are characterised by larger grains within an overlapping size distribution, although the largest grains pertain to *P. pinaster*. These studies use a measurement of total grain diameter (including sacci), which is not useful for fossil grains due to the frequent collapse or crumpling of the sacci. Therefore, the sizes are not directly comparable to those obtained here. If, based on observation, it is assumed that the total diameter is about 20% greater than the grain body diameter, the modes observed in the CM5 dataset at 40 and 55 μm would correspond to total grain diameters of 48 and 66 μm . These figures correspond with the modes observed by Queiroz (1999) in modern samples (Figure 7.5b). The best explanation for the patterns observed in the CM5 data is that the *Pinus* pollen represents more than one species, and that a population of small sized grains within the data set is derived from *P. sylvestris*. This population is more strongly represented in the lower part of the record, and declines in the upper part. This trend is of ecological interest because *P. sylvestris* is a tree of montane forest habitats at altitudes above 500m (and not occurring in the modern flora of southern Portugal), while *P. pinea* and *P. halepensis* are lowland pines typical of the thermomediterranean coastal zone (Barbéro *et al.*, 1998). *P. pinaster* is a

tolerant species, and occurs across a wide altitudinal and thermic range (Carrion *et al.*, 2000).

7.2.2 P2 Arade

The P2 core is characterised by good pollen preservation in the central section of the core corresponding to sediment zone P2s-3, and the virtual absence of palynomorphs in the underlying and overlying sections corresponding to sediment zones P2s-2 and P2s-4. Two samples were recovered from a silty layer contained within sediment zone P2s-4a. Further investigation of these upper core sections may in the future yield further sections with pollen preservation; however, overall, the sandy layers of P2s-4 are not suitable for pollen analysis.

The pollen diagram (Figure 7.6 percentage data, Figure 7.7 concentration data) shows the results obtained from the analysis of 14 samples. All recorded taxa are plotted. Two sediment zones and two subzones are defined:

P2-I: 1722–1024 cm (8310–7690 cal BP)

P2-I is characterised by high frequencies of Sum *Quercus* (>30 %), and decreasing frequencies of *Pinus* pollen. *Quercus coccifera* type, *Olea*, *Phillyrea* and *Pistacia* are well represented. These taxa are accompanied by a moderate presence of Sum Cistaceae, reflecting mainly *Cistus ladanifer*/ *populifolius* types, and Sum Ericaceae, reflecting chiefly *Erica arborea* and *Erica australis* types.

The wetland taxa are characterised by a strong representation of Asteraceae (Lactuceae) (~10 %), Chenopodiaceae (5 – 10 %), Poaceae (~10 %) and *Isoetes* undiff. (~25 %). Riparian tree taxa are well represented with high frequencies of *Alnus* (10 – 20 %) and an important presence of *Fraxinus* (~5%). Frequencies of the dinoflagellate *Lingulodinium machaerophorum* are high toward the base of the biozone, and decrease in the upper part. *Spiniferites* sp. displays a reverse trend, with higher values towards the top of the biozone.

Pollen concentrations are high, both for dry ground taxa ($\sim 15 - 25 \times 10^3$ grains·cm⁻³) and wetland taxa ($\sim 20 - 35 \times 10^3$ grains·cm⁻³).

Two subzones are distinguished on the basis of the curves for *Pinus* and Ericaceae pollen types:

–P2-Ia: 1722–1498 cm (8310–8270 cal BP)

The lower subzone is characterised on the basis of high frequencies of *Pinus* pollen (>30 %), and low frequencies of all Ericaceae pollen types.

–P2-Ib: 1498–1024 cm (8270–7690 cal BP)

P2-Ib displays reduced frequencies of *Pinus* pollen, declining across the subzone from around 25 to 20 %. Values for Sum Ericaceae are increased, reflecting increased frequencies of *Erica arborea* and *E. australis* types. Values for *Quercus* deciduous are slightly increased.

P2-x (barren): 1024–562 cm

No pollen was recovered from samples in this section of the core.

P2-II: 562–546 cm (5220–5070 cal BP)

The two uppermost samples from the P2 core present a marked contrast with the samples from biozone P2-I, and an upper biozone is tentatively proposed on this basis. The samples display greatly reduced values for *Pinus* (~ 5 %) and reduced values for Sum *Quercus* (chiefly reflecting decreased values for *Quercus* deciduous type) with frequencies less than 20 %. Frequencies of *Olea*, *Phillyrea* and *Pistacia* pollen are slightly reduced. The samples are also distinguished by the presence of *Myrtus*, high frequencies of Sum Cistaceae, including an occurrence of *Tuberaria guttata*, and by a major increase in Sum Ericaceae with notable high values for *Calluna vulgaris*.

The overall composition of the wetland pollen assemblage from P2-II is more similar to P2-I. Frequencies for the majority of wetland taxa fall within the range of values observed in the underlying zone. Increases in *Artemisia* and *Armeria/Limonium* are noted. Increased frequencies of indeterminate grains are also recorded. Dinoflagellates are recorded in low frequencies.

Pollen concentration in these samples is low, both for dry ground taxa ($\sim 3 \times 10^3$ grains·cm⁻³) and for wetland taxa ($< 3 \times 10^3$ grains·cm⁻³).

7.2.3 P5 Boina

The P5 core is characterised by variable pollen preservation, with several hiatuses in the pollen record corresponding to sandy/gravelly sediments in sediment zones P5s-2b, P5s-2d and P5s-4. This means that the pollen record is not continuous, but represents different sedimentation phases at the site. Breaks in the pollen curves are intended to show this discontinuity. However, the zonation of the pollen data, in line with the other sites, has been undertaken with respect to the composition of recovered samples and without respect to sediment stratigraphy. A hiatus is marked in the pollen assemblage biozone stratigraphy between P5-Ib and P5-Ic, because the length of elapsed time represented by this hiatus is much greater than either of the lower breaks. However, as described in Chapter 5, the age-model is poorly constrained for the upper part of sediment zone P5s-3, corresponding here to P5-Ic. A single sample was recovered from a silty lens within sediment zone P5s-4, and a sub-zone in the pollen stratigraphy (P5-Ic) is tentatively defined on the basis of this single sample. However, further research must be undertaken to confirm the reliability of this pollen spectrum.

Depth (cm)	Taxon
160	<i>Frankenia laevis</i> type
210	<i>Ilex aquifolium</i>
320	<i>Herniaria</i> type
320	<i>Valerianella</i>
590	<i>Gynandris sisyrinchium</i>
660	<i>Jasione montana</i> type
700	<i>Sambucus ebulus</i>
1305	<i>Rhus</i>
1565	<i>Scrophularia</i> type
2100	<i>Corylus</i>
2240	<i>Teucrium</i>
4706	<i>Convolvulus</i>
4745	<i>Viburnum tinus</i>
4762	<i>Halimium/Tuberaria</i>

Table 7.5. Taxa occurring in only one sample, P5.

The pollen diagram (Figure 7.8 percentage data, Figure 7.9 concentration data) shows the results of analysis of 21 samples. Taxa occurring in only one sample are not plotted, but are listed in Table (7.5).

Two biozones and three sub-zones are defined:

P5-I: 1570–1257 cm (8210–8030 cal BP)

P5-I is characterised by high frequencies of *Pinus* pollen (~30 %). Well represented pollen types include *Quercus* (excl. *coccifera* type). (~30%), *Quercus coccifera* type (~15 %), *Olea*, *Phillyrea* and *Pistacia*. Low frequencies of Sum Cistaceae and Sum Ericaceae are recorded. P5-I is distinguished by high values for *Alnus* (~20 %) accompanied by relatively high frequencies of *Fraxinus* and the occurrence of *Ulmus* pollen. Relatively low values for the well represented *Isoetes* undiff. (~20 – 30 %) are recorded. Other taxa well represented in the biozone include Asteraceae (Lactucaee) (~15%), Chenopodiaceae (~10 %), Poaceae (~10 %) and Cyperaceae (up to 5 %). A peak in abundance of Apiaceae undiff. is observed at the base of the biozone. High frequencies (up to 20%) of indeterminate grains are recorded. Dinoflagellates are recorded at frequencies around 5 – 10 %. Minor peak values for *Lingulodinium machaerophorum* occur in this biozone.

Pollen concentration for dry ground taxa is moderate ($\sim 20 \times 10^3$ grains·cm⁻³), and moderate for wetland taxa ($\sim 30 \times 10^3$ grains·cm⁻³). A strong peak in pollen concentration values occurs in one sample, affecting all taxa, with dry ground pollen concentration in excess of 50×10^3 grains·cm⁻³, and wetland pollen and spore concentration reaching 85×10^3 grains·cm⁻³.

P5-II: 1257-505 cm (8030–3740 cal BP)

This zone is characterised overall by reduced values for *Pinus* and *Alnus*. Three sub-zones and a significant hiatus in pollen preservation are recorded:

–P5-IIa: 1257–870 cm (8030–7550 cal BP)

P5-IIa is characterised by reduced frequencies of *Pinus* pollen (~15 %). Frequencies of *Quercus* (excl. *coccifera* type) are high, accompanied by high values for *Quercus coccifera*

type (~15%). *Olea*, *Phillyrea* and *Pistacia* are also well-represented, with the curves for *Phillyrea* and *Pistacia* showing a close affinity. A small decline in *Quercus* near the top of P5-IIa corresponds with slight increases in *Quercus coccifera* type, *Phillyrea* and *Pistacia*. Low frequencies of Sum Cistaceae and Sum Ericaceae are recorded. P5-IIa is characterised by relatively high frequencies of Chenopodiaceae and Poaceae, with rising curves and peak values at the top of the subzone (>10 % for Chenopodiaceae and >15 % for Poaceae). Frequencies of *Alnus* decline across the sub-zone. Values for *Isoetes* undiff. are intermediate (~30 %). Dinoflagellate frequencies are stable around 7 %, reflecting chiefly *Spiniferites* sp .

Pollen concentration for dry ground taxa is moderate ($10 - 25 \times 10^3$ grains·cm⁻³). Concentration values are strongly reduced for *Pinus* are reduced from P5-I, while other taxa show only slight reductions. Pollen and spore concentration for wetland taxa is moderate to high (~20 – 40 × 10³ grains·cm⁻³).

–P5-IIb: 870–656 cm (7550–7210 cal BP)

In P5-IIb, frequencies of *Pinus* display a further slight reduction. Values for *Q. coccifera* type decline to less than 10%, accompanied by a slight decline in *Phillyrea*. Small increases in Sum Cistaceae, reflecting *Cistus ladanifer/populifolius* types and *C. monspeliensis* type are recorded. Increased frequencies of Sum Ericaceae are also recorded, reflecting primarily *Erica arborea* and *E. australis* types. *Rumex acetosella* type and *Plantago coronopus* show slight increases relative to P5-IIa. Reduced frequencies of Chenopodiaceae (~5 %) and Poaceae (~8 %) pollen are recorded. Frequencies of *Isoetes* undiff. reach peak levels (~50 %). Increased frequencies of dinoflagellates are observed, reflecting peaks in the abundance of *Spiniferites* sp..

Pollen concentration for dry ground taxa is moderate ($10 - 25 \times 10^3$ grains·cm⁻³).

Pollen and spore concentration for wetland taxa is high (~25 – 60 × 10³ grains·cm⁻³). Concentration values for most wetland taxa (Chenopodiaceae, Poaceae, *Alnus*) are actually rather stable, with increases in concentration reflecting greater abundances of *Isoetes* undiff.

–P5-x (barren): 656–505 cm (7210–3740 cal BP)

No pollen was recovered from this section of the core.

–P5-IIc: 505 cm (3740 cal BP)

The uppermost sample is marked by greatly reduced frequencies of *Pinus*, *Quercus* (excl. *coccifera* type), *Olea* and *Phillyrea* pollen and peak values for a range of shrub and herb pollen types including *Myrtus*, *Erica arborea* and *australis* types, *Cistus monspeliensis* type., *Tuberaria guttata* type, *Plantago lanceolata* type and *Rumex acetosella* type. These types, although generally present in biozones P5-I and P5-II (either in low frequencies or sporadic occurrences), occur in combination and at increased frequencies, setting this sample (depth 505cm) strongly apart from the rest of the sequence. In terms of the wetland taxa, frequencies of Chenopodiaceae and Poaceae are increased, and frequencies of *Isoetes* undiff. are decreased relative to P5-IIb. Dinoflagellates are virtually absent.

Pollen concentration in this sample is low for both dry ground taxa (6×10^3 grains·cm⁻³) and wetland taxa (9×10^3 grains·cm⁻³).

CM5 Guadiana Summary pollen percentage diagram

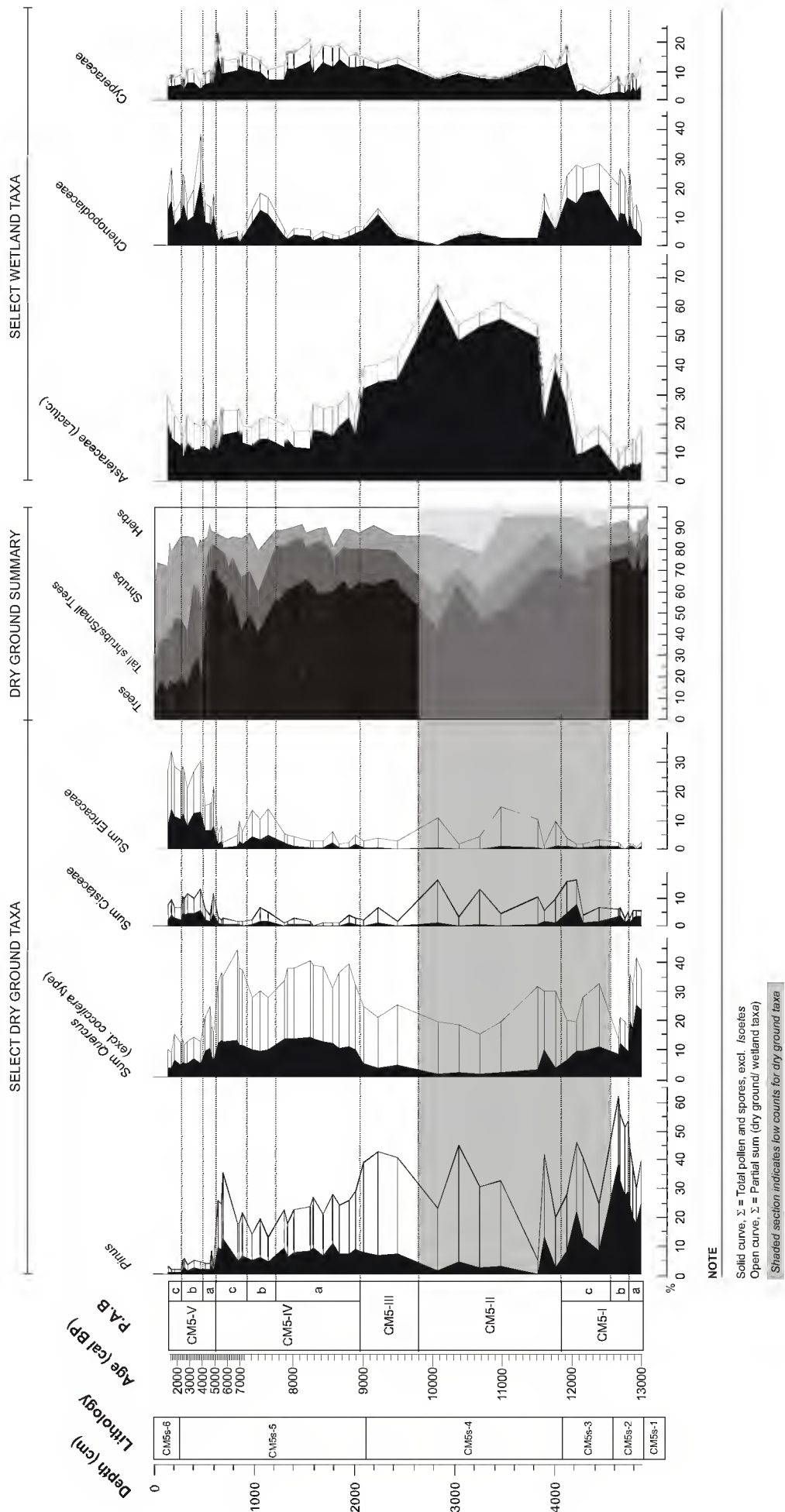
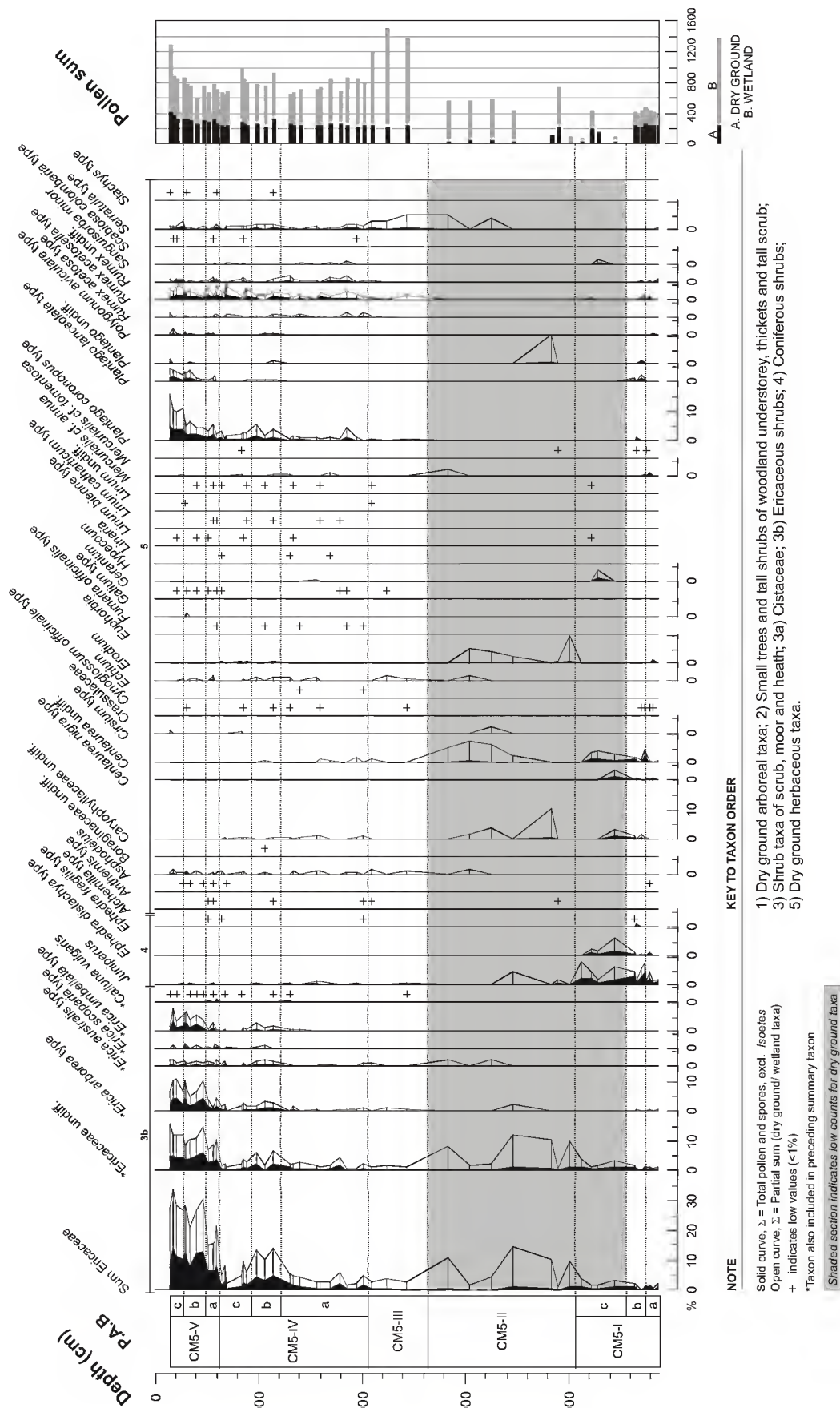


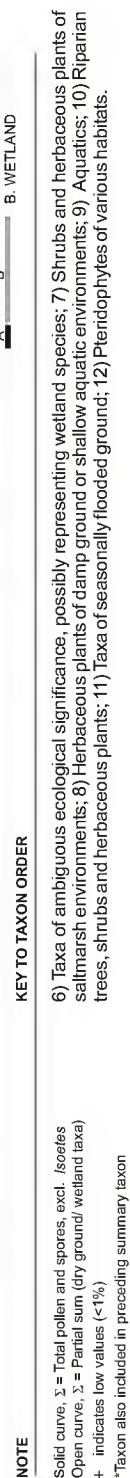
Figure 7.2. Summary pollen percentage diagram, CM5.



CM5 Guadiana Pollen percentage diagram, page 2/5 (dry ground taxa)









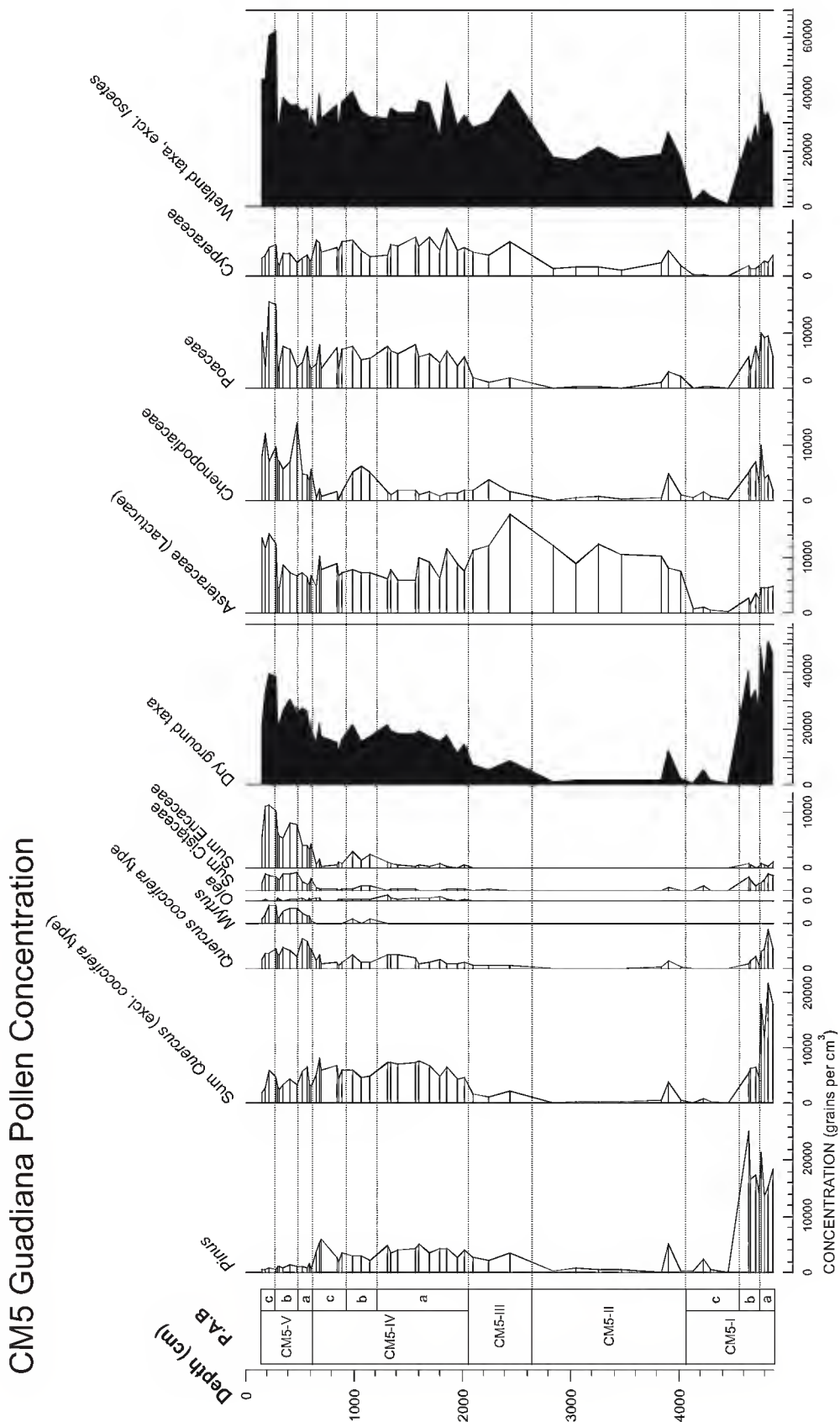


Figure 7.4. Concentration diagram, CM5, select taxa.

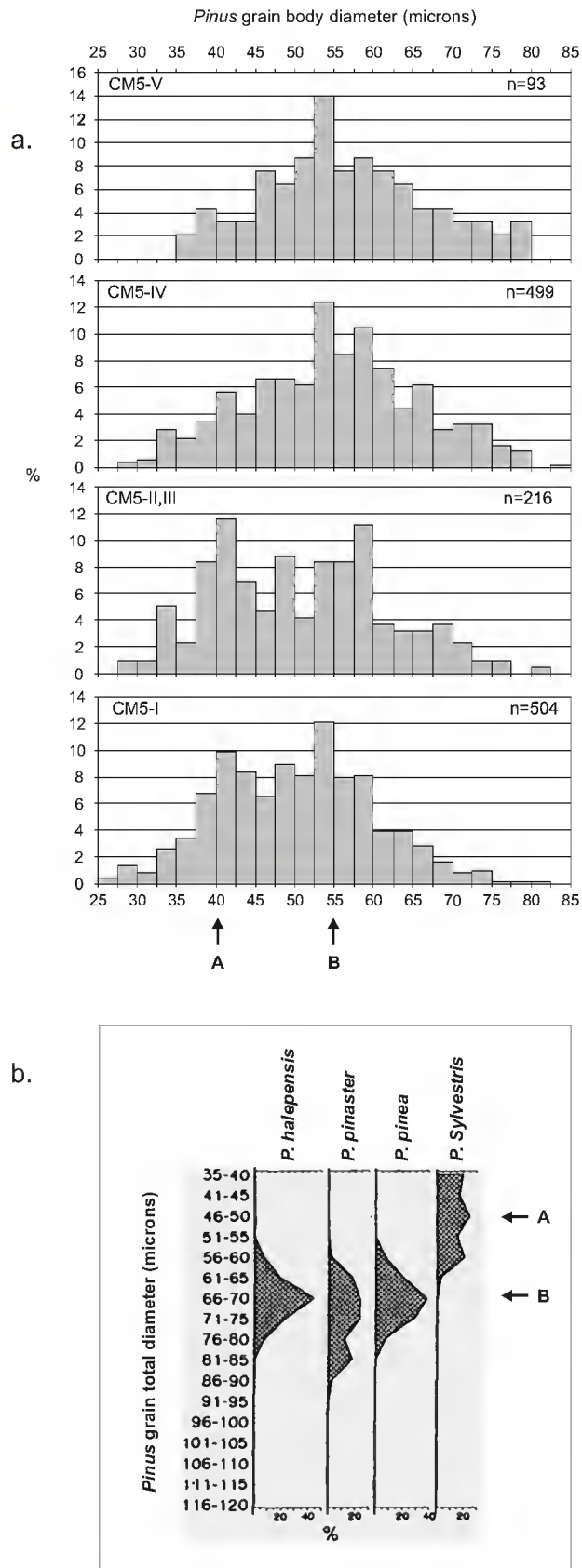
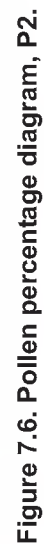


Figure 7.5. *Pinus* morphometric analysis.

a. Distribution of *Pinus* grain body diameter measurements by biozone (core CM5).

b. Frequency curves of total grain diameter for Portuguese *Pinus* species (from Queiroz, 1999).





Solid curve, Σ = Total pollen and spores

Solid curve, Σ = Total pollen and spores
Open curve, Σ = Partial sum (dry ground/ wetland taxa)

+ indicates low values (<1%)

*Taxon also included in preceding summary taxon

KEY TO TAXON ORDER

1) Dry ground arboreal taxa; 2) Small trees and tall shrubs of woodland understorey, thickets and tall scrub; 3) Shrub taxa of scrub, moor and heath; 3a) Cistaceae; 3b) Ericaceous shrubs; 4) Coniferous shrubs; 5) Dry ground herbaceous taxa.



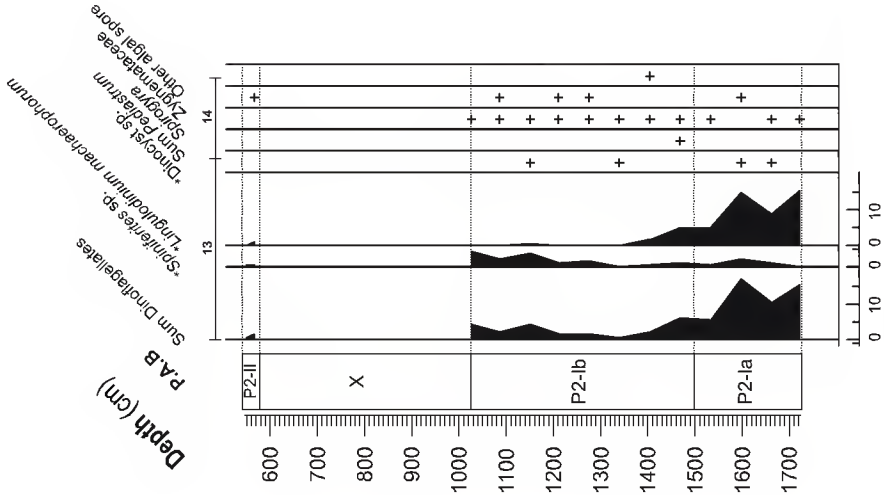
Solid curve, Σ = Total pollen and spores, exd. /soetes
Open curve, Σ = Partial sum (dry ground/ wetland taxa)
+ indicates low values (<1%)

*Taxon also included in preceding summary taxon

KEY TO TAXON ORDER

6) Taxa of ambiguous ecological significance, possibly representing wetland species; 7) Shrubs and herbaceous plants of saltmarsh environments; 8) Herbaceous plants of damp ground or shallow aquatic environments; 9) Aquatics; 10) Riparian trees, shrubs and herbaceous plants; 11) Taxa of seasonally flooded ground; 12) Pteridophytes of various habitats

P2 Arade Pollen percentage diagram, page 4/4 (non-pollen microfossils)



NOTE

Solid curve, Σ = Total pollen and spores, excl. /scotels
+ individual sum
+ indicates low values (<1%)
*Taxon also included in preceding summary taxon

KEY TO TAXON ORDER

13) Dinoflagellates, 14) Algal remains.

P2 Arade Pollen concentration, select taxa

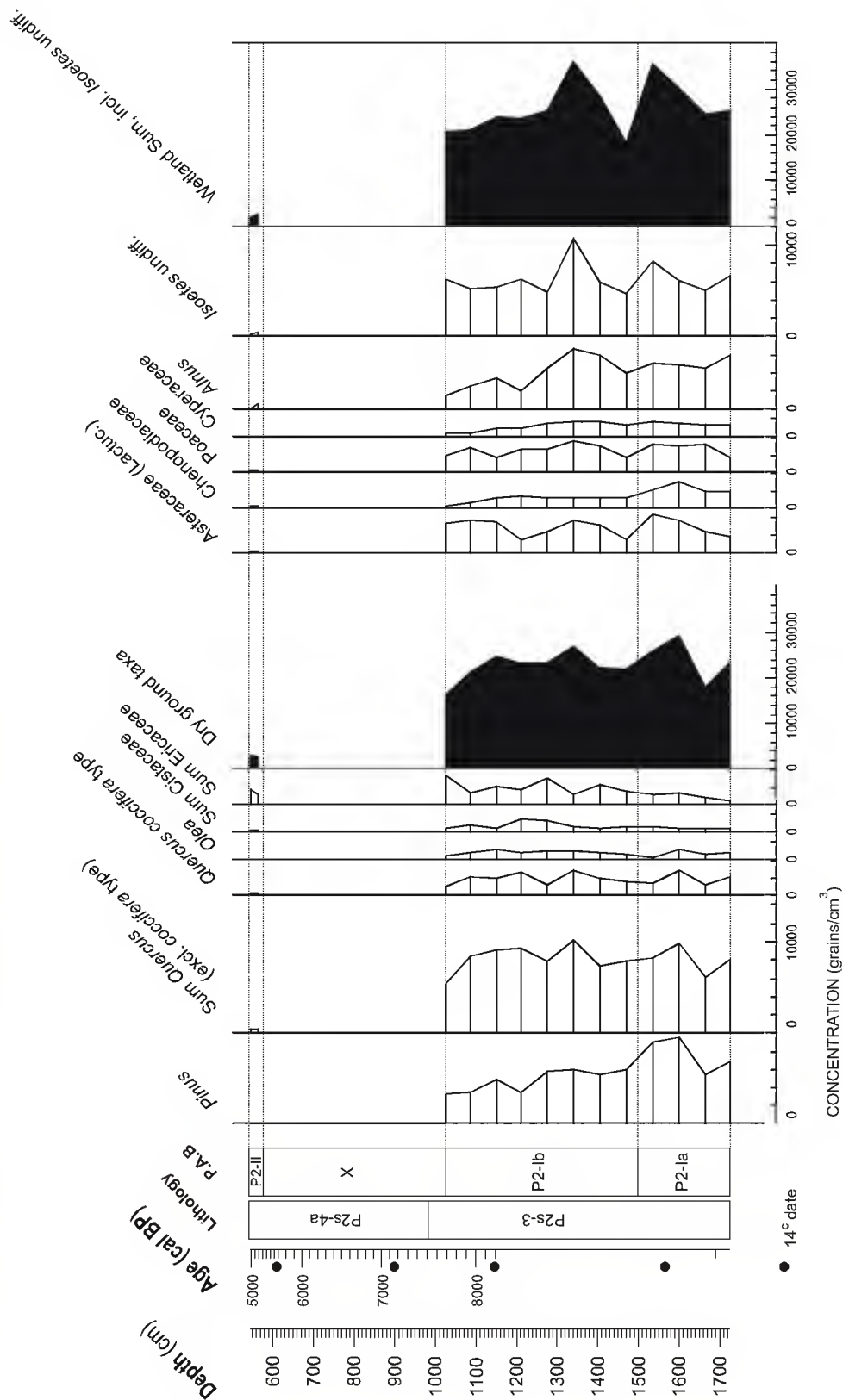


Figure 7.7. Concentration diagram, P2, select taxa.

P5 Boina Pollen percentage diagram, page 1/4 (dry ground taxa)

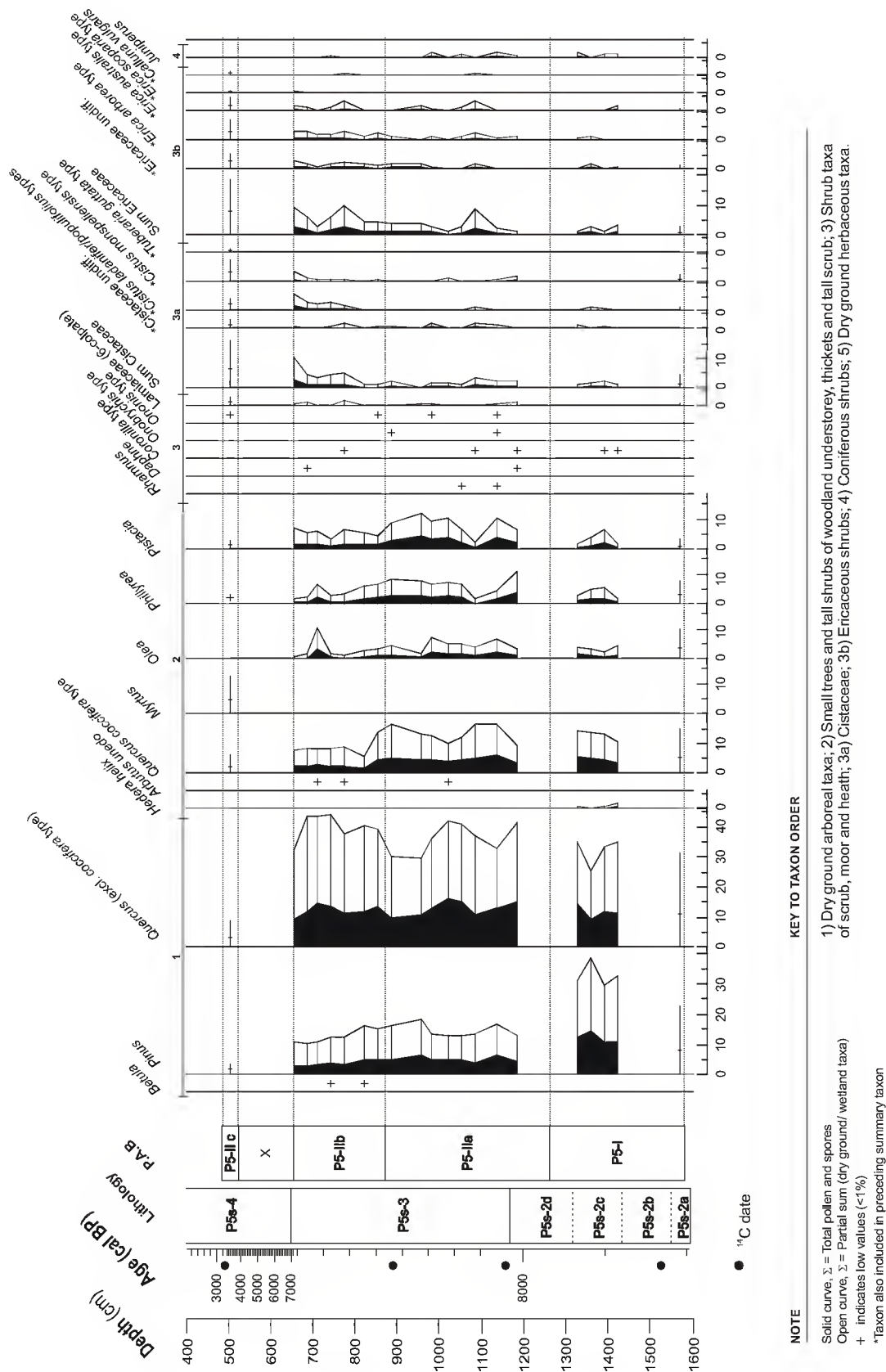
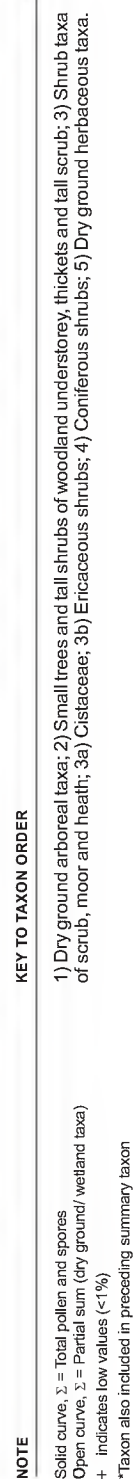
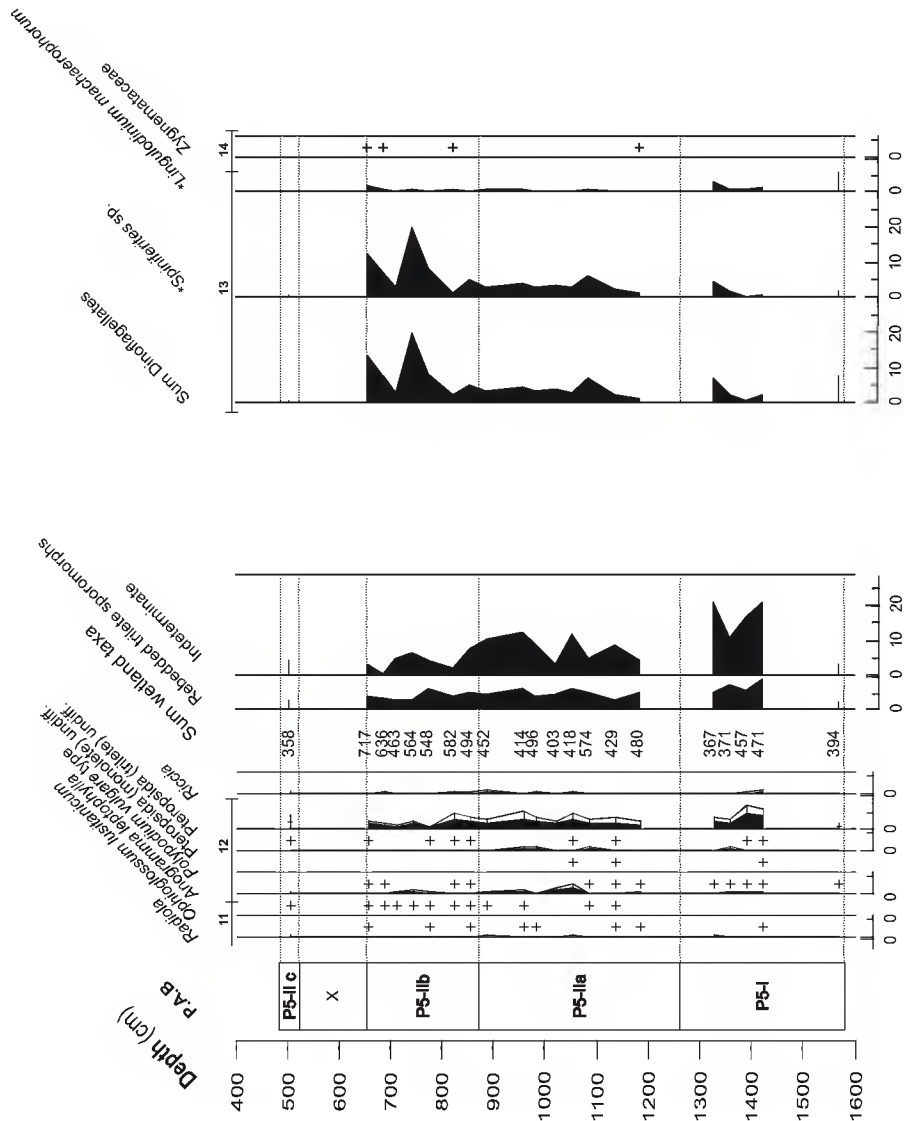


Figure 7.8. Pollen percentage diagram, P5.





P5 Boina Pollen percentage diagram, page 4/4 (wetland taxa and non-pollen microfossils)



NOTE

Solid curve, Σ = Total pollen and spores, excl. /scetes
Open curve, Σ = Partial sum (dry ground/ wetland taxa)
+ indicates low values (<1%)
*Taxon also included in preceding summary taxon

KEY TO TAXON ORDER

6) Taxa of ambiguous ecological significance, possibly representing wetland species; 7) Shrubs and herbaceous plants of saltmarsh environments; 8) Herbaceous plants of damp ground or shallow aquatic environments; 9) Aquatics; 10) Riparian trees, shrubs and herbaceous plants; 11) Taxa of seasonally flooded ground; 12) Pteridophytes of various habitats; 13) Dinoflagellates; 14) Algal remains.

P5 Boina Pollen concentration, select taxa

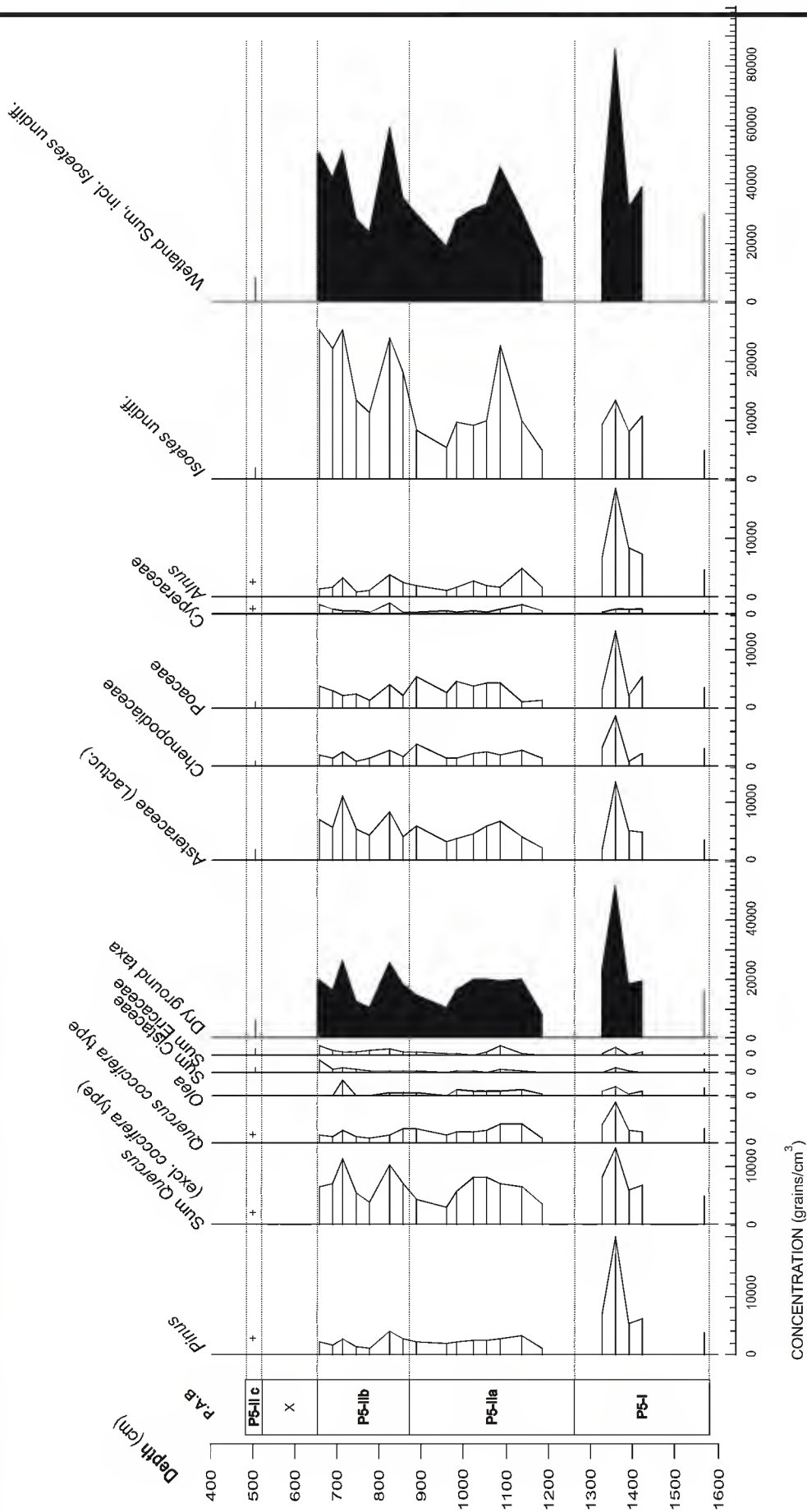


Figure 7.9. Concentration diagram, P5, select taxa.

8 Discussion: pollen data

8.1 On the interpretation of pollen percentage data

8.1.1 Pollen production, dispersal and preservation

The range of pollen types and the proportions in which they occur reflect the vegetation growing at and around the site from which they are recorded. While this statement provides the rationale for pollen analysis, it cannot be accepted without qualification. The extent to which the results of pollen analysis, particularly as presented in terms of relative frequencies within a pollen sum, provide an accurate reflection of past vegetation cover will be conditioned by a range of factors. Some general factors — pollen production, dispersal and preservation — which concern all pollen studies are considered first.

The conditioning factors of differential pollen production and dispersal relate to the field of pollination ecology (Faegri & van der Pijl, 1971). These factors alter the representation of pollen types reaching a sample location or point of deposition (i.e. in the “pollen rain”) relative to the representation of species in the surrounding vegetation. Plants produce widely differing quantities of pollen. Pollen production varies greatly between taxa, and is strongly influenced by ecological and climatic conditions. A number of northern European examples are well-known; for example, oak (*Quercus robur*) produces more than 5 times as many

pollen grains per inflorescence as beech (*Fagus sylvatica*), and birch (*Betula pubescens*) more than 30 times as many (Erdtman, 1969). In the common oak species of southern Iberia, differences in the number of pollen grains produced per stamen were observed, in the ratio 1: 3: 3: 6 (*Q. coccifera*, *Q. ilex* ssp. *ballota*, *Q. faginea* and *Q. suber*) (Gómez-Casero *et al.*, 2004). Differences in pollen production are related, in part, to different strategies for reproduction and modes of pollination (Dafni, 1992). On the whole, wind-pollinated (anemophilous) plants tend to produce more pollen than animal pollinated (zoophilous) plants due to the relative efficiency of the latter as a pollination strategy (Faegri & van der Pijl, 1971). However, pollen production in some zoophilous plants (e.g. *Calluna*) is comparable with anemophilous types. The efficiency of pollen dispersal from the parent plant is also very variable, both related to individual species characteristics and to the structure of the vegetation stand (Faegri & Iversen, 1989). A general model of the exponential decline in pollen representation with increasing distance from source is well understood (Janssen, 1966) (Figure 8.1), but the actual nature of pollen dispersal is conditioned by a host of species- and site-specific factors, including flower structure, size and aerodynamic properties of different pollen types, and meteorological conditions.

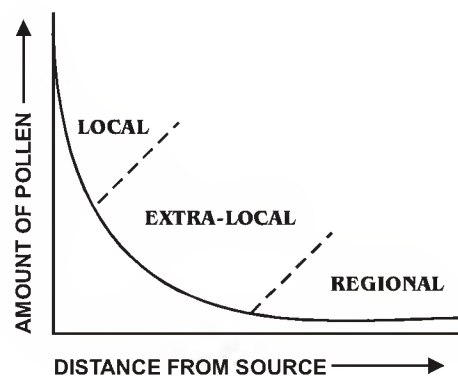


Figure 8.1. Theoretical pollen dispersal curve (after Janssen, 1966). The bulk of pollen is dispersed within only a few metres from the source, deposited in the form of individual grains and also intact anthers and catkins, by gravity and water runoff from leaves and stems (local pollen). Some pollen is dispersed over tens of metres in diffuse clouds, more or less parallel to the ground, to be scavenged by ground cover (extra-local pollen). A small proportion of pollen will be dispersed over hundreds to thousands of metres (up to hundreds of kilometres) by thermal updraughts and air-currents (regional pollen).

Where pollen surface studies enable the direct comparison of the representation of a pollen type and the abundance of the source plant in the vegetation cover, numerical correction factors (R-values (Davis, 1963)) may be developed to account for differences in pollen production and dispersal. This technique has been successfully applied in a number of studies (e.g. Bradshaw, 1981) where the modern and palaeovegetation are not widely different and where the pollen source area is clearly defined. While refinement of numerical techniques for the calibration of pollen data continues (e.g. Sugita, 1994), in practice most palynologists rely on an observational approach. As no numerical models or correction factors exist for the vegetation of southern Iberia, this study must fall into the latter category. A number of general observations regarding pollen production and dispersal for some of the pollen types encountered in this study may be gathered from surface sample studies presented in Stevenson (1985a) for the Doñana area in southwest Spain and Queiroz (1989) for the Serra da Arrábida in western Portugal. For example, Queiroz observes that the main pollen producers are *Quercus faginea* (*Quercus* deciduous pollen type), *Quercus coccifera*, *Olea europea*, *Pistacia lentiscus*, *Phillyrea*, *Erica arborea*, *Juniperus* and *Viburnum tinus*. These plants display high levels of pollen production and successful dispersal, being well represented in all samples and showing highest percentages where they occurred more frequently. In contrast, a number of pollen types, including *Acer*, *Cistus*, *Ophioglossum* and *Selaginella*, display high local representation but poor dispersal. Pollen of *Arbutus unedo* was observed to be distinctly underrepresented at all sites, despite being abundant in the vegetation and flowering profusely. Similarly, Stevenson (1985a) notes that leguminous shrubs may be severely underrepresented even where they form a major component of the vegetation cover.

Taphonomic influences related to differential pollen preservation may have an important effect on the representation of pollen types, altering the representation of pollen types within the fossil assemblage relative to their representation in the pollen rain. Experimental investigations have demonstrated that pollen and spores are susceptible to decay through

biological and chemical attack, and that susceptibility varies between types. Sangster & Dale (1961, 1964) demonstrate that rates of decay and fossilization potential varied between different pollen types, and that decomposition of the same pollen types varied with depositional environment, e.g. pond, lake, swamp, or bog. Havinga (1984), presenting the results of a 20 year experimental investigation into pollen decay in soils, demonstrates that different types show different susceptibility to degradation. Both rates of decay and the nature of degradation of the exine (e.g. corrosion, cavitation, thinning) varied between different soil environments (river clay, podzolised sand, peat). However, certain types demonstrate generally lower susceptibility to decay; these include Pteridophyte spores (*Lycopodium*, *Polypodium*), bisaccate pollen grains of *Pinus*, and fenestrate pollen of Asteraceae (*Taraxacum*). Laboratory-based experimental investigations (Campbell, 1991; Campbell & Campbell, 1994) also highlight the susceptibility of pollen grains to physical degradation when exposed to repeated wet-dry cycles. While differential preservation is a concern for the interpretation of pollen records, in practice, anaerobic sediments probably preserve most pollen grains of most types (Bennett & Willis, 2001). However, the extreme susceptibility of a few pollen types to extremely rapid decay may underline their absence or under-representation in pollen records. In this study, for example, the absence of *Populus* or *Juncus* pollen may be related to this phenomenon.

8.1.2 Pollen in the estuarine environment: source areas, transport and deposition

In addition to an awareness of the preceding factors, interpretation of pollen records must be undertaken with consideration of the pollen source area. This requires an understanding of nature of the depositional setting and the modes of transport by which pollen arrives at the site. In general, models for pollen transport and deposition have concentrated on aerial, fluvial and lacustrine systems (Traverse, 1988). In some settings, notably lake basins in forested environments, extensive research has yielded a strong understanding of the relationship between the depositional location and the pollen source area for certain settings. For example, the general relation between increasing size of a lake basin and increasing pollen source area is well defined (Jackson, 1994). In contrast, the understanding of pollen

transport and deposition within the estuarine environment is less advanced (Chmura & Eisma, 1995).

A model for the pathways of pollen transport into estuarine sediments, adapted from the classic model of Tauber (1965), is presented in Figure 8.2. Overall, pollen in the estuarine setting is considered to derive from both airborne and waterborne sources, and be subject to varying degrees of homogenisation within the tidal water body. The pollen entering the estuary is viewed as the sum of different source components. These components illustrate the variety of mechanisms by which pollen may be transported into an estuary and, by extension, highlight the possibility for changes in the relative importance of different

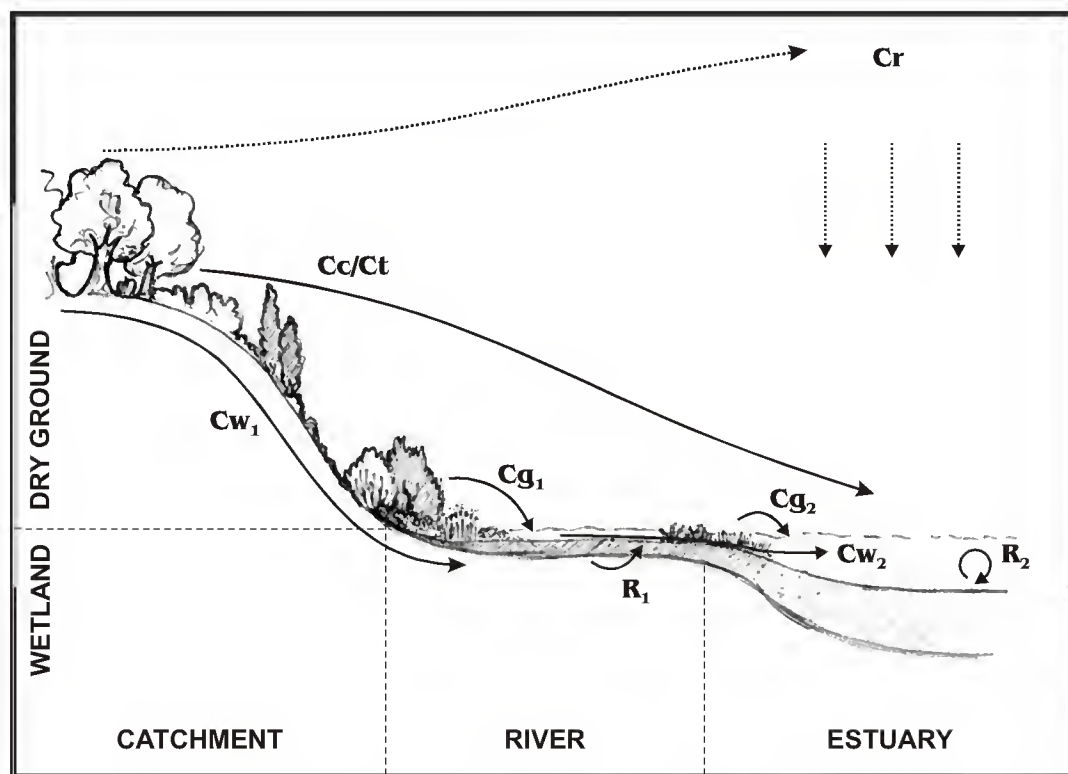


Figure 8.2. Transport pathways of pollen entering an estuary; adapted from Tauber (1967).

Cr : atmospheric airborne pollen component (long-distance)

Cc/Ct : canopy/trunk-space airborne component (short to medium distance)

Cg_1 : gravity component entering the fluvial system from riparian vegetation

Cg_2 : gravity component from wetland vegetation within the estuary

Cw_1 : inwashed component entering the fluvial system from soil and vegetation runoff

Cw_2 : total inwashed component of waterborne pollen entering the estuary

R_1 : recycled/reworked component from alluvial sediments and soils

R_2 : resuspended tidal component

transport mechanisms to produce variation within the pollen assemblage reaching the estuary (Jackson, 1994).

A local or gravity component is composed of pollen falling more or less vertically from plants growing within or on the fringes of the estuary (Cg_1). This component may be deposited in the form of clumps of pollen or intact anthers, and may result in a strong over-representation of local vegetation types of marsh vegetation, e.g. Poaceae and Chenopodiaceae. A component derived from vegetation neighbouring the estuary, and transported by low to high velocity air currents more or less horizontally, is comparable to the trunk-space (Ct) and canopy (Cc) components of Tauber. A distinction between the two is probably not appropriate in a landscape where a mosaic type vegetation may be more common than closed canopy forest. This combined component (Cc/Ct) is carried on turbulent winds close to the ground, and is considered to derive from dry ground vegetation of hillslopes and upland areas at distances from several metres to several kilometres from the estuary. Stevenson (1985a), for example, observed that in the complex mosaic type vegetation of the Coto de Doñana park, the movement of pollen from one vegetation type to another is a very important source of non-local pollen. The rain component (Cr) represents pollen dispersed by air currents from the source vegetation, lifted to high-altitude by convection, and deposited in rain droplets. As pollen may be transported long distances on high-altitude currents, the rain component may represent pollen sources at distances of hundreds of metres to hundreds of kilometres from the site, both within the drainage basin and beyond. The inwashed or fluvial component (Cw_2) comprises pollen entering the estuary via the river system and represents pollen sources within the entire drainage basin. The inwashed component contains pollen from dry ground vegetation entering rivers via surface runoff and tributary streams (Cw_1). The fluvial pollen load will also include its own gravity component (Cg_2) derived from riparian and aquatic vegetation growing in the river system and along its banks and floodplains. The fluvial pollen load is likely also to include recycled pollen, which repeatedly re-enters the stream in times of peak flow, and reworked palynomorphs from sediments eroded by the river (R_1) (Traverse, 1990; Campbell & Chmura,

1994). Another source of recycled pollen is tidal currents within the estuary, which promote resuspension of surface sediments, mixing and redeposition (R_2).

Within the estuary, deposition of pollen grains on the sediment surface is controlled by processes within the estuary. A large proportion of the pollen transported into the estuarine domain will enter the tidal water body, either via the fluvial system or at the air/water interface. A proportion of the airborne pollen supply may settle directly onto the sediment surface, but will be subject to resuspension during high tides. The tidal water body therefore represents a major proximal source of pollen for estuarine sediments. Estuarine waters typically contain high concentrations of pollen (10^5 grains/ 100 l), one order of magnitude higher than nearshore coastal waters and two orders of magnitude higher than open marine waters (Traverse, 1990). Pollen grains, once they contain sufficient water to sink, are generally considered to behave in a similar manner to other particulate matter, with settling velocities determined by size, specific gravity, shape and surface texture (Brush & Brush, 1994). Pollen grains have settling velocities equivalent to mineral grains between 5 and 15 μ m (fine silts, ~6 to 8 phi) (Brush & Brush, 1994; Chmura & Eisma, 1995). Pollen in the tidal water body should move in suspension in tidal currents, and be deposited during slack water periods. While settling velocities vary between pollen types, the hydrodynamic properties of individual grains probably do not exert a strong control over the deposition of pollen from the tidal water body. This is because pollen and spores are likely to be incorporated into aggregate particles, both floccules and bioaggregates (faecal pellets of bivalves and zooplankton), with higher settling velocities than individual grains. Pollen settling onto the sediment surface is subject to remobilization by tidal currents and mixing in the tidal water body (Clark & Patterson, 1985; Chmura & Eisma, 1995). The extent of resuspension will vary with current strength and whether the sediment surface is vegetated. Where the surface is vegetated by marsh plants, these act as a baffle, trapping sediment and organic debris and reducing the extent of remobilisation (Allen, 2000).

The study of the pollen content of surface sediments from the Ems-Dollard tidal basin (Germany/Netherlands border) (Chmura & Eisma, 1995) provides some important insights into the behaviour of pollen within a tidal basin. The authors demonstrate that while total pollen concentration in surface samples is conditioned by hydrodynamic factors related to mud flat topography and current energy, pollen percentages show little variation. The minimal sorting of pollen by taxa or by condition (preservation state) is attributed to two factors. First, processes of flocculation and bioaggregate pellet formation diminish the importance of variation in settling velocities between different pollen types. Evidence for the important role of bioaggregation is shown in the recovery of pollen and spores from the stomach contents of bivalves and from intact faecal pellets recovered from sediment samples (Chmura & Eisma, 1995). Second, resuspension of surface sediments promotes homogenisation of the pollen content.

Some pollen, notably the gravity component derived from local marsh vegetation (Figure 8.2, Cg₂), and airborne components from neighbouring vegetation or the regional pollen rain (Cc/Ct, Cr), may be supplied directly to the sediment surface of marshes or tidal flats. As vegetation tends to reduce current velocities and promote sediment trapping (Allen, 2000), pollen deposited within a vegetated marsh setting is less likely to be redistributed. Saltmarshes therefore tend to concentrate pollen derived both from local vegetation and from the tidal water body (Clark & Patterson, 1985; Chmura & Eisma, 1995).

Opinions differ regarding the relative importance of windborne and fluvial pollen sources for estuaries. On the one hand, rivers are effective pathways for the transport of pollen, and fluvial pollen supply is significant in a range of sedimentary settings including lakes (e.g. Peck, 1974; Bonny, 1978) and shallow marine environments (Heusser, 1978). A number of studies have demonstrated positive correlations between pollen concentration, suspended sediment load and discharge in river water (Groot, 1966; Chmura & Liu, 1990). As estuaries and surrounding marshes are major sinks for fine-grained sediments of fluvial origin (Dark & Allen, 2005), a significant contribution of fluvially-derived pollen should be anticipated.

In the Delaware river estuary (Atlantic coast, USA), Groot (1966) observes correlations between suspended pollen concentration and suspended sediment load. Groot also observed a good correspondence between the composition of pollen spectra and the vegetation cover across the entire drainage basin, both for suspended and bottom sediments. These observations suggest a predominantly fluvial source of pollen in this case. This view is maintained in a number of palynological studies of estuarine sediments, where the pollen source area is equated with the fluvial drainage basin (e.g. Sánchez Goñi, 1996; Santos & Sánchez Goñi, 2003).

In contrast, in studies of the Chesapeake Bay (Atlantic coast, USA) Brush and Brush (1994) found that pollen content of surface samples correlates with the vegetation cover of adjacent areas to the estuary. These authors suggest a predominantly airborne pollen supply and a model whereby pollen grains entering the estuary eventually settle to the bed in approximately the same place, after a period of back and forth movement under tidal action (Brush & Brush, 1994). Debenay *et al.* (2003) also observe correlations between pollen content and vegetation cover of adjacent areas along a longitudinal transect of sediment samples in the Vendée estuary in western France. However, it is not clear that spatial variation in pollen content demands that aerial pollen sources be dominant. Chmura *et al.* (1999) note that even in high order rivers, surface runoff from river banks and tributary inputs may introduce pollen from local plants which is detectable in suspended pollen assemblages. Similarly, spatial variation within estuarine waters and surface sediments may also reflect localised variation in the inwashed component. To conceive of a basin-wide dominance of either fluvial or aerial sources is probably unrealistic. As Chmura (1994) demonstrates for modern sediments of the Mississippi delta plain, pollen content and the ratio of local to regional pollen vary systematically across different sub-environments, related to the relative importance of local (gravity component), fluvial and aerial pollen sources. The relative importance of these components is understood to vary according to flooding regimes, proximity of fluvial sources, conditions of sediment trapping and the extent of vegetation of the sediment surface.

In terms of interpreting pollen assemblages from estuarine sediments, the likely contribution of fluvially-transported pollen introduces certain difficulties. Differential transport of pollen and spores has been shown to occur in flume experiments (Brush & Brush, 1972; Holmes, 1990), and has been considered by some researchers to be a significant control on the composition of alluvial pollen assemblages (e.g. Catto, 1985; Fall, 1987). However, studies of spatial variability in pollen content within river water samples have not demonstrated strong correlations between pollen content and stream velocities (Campbell & Chmura, 1994; Smirnov *et al.*, 1996), supporting the view that fluvial transport “should not be expected to cause distortion of pollen assemblages in sediments” (Smirnov *et al.*, 1996: 80). While the action of fluvial transport itself is not considered to represent a serious problem for the interpretation of sediments which contain a major inwashed component, the contribution of recycled and reworked pollen of mixed ages does present a challenge for the interpretation of pollen in sediments receiving a major fluvial contribution (Burrin & Scaife, 1984). High frequencies of pre-Quaternary spores or degraded pollen grains may provide critical indications of the extent of erosion and reworking. While a major inwashed component presents this difficulty, a benefit arises from the more inclusive incorporation of pollen from plants which are not wind-pollinated and which may only disperse pollen over short distances (e.g. entomophilous plants, understorey plants and some spore producers) (Chmura *et al.*, 1999). The record of members of the Cistaceae family encountered in this study, for example, is considered to reflect the influence of an inwashed pollen component.

For the sites studied here, the pollen components that are considered likely to dominate the pollen record are 1) local vegetation growing near the coring site (Cg2), and 2) inwashed pollen from the fluvial drainage basin (Cw2). This latter component will contain both dry ground (Cw1) and wetland pollen types (Cg1). Given the sedimentary (particle size) evidence for the predominant deposition of fine-grained particles in the form of aggregate particles from the tidal water body, and the focusing of sedimentary and organic material of fluvial origin which occurs within an estuary, these sources are considered more important than

airborne pollen sources. However, airborne sources at a range of distances from the core sites (Cc/Ct/Cr) will also have contributed to some extent to the pollen record, and this contribution may have varied over time with respect to prevailing winds, changes in the morphology of the estuary and the structure of local vegetation.

Overall, the main (non-local) pollen source areas for the P2 and P5 cores are considered the drainage basins of the Boina and Arade valleys, respectively. These include large areas of the upland *Serras*, and (for P5) the slopes of the Monchique massif. These also include numerous small valleys of tributary streams, and small areas of limestone *Barrocal* lowland on the margins of the estuary. For core CM5, an important pollen source area is considered the drainage basin of the Beliche tributary. In common with the Boina and Arade basins, this includes a large area of upland terrain, dissected by small valleys. Fluvial input from this tributary system may dominate the pollen content at the core site. However, as part of the Guadiana estuarine system, the pollen record may contain a significant pollen component derived from the tidal water body or remobilised from other areas of the estuary (R2). This component will increase the geographic range of pollen source areas to include a much wider region of the Guadiana basin.

8.1.3 Taxonomic precision

A difficulty in interpretation of the pollen record relates to the low taxonomic precision of some pollen types. Poaceae, the grass family, is an important example. Grass pollen is generally well represented in the pollen records studied here, but its significance is not easy to determine. Grasses are an important floristic component of a variety of vegetation communities, representing lower intertidal saltmarshes, river floodplains, meadows and agricultural ground. Asteraceae (Lactucaee), with representative species in many open ground habitats including saltmarsh, is another example. Overall, these problems are exacerbated in the study of tidal sediments due to the likely extent and range of pollen source areas. The basic division of the pollen records into two sets, dry ground and wetland taxa, is an important step towards improving the interpretation of the pollen data (Clark & Patterson, 1985). However, some broad taxonomic pollen groups taxa are likely to straddle this basic

division. While it is considered likely in this case, due the nature of pollen dispersal, that local wetland sources may be more significant than dry ground sources within the pollen source area, this cannot be proved. High and fluctuating pollen percentages are generally recognised to indicate pollen inputs from local vegetation (Rybníèková & Rybníèek, 1971), but this may not provide such a reliable indicator where resuspension and mixing of pollen grains by tidal currents take place. In cases where a dry ground or regional contribution to a designated wetland type is suspected, specific mention is made in the text.

8.1.4 Proportional data

Finally, it is recognised that pollen percentages are subject to certain difficulties which arise from the nature of proportional data. The most obvious difficulty is that high values for one taxa will depress the values for other taxa. Where changes reflect different areas within the pollen catchment, this may lead to difficulties in interpretation. Less obvious is what Faegri and Iversen refer to as the ‘law of diminishing return’, whereby as a taxon approaches 100% a large absolute change in pollen input will result in very little change in representation in terms of percentage values (Faegri & Iversen, 1989). The interpretations drawn from percentage data should be checked against concentration values, by which means the input of any given pollen type may be considered independently.

8.2 CM5 Guadiana

8.2.1 Late-glacial vegetation, c. 13,000–11,860 cal BP

The well-preserved pollen from samples of Late-glacial age is, in the broader perspective, a valuable and unusual feature of the CM5 core. In terms of the dry ground assemblage, one of the most distinctive features of CM5-I is the combination of high values for *Juniperus* associated with the occurrence of *Ephedra distachya* type. *Ephedra distachya* is a plant of arid conditions on sandy terrain, such as stabilised dunes, and does not occur in the modern vegetation of Portugal. The combination of juniper and *E. distachya* suggests a floristic community occurring in xeric conditions during the Late-glacial, perhaps similar to the permanent shrub communities of *J. phoenicea* ssp. *turbinata* and *E. distachya* growing on coastal sand dunes and palaeodunes in semi-arid to sub-humid areas of the western

Mediterranean and Maghreb (Rivas-Martínez *et al.*, 2001). Although these junipers grow as small trees and shrubs on dry rocky slopes within the modern basin of the Guadiana (Capelo, 1996), the increased representation of *Juniperus* pollen and presence of *E. distachya* in the Late-glacial suggest that this floristic community did not persist into the Holocene. Other indications of drier than present conditions may include the occurrence of *Centaurea* (*C. nigra* type and *Centaurea* undiff.), associated with steppic or dry grassland environments, in CM5-I. Also, the virtual absence of typical sclerophyllous thermomediterranean taxa, *Olea*, *Phillyrea* and *Pistacia*, in CM5-I may reflect cooler as well as drier conditions.

During the period of time represented by CM5-Ia and CM5-Ib (*c.* 13,000–12,550 cal BP) the record for *Pinus* and *Quercus* presents indications of dynamic changes in arboreal populations. In the lowermost samples (CM5-Ia), values for Sum *Quercus* (the individual records of the constituent types will be considered later) are as high as any recorded during the Holocene. Values decrease across the sub-zone, and are then dramatically reduced at the transition to CM5-Ib (*c.* 12,800 cal BP), decreasing to frequencies as low as those observed in the upper part of the core where major human impact may be considered a likely factor. A concomitant decline in *Quercus coccifera* type is also observed, with core low values occurring at the base of CM5-Ib. In contrast, values for *Pinus* increase across the sub-zone boundary, reaching peak values for the core. The pollen concentration values suggest that decreased input of *Quercus* pollen is the main cause for changes in the frequency values. This major decrease in the representation of *Quercus* — a genus characterised by good pollen production and dispersal — is interpreted as a decline in regional forest cover. This event probably reflects climatic factors, namely a relative shift from wet to dry conditions, which is supported by the record of several other taxa at the CM5-Ia/Ib boundary. Increases in *Juniperus*, *Ulex* type (gorses and brooms) and several herbaceous taxa associated with open dry terrain, namely *Plantago lanceolata* type, *Centaurea* undiff. and Caryophyllaceae, are consistent with this interpretation. The contribution of *Pinus*, probably reflecting both coastal pinewoods on sandy soils and upland stands, appears to have been more stable, and percentage values are enhanced in relation to the other taxa. The

identification of a morphometric group ascribed to *P. sylvestris* indicates a long-distance pollen contribution from montane areas in the Portuguese interior. In CM5-Ic, percentage values show a reduction for *Pinus* and an increase for *Quercus*. The significance of these changes in terms of forest cover is difficult to assess, because they correspond with a dramatic reduction in pollen concentration for virtually all taxa. *Quercus* displays an apparent recovery from the decline observed in CM5-Ib.

In terms of wetland vegetation, CM5-I presents evidence for a transitional phase from floodplain to saltmarsh vegetation. At the base of the core, high values for Apiaceae, Asteraceae (Lactucaee), Poaceae and Cyperaceae suggest open conditions around the core site. Although the taxonomic precision of these taxa is low, the affinity between the pollen curves for these taxa suggest that they may in large part reflect a common floristic element, which is considered to be floodplain and freshwater marsh vegetation. Across CM5-Ia and CM5-Ib, these types decline relative to *Artemisia*, Chenopodiaceae and *Armeria/Limonium*, suggesting a transition in the wetland environment towards the development of halophytic communities. CM5-Ic is characterised by a well developed halophytic vegetation, with high frequencies of Chenopodiaceae, *Aster* type, *Artemisia* and *Armeria/Limonium*.

The development of the halophytic vegetation may reflect a localised expansion of saltmarshes near the CM5 site. However, there are indications that the evidence for increased salinity does not pertain simply to local vegetation at this time. High values for *Artemisia* and Chenopodiaceae are a characteristic feature of southern European pollen records for the Late-glacial period (e.g. Pons & Reille, 1988; Giralt *et al.*, 1999; Lawson *et al.*, 2004) and are considered an indicator of arid climatic conditions, representing a steppic vegetation without clear modern analogues. In a coastal setting, it may be difficult to distinguish between climatic aridity and hydrographic salinity signals in the pollen record, as the two pose a similar effective pressure for plant life. Aridity and salinity may of course be related in the coastal zone; for example, decreased freshwater supply and increased evaporation promote the salinisation of marginal areas and encourage the development of salt crusts. Although

Artemisia is included with the wetland group of pollen types because of the occurrence of certain species within halophytic marsh vegetation communities, e.g. *A. caerulescens* (Lousã, 1986), the increased importance of *Artemisia* during the Late-glacial may well represent the wider development of arid environments during this period. Indeed, while a local saltmarsh signal for *Artemisia* is suggested by occasional minor peaks in association with elevated values for Chenopodiaceae in other zones (CM5-Ivb, CM5-V), the nature of the signal in CM5-I is different. The representation of *Artemisia* is much stronger, more consistent between samples, and shows evidence for changes which parallel the aforementioned trends across CM5-Ia/Ib in dry ground taxa such as *Pinus* and *Juniperus*. These observations suggest a regional signal, reflecting a wider development of arid or saline environments within the Guadiana basin.

In summary, the Late-glacial pollen spectra display a distinct overall character, with evidence for arid climatic conditions in the representation of a xerophytic shrub community (*Juniperus* and *Ephedra distachya*) and a range of dry ground herbaceous taxa. The lower sub-zones (CM5-Ia/Ib) record marked changes in a number of taxa, including a major decline in *Quercus*. These changes are interpreted as evidence of an arid climate event. Pollen types within the wetland group suggest a trend towards conditions of increased salinity. This trend may reflect changes in the local environment from freshwater floodplain to saltmarsh. However, the trend may be representative of arid conditions in the wider region.

8.2.2 Early Holocene vegetation, c. 11,860–8960 cal BP

CM5-II has unusual characteristics which make interpretation of the pollen spectra difficult. The record of dry ground taxa suffers from a combination of poor preservation and low pollen concentration. Dry ground taxa represent only a minor component of the total pollen assemblage, which accounts for depressed pollen percentage values relative to the total sum. In this case, the percentage values relative to the partial sum should provide insights into the composition of dry ground vegetation. However, the pollen counts for dry ground taxa are low, so the percentage values cannot be considered robust. Therefore, the interpretation of this part of the record in terms of vegetation is tentative. Overall, the main

arboreal types are well represented, with slightly higher frequencies for *Pinus* than *Quercus*. The important role for *Juniperus* and *Ephedra distachya* type is not evident in CM5-II, although the overall evidence for a mixed woodland and scrub landscape continues into the early Holocene, with relative high frequencies for a number of open ground herbaceous types (*Centaurea*, *Erodium*, *Serratula* type) and shrub taxa (*Coronilla* type, Cistaceae and Ericaceae).

The total pollen and spore assemblage is dominated by a small number of taxa, namely Cyperaceae, *Ophioglossum lusitanicum*, and especially Asteraceae (Lactucaee). *Isoetes* spores are also very abundant, particularly near the top of the biozone, being up to 5 times more numerous than the entire population of other pollen and spores. The combination of *Isoetes*, *Ophioglossum lusitanicum* and *Pilularia globulifera* (a relatively minor taxon which is best represented in this zone) suggests a particular set of ecological conditions. *Ophioglossum lusitanicum* and *Pilularia globulifera* are both amphibious plants of shallow depressions, seasonal ponds and temporary wetlands on minerogenic soils, and are typically found in vegetation communities associated with *Isoetes* (Rivas-Martínez *et al.*, 2001; Grillas *et al.*, 2004). *Isoetes* today occupies shallow, oligotrophic pools and in southern Europe is especially characteristic of seasonal pools, a special and generally threatened biotope with a rich and distinct flora (Quezel, 1998). The genus *Isoetes* in southern Portugal includes both terrestrial plants of damp grassy areas on the fringes of temporary ponds (*I. histrix*, *I. durieui*) and amphibious plants of seasonal pools (*I. velata*, *I. setacea*) (Grillas *et al.*, 2004). A sub-population of the *Isoetes* spores was distinguished on the basis of a distinctive fibrous sculpturing of outer coating (perine) which is considered specific to *I. histrix* (Berthet & Lecocq, 1977). This type was only recorded in the upper part of the core, CM5-IV/V. This suggests that the population of *Isoetes* spores in CM5-II and CM5-III may predominantly reflect the amphibious group of *Isoetes*. However, the contribution of *I. durieu* and the resilience of the sculpturing of *I. histrix* over time are not known.

The abundance of Asteraceae (Lactucaee) grains may reflect a large presence in the local vegetation. However, the recognised resilience of this particular pollen morphology may suggest a taphonomic influence on the assemblage. The fenestrate morphology of this pollen type is extremely robust and the pollen type may survive under conditions of poor preservation when other pollen grains are destroyed (Havinga, 1984). The very strong representation of this pollen type may reflect a reworked component from soils or alluvial sediments which have been exposed to subaerial weathering, as suggested for high abundances of Asteraceae (Lactucaee) in fluvio-estuarine sediments in Sicily (Collins *et al.*, 2001). Another indicator of reworked sediment input, namely rebedded trilete spores, shows increased values in this biozone although frequencies of indeterminate grains are not significantly greater than in other biozones, and are in fact much reduced from the preceding biozone, CM5-Ic.

In contrast with CM5-II, CM5-III is characterised by modest pollen concentration and larger pollen counts for dry ground taxa. Two distinctive features of CM5-III are: 1) the strong representation of *Pinus*, suggesting an important pollen contribution from both lowland pinewoods and more distant upland pines (*P. sylvestris*), and 2) the beginning of the continuous curve for *Olea*, and the beginning of increased importance for *Phillyrea* and *Pistacia*. These pollen types show a general affinity throughout the core (and in cores P2 and P5) and are considered to represent areas of evergreen woodland and thickets. The status of these taxa during the early Holocene (CM5-II) cannot be ascertained with certainty due to the poor record overall for dry ground taxa. However, despite a well preserved pollen assemblage, these taxa are virtually absent from CM5-Ia and CM5-Ib. This contrast between the Late-glacial and Early Holocene representation of these sclerophyllous Mediterranean taxa suggests a vegetation response to warmer conditions after c. 10,000 cal BP.

8.2.3 Holocene forest conditions, c. 8960–5200 cal BP

CM5-IV shows high values for all *Quercus* pollen types and suggests the most important development of regional *Quercus* forests during the Holocene. Frequencies for *Pinus* are

reduced from CM5-III, and morphometric indications suggest a reduced component of *P. sylvestris* pollen. Examination of the concentration curves shows that the expansion of *Quercus* at the transition from CM5-III to CM5-II is more significant than the reduction in *Pinus*. Small evergreen trees or large shrubs of *Olea*, *Phillyrea* and *Pistacia* are well represented. The concomitant expansion of *Quercus* and these evergreen types probably reflects a forest expansion structured by microclimatic and edaphic conditions, with oaks growing on the deeper, moister soils in the valleys and evergreen thickets occurring on thinner soils on south-facing slopes and other xeric locations. The consistent presence of *Olea* in this biozone demonstrates the status of *Olea* as a constituent member of the natural vegetation cover in association with other Mediterranean evergreen taxa such as *Phillyrea* and *Pistacia*. This contrasts with its status in northern Portugal where *Olea* chiefly provides a signal of human activity through cultivation (van den Brink & Janssen, 1985). Other shrub taxa are not strongly represented in this biozone. Fairly low frequencies of Cistaceae and Ericaceae may reflect shrubs growing as part of the forest understorey and/or an overall limited extent of shrubland vegetation. While this zone presents evidence for a maximum development of forest conditions, the structure of the vegetation cover probably was not fully closed. In general, arboreal taxa (*Pinus* and *Quercus*) and small tree/tall shrub taxa account for around 80% of dry ground taxa, and a much smaller proportion of the total pollen and spores. The occurrence of small clearings, forest edge habitats and grassy places are indicated by the sporadic presence of a range of herbaceous taxa at low pollen percentages, e.g. *Echium*, *Erodium*, *Linum* types, *Sanguisorba minor* and others.

In CM5-IV, peak values are recorded for *Q. suber* type. The record of *Quercus suber*, the cork oak, is of considerable ecological interest, both in terms of the tree's role in the original forest cover of southern Portugal and for the economic importance of the plant. The identification of *Quercus suber* type, however, which is undertaken on the basis of the size of the polar area of the pollen grain and the size of verrucate sculpturing on the exine (Saenz de Rivas, 1973), relies on good preservation of fossil grains. The type may also show considerable overlap with the *Quercus deciduous* type (Mateus, 1992). The curve for

Quercus suber type from core CM5 at a number of depths in CM5-IV shows an inverse relationship with *Quercus undiff.* suggesting that the successful identification of *Quercus suber* type was conditioned by preservation state or other sample specific factors unrelated to the actual influx of *Q. suber* pollen to the site. Nevertheless, the broad pattern which emerges from the CM5 record is that *Q. suber* was a relatively minor constituent of the Late-glacial and early Holocene forests, but increased in importance after 9000 cal BP (biozone CM5-IV) as part of the Holocene maximum forest development. In light of the preference of *Q. suber* and the semi-evergreen oaks (*Q. faginea*, *Q. canariensis* = *Q. deciduous* type pollen) for sub-humid to humid conditions (Polunin & Smythies, 1973; Capelo, 1996), the expansion of *Q. suber* and *Q. deciduous* type at this time suggests a climatic transition from warm, dry conditions to warm, moist conditions.

In terms of the wetland environment, CM5-IV presents evidence for input from a range of fresh and brackish habitats. Overall a well developed marsh vegetation with high frequencies of *Aster* type, Poaceae and Cyperaceae is recorded. Chenopodiaceae occur at fairly low frequencies. This may indicate that the depositional environment was low in the tidal frame, with a surrounding marsh vegetation dominated by grasses such as *Spartina* spp. rather than Chenopodiaceae. Alternatively, if conditions were of fairly low salinity, other taxa might be more competitive than the Chenopodiaceae. CM5-IV shows an increased input of pollen from freshwater wetlands. The extensive development of forests on dry ground environments is accompanied by a strong development of riparian woodlands with *Fraxinus* and *Salix* accompanied by *Osmunda regalis*. Together with oak forests and the evergreen forest fringe of *Olea* and *Phillyrea*, riparian woodland completes the picture of maximum forest development across the full spectrum of xeric to moist edaphic and microclimatic conditions. Freshwater marshes and pools are also recorded with *Typha/Sparganium* and *Myriophyllum alterniflorum*. Bearing in mind the likely contribution of many wetland pollen types via the tidal water body, it is also likely that the diverse wetland pollen assemblage reflects a variety of habitats around the estuary.

8.2.4 A mid-Holocene deforestation event, c. 7760–7350 cal BP

Within sub-zone CM5-IVb, an event is detected which impacts upon the pollen records of several major taxa. In this sub-zone, a decline in the main arboreal taxa is detected. Pollen percentages and concentration values for *Pinus* and Sum *Quercus* (excl. *coccifera* type) are slightly reduced and a range of shrub and open ground indicators show increases. *Myrtus* pollen is recorded for the first time. *Myrtus* is a fairly common shrub and occurs both as an understorey component of oak woodland and as an element of evergreen thickets, scrub and heath communities (Simonson & Sturgess, 1986). Only a single occurrence of *Myrtus* is detected before this sub-zone, in CM5-IVa. It would seem unlikely that *Myrtus* was not present in the landscape during the early Holocene. Rather, the sudden appearance of *Myrtus* as an important component of the upper pollen spectra suggests a possible change in either pollen production or dispersal efficiency related to a change in role for *Myrtus* from an understorey element to a member of more open shrub communities. This change might be associated with a reduction in arboreal cover associated with human activity, namely cutting and felling. A number of other shrub taxa which rise to prominence in the upper part of the record are detected in slightly increased frequencies in this sub-zone, including *Cistus ladanifer* type, *Erica scoparia* type and *E. umbellata* type. *Plantago lanceolata* type also shows a continuous curve during this sub-zone. These changes suggest a short-lived episode of reduced forest cover, with an expansion of *Cistus* scrub and ericaceous heaths.

Contemporaneous changes in the wetland taxa are also observed. A peak in Chenopodiaceae pollen accompanied by slightly elevated values for *Artemisia* suggests a flourishing of halophytic vegetation associated with a short-lived phase of marsh development. Certain freshwater indicators diminish during this phase (*Typha/Sparganium*, *Myriophyllum spicatum*) and *Isoetes* undiff. is also reduced. The changes observed in CM5-IVb appear to have been fairly short-lived and a renewed dominance of the arboreal taxa is observed in CM5-IVc, which is palynologically similar to CM5-IVa. Estimates from the age-model suggest a period of about 400 calibrated years for the duration of CM5-IVb.

8.2.5 Indications of anthropogenic impact, c. 5200–1430 cal BP

CM5-V contains evidence for a series of major changes in vegetation cover and composition. Overall, percentage values suggest a significant decline in both *Pinus* and *Quercus* (excl. *coccifera* type) at the CM5-IV/V boundary. Percentage values for both *Pinus* and *Quercus* then show a series of step-like decreases at the CM5-Va/Vb/Vc boundaries. These changes suggest a progressive reduction in the regional forest cover. This reduction is supported by changes in the concentration values, particularly bearing in mind that total concentration increases in CM5-V. The decline appears even more marked for *Pinus* than *Quercus*. The absence of a significant *P. sylvestris* component in the upper zones (CM5-IV/V) suggests that the declines recorded in CM5-V reflect a major impact on lowland and coastal pinewoods at this time.

Accompanying the first reduction in *Quercus* (excl. *coccifera* type) and *Pinus* frequencies (CM5-Va) is an increase in frequencies of *Q. coccifera* type, accompanied by increases in *Myrtus*, Cistaceae and Ericaceae. The contrast between high values for *Q. coccifera* type and reduced values for the other *Quercus* types suggests that *Q. coccifera* in this zone does not reflect woodland trees but rather shrub vegetation. In CM5-Vb, frequencies for all *Quercus* types, including *Q. coccifera*, are reduced, and Cistaceae and Ericaceae become more dominant. Finally, in CM5-Vc, *Pinus* and *Quercus* types are further reduced, while Ericaceae and open ground herbaceous taxa, *Plantago coronopus* and *P. lanceolata* types, increase.

The processes underlying this series of changes in the pollen record of CM5-V reflects the major development of shrubland vegetation communities, and are best explored in light of the ecological significance of some of the key pollen types. In the study of *Quercus* pollen, ambiguity results from variability in growth habit (Grove & Rackham, 2001) and from the inclusion of multiple species of different habit and ecology within pollen types. While the distinction of a *Quercus coccifera* pollen type is relatively straightforward, the interpretation of the resultant curve may not be. The *Q. coccifera* type includes pollen grains of *Q. coccifera*,

which may display a variety of growth habits depending on the extent of disturbance. *Q. coccifera* may grow as a small tree, and is considered a natural constituent of oak woodland alongside other shrubs which may reach the status of fully-fledged small trees in the absence of human interference (Braun Blanquet *et al.*, 1956). Following the first clearance of semi-evergreen forest of *Q. faginea*, tall scrub dominated by *Q. coccifera*, the *carrascais*, results due to the regenerative capabilities of *Q. coccifera*, with shrubs around 2 m high. Where burning is employed for pastoral activities, *Q. coccifera* gives way to scrub communities dominated by *Cistus*, *Erica* and leguminous shrubs, e.g. *Ononis*, *Ulex*. The *Q. coccifera* pollen type also includes part of the pollen of *Q. rotundifolia*, which is considered a primary constituent of the original forest under dry to sub-humid conditions (Capelo, 1996). *Q. rotundifolia* is also one of the principal oak species of the “montados”, or semi-natural parklands that characterise the continental interior of southern Portugal.

The curve for *Q. coccifera* type from the CM5 core is more or less parallel to the curves for *Q. deciduous* type and *Quercus* undiff. throughout the lower part of the sequence (biozones CM5-I, II and III). This close affinity is not observed in biozone CM5-IV, where a more individual behaviour is observed. In biozone CM5-V, the *Q. coccifera* type curve breaks fully from the other *Quercus* types, notably in CM5-Va, displaying a major increase in representation while other types undergo a severe reduction. The interpretation of this changing affinity between the types is considered to reflect a combination of two factors: 1) an increased representation of *Q. coccifera* compared with *Q. rotundifolia* associated with the expansion of tall scrub communities relative to forest, and 2) a changing role for *Q. coccifera*, from a component of the original forest cover to an individual response in reflecting the expansion of *Q. coccifera* scrubland. This individual response is best expressed in CM5-Va. Overall, CM5-Va is considered to reflect a first phase of forest clearance.

In CM5-Vb, a further reduction of *Quercus* types is recorded, this time including *Q. coccifera* type also, which corresponds with the maximum development of *Cistus ladanifer*/*populifolius*, *E. arborea* and *E. umbellata* types. These changes suggest a widespread decline

of oak forests, accompanied by the development of extensive *Cistus* scrub and ericaceous heaths. The development of these vegetation communities is promoted by burning, because of the regenerative response of the Cistaceae and Ericaceae following fire, through enhanced seed germination for the Cistaceae and through resprouting for the Ericaceae (Mabberley & Placito, 1993). As described by Braun Blanquet *et al.* (1956), traditional pastoral activities included intentional burning of the vegetation to promote lush regrowth of annual and herbaceous plants. This burning, however, ultimately promotes the further development of scrub and heath communities of Cistaceae and Ericaceae, resulting in a cycle of repeated burning and regrowth. *Daphne*, also notable for its recovery following fire (Mabberley & Placito, 1993), is most frequently recorded in this sub-zone. Overall, CM5-Vb is considered to reflect the maximum extension of semi-natural shrublands, probably under a regime of pastoral activity and anthropogenic burning.

In CM5-Vc, *Pinus* and *Quercus* types reach their lowest values, following a trend of declines observed across the biozone. Distinctive to CM5-Vc, however, are declines in the sclerophyllous taxa *Olea*, *Phillyrea* and *Pistacia*, and the riparian arboreal taxa. These declines suggest the destruction of natural woodland and tall shrub communities across the full range of edaphic and micro-climatic environments. These declines are accompanied by the maximum expansion of open ground indicators (*Plantago* types) and ericaceous heaths. The taller shrubs of *Cistus ladanifer*/ *populifolius* types decline, with the smaller species represented by *C. monspeliensis* type (*C. monspeliensis*, *C. salvifolius*) becoming more important. These changes are considered to reflect an intensification of human pressure through cutting, burning and pastoral activity and the degradation of some shrubland formations which found their maximum expression in CM5-Vb.

8.2.6 Agricultural indicators

“Primary indicators” (Behre, 1990) of anthropogenic activity, i.e. cultivated species of fields, orchards and gardens, are not clear in the CM5 record. Sporadic occurrences of large Poaceae pollen (diameter >38 μ m, pore > 8 μ m) are recorded in CM5-IV and CM5-V (shown in the column following Poaceae in Figure 7.3). In general, grains of this description may be

derived from cultivated cereals, although some wild grasses, notably *Glyceria* and other wetland species, produce grains of similar proportions (Bottema & Woldring, 1990; Moore *et al.*, 1991). In the CM5 record, some minor peaks in Poaceae D>38 P>8 correspond with local maxima for Poaceae, suggesting that these grains may in part simply represent a portion of a normally-distributed population of grass grains of various sizes. No clear correspondence is observed between peaks in Poaceae D>38 P>8 and indicators of open ground areas. While it is considered possible that some of the grains recorded in this category do originate from cultivated cereals, a clear signal for arable cultivation is not detected.

Of note is the record of the *Vitis* pollen type. *Vitis vinifera* is a sun-seeking creeper, often found growing on moisture loving trees and shrubs, for which the native range and history of cultivation are not fully known (Rivera Nuñez & Walker, 1989). *Vitis* pollen is plotted with the riparian taxa in Figure 7.3. At the outset of this study, the *Vitis* pollen type was considered likely to be an important indicator of viticultural activities. However, *Vitis* pollen was encountered routinely in the CM5 core (and also the P2 and P5 cores) in samples of mid-Holocene age, the earliest dating to 8820 cal BP (CM5, 1905 cm). These occurrences pre-date by several millennia the earliest archaeological or palynological evidence for viticulture or wine-making (Rivera Nuñez & Walker, 1989). This finding suggests that *Vitis* is an element of the native flora. The native range of *Vitis* is not well known, predominantly because of the widespread naturalisation of *Vitis* cultivars, but is generally considered to extend only to southeastern Europe (e.g. Tutin *et al.*, 1964–1980). However, evidence from a range of palynological and archaeological sources suggest that the native range, and hence the potential for domestication, may be much wider than generally accepted (Rivera Nuñez & Walker 1989).

Vitis is generally considered a poor pollen producer, and its detection in the pollen record is generally considered indicative of a local presence (Bottema & Woldring, 1990). At Laguna de las Madres in southwest Spain (Stevenson, 1985b), strong evidence for viticulture with *Vitis* pollen percentages reaching 40–50 % dates to at least 4500 ¹⁴C bp (c. 5300 cal BP).

Modest percentages are also found in spectra of similar age at the nearby site of El Acebron (Stevenson, 1988). In this case, a viticultural source is not clear. In the modern vegetation near this site, *Vitis vinifera* grows commonly as a liane among a carr vegetation of willows and ash, and fossil *Vitis* pollen percentages show affinities with *Salix* and *Fraxinus* pollen in some phases. However, in other phases, *Vitis* shows an affinity with disturbance indicators in the pollen record. In pollen records from the Alentejo littoral, sporadic occurrences of *Vitis* pollen are recorded at Lagoa Travessa from c. 6000 cal BP (Mateus, 1992). At Vale da Carregueira (Queiroz, 1999), *Vitis* pollen is recorded more abundantly, associated with *Alnus*, in a record extending to c. 6100 cal BP. In the CM5 record, the *Vitis* curve shows an affinity with the *Fraxinus* curve in CM5-IV and CM5-Va, and it is this represents wild plants of *Vitis* growing in riparian woodland in the surrounding valleys. Only in CM5-Vb and CM5-Vc, where *Vitis* frequencies show a modest increase, is a possible viticultural signal detected (i.e. after c. 4000 cal BP).

Castanea is recorded only in pollen spectra of CM5-Vb and CM5-Vc. Although there is evidence for a native status for the sweet chestnut in the Iberian peninsula with refugial populations present during the last Glacial period, *Castanea* is documented at the CM5 site only in the last 3000 years. This suggests that the traditional model for the spread of *Castanea* in Iberia, namely through introduction from more eastern parts of the Mediterranean region, holds for this locality. Although the Romans are generally credited with the widespread planting of *Castanea*, the earliest occurrence in core CM5 as determined by the age model (depth 340cm, c. 2860 cal BP) precedes the Roman invasion of Iberia of around 200BC by several centuries. Two explanations may be considered: first, the age-model may not be sufficiently accurate, and second, *Castanea* may have been brought to this region during pre-Roman times. The centuries preceding the Roman invaders were certainly a period of widespread contacts between southern Portugal and the eastern Mediterranean via Greek and Phoenician traders (Rouillard, 1991).

Several reasons may be posited for the limited record of primary indicators. One may be a large pollen source area producing a generalised picture of the vegetation cover below the resolution of small-scale prehistoric agricultural activities (In general, the best sites for palynological detection of early agriculture are those with small pollen source areas that include archaeological settlements (Willis & Bennett, 1994)). Another may be that pastoral, rather than agricultural activities may have been more important in terms of influence on the vegetation cover. In contrast, the record of “secondary indicators” (Behre, 1990) of anthropogenic activity is much stronger. These secondary indicators include species which are not intentionally grown by man but are either favoured or unintentionally introduced by human activities. In the CM5 record, taxa which appear to be associated with human impact include several shrub taxa which flourish only in the upper part of the record, e.g. *Myrtus*, *Erica scoparia* type and *E. umbellata* type. As mentioned, although *Myrtus* is likely to have been a constituent of a natural woodland vegetation communities, palynologically it is only associated with the expansion of semi-natural shrublands in the upper part of the record. This pattern holds true for the P2 and P5 records. The Cistaceae family are also important indicators of the development of semi-natural shrublands. Within the Cistaceae pollen taxa, three types — *Halimium halimifolium* type, *Helianthemum salicifolium* type and *Tuberaria guttata* type — show their maximum development in CM5-V. These types include dwarf shrub species and, in the case of *Tuberaria guttata*, herbaceous annuals, of low scrub and steppe vegetation. Although present in low frequencies, these types provide an important record of strong anthropic pressure through pastoral activity and the creation of degraded scrub vegetation. A contrast is also observed between the curves for *Cistus ladanifer/populifolius* types and *C. monspeliensis* type. The smaller species included in the *C. monspeliensis* type are more clearly associated with the semi-natural landscapes of CM5-V. Although direct pollen evidence for the cultivation of cereals is ambiguous, a number of ruderal species are recorded in CM5-V which probably reflect waste ground and field boundaries. These include *Anthemis* type, *Galium* type, *Fumaria officinalis*, *Valerianella* and *Scabiosa colombaria* type.. In general, however, these types are recorded only in low frequencies. *Plantago lanceolata* type, considered one of most

reliable anthropogenic indicators in the eastern Mediterranean (Behre, 1990; Bottema & Woldring, 1990), is strongly associated phases of forest decline, and is considered a reliable anthropogenic indicator here also. The more abundant *P. coronopus* type probably represents a mixed signal of human impact and terrestrialisation of estuary, given the tolerance of the species *P. coronopus* for saline soils.

8.2.7 Saltmarsh development, c. 5200–1430 cal BP

In CM5-V, fluctuating high values for Chenopodiaceae accompanied by small peaks in the curve for *Artemisia* suggest a local development of halophytic vegetation. Small increases in *Tamarix* in CM5-V may indicate marsh terrestrialisation and the encroachment of brackish ground at the marsh fringes. Declines in Cyperaceae and a progressive decline of *Isoetes* undiff. suggest a trend towards drier conditions. These changes are considered to reflect infilling of the depositional basin and a relative elevation with respect to the tidal frame. Riparian woodlands are well represented during most of this phase, declining only in the uppermost part of the record (CM5-Vc) after c. 2500 cal BP.

8.2.8 Dinoflagellates and other micro-fossils

A small number of dinoflagellate taxa are recorded from the CM5 sediments. Two important constraints must preface any interpretation of the dinoflagellate assemblage. First, dinoflagellates were only counted that were observed during pollen counts, i.e. the sum of dinoflagellates varies significantly between samples. Second, the use of oxidising chemical treatments during the routine pollen preparation may bias the preservation of dinoflagellate cysts towards the more resistant types (generally the autotrophic dinoflagellates) and result in the total destruction of some less resistant types (particularly the heterotrophic dinoflagellates) (Debenay *et al.*, 2003).

Nevertheless, some important observations arise from the dinoflagellate data. First, dinoflagellates are observed in every sample from the CM5 record. This suggests at least some tidal influence throughout the period of infilling (Jennings *et al.*, 1993). However, it is recognised that biological indicators of brackish or marine conditions may occur well

upstream of sedimentary tidal influence, relating to periods of reduced river discharge (Frey & Howard, 1986). Second, the samples are dominated by two types, *Spiniferites* sp. and *Lingulodinium machaerophorum*. These taxa are typical estuarine types tolerant of low salinities and their dominance (and the low diversity of types in general) is typical of the estuarine environment (Morzadec-Kerfourn, 1992; Debenay *et al.*, 2003; Morzadec-Kerfourn, 2005). Third, a slight increase in dinoflagellate diversity is noted in CM5-IV, with taxa of probable neritic or shelf origin (*Operculodinium centrocarpum*, *O. israelianum*, *Polysphaeridium zoharyi*) (Debenay *et al.*, 2003). This suggests a stronger tidal influence in this biozone, with the transport of dinoflagellates from more open coastal waters at the estuary mouth to the core location.

Pediastrum, considered an indicator of freshwater conditions (Round, 1965) are fairly abundant in many parts of the core, notably in biozones CM5-III and CM5-IV. In CM5-III the peak abundance of *Pediastrum* colonies corresponds to lowest values for dinoflagellates, and may suggest a low salinity wetland phase. In the pollen spectra, this zone displays the maximum frequencies of *Isoetes* undiff. However, high values of *Pediastrum* also occur in CM5-IV, associated with peak dinoflagellate abundance and diversity. This juxtaposition of freshwater and salinity indicators is considered to reflect a well-mixed tidal source of palynomorphs and algal bodies. Other algal fossils do not show a clear association with the pollen biozones. Spirogyra and Zygnemataceae, possibly also freshwater indicators, occur throughout the core, although peak frequencies occur in the lower biozones. *Concentricystes* (syn. *Pseudoschizaea*), a microfossil of uncertain but possible soil provenance, occurs rarely in CM5-V. In pollen records from southeastern Spain (Pantaléon Cano *et al.*, 2003), this fossil has been considered an indicator of input of eroded soil material, and its occurrence in the CM5 core may tentatively be ascribed to the same cause.

8.3 P2 Arade

Due to the nature of the sedimentary record, the P2 core contains two distinct palynological assemblages pertaining to two discrete time periods. The radiocarbon dates from P2 suggest

a very rapid sedimentation rate in the lower part of the core and suggest that P2-I spans a period of around 600 calibrated years between *c.* 8300 and 7700 cal BP. During this period, the overall palynological assemblage is fairly stable. Some important trends are noted, however. The age for the uppermost two samples (P2-II), is suggested to be around 5200 cal BP. In terms of the content of dry ground pollen, these samples present a marked contrast to P2-I.

Samples from the lower part of the core (P2-I) show high frequencies of deciduous *Quercus*, *Q. suber* and *Q. coccifera* types, and moderate frequencies of *Olea*, *Phillyrea* and *Pistacia*. These taxa display fairly stable concentration values, and suggest a well-developed regional oak forest with evergreen thickets occurring in dry areas of the landscape and on thin soils. Frequencies of *Pinus* decline steadily from high values towards the base (P2-Ia), a trend which is observed also in the concentration values. Percentage and concentration values for Sum Ericaceae show a slight increase from P2-Ia to P2-Ib. A possible explanation for these trends is a decline of pinewoods and replacement by open pine-heath in lowland areas.

The pollen assemblage of P2-II is characterised by changes in all the major dry ground taxa relative to P2-I. Frequencies of *Pinus*, *Quercus suber* and *Q. deciduous* types, *Olea*, *Phillyrea* and *Pistacia* are reduced, while Cistaceae and Ericaceae (notably *Calluna vulgaris*) display increased percentage values. Frequencies of *Quercus coccifera* type remain high. As discussed for the upper part of the CM5 sequence, the discrepancy between the *Quercus* types may relate to the different growth habits displayed by *Q. coccifera* and its regenerative capabilities following cutting. The first occurrence of *Myrtus* is recorded. These changes suggest significant alterations in the regional vegetation cover in the intervening period between P2-I and P2-II. A reduction in both pinewoods and oak forest is suggested, with widespread replacement of forested areas by tall scrub formations of *Q. coccifera* and *Myrtus*, *Cistus* scrub and ericaceous heaths. The marked reduction in forest and woodland taxa between P2-I and P2-II suggests a major phase of deforestation prior to 5200 cal BP.

Moreover, the evidence for a range of scrub and heath habitats in P2-II is considered to reflect widespread anthropic pressures in the Arade basin through grazing and burning.

In contrast with the dry ground pollen assemblage, changes in the wetland landscape appear to have been more moderate. Overall, the wetland pollen assemblage suggests pollen input from saltmarshes in the estuarine domain with Asteraceae (Lactucae), Chenopodiaceae, *Aster* type, Poaceae and Cyperaceae, and from riparian woodland with *Alnus* and *Fraxinus*. Riparian woodland is more strongly represented than at the CM5 site, with high values for *Alnus* in particular, suggesting a localised development of riparian carr vegetation in the tributary valleys. As discussed for CM5, the occurrence of *Vitis* pollen probably reflects wild vines growing in the riparian woodlands. A pollen component from shallow, seasonally flooded ground is also recorded with *Isoetes* and *Pilularia globulifera*. Inevitably, the juxtaposition of wetland pollen types of different habitats reflects the contribution of multiple pollen source components mixed in the tidal water body. Substantial differences between P2-I and P2-II are not observed for the wetland pollen types, suggesting that the vegetation of the local environment did not undergo significant changes. An increase in indeterminate pollen grains and a considerable decrease in pollen concentration reflect changes in the sedimentary environment.

Of non-pollen microfossils, only the dominant estuarine dinoflagellates *Lingulodinium machaerophorum* and *Spiniferites* sp. are recorded consistently. The two types show a negative affinity, with *L. machaerophorum* dominance giving way to increased abundance of *Spiniferites* sp. This negative affinity has been recorded in estuarine sediments from the Atlantic coast of Brittany (Morzadec-Kerfourn, 2003), and is considered to reflect the greater tolerance of *L. machaerophorum* for nutrient-rich waters of the fluvial estuarine domain. Following this interpretation, the changing dominance observed in the P2 sequence may reflect a transition from fluvial to open estuarine conditions over the course of biozones P2-Ia to P2-Ib.

8.4 P5 Boina

The P5 core contains a pollen record which more or less parallels that of the P2 core from the neighbouring Arade valley. With the exception of the uppermost sample, the pollen record is characterised by high frequencies of *Quercus*, *Olea*, *Phillyrea* and *Pistacia* pollen, with a small component of Cistaceae and Ericaceae pollen. However, some significant transitions are recorded in the period from c. 8200–3400 cal BP.

In P5-I, high frequencies of *Pinus*, *Quercus* spp., *Olea*, *Phillyrea* and *Pistacia* are recorded, probably reflecting a forested landscape in the Boina basin. The different taxa probably correspond to different thermal, pluvial and edaphic zones, with *Pinus* woodland on dry, sandy soils in the littoral zone, woodland and thickets of evergreen, sclerophyllous taxa (*Q. coccifera* type, *Olea*, *Phillyrea*, *Pistacia*) in the dry lowland areas, and semi-evergreen oaks (represented by *Quercus* (excl. *coccifera* type)) in the higher, moister areas of the basin. Low frequencies of *Cistus* and *Erica* pollen plants probably reflect a woodland understorey component.

From c. 8000 cal BP (P5-IIa) a marked reduction in *Pinus* percentage and concentration values suggests a decline in pinewoods. In contrast, populations of *Quercus* spp., *Olea*, *Phillyrea* and *Pistacia* continue without decline. Peak values for *Q. coccifera* type are observed, which may reflect either dry forest with *Q. rotundifolia* or shrubs and small trees of *Q. coccifera*. In contrast, high values of *Quercus* (excl. *coccifera* type) probably reflect a maximum development of evergreen and semi-evergreen oaks (*Q. suber*, *Q. faginea*, *Q. canariensis*) in the sub-humid upland areas of the Boina basin.

After c. 7210 cal BP (P5-IIb), frequencies of *Q. coccifera* type, *Phillyrea* and *Pistacia* decline. The affinity in the curves for these taxa suggest that they represent a common vegetation community, probably a lowland vegetation of mature thickets of tall shrubs and small trees occurring on the limestone slopes surrounding this part of the Boina valley. The decline in these taxa is accompanied by small expansions of *Cistus* scrub (*Cistus ladanifer*/

populifolius type) and heaths. These changes suggest the development of patches of more open scrub vegetation. However, continued strong representation of *Quercus* (excl. *coccifera* type) suggests that these changes were not of widespread impact across the Boina basin, particularly in the upland areas.

In contrast, the sample from the upper part of the core (505 cm, 3740 cal BP) provides an indication of much more extensive vegetation changes. Arboreal pollen types, *Pinus* and *Quercus* (excl. *coccifera* type), are poorly represented, as are the evergreen sclerophyllous taxa *Olea*, *Phillyrea* and *Pistacia*. In their place, populations of shrub species, notably Ericaceae and *Cistus* spp., and open ground ruderals *Plantago lanceolata* and *Rumex acetosella* are strongly represented. These changes suggest a major reduction in the extent of both oak forests and mature shrub communities of sclerophyllous taxa such as *Pistacia*. In common with the records from cores CM5 and P2, evidence for major forest reduction is accompanied by the appearance of *Myrtus* in the pollen record. As discussed for CM5, this is considered to reflect a new role for *Myrtus* as a taxon of scrub vegetation as opposed to woodland understorey, possibly associated with increased efficiency of pollen dispersal. The record of *Tuberaria guttata* in this sample attests to the presence of highly degraded areas of scrub vegetation. Overall, the major changes probably reflect widespread human impact in terms of deforestation and grazing pressures across the Boina catchment.

The P5 core also records some important changes in the wetland vegetation during the period of transgression at the site. As in the CM5 and P2 records, the diversity of wetland pollen types indicates the transport of pollen from a number of different habitats, of which saltmarsh and riparian woodland are particularly well represented. The more marked changes which occur in the records for certain pollen types, notably *Alnus*, *Isoetes* undiff., Chenopodiaceae and Poaceae, are likely to be related to hydrographic changes in the Boina valley. In P5-I, a maximum development of riparian woodland is recorded, with *Alnus*, *Salix*, *Fraxinus* and *Ulmus*. In P5-IIa and IIb, frequencies of *Alnus* pollen show a gradual decline. Because other arboreal riparian taxa (*Fraxinus*, *Salix*) do not show the same pattern

of diminishing values along the core, it may be that *Alnus* woodland was fairly localised, occupying the low-lying areas of the valley and giving way to more open conditions with progressive drowning of the area. The decline of *Alnus* in the wetland environment parallels that of *Pinus* on dry ground. While the two types represent different parts of the landscape — *Alnus* in fluvial freshwater wetlands, *Pinus* on sandy soils and stabilised dunes — both trees may have been adversely affected by changes in the littoral zone during the Holocene transgression. The pollen curve for *Alnus* contrasts with that of *Isoetes* undiff., which increases up core from P5-I to P5-IIb. This contrast probably reflects a declining contribution from dense carr vegetation on organic rich substrates and an increased contribution from open herbaceous swards on mineral rich substrates. The change, reflecting sedimentary conditions in the local environment, may have been occasioned by progressive drowning of the Boina valley.

Only two dinoflagellate taxa were observed in the P5 samples, the dominant estuarine dinoflagellates *Lingulodinium machaerophorum* and *Spiniferites* sp.. These taxa show a slight negative affinity, with frequencies of *L. machaerophorum* higher near the base of the sequence and of *Spiniferites* sp. towards the top. This pattern is comparable to that observed in the P2 core, and may suggest a similar hydrological development related to the evolution of the combined Boina-Arade estuary, with progressively more open estuarine conditions being established during the course of transgression.

9 Integration

In the following sections an interpretation of changes in the sedimentary environments is proposed on the basis of the combined information from the core descriptions, sedimentary analyses and pollen analysis. This is followed by an outline of regional vegetation history based on the new pollen evidence.

9.1 Estuarine evolution and environments of deposition

9.1.1 *Beliche-Guadiana (Core CM5)*

Table 9.1, showing the summary of sedimentological and palynological findings from the CM5 core, and Figure 9.1, showing pollen data plotted against age, accompany the following interpretations of palaeoenvironmental changes in the Guadiana estuary.

9.1.1.1 Pre-estuarine fluvial sediments (CM5s-1; prior to 13,000 cal BP)

The gravelly basal fill (lithozone CM5s-1), composed of coarse sands and rounded fragments of basement rocks, indicates deposition under a highly energetic fluvial regime. The coarse clast sizes and heterogeneous composition suggest a braided river setting subject to a flashy flow regime and characterised by the frequent migration of small channels. The presence of lenses of charcoal and plant detritus indicate the deposition of terrestrial detritus in flood deposits. The predominance of rounded greywacke and schist cobbles indicates that most of the coarse clastic material could be derived from local bedrock lithologies outcropping

AGE (ka cal BP)

GRIP EVENT CHRONOLOGY

LITHOZONE

DOMAIN

ENVIRONMENT OF DEPOSITION

WETLAND VEGETATION

P.A.B.

REGIONAL VEGETATION

ARCHAEOLOGICAL PERIOD

0

2

4

6

8

10

12

HOLOCENE

GS-1

GI-1

CM5s-6	Upper saltmarsh	ESTUARINE (MARINE)	CM5-V	Chenopodiaceae (upper saltmarsh flora)	No record	Further decline of oak and pine; decline of sclerophyllous thickets and maquis; expansion of heaths and open ground	Epipalaeolithic/ Mesolithic	Post-Roman			
	Lower saltmarsh/Tidal flat (influence of tidal currents)							CM5-IV	Poaceae/Cyperaceae/Aster type (lower saltmarsh flora)	Maximum development of oak forest (expansion of <i>Q. suber</i>), evergreen thickets of <i>Olea</i> , <i>Phillyrea</i> and <i>Pistacia</i> , and <i>Fraxinus</i> wet woodland; gradual decline of pinewoods	Neolithic
	Sheltered mudflat (low-energy)							CM5-III	Pinewoods and oak forest well established; presence of <i>Olea</i> , <i>Phillyrea</i> , <i>Pistacia</i>	Poor record of dry ground vegetation	Roman
	Fluvial/tidal channel (high energy, tidal influence) Floodplain/deltaic marsh (increasing tidal influence)							CM5-I	Presence of oak and pine, maximum development of <i>Juniperus</i> and <i>Ephedra distachya</i> Major decline of oak forest, expansion of pine, xeric scrub and steppe elements Established oak forest and pinewoods	Iron Age	
	CM5s-3							CM5-II	Decline of pinewoods and regional oak forests, development of sclerophyllous maquis with <i>Q. coccifera</i> and <i>Myrtus</i>	Major expansion of shrublands with <i>Cistus</i> and <i>Erica</i> spp.	Bronze Age
CM5s-2	CM5-I	Decline of pinewoods and regional oak forests, development of sclerophyllous maquis with <i>Q. coccifera</i> and <i>Myrtus</i>	Major expansion of shrublands with <i>Cistus</i> and <i>Erica</i> spp.	Copper Age							
CM5s-1	CM5-I	Decline of pinewoods and regional oak forests, development of sclerophyllous maquis with <i>Q. coccifera</i> and <i>Myrtus</i>	Major expansion of shrublands with <i>Cistus</i> and <i>Erica</i> spp.	Neolithic							

CM5s-1	FLUVIAL	Inactive floodplain (subaerial exposure, erosion)	No record	No record
--------	---------	---	-----------	-----------

PLEISTOCENE

Table 9.1. Summary of sedimentological and palynological findings from core CM5.

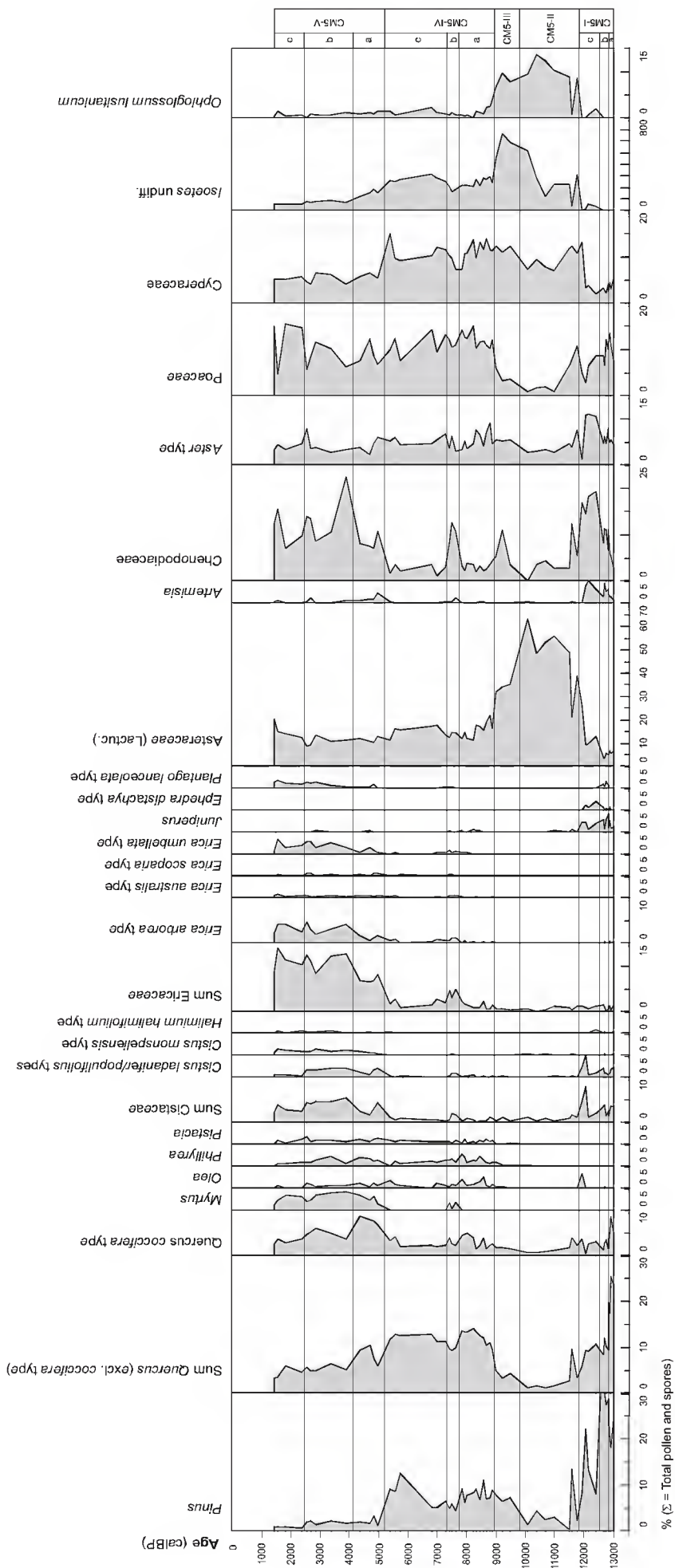


Figure 9.1. CM5 pollen percentage data plotted against age (cal BP). Sample ages calculated on the basis of the age-depth model proposed in chapter 5 (Figure 5.1).

within the drainage catchment of the Beliche tributary. However, the rare presence of fractured quartzites indicates transport of some of the fill material over longer distances from more continental areas. In the Guadiana setting, quartzites indicate recycling of material from *rañas* (Boski *et al.*, 2002), continental surface deposits of Plio-Pleistocene age that cover wide areas of the Pliocene planation surfaces of the Iberian peninsula (Espejo, 1987). Although not directly dated, radiocarbon dates from overlying zones indicate that CM5s-1 was deposited during the Pleistocene.

Although not directly dated, similar deposits have been previously recorded and some information is available that helps to constrain their age. A gravelly layer composed of recycled quartz pebbles and basement rock fragments is recorded at the base of four cores and several destructive drillings in the Guadiana estuary, reaching thicknesses of up to 45 m in the deepest part of the palaeovalley (Boski *et al.* 2002). Seismic stratigraphy reveals that the surface of the gravels can be traced throughout the Guadiana valley, and show morphological characteristics associated with subaerial exposure and erosion (Lobo *et al.* 2003). Comparable deposits are recorded from nearby estuaries of the Gulf of Cadiz (Borrego *et al.*, 1999; Dabrio *et al.*, 2000). Radiocarbon dates of *c.* 25,000 to 30,000 ¹⁴C bp for wood fragments from the basal fills of the nearby Odiel estuary have been obtained (Dabrio *et al.* 2000) indicating deposition prior to the Last Glacial Maximum. This suggests that these fluvial fills correspond with the sea-level highstand of Isotope Stage (IS) 3 (Boski *et al.*, 2002; Lobo *et al.*, 2003). The Last Glacial Maximum (LGM), in contrast, was a period of sediment bypassing and down-cutting with the rivers of southwest Iberia reaching a peak of eroding capacity associated with a mean sea-level *c.* 120 to 140 m lower than present and a coastline located *c.* 10 km offshore at the shelf margin (Dias *et al.*, 2000). The depth of the gravel surfaces therefore reflects the inherited palaeorelief following the Last Glacial Maximum.

9.1.1.2 Fluvial-estuarine transition (CM5s-2, s-3; 13,000–11,900 cal BP)

The lower part of the CM5 core (CM5s-2, s-3) contains sediments of Late-glacial age which attest to a transition between fluvial and estuarine conditions at the core location.

The onset of sedimentation at *c.* 13,000 cal BP is considered to reflect a change in base-level under a regime of eustatic sea-level rise related to deglaciation (Dias *et al.*, 2000). Rapidly rising sea-level during the period 13-11 ka ¹⁴C (~15,000–13,000 cal BP) drowned the terminal segment of the Guadiana river valley, effecting a transition from sediment bypassing under a fluvial regime to sediment trapping and accumulation. The approach of sea-level to around 50 m below present level would have brought the CM5 location within the domain of tidal influence. The coastline and estuary mouth, however, would have been located *c.* 20 km from the Beliche tributary (Dias *et al.*, 2000).

In contrast with the underlying gravel fill, CM5s-2 is composed primarily of fine-grained sediments, indicating the general conditions of a low energy sedimentary environment. Particle size analyses indicate an overall calm depositional environment dominated by settling processes. The zone is punctuated by evidence for periodic flood events. Discrete laminae of fine sand suggest the recurrence of low magnitude flood events. A thin layer of sand overlying an abrupt contact at 4740cm provides evidence of an individual flood event possibly accompanied by erosion. In addition to sands, flood events are likely to have been the source of allochthonous organic matter, represented by charcoal lenses, which occur in some parts of the zone. Small schist fragments at the base of the zone are likely to have been reworked by fluvial action from the underlying gravel fill.

The interlamination of sands and silts indicate a generally calm environment associated with settling processes was subject to recurrent flood events bearing coarser sediments and organic material. The occurrence of episodic alluviation within a marsh environment explains the presence of loading structures in several layers within the zone. Loading structures occur where relatively dense sand layers are deposited onto unstable soft sediments of lower density causing post-depositional deformation of the underlying layer. Loading and deformation structures suggest bursts of sedimentation (Lajeunesse & Allard, 2002), and are consistent with the interpretation of the sandy layers within the zone as flood deposits which settled rapidly onto the surface of fine-grained marsh deposits. The environmental

setting for this zone is considered to be an alluvial marsh environment located on the landward fringes of the developing estuary. In terms of the sedimentary characteristics, CM5s-2 is comparable to the fluvial floodplain facies described for the Huelva coast (Pendón *et al.*, 1997), which is observed today in the fluvial estuarine domain in areas subject to inundation by fluvial floodwaters and occasionally by high tides.

Wetland pollen types suggest a transition from a more freshwater floodplain vegetation with Apiaceae, Poaceae and Cyperaceae towards a halophytic vegetation dominated by Chenopodiaceae, *Artemisia* and *Armeria/Limonium*. This trend may indicate increasingly brackish conditions related to a gradual increase in tidal flooding. However, the interpretation of the halophytic pollen types may be complicated during this Late-glacial period by the contribution of Chenopodiaceae and *Artemisia* from steppe vegetation. However, the presence of dinoflagellates from the base of lithozone CM5s-2 indicates a contribution of sedimentary particles from tidal waters, and these show an increase towards the top of lithozone CM5s-2, supporting the view of increased tidal influence. The interpretation of the environmental setting as a marsh of fluvial/alluvial sedimentary character but with indications of tidal influence (in terms of the vegetation and dinoflagellates) is consistent with that predicted by general models of estuarine evolution (Roy *et al.*, 1980; Dalrymple *et al.* 1992) for the oldest deposits of a transgressive sequence. These models predict a bay-head delta within the fluvial estuarine domain, characterised by sediments of generally fluvial character but with indications of marine influence.

The transition from lithozone CM5s-2 to CM5s-3 represents a shift towards higher energy depositional conditions. The sediments display evidence of tidal action with interbedded sands and clays including sections of flaser-type bedding of clay drapes within fine sands. Flaser bedding results usually, though not exclusively, from the action of tidal currents and associated energy fluctuations (Reineck & Wunderlich, 1968; Frey and Howard, 1986), with clay drapes deposited between sand layers at times of slack water between the flood and ebb tides. The preferred environments are intertidal zones where alternations occur

between slack and turbulent water and where a range of sediment sizes are present (Reineck & Wunderlich, 1968). Although distinctive of tidal environments, flaser bedding may occur in a number of different estuarine sub-environments including sandy or mixed intertidal flats (Dalrymple 1992), tidal bars (Fenies & Tastet, 1998) and channels. In the modern estuary of the Guadiana, flaser bedding is associated with shallow sub-tidal channels in lateral areas of the central estuary (Borrego *et al.*, 1995). Here flaser and wavy bedding forms are characteristic features of a shallow-channel facies comprising finer sands (up to 3.5 ϕ) interbedded with silty-argillaceous sediments consisting of grain sizes associated with flocculation (Borrego *et al.*, 1995: 160). Fine 'flame' and 'dyke' structures are also observed in the lower part of CM5s-3. These post-depositional sedimentary structures arise from the injection of high-porosity, low-density sediments, (typically clays) into overlying sediments of low-porosity and high-density (typically sands). The presence of these structures indicates bursts of coarse-grained sedimentation and provide additional evidence of a sedimentary setting characterised by high-energy fluctuations.

Both CM5s-2 and CM5s-3 are distinct from the overlying sediments in terms of magnetic susceptibility properties. They display high values for χ_{lf} and significant values for χ_{fd} ($>2\%$), which are broadly associated with the input of sand sediment fractions. These high values are considered to reflect the input of terrigenous ferrimagnetic minerals associated with a coarse sediment fraction, and probably relate to conditions of high sediment supply from slope sediments and soils via the fluvial system.

The preservation of laminations and bedding features in zone CM5s-3 suggests low levels of biological activity and the absence of bioturbation; this is to be expected for a sandy environment subject to frequent sediment movement (Dalrymple, 1992). Shells are absent, and the zone is generally poor in organic matter although some detrital plant matter is contained within the fine-grained layers. Very low pollen concentration suggests that vegetation was not well developed in the immediate local area or that winnowing of pollen occurred under current action; both possibilities relate to current activity and shifting

substrate at the site. High abundances of *Chenopodiaceae*, *Artemisia* and *Aster* type pollen represent aridity and salinity tolerant vegetation, and may reflect salt marshes in the Guadiana valley. However, the low pollen concentration and coarse, fluvial sediment supply suggest that the source areas for these pollen types may extend beyond the wetland zone, representing a signal of widespread arid conditions.

CM5s-3 represents a high-energy, current-dominated environment with tidal influence and low biological activity. Without evidence from multiple boreholes, it is not possible to determine whether the interbedded sands recorded in this zone are a relatively localised phenomenon related to channel influence at the core location or whether they are characteristic of hydrodynamic changes in the wider fluvio-estuarine setting. However, some information suggests that the changes in depositional environment between CM5s-2 and CM5s-3 may be related to wider sedimentary patterns. The estimated period of deposition for this unit is 12,580–11,880 cal BP, constrained by a radiocarbon date within the zone and dates from the overlying and underlying zones. This places the time of deposition during Greenland Isotope Stadial 1 (GS-1, Björck *et al.*, 1998) or the Younger Dryas (YD) chronozone (Mangerud *et al.*, 1974). Evidence from the Portuguese shelf suggests that the YD was characterised by the transport of large volumes of coarse sediments to the shelf, reflecting enhanced sediment supply and renewed river erosion of the sedimentary infill of estuaries (Rodrigues *et al.*, 1991, 2000; González *et al.*, 2004). Worldwide, a decline in deglacial meltwater contribution led to a decrease in the rate of eustatic sea-level rise (Fairbanks, 1989; Flemming *et al.*, 1998), although different models have been proposed for whether sea-level continued to rise during this period, or whether a mid-deglacial pause in ice volume loss, or even a mid-deglacial reversal with significant ice regrowth occurred. Dias *et al.* (2000) propose a 20 m fall in sea-level on the Portuguese coast for the YD (from -40 to -60 m relative to present sea-level), based on studies of offshore geomorphological features. A fall in base-level of this magnitude does not accord with the CM5 record, which contains tidal sedimentary structures and estuarine dinoflagellates (*Lingulodinium machaerophorum* and *Spiniferites* sp.) in CM5s-3 at about 40 m below present sea-level.

However, a minor fall or stabilisation in sea-level during the YD at around 40 m below present sea level is not inconsistent with the CM5 record, and may underline changes in channel activity at that time. Also, increased coarse sediment supply related to a reduced vegetation cover and an arid climate regime (discussed in the next section) may have had widespread impact on sedimentation regimes in fluvio-estuarine environments at this time.

The deposits of CM5s-2 and s-3 are unusual because drowned fluvio-estuarine environments of Late-glacial age are typically located offshore. There are few comparative records for this part of the sequence. Core CM2 (Boski *et al.*, 2002), located in a confined sector of the Guadiana estuary and distant from the main estuarine channel, contains a 1 m thick layer of fine, micaceous sand overlying basal gravels. Unidentified shell material within this layer has been dated to $10,130 \pm 200$ ^{14}C bp, suggesting a possible deposition during the YD chronozone. This layer is located at a depth of only about 9 m below sea-level, and therefore corresponds to a fluvial environment of a small tributary, located at a higher altitude than the CM5 site in the Beliche tributary. A stratigraphically and lithologically similar layer (but without radiocarbon date) is also observed in core CM4, located in the prograding delta area of the Guadiana estuary mouth (Boski *et al.*, 2002). If of YD age, this deposit also corresponds to a fluvial environment, being situated at about 14 m below sea-level. Combined with evidence from CM5s-3, these fragmentary records may indicate that a thin layer of sands was deposited in the estuary and its surrounding valleys during the YD, most likely related to enhanced sediment supply.

9.1.1.3 Early Holocene transgression (CM5s-4; 11,900–9000 cal BP)

The upper part of the CM5 sequence contains fine-grained sediments deposited under a low energy sedimentation regime that prevailed at the site throughout most of the Holocene. Lithozone CM5s-4 is a thick (*c.* 20 m) deposit of homogeneous, minerogenic silts, which accumulated at a rate of about 7mm/yr, i.e. paced by eustatic sea-level rise. Particle size analysis indicates the dominance of a population of grain sizes associated with aggregation processes and the virtual absence of a medium or coarse sand fraction. These characteristics suggest a sheltered intertidal setting. The virtual absence of sands coarser than 3 phi indicates

a minimal contribution of bedload material. This relates to a greatly reduced fluvial influence at the site, and a weak influence of tidal currents. The dominance of fine grain sizes associated with transport in suspension may also reflect the proximity of the turbidity maximum within the Guadiana estuary during this period, resulting in a high degree of sediment sorting and large supply of fine suspended sediment to marginal flats and marshes. This would be consistent with the landward intrusion of the saline water body during the transgressive phase, and with a sedimentary location in the inner area of the estuary (Hewlett & Bernie, 1996).

Although shells are not present in the sediments, traces of bioturbation provide an indication of biologically active conditions typical of low-energy estuarine environments with burrowing by annelids or crustaceans. Thin, discrete peaty layers indicate the recurrence of stagnant conditions in shallow brackish or freshwater ponds occurring on the marsh surface, possibly associated with short periods of reduced sedimentation rate and/or freshwater influence. Reduced χ_{f} values relative to CM5s-2/3 and a negligible superparamagnetic component ($\chi_{\text{fd\%}} < 2\%$) may indicate a reduced detrital mineral component of fluvial origin. However, the sedimentary characteristics of high sedimentation rate and presence of iron sulphides indicate of a reducing environment with the potential for rapid post-depositional dissolution of ferrimagnetic minerals.

Low percentages and concentrations of Chenopodiaceae, Poaceae and *Aster* type pollen suggest that local vegetation was not dominated by the typical halophytic flora associated with saltmarshes in the intertidal and supratidal zones of the modern estuary. Instead, an assemblage dominated by *Isoetes*, *Ophioglossum* and Cyperaceae suggests a wetland vegetation of fresh to brackish conditions and an unstable minerogenic substrate subject to periodic drying out. Low concentration of all pollen types except *Isoetes* and Asteraceae (Lactucaee), combined with low organic matter content, suggest a sparsely vegetated or non-vegetated sediment surface, i.e. a mud-flat environment. High concentrations of Asteraceae (Lactucaee) grains and a modest contribution of rebedded trilete spores may be

indicative of recycling of palynological material within the estuary and reworking from alluvial sediments.

The onset of silty sedimentation in CM5s-4 is considered to reflect renewed transgression and rapid submergence of the Guadiana valley at the start of the Holocene. The sedimentary changes suggest an areal expansion of the Guadiana estuary and a landward shift of the fluvial-dominated estuarine zone. The evidence for rapid sedimentation fits well with the proposed rapid sea-level rise for the early Holocene (Dias *et al.*, 2000). These interpretations are also consistent with general models for estuarine sedimentary response to transgression, which predict the deposition of fine-grained sediments in the central part of the estuarine basin during the transgressive phase (Roy *et al.*, 1980; Dalrymple *et al.*, 1992; Allen & Posamentier, 1993). This transgressive sedimentary phase in the CM5 core corresponds with a period of generally fine-grained sedimentation in the central area of the Guadiana estuary, as recorded in the sediment record from destructive drillings (Figure 2.5, Unit 2, Boski *et al.*, 2002).

9.1.1.4 Mid-to late Holocene estuarine infilling (CM5s-5; 9000–2160 cal BP)

At *c.* 9000 cal BP, a number of distinct changes in the local environment are recorded in both sedimentary and biotic parameters. Although changes in sedimentation rate may have occurred during the transition from CM5s-4 to s-5, long-term average sedimentation rates of 7 mm/yr were maintained until *c.* 7000 cal bp. At *c.* 9000 cal BP, a change from a sheltered to relatively open estuarine sedimentary environment took place. The sediments continued to be dominated by a population of fine-grained sediments associated with the deposition of flocculated/aggregated particles from suspension, indicating that settling conditions prevailed at the site. However, CM5s-5 is distinguished by increased quantities of sand (medium sand, 3–2 phi). These minor peaks in sand content were probably transported to the site via tidal currents, being derived from bedload material in the main estuarine channel and tidal creeks. Sand may also have been recycled across the sediment surface by the rapid migration of small ebb channels; this is characteristic of the surface of marshes and flats in the modern estuary (Borrego *et al.*, 1995).

CM5s-5 is also relatively rich in both intact and fragmented shell material, probably reflecting a mixture of *in situ* preservation and detrital sources. An open connection with marine-influenced waters is suggested by peak dinoflagellate abundance and diversity (including shelf taxa), and by peak values for carbonate content, which is considered to reflect predominantly biogenic sources. These indications for increased influence of the marine water body suggests that the sand in this section of the core may be of mixed fluvial/marine origin, derived in part from the Guadiana shelf area. Reduced fluvial supply of coarse-grained ferrimagnetic minerals may underline very low values for magnetic susceptibility in this zone. However, it is considered likely that significant post-depositional diagenesis occurred, with a dissolution of ferrimagnetic minerals and the production of paramagnetic minerals by way of pyrite formation.

The particle size distribution, presence of benthic shell fauna, increased channel activity (shell detritus and sand content) and increased marine influence suggest a low-energy tide-dominated environment. Similar characteristics are described for sedimentary facies of the modern Guadiana estuary occurring in an intermediate position between channel and saltmarsh, described variously as a “muddy tidal-flat facies” (Morales, 1997) or “channel margin” facies (Borrego *et al.*, 1995). The term channel margin is used by the latter authors because classic, low-gradient, extensive tidal flats are not developed within the Guadiana estuary. High organic matter content relative to CM5s-4 suggests that the sediment surface may have been vegetated, promoting trapping of organic debris. The abundance of Poaceae, Cyperaceae and Aster type pollen suggest a predominant wetland vegetation of low or pioneer saltmarsh, with species such as *Spartina maritima* and *Scirpus maritimus*.

The evidence for maximum marine influence (dinoflagellate, shell, carbonate content) suggests that the period 9000–5200 cal BP saw the maximum landward expansion of the Guadiana estuary and the intrusion of the marine-estuarine domain inland as far as, or beyond, the Beliche tributary. The pollen record suggests that this expansion of the estuary

was accompanied by a diversification of wetland habitats, including colonisation of river valleys by riparian woodland.

The age-depth profile for the CM5 sequence suggests a significantly reduced rate of long-term average sedimentation from around 7000 cal BP. This decline is consistent with the transition from the Holocene sea-level transgression to highstand phases. Perhaps surprisingly, this decline in sedimentation rate is not accompanied by direct changes in sedimentary characteristics. In the pollen record, a possible indication of the sea-level deceleration is recorded in an expansion of halophytic vegetation (*Chenopodiaceae*) reflecting a period of saltmarsh development between *c.* 7760 and 7350 cal BP. This development may relate to stabilisation and aridification of marsh surfaces contemporaneous with the earliest phase of barrier progradation along the Gulf of Cadiz coasts (Zazo *et al.*, 1994). However, this period is associated with changes in the dry ground vegetation which are difficult to interpret (discussed below), and the causes for changes in the pollen record during this phase are not clear.

From *c.* 5200 cal BP, major increases in *Chenopodiaceae* pollen and a reduced pollen contribution from moisture-dependent taxa such as *Cyperaceae* and *Isoetes* indicate the expansion of upper or mature saltmarshes, characterised by high salinity and evaporative aridity. This expansion probably relates to the progressive infilling of the estuary, and a change from vertical accretion to prograding sedimentation in marshes of the tributary valleys. The development of saltmarshes corresponds with major changes in the vegetation cover in dry ground environments, accompanying evidence for deforestation and the extension of shrublands. The infilling process is considered a natural progression in the evolution of a drowned valley, leading ultimately to sediment bypassing and delta formation (Roy *et al.*, 1980; Heap *et al.*, 2004). However, increased sediment supply as a result of disturbance and reduced vegetation cover may have promoted the infilling process.

While the transition at *c.* 9000 cal BP from sheltered to open tidal conditions may be related to the crossing of a local threshold, for example the breaching of a levée or tidal bar structure, evidence from other borehole locations in the Guadiana suggests a more widespread transition to tide-dominated conditions and sandy sedimentation (Boski *et al.*, 2002). This is observed in the cross-section of destructive drillings (Figure 2.5, Unit 3).

9.1.1.5 Late-Holocene saltmarsh and soil development (CM5s-6; 2160 cal BP to present)

In CM5s-6, signs of oxidation, including sediment reddening and the deterioration of shell material, indicate an elevation of the sediment surface relative to the tidal frame. Oxidation is typical of saltmarsh deposits occurring above mean high water (Pendón *et al.*, 1998). While a process of terrestrialisation is recognised in the pollen record of saltmarsh development from *c.* 5200 cal BP, these sedimentary changes are not recorded until *c.* 2160 cal BP. This may reflect a process of terrestrialisation beginning at the fringes of the valley and progressing towards the core location. The uppermost 90 cm of the core display the development of a soil surface, indicating conditions of low frequency of tidal flooding and reduced sedimentation which characterise the modern supra-tidal saltmarsh environment at the core location. This final sedimentary phase at the CM5 site corresponds with a period of rapid deltaic progradation at the Guadiana estuary mouth under regime of sediment bypassing of the infilled central estuarine sector (Morales, 1997).

9.1.2 Boina-Arade estuary (Cores P2 and P5)

In terms of the sedimentary sequences, the P2 and P5 cores show a number of important similarities related to the development of the combined Boina-Arade estuary. The developmental stages of the two sequences are considered in parallel; age ranges for these stages are broadly defined, accommodating differences on the order of a few centuries between the sites. Sedimentological and palynological findings are summarised in Table 9.2.

9.1.2.1 Pre-Holocene fluvial sediments (P2s-1, P5s-1; prior to 8,500 cal BP)

Coarse gravels compose the basal fill of both the P2 and P5. The coarse composition and varied clast sizes (coarse sand to cobbles) indicate transport under high energy conditions,

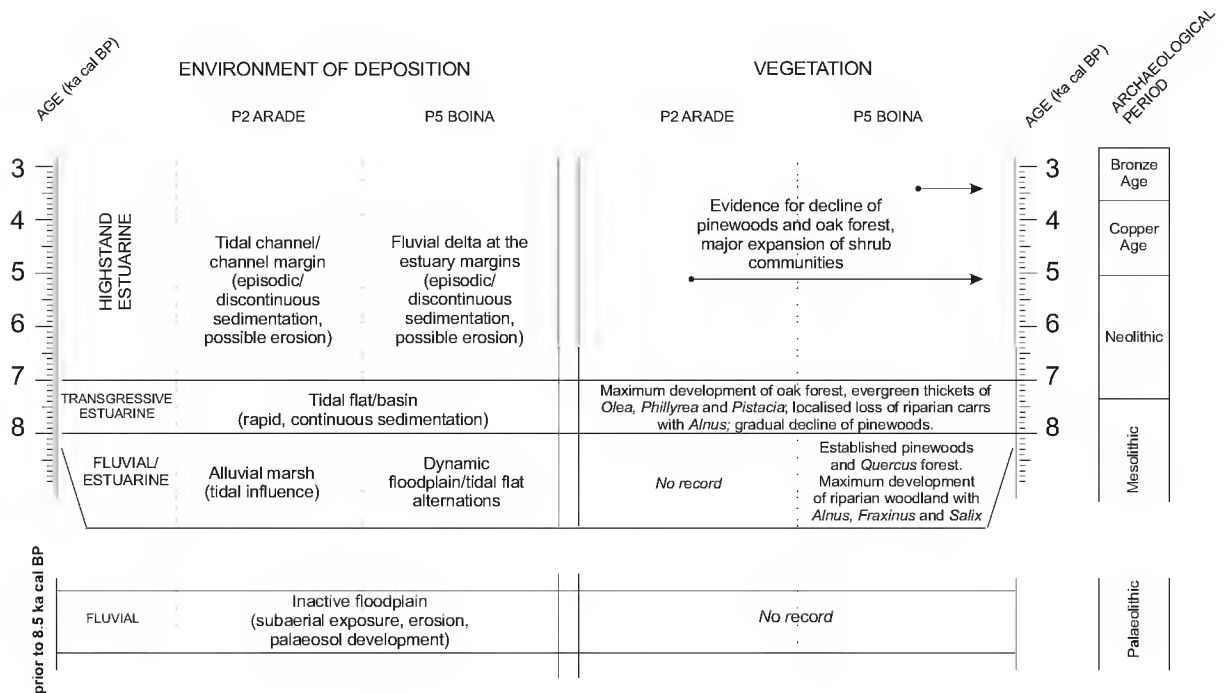


Table 9.2 Summary of sedimentological and palynological findings, Boina-Arade estuary

probably associated with an episodic or flashy fluvial regime. The prevalence of greywacke lithologies suggests the fill material was derived predominantly from the Palaeozoic bedrock which outcrops over wide areas of the Boina and Arade basins. In the P2 core, the morphology of the gravels (generally angular and of low sphericity) in part reflects the platy structure of *Serra* metasediment lithologies. It also suggests, however, that the fill material was not subject to transport over long distances, and perhaps incorporates material of colluvial or slope-derived origin. In contrast, the P5 basal fill contains more polished clasts, including occasional fragments of lamprophyre and syenite indicating transport from upstream areas of the catchment on the Monchique massif. This contrast may reflect the difference in gradients between the two rivers, with greater transport capability in the higher gradient Boina river. The coarse deposits which occur at the base of both cores represents the gravel fill which occupied the valley floor of the Arade and Boina rivers during the previous sea-level lowstand, and which may have been subject to phases of erosion, reworking and redeposition. As in the Guadiana valley, the depth of the gravel surfaces is considered to reflect the inherited palaeorelief of the valleys following the Last Glacial Maximum.

The uppermost 85 cm of the gravelly deposit of the P5 core (P5s-1) are rich in clay and show signs of intense weathering, and may represent a palaeosol developed on the fluvial valley fill. This interpretation is proposed in light of the evidence of a highly reddened colour, very strong magnetic susceptibility with significant values for frequency dependent susceptibility, an unusual polymodal particle size distribution including a significant component of very fine clays (<9 ϕ). The only palynomorphs recovered from this unit were degraded trilete sporomorphs, consistent with the interpretation of an environment characterised by subaerial exposure and oxidation processes.

9.1.2.2 *Fluvial-estuarine transition (P2s-2, P5s-2; c. 8500–8000 cal BP)*

Extrapolation from radiocarbon dates indicates that renewed sedimentation began prior to 8300 cal BP at the P2 location in the Arade valley, and c. 8200 cal BP at the P5 location in the Boina valley. The onset of sedimentation during the Holocene at the two sites is considered a common response to inundation of the Boina-Arade palaeovalley by sea-level rise and the consequent creation of accommodation space. The earlier onset of sedimentation at the Arade site reflects the lower altitudinal position of the surface of the basal gravel fill at this site (1925 cm vs. 1614 cm). (Depths are relative to the modern surface, which at each site lies within the modern intertidal range c. 1m above mean sea-level; precise correlation of the surface altitudes is not available.) In the lower core sections, both sites present evidence for a transitional phase from fluvial to estuarine conditions with intercalated coarse- and fine-grained sediments.

In core P2 (Arade valley), lithozone P2s-2 suggests an alluvial marsh environment under tidal influence. Alternating layers of sandy and fine-grained sediment, in parts showing fine-scale laminations, suggest variable energy conditions associated with periodic inundation. Input of terrigenous detrital material is recorded in the presence of fine accumulations of carbonised plant fragments, and is also suggested by higher values for magnetic susceptibility near the base of the sequence. Indications of oxidation in some of the sandy layers suggest episodes of subaerial exposure, while thin peaty layers suggest

periods of wetter conditions, occurring for example in shallow temporary pools. Towards the top of the zone, sedimentary structures in the form of branching cracks may represent either root casts or desiccation features, indicating a phase of stabilisation and either vegetation or exposure of the sediment surface. At 1832cm, an irregular contact indicates an erosional event. The discrete lines of evidence for episodes of inundation, subaerial exposure, stabilisation and erosion suggest an environmental setting of an alluvial marsh or floodplain. Low carbonate content and the absence of shell material probably reflect conditions of strong fluvial/terrigenous influence and weak marine influence.

In the P5 core, the P5s-1/2 boundary is an abrupt contact between the reddened fluvial/palaesol deposit and the overlying silts. This contact may be a flooding surface formed by the ingress of tidal water into the valley (Allen & Posamentier, 1993). In this newly inundated setting, a series of intercalated fine- and coarse-grained deposits (P5s-2) were laid down, which display characteristic alternations in organic content and magnetic susceptibility. The alternations in grain size and other sedimentary parameters is considered to reflect a dynamic sedimentary environment during a phase of transitional fluvial/estuarine conditions. Layers of clayey and sandy silts (P5s-2a, s-2c) display an estuarine character, with the presence of shell fragments, increased CaCO_3 content, the dominance of fine grain sizes in the range 9 to 5 phi associated with flocculation and bioaggregation processes, and the presence of dinoflagellates. Pockets of fine sands within the muds are interpreted as low-energy tidal sedimentary structures (Reineck & Wunderlich, 1968). The silty layers reflect calm, settling conditions in a mud-dominated tidal environment. Layers rich in sands and gravels (P5s-2b, P5s-2d) indicate episodes of fluvial influence associated with high energy flood events or migration of the river channel. The combination of high mineral residue (low organic and CaCO_3 content), high magnetic susceptibility and the dominance of coarse grain sizes is considered a strong signature of fluvial input of terrigenous sediments. This signature is best developed in the gravel-rich sediments of P5s-2b. The coarse grained sediments of P5s-2 are distinguished from true fluvial deposits by the presence of shells and shell debris, and in P5s-2d, by clay drapes and silt-sand ball sedimentary structures,

reflecting slack-water sedimentation and the action of tidal currents, respectively. Across P5s-2 as a whole, evidence for an increasingly estuarine character is shown in rising CaCO_3 content and increasing abundance of shell material. The depositional setting for P5s-2 is considered to be a deltaic environment located at the head of the developing estuary.

Although pollen was not recovered from lithozone P2s-2, high frequencies of *Alnus* pollen with *Fraxinus* and *Ulmus* from lithozone P5s-2 (Boina valley) suggest a well-developed riparian woodland vegetation occupying the floodplain and terraces of the valley. A significant contribution from *Chenopodiaceae* and *Poaceae* also suggests a saltmarsh vegetation which must have been located in tidal areas of the developing estuary.

The duration of this transitional phase at the P2 location is not constrained by the available radiocarbon data. However, the relatively thin depth of this deposit suggests that deposition time may have been fairly short, and that a fairly rapid and smooth transition from a fluvial to estuarine setting took place, being accomplished by *c* 8300 cal BP (P2s-2/3 boundary). In the Boina core, lithozone P5s-2 contains two radiocarbon dates, from which an accumulation time of around 200 cal yr is extrapolated. This estimate must be considered tentative given the episodic pattern of deposition suggested by the alternating fine/coarse sediments. Nevertheless, very rapid sedimentation is suggested. In contrast with the P2 sequence, the rather thick and more complex sequence of intercalated deposits in the P5 core suggests that the fluvial/estuarine transition was characterised by a more dynamic interaction of fluvial and estuarine processes. This contrast probably reflects the characteristics of the two valleys. The Boina river rises rapidly behind the core location, with a high-gradient and deeply incised valley, while the reaches of the Arade river upstream of the P2 core location are relatively broad and low gradient, corresponding to the geomorphological trough developed on the Silves series lithologies. The contrast in gradient and valley morphology underlines on the one hand a greater potential for coarse sediment transport by flash floods in the Boina, and on the other, a more open connection of the Arade valley with the sea.

9.1.2.3 Transgressive estuarine sediments (P2s-3, P5s-3; c. 8000–7000 cal BP)

At both sites, the middle section of the cores contain fine-grained deposits pertaining to open estuarine conditions. At the P2 location in the Arade valley, a thick deposit of shelly silts (P2s-3) provide evidence for estuarine conditions. The presence of fine, undulating sand laminae relate to the action of tidal currents, with small quantities of sand transported under flood tides and buried beneath muds during the slack water period (Dalrymple, 1992). Particle size analysis indicates the predominance of a population of fine grain sizes associated with flocculation/aggregation processes accompanied by small quantities of coarser sands (3 phi and coarser), suggesting an overall low-energy settling environment influenced by tidal currents. A mixture of intact and fragmented shell material probably represents both an *in situ* estuarine benthic fauna and detrital material. Increasing carbonate and shell content across the lithozone reflect the development of the local calcareous fauna and probably correspond to increasing marine influence across the zone. The environment of deposition for zone P2s-3 is considered to be an intertidal mudflat. The two available radiocarbon dates from this zone suggest very high sedimentation rates (up to 60 mm/yr) during this phase, exceeding the rate of sea-level rise.

At the P5 location in the Boina valley, a similar deposit (P5s-3) of silty sediments is recorded, characterised by abundant shells, high CaCO_3 content and rapid sedimentation rate (up to 20 mm/yr). As in core P2, pockets and fine layers of sand within the sediments are indicative of low energy tidal currents. Gravel clasts, which are considered to reflect fluvial sediment supply, are generally absent although fluctuating sand content and magnetic susceptibility values suggest continued episodic contribution of coarse fluvial sediments. These characteristics also point to a tidal-flat environment.

This phase of predominantly silty sedimentation is considered to relate to the maximum expansion of the Boina-Arade estuary and the landward retreat of the fluvially dominated inner areas of the estuary. The P5 core contains slightly stronger indications of fluvial influence, which again is probably related to the nature of the Boina valley, sediment supply

and fluvial regime. The high sedimentation rate observed at each site relates to the role of the estuary as a highly efficient sink for fine sediments during the transgressive phase.

During this phase, wetland pollen types indicate a well-developed riparian woodland with *Alnus* and *Fraxinus* in the Arade valley. In the Boina valley, a decline in *Alnus* pollen frequencies occurs at the onset of the estuarine phase. The replacement of *Alnus* by Poaceae and *Isoetes* suggests that *Alnus* woodland may have been fairly localised, occupying the low-lying areas of the valley and giving way to more open conditions with progressive drowning of the area. The pollen curve for *Alnus* contrasts strongly with that of *Isoetes*, which displays major abundance during the more developed estuarine phases at the site.

9.1.2.4 Highstand conditions (P2s-4 & s-5, P5s-4 & s-5; post 7000 cal BP)

The upper part of the P2 and P5 cores document marked changes in the depositional environments at both sites, with a switch to high energy conditions. Sedimentation trends at both sites suggest a deceleration in accumulation rate after *c.* 7000 cal BP, with long-term average sedimentation rates below 2 mm/yr. The exact timing of the transition from low to high energy environments is currently not well constrained. Radiocarbon dates are not available for the uppermost part of the fine-grained deposits (P2s-3/P5s-3), and the overlying lithozone boundaries may represent a major change in sedimentation rate. Also, the change in lithological characteristics suggests a major change in depositional regime, from gradual/ continuous to punctuated/ episodic. Also, the transition from a low- to high-energy environment may have resulted in erosion of the underlying deposits.

In the P2 core, thick deposits of shelly sands in lithozone P2s-4a suggest a shift from low energy tidal conditions to higher energy current conditions. Higher energy conditions associated with proximity to a main channel are indicated by the predominance of fine and medium sands and reduced silt and clay content. The indications of stronger channel influence may relate to a shift in the location of the main estuarine channel. High values for χ_{fr} and $\chi_{\text{rd}\%}$ suggest a greater input of terrigenous material of fluvial origin derived from eroded soils and sediments, although this may relate to reduced diagenesis accompanying

the shift from a reducing to oxidising geochemical environment. Shell and CaCO_3 content are high. The depositional environment for this is considered to be a tidal channel or channel margin setting, with strong tidal influence and open marine connection.

In the P5 core, the deposition of a series increasingly coarse sandy layers and the presence of gravel clasts suggests a return to fluvially-dominated conditions. At both sites, increased values for χ_{lf} and $\chi_{\text{id}\%}$ may indicate a greater input of terrigenous material of fluvial origin derived from eroded soils and sediments, although changes in the geochemical environment are likely also to have occurred with ramifications for the mineral magnetic assemblage. The depositional environment is considered a transitional fluvial/estuarine floodplain.

The primary factor underlying the changes in sedimentation in the upper part of the cores is likely to be deceleration in eustatic sea-level rise at the transgressive to highstand transition. The major reduction in sea-level rise would have curtailed the creation of accommodation space in the Boina and Arade valleys, prompting a change from vertical accretion to lateral progradation. A sensitive record of this change is observed at the P5 core site, due to its location near the margins of the estuary, and due to the characteristics of the Boina basin (high gradient, high rainfall) which promote coarse fluvial sediment supply. At the P2 core site, the upper deposits retain a stronger estuarine character, related to the more open tidal aspect of the Arade river.

Another factor which must be considered is the role of human activity in the river catchments and the potential influence on sediment supply to the estuary. The pollen records provide strong indications of deforestation in the Guadiana valley from *c.* 5200 cal BP, which are complemented by pollen spectra showing the loss of forest and the development of scrub and heath vegetation in the Arade basin by *c.* 5100 cal BP, and in the Boina basin by at least 3400 cal BP (discussed in the next section). These changes are currently poorly constrained, due to the general unsuitability of the upper sections of the P2 and P5 cores for pollen analysis. However, the hypothesis is put forward that reduction of the vegetation cover

through land clearance and pastoral activities in prehistoric times promoted sediment supply to the estuary, influencing the channel behaviour, depositional patterns and morphological characteristics of the estuary during the sea-level highstand period.

The uppermost sections of the cores, which have not been studied in detail, reflect the late-Holocene infilling of Arade-Boina estuary. In the Arade core, open tidal conditions are suggested by the development of thick shell-beds in a sandy sediment matrix (P2s-4b). In the Boina core, fluvial sedimentary input is more important, with intercalated accumulations of sands and gravels. The top sections of both sequences record a phase of fine-grained sedimentation, surface stabilisation and soil development, which may relate to siltation of the estuary in the historical period (Chester & James, 1999), and anthropogenic activities in the estuary (drainage, land reclamation and agriculture).

9.1.3 Summary: Holocene changes in the estuarine domain

Some final observations arise from the comparison of the sedimentary records from the two estuaries, relating to the Holocene history of the estuaries. The basal fill at each of the studied sites reflects a phase of deposition under a fluvial regime and lower than present sea-level. These fluvial deposits are not considered to represent the initial deposits of the transgressive sediment sequence, but rather relict features of a previous highstand phase which were exposed to weathering and erosion during the LGM.

The lowest transgressive sediment sequences at each site pertain to a transitional fluvial/estuarine phase. The age of these deposits relates to the depth of the palaeovalleys, with deposits of Late-glacial age preserved in the more deeply incised Guadiana valley system. The transgressive phase is characterised in both estuaries by the rapid accumulation of fine-grained sediments characteristic of the low-energy central basin domain (Roy *et al.*, 1980). Comparable transgressive deposits are recorded in southwestern Spain (Borrego *et al.*, 1999; Dabrio *et al.*, 2000), and attest to the dominant control of eustatic sea-level rise on sedimentation in the estuaries of the Gulf of Cadiz during this period.

The end of the transgressive phase (c. 7000 cal BP) saw a diversification of estuarine geomorphologies. While a low-energy tidal-flat regime predominated in the Beliche tributary of the Guadiana, coarse-grained deposits associated with tidal and fluvial channel activity are recorded from the Arade and Boina sites. The contrasts between the sites relate to differences in basin morphology, the location of the sites relative to the main estuarine channels, and the nature of fluvial regimes and sediment supply in the river basins. This divergence is considered typical of the highstand phase, in which local factors replace sea-level rise as the dominant control on patterns of sedimentation. In estuaries of southwest Spain, the highstand phase is characterised by a shift from vertical to lateral (prograding) accretion in the estuaries, and the development of spit and barrier forms in the coastal zone (Rodríguez-Ramírez, 1996; Dabrio *et al.*, 2000).

9.2 Vegetation history and landscape changes

9.2.1 Late-glacial

The lowest pollen spectra from CM5 (13,000–12,840 cal BP) record a developed oak forest in the Guadiana valley and its tributaries with evergreen and semi-evergreen oaks (*Quercus* deciduous, *suber* and *coccifera* types) accompanied by *Cistus* shrub formations. This forested phase is distinguished from the main Holocene forest phase by the absence of the sclerophyllous evergreen taxa *Olea*, *Phillyrea* and *Pistacia* from the pollen record, and by the presence of relatively high levels of *Juniperus* pollen. The strong arboreal development suggests a fairly warm, moist climate, although the absence of the typical thermomediterranean sclerophyllous taxa may indicate a continental seasonality with relatively cold winters. Historical factors related to the location of these taxa during the Last Glacial Maximum (LGM) may be critical, although a delayed response resulting from migration is not expected for a southern Iberian location (Bennett *et al.*, 1991). This phase is attributed to the Late-glacial interstadial, equivalent to the Greenland Isotope Interstadial 1 (GI-1, Björck *et al.*, 1998) or the Allerød chronozone (Mangerud *et al.*, 1974). During this period, the North Atlantic was not strongly influenced by meltwater (Phase IIb, Ruddiman & McIntyre (1981)), and isotope records and dinoflagellate assemblages from

the Portuguese margin record a phase of warm sea-surface temperatures (Boessenkool *et al.*, 2001). In the Serra da Estrela, the period 14,060–12,850 cal BP (dated by radiocarbon and correlation with the GISP2 Greenland ice-core records) is characterised by a significant contribution of lowland *Quercus*, a high altitudinal vegetation limit, and high lake levels, and is considered to reflect a relatively warm and moist climate (van der Knaap & van Leeuwen, 1997). At Padul, zone P3k, attributed to the Late-glacial interstadial, shows the development of evergreen oaks (*Q. ilex* type) at low and middle elevations, and *Juniperus* at higher elevations (Pons & Reille, 1988).

At *c.* 12,840 cal BP, a set of changes are observed which suggest a rapid contraction of oak forest, an expansion of pinewoods, xeric scrub and steppe environments, with *Juniperus*, *Ephedra distachya* type, *Centaurea* and *Plantago lanceolata* type. Peak values for *Artemisia* and Chenopodiaceae are considered to reflect their role as an element of steppic vegetation, contrasting with a predominant role as saltmarsh taxa during the Holocene. Both in timing and character, these changes are consistent with a climatic deterioration (cooling and drying) during the Greenland Isotope Stadial 1 (GS-1, Björck *et al.*, 1998) or the Younger Dryas (YD) chronozone (Mangerud *et al.*, 1974). During the YD, the polar front migrated southwards, reaching the coasts of northern Iberia (Phase IIIb, Ruddiman & McIntyre (1981)). Rapid cooling in sea surface temperatures is recorded on the Portuguese margin (Boessenkool *et al.*, 2001), and the movement of the polar front is likely to have strongly influenced cyclonic trajectories and patterns of heat and moisture transport. In the Serra da Estrela, the boundary between the Allerød and YD is marked by a strong reduction of open woodland, a reduced contribution of lowland *Quercus*, and low lake levels (van der Knaap & van Leeuwen, 1997). This boundary is dated to 12,850 cal BP. At Padul, zone P3l, attributed to the YD, is characterised by a reduction in evergreen *Quercus*, and increased values for *Artemisia*, *Ephedra* and Chenopodiaceae (Pons & Reille, 1988).

Within the CM5 pollen record for the period 12,840–11,860 cal BP (YD), an early phase with high *Pinus*, low *Quercus* (CM5-Ib) is distinguished from a later phase with moderate

Pinus, moderate *Quercus* and expansion of *Juniperus*, *Ephedra distachya* type, *Centaurea* and *Artemisia* (CM5-Ic). The estimated age for CM5-Ib/Ic boundary is 12,550 cal BP. This boundary corresponds with a significant change in lithological characteristics and inferred sedimentary environment (marsh to channel) and a marked reduction in pollen concentration. On the one hand, changes in pollen spectra above this boundary may simply reflect a change in pollen source components resulting from an increased fluvial pollen supply, and a more continental record of inner areas of the Guadiana basin. On the other hand, the changes may accurately reflect climatic influences affecting the lower Guadiana valley, with an expansion of arid scrub and steppe vegetation during the course of the YD. This expansion may signal a generally lower vegetation cover, which resulted in increased supply of coarse-grained sediments to the estuary.

In southern Portugal, an unpublished pollen study from Lagoa de Golfo on the Alentejo littoral (Queiroz, 1999) records a series of vegetation changes occurring in an undated sediment sequence which underlies dated Holocene deposits. A phase with low frequencies of *Pinus* and elevated frequencies of *Quercus* deciduous type is attributed to a phase of climatic amelioration (Allerød). The subsequent phase records an increase in *Pinus*, *Juniperus*, *Calluna* and *Plantago*, a reduction in *Quercus* deciduous type, and occurrences of *Ephedra distachya* type, and is attributed to a phase of climatic deterioration (YD). The strong similarities with the assemblage recorded in the CM5 core (CM5-Ib/Ic) supports the view that the YD climate event was clearly expressed in the vegetation cover in the southern part of Portugal. The record of xeric vegetation elements during the YD (*Juniperus*, *Ephedra distachya* type) is consistent with geomorphological evidence for extreme aridity in the littoral zone with the formation of mass-wasting deposits and aeolian sand bodies in the Alentejo and western Algarve (Dias *et al.*, 2000). However, the continued contribution of pollen of *Quercus* deciduous and *Q. coccifera* types attests to the presence of oak woodlands in sheltered locations.

9.2.2 Early Holocene

The sedimentary transition to fine-grained estuarine muds corresponds to the transition to biozone CM5-II, and these changes are considered to signal the onset of the Holocene. The impact of climatic amelioration at the Late-glacial/ Holocene transition on the regional vegetation is difficult to determine because of the poor record of dry ground pollen types in CM5-II. A distinctive pollen assemblage dominated by Asteraceae (Lactuceae), Cyperaceae, *Isoetes* undiff. and *Ophioglossum lusitanicum* is observed, with a very poor record of arboreal and shrub taxa. It would seem that a wetland vegetation response to sea-level rise and wetter climatic conditions at the onset of Holocene is the dominant signal recorded in the CM5 pollen spectra. The very high abundances of Asteraceae (Lactuceae) pollen may represent a reworking of pollen from soils and fluvial sediments. This may have been associated with increased precipitation, the mobilisation of slope sediments and the reactivation of fluvial floodplains. Planchais (1987) identifies a similar assemblage at the base of an estuarine sediment sequence from the Languedoc coast dominated by Poaceae, Asteraceae, *Isoetes* and *Ophioglossum*. Planchais considers the assemblage characteristic of transgressive conditions within the estuary and development of unstable substrates in the wetland zone. Although a modern analogue for these pollen assemblages does not exist, Planchais suggests that this is because the rate of transgression is also without modern parallel. The particular conditions created during periods of significant sea-level rise may underlie the abundance of *Isoetes*. It would appear that rapid sea-level change with strong sediment supply created unstable, minerogenic settings associated with much flooding and brackish conditions which were especially suitable for *Isoetes*.

The expansion of *Isoetes* at the start of the Holocene is insignificant at other terrestrial sites in Portugal and Spain, but is clearly recorded in marine pollen records. *Isoetes* shows strongly increased abundances in marine pollen records from the Portuguese margin and offshore Morocco (Hooghiemstra *et al.*, 1992; Marret & Turon, 1994; Turon *et al.*, 2003) during the early Holocene, and also during the early part of the previous Interglacial, Isotope Stage 5e (Sánchez Goñi *et al.* 2000), and is considered an indicator of wetter climatic conditions.

The abundance of *Isoetes* spores and presence of megaspores in the CM5 sediments suggests that swards of *Isoetes* were located in developing estuarine areas and constitute an indicator of rapid transgression. This signal is recorded in the marine pollen records because of the transport of pollen from the estuarine to the marine environment by river currents.

The plotting of pollen curves on the basis of a partial sum of dry ground taxa (Rybníèková & Rybníèek, 1971) provides some insights into the composition of the dry ground vegetation. A mosaic of forest, scrub and open ground vegetation is suggested for the period 11,860–9800 cal BP, with *Pinus*, *Quercus* types, Cistaceae, Ericaceae, *Centaurea* and *Erodium* well represented. Vegetation elements of Late-glacial affinity, *Juniperus* and *Ephedra distachya* type, decline. A parallel disappearance of *Juniperus* is recorded at Padul in the early Holocene; there, as in the CM5 record, the presence of *Juniperus* strongly differentiates between the Late-glacial and Holocene (Pons & Reille, 1988). *Pinus*, in general, is more strongly represented in the dry ground taxa than in the mid-Holocene, and *Quercus coccifera* type (evergreen oaks) is more strongly represented than *Q. suber* or *Q. deciduous* type (probably representing the semi-evergreen species *Q. faginea* and *Q. canariensis*). Overall, however, the poor preservation state of these grains, and the overall greatly reduced concentration values for dry ground taxa leaves some unanswered questions regarding pollen sources areas, transport pathways and taphonomy for this period, and a fundamental question regarding the response of forest vegetation at the onset of the Holocene. The other available records for southern Portugal for this period, two sites from the Alentejo coast (Lagoa do Golfo (Queiroz, 1999) and Lagoa de Santo André (Santos & Sánchez Goñi, 2003), show expansions of *Quercus* deciduous type, evergreen *Quercus* and *Olea* in the early Holocene, suggesting a rapid forest response to Holocene climatic conditions with wider parallels at Serra da Estrela and Padul.

A clearer picture of early Holocene vegetation emerges in the Guadiana valley for the period 9800–8960 cal BP. A forested environment with *Pinus* and *Quercus*, with sclerophyllous thickets of *Olea*, *Phillyrea* and *Pistacia*, is recorded. An equivalent forest

phase with a particularly strong development of pinewoods is recorded in other lowland sites in southern Portugal (Lagoa do Golfo, Lagoa de Santo André). These parallels are interpreted as evidence of a regional belt of pinewoods occurring in the littoral zone on sandy soils. This formerly increased extent of pinewoods may reflect the still enlarged coastal plain at this time, with sea-level more than 20 m below present and the coastline located *c.* 5 km offshore at the mouth of the Guadiana. A contribution of the montane *Pinus sylvestris* is also recorded in the early Holocene samples (as inferred from grain size measurements), although this contribution is not dominant. This may represent either an extra-regional pollen contribution, or the presence of an upland pine vegetation in the Algarve which diminished during the mid-Holocene and is no longer recorded in Portugal. Overall, an early Holocene forest vegetation with strong representation of *Pinus* is rather characteristic of many areas of the Iberian peninsula (Múgica *et al.*, 1998; Taylor *et al.*, 1998 Carrion *et al.*, 2001; Dorado Valiño *et al.*, 2002), and may reflect a prevailing dry climate during the first millennia of the Holocene.

9.2.3 Mid-Holocene

From 8960 to 5200 cal BP (corresponding to the Atlantic chronozone (Mangerud *et al.*, 1974)), the CM5 pollen spectra record a forest phase with the maximum development of semi-evergreen and evergreen oaks, including *Quercus suber*, the cork oak. In addition to oak forest, this phase corresponds to the maximum development of the sclerophyllous taxa *Olea*, *Phillyrea* and *Pistacia*, which are considered to represent a natural vegetation community of mature shrublands comprising thickets of tall evergreen shrubs. This community probably occurred in xeric micro-climates and on stony ground, in contrast to the development of oak forest on deeper, humus rich soils in moister areas. Low values for Cistaceae and Ericaceae pollen types indicate a limited development of scrub and heath vegetation, and may reflect understorey elements of the oak forests. A parallel development of oak forest is recorded in the Boina and Arade valleys, with pollen spectra for the period between *c.* 8500 and 7000 cal BP showing very similar composition to the CM5 record. The maximum development of oak forest, and in particular the increased representation of moisture-demanding *Quercus suber* and *Q.* deciduous types, is considered to reflect increased

precipitation from *c.* 9000 cal BP. The maximum development of the frost-sensitive sclerophyllous taxa suggests an oceanic, thermomediterranean climate with mild winters. This contrasts with the forested phase of the Late-glacial Interstadial, where the absence of the thermomediterranean taxa points to a more continental climate with cold winters.

In the CM5 record, the transition from an early Holocene vegetation with higher frequencies of *Pinus* to a mid-Holocene vegetation with higher frequencies of *Quercus* corresponds with a change in the sedimentary environment and increased tidal influence. Therefore, it is recognised that the transition in the dry ground pollen record may be conditioned by changes in pollen transport and taphonomy. However, both in character and timing, the transition has several important parallels at other Iberian sites. In the Serra da Estrela, a transition to a wetter, more oceanic climate is recorded at *c.* 9000 cal BP (van der Knaap & van Leeuwen, 1995), although the taxa involved are different. At that site, a slight increase of mesophytic taxa, including *Pinus*, *Pteridium aquilinum*, and *Alnus*, relative to xerophytic taxa, such as *Quercus ilex* type, support the climatic interpretation. At Padul, the establishment of *Quercus suber* occurred at about 8000 ¹⁴C bp (*c.* 8800 cal BP), and is considered to reflect a thermic and humidity optimum during the Holocene.

A climatic interpretation for the *Quercus maxima* observed across the Algarve is consistent with evidence for a mid-Holocene humidity maximum from the Laguna de Medina, near Cadiz (Reed *et al.*, 2001), and for the onset of warmer, wetter conditions from 8000 ¹⁴C bp (*c.* 8800 cal BP) in the upper Guadiana basin in central Spain (Dorado Valiño *et al.*, 2002). Marine pollen records from the Atlantic offshore Portugal and Morocco indicate an onset of humid conditions at the slightly earlier date of 8500 ¹⁴C BP (~9500 cal BP) (Hooghiemstra *et al.*, 1992; Marret & Turrón, 1994).

One of the characteristic features of the Guadiana and Boina-Arade pollen records is declining values of *Pinus* pollen during the mid-Holocene. In the CM5 and P2 records, gradually declining values are observed (at least for the period prior to 5200 cal BP). In the

P5 record, a more distinct decline is noted at *c.* 8030 cal BP. Several causes may underline the declining trend of *Pinus*. One factor, as suggested by morphometric observations on the *Pinus* pollen content of CM5, is a reduced pollen contribution from montane pines (*P. sylvestris*) which may have been less suited to climatic conditions after the Late-glacial. Macrofossil evidence (wood charcoal) from sites in central and northern Portugal indicates a progressive northward retreat and overall diminished occurrence of montane pines since the onset of the Holocene (Figueiral & Carcaillet, in press). A second factor may be inter-specific competition with angiosperm trees and a generally poor adaptation of pines in general, both lowland and upland, to warm-moist mid-Holocene climate conditions. A third factor may be destruction of pinewoods as a direct result of human clearance activities. Declining values of *Pinus* during the mid-Holocene are observed in the pollen records from the Alentejo littoral, although a complex picture emerges of the nature and timing of the decline. In the Lagoa Travessa sequence (Mateus, 1989), which begins *c.* 8300 cal BP, a gradual decline is observed. At the Lagoa de Santo André (Santos & Sánchez Goñi, 2003), a rapid decline is recorded after 6200 cal BP. Further north, at the site of Apostiça, a rapid decline occurs much later, after 3900 cal BP (Queiroz & Mateus, 1994). These contrasting patterns suggest that the pine decline is a mixed response to climatic, ecological and anthropogenic factors.

Between *c.* 7760 and 7350 cal BP, a decline in the forest cover in the Guadiana basin is recorded (CM5-IVb). During this phase, a number of shrub taxa which rise to prominence after 5200 cal BP show moderate expansions. This phase corresponds with an apparent expansion of saltmarsh (increased *Chenopodiaceae*), and a reduced input of some freshwater taxa. This oscillation in both the pollen record for both dry ground and wetland vegetation suggests a complex interaction of hydrographic and either climatic or anthropogenic impact on the opening of the vegetation cover. A number of arid climatic events are recorded in lake level and aquatic pollen records from southwestern Spain (Reed *et al.*, 2001), and such an event might explain the combination of dry ground and wetland impacts. However, the timing of this event does not correspond with the aridification events identified by

Reed *et al.* (2001). A short-term sea-level fluctuation may underlie the phase of saltmarsh development, but this does not explain the changes in dry ground taxa. Perhaps a phase of early and reversible human impact is detected, related to the activities of people during the late Mesolithic (the very earliest Neolithic cultural remains in the Algarve date from *c.* 7500 cal BP (Cardoso *et al.*, 1998)). The late Mesolithic period saw an expansion of human activities in the Tagus and Sado basins (Bicho, 1994) and in the western Algarve (Calado *et al.*, 2003; Stiner *et al.*, 2003). However, no clues as to the scale of Mesolithic activity in the Guadiana basin are available.

9.2.4 Late Holocene

From 5200 cal BP, major changes in the vegetation cover are detected with the widespread replacement of forest by scrub communities and open ground. In the CM5 record, a series of changes are recorded which suggest a progressive intensification of anthropogenic pressure. Between *c.* 5200 and 4100 cal BP, an expansion of *Quercus coccifera* type pollen is interpreted as the development of tall maquis in response to forest clearance. This phase corresponds with the Chalcolithic period or Copper Age period which began at 4500 ¹⁴C bp (*c.* 5200 cal BP) (Straus, 1989), and saw a major expansion of human activity into the uplands and hinterlands of southern Portugal (Kalb, 1989). In the northern slopes of the Beliche valley a cemetery pertaining to this period is known. Between *c.* 4100 and 2500 cal BP, the maximum development of *Cistus* scrub is recorded, suggesting impacts from pastoral activities (grazing and burning). This phase includes the Bronze Age (1800–800 B.C. (Gomes, 1995)) and the early Iron Age. Between *c.* 2500 and 1400 cal BP, the expansion of open ground indicators such as *Plantago lanceolata* accompanied by declines in both arboreal and some shrub taxa, and the planting of *Castanea*, indicates the further intensification of human activities. This phase corresponds with the late Iron Age and Roman periods.

In the P2 and P5 records, the shift from fine- to coarse-grained sedimentation after *c.* 7000 cal BP does not allow detailed palynological investigation of changes occurring during this period. However, the recovery of pollen from a small number of samples in the upper part

of the cores provides a glimpse of vegetation conditions for a date *c.* 5100 cal BP from the Arade core, and *c.* 3400 cal BP in the Boina core. At both sites, a major development of maquis and open ground vegetation communities is recorded. Although the understanding of these changes can only be considered rudimentary at present, they suggest deforestation and human pressure on the landscapes of the Boina-Arade basin. They support the possibility that the supply of coarse-grained sediments was conditioned by reduced vegetation cover in the catchments.

It is recognised that the timing is consistent with declines in subhumid forests across Mediterranean Spain and the Balearics (Yll *et al.*, 1997; Carrion *et al.*, 2001; Gil García *et al.*, 2002; Pantaléon-Cano *et al.*, 2003) at around 5000 cal BP. These authors argue for a climatic aridification around 5000 cal BP. Evergreen/deciduous pollen ratios in Mediterranean France and Spain have also been used as a climate proxy to demonstrate increased aridity from 5000 cal BP (Jalut *et al.*, 2000). This aridification is supported by lake and river records from Spain and the western Mediterranean region (Reed *et al.*, 2001; Dorado Valiño *et al.*, 2002; Magny *et al.*, 2002). The possibility that the major change in the CM5 pollen record at 5200 cal BP reflects increased aridity must therefore be considered.

Throughout the CM5 record, a range of taxa are recorded which probably relate to the different moisture and thermicity gradients observed in the Algarve. The CM5 record after 5200 cal BP not only shows an increased representation of shrub taxa, but the presence of new taxa, such as *Helianthemum salicifolium* and *Tuberaria guttata*. Other taxa, such as *Erica scoparia* and *E. umbellata* types, show a distinct expansion only after 5200 cal BP. These features of the pollen record are considered to reflect not a readjustment of the existing vegetation to climatic change, but the creation of a greater diversity of shrubland vegetation communities across both dry and subhumid areas (i.e. *Cistus* scrub and ericaceous heathlands). This diversification of shrublands accompanied the loss of both pinewoods and oak forests from 5200 cal BP, and, certainly from 4140 cal BP, the destruction of woodlands and thickets of the oaks of drier ombrotypes (*Q. coccifera* and *Q. rotundifolia*).

These changes do not suggest a competitive readjustment to a climatic aridification, but human impact through clearance, fire and pastoral activities across both upland and lowland environments. Finally, from around 2400 cal BP, declines of both the sclerophyllous taxa of thickets and maquis, such as *Olea*, and the decline of riparian woodlands, demonstrate the ultimate reduction of all arboreal taxa, regardless of climatic preferences, and suggest the extension of cutting and clearance activities into the both the driest and wettest areas of the landscape. While climatic aridity may have exacerbated the impact of human activities, the view here is that anthropogenic influence is the primary factor underlying the distinct changes in the pollen record after 5200 cal BP.

The decline of oak forests and the rise of scrub and particularly ericaceous heath communities is readily identified in several mid- to late Holocene pollen records from Portugal. In the Serra da Estrela, a significant increase in human activity is recorded from *c.* 6300 cal BP, large scale deforestation from *c.* 3600 cal BP, and total disappearance of the forests during the Medieval period (van der Knaap & van Leeuwen, 1995). At the site of Alpiarça, in the lower Tagus valley (van Leeuwaarden & Janssen, 1985), declines in arboreal taxa (*Pinus* and *Quercus*) and concomitant increases in Ericaceae and Poaceae occur between 5400 and 3600 cal BP. Sites from the Alentejo littoral suggest major human impact between 4000 and 3000 cal BP. At Estacada (Queiroz, 1989), the disappearance of pine and oak woodlands (zone LAL-I) and their replacement by shrub formations with *Q. coccifera*, *Erica arborea* and *E. scoparia* (zone LAL-II) is recorded at around 3600 cal BP, although a possible hiatus means that the transition may have occurred earlier. At Apostiça (Queiroz & Mateus, 1994), the replacement of pinewoods and *Olea* by maquis and heathlands is recorded (zone APO III) by about 3800 cal BP. At Lagoa Travessa (Mateus, 1989), a strong forest decline and expansion of sclerophyllous scrub and ericaceous heaths is recorded after about 3200 cal BP, although indications of human influence on the forest cover occur earlier, from *c.* 5000 cal BP. The evidence from these lowland sites in southern Portugal suggests a widespread period of forest reduction and the extension of semi-natural shrublands between 5000 and 3000 cal BP (~3000–1000 BC, Copper and Bronze Ages). This contrasts

with the evidence from the coastal Huelva region further to the east. Records from El Acebron and Laguna de las Madres (Stevenson, 1985b, 1988; Stevenson & Harrison, 1992) begin at *c.* 5000 cal BP. Anthropogenic clearance is detected in the loss of pinewoods, but levels of *Quercus* remain high throughout the prehistoric period. This is considered to reflect the prevalence of a managed woodland landscape and the prehistoric development of the *dehesa*, or oak parkland.

The new data from the CM5 core suggest an early impact on the forest cover during prehistoric times (since the Copper Age), and an intensification of human pressure through the Bronze and Iron Ages, culminating in the most open landscape during the Roman period. The sequence of vegetation changes from pine and oak forest to evergreen thickets of *Q. coccifera* and *Myrtus*, then to *Cistus* and ericaceous scrub and heath, and finally to more open shrublands is consistent with a view of progressive alteration of the natural landscape. This finding supports the view that anthropogenic influence is a major agent of landscape change in the Algarve (Chester & James, 1991, 1999). While increased soil erosion and sediment supply are considered a likely consequence of degradation of the vegetation cover, a clear sedimentological impact of deforestation is not recorded in the CM5 core. Minor peaks in low frequency magnetic susceptibility and fine sand content are noted towards the top of the core, but are not clearly differentiated from patterns observed in grain size or magnetic parameters in lower core sections. However, the period of human impact after 5200 cal BP corresponds with palynological indications for terrestrialisation and the development of saltmarsh around the core site. It is possible that the process of infilling which led to the development of upper saltmarshes and halophytic vegetation was promoted by fine sediment supply to the marsh resulting from human activities in the Beliche and Guadiana basins.

9.3 Evaluation and prospects for future research

The combination of sedimentary and pollen analyses proves valuable for the interpretation of environmental changes both at the site of deposition and in the wider landscape. The

combination is considered particularly important for the interpretation of pollen records from the dynamic estuarine environment where changes in sedimentary conditions may be associated with changes in pollen source area. In the course of this study, it was recognised that other lines of investigation could complement those chosen here, and could lead to more secure palaeoenvironmental interpretations. Certain techniques which were either not available or not feasible within the timeframe of this study, but which would be valuable additions include:

X-ray core scans. The recognition and accurate description of sedimentary structures in tidal sediments provides important clues regarding the environment of deposition and post-depositional changes. In many cases, in particular with muddy sediments, it may be difficult to observe certain sedimentary structures by eye. Features such as fine sand laminae, bioturbation structures or slumping are more readily identified in X-ray radiographs (e.g. Borrego *et al.*, 1995), providing an additional level of information leading to more secure interpretations of sedimentation history and environments of deposition.

Other microfossil analyses. Although pollen provides information regarding wetland environments, and may reflect, either by changes in composition or concentration, changes at the site of deposition, pollen does not provide a very sensitive indicator for tidal depth. This is both because of the taxonomic imprecision of several groups of saltmarsh taxa (Chenopodiaceae, Poaceae, Cyperaceae) and because pollen from several saltmarsh zones may be mixed in the tidal water body. In contrast, species identifications for foraminifera, ostracoda or diatoms may provide much more specific indications of water chemistry and tidal depth. This information would complement the results of analysis of the physical properties of the sediment sequence, and improve the understanding of the relationship between changes in the pollen record and changes in the local environment

Other magnetic parameters. The measurement of magnetic susceptibility in this study reveals a large variability in susceptibility values. It is also suspected that early iron

mineral diagenesis may be characteristic of the transgressive estuarine deposits investigated here. In order to understand the effect and variability of these processes, it is clear that much further research is required. Ongoing research into the sequence of iron mineral diagenesis and the identification of iron minerals by transmission light microscopy, electron microprobe and X-Ray powder diffraction is taking place at CIMA (Universidade do Algarve). This research would be complemented by further study of mineral magnetic properties of the sediments (for example, remanence measurements (anhysteretic remanent magnetisation (ARM) and saturated isothermal remanent magnetisation (SIRM))). These might not only permit more secure identification of detrital terrestrial signals (Oldfield, 1994), but lead to a more complete understanding of diagenetic processes which in themselves are of interest, being related in a systematic way to changing environmental conditions at the depositional location (e.g. Reitz *et al.*, 2004).

Charcoal analysis. Although charcoal was observed during pollen and sediment preparations, the content was not quantified as part of this study. The identification in the pollen record of phases of strong human impact and the development of semi-natural shrublands in the pollen records suggests that the incidence of anthropogenic fires should increase in the upper part of the sediment sequences. This hypothesis could be tested in the future by analysis of the charcoal content of the sediment.

This study has demonstrated that silty estuarine sediments contain pollen derived from both wetland and dry ground environments, and that the pollen record may contribute to the understanding of changes in the regional landscape and vegetation. Given the presence of extensive saltmarshes in other Algarve estuaries, it is clear that there is the potential for further studies in many locations in the Algarve. These are necessary, of course, to confirm and develop the findings of this study. One of the potential drawbacks of estuarine sequences, however, as encountered in the P2 and P5 cores, is the discontinuity of fine-grained sedimentation and hence pollen preservation. In this respect, the CM5 sequence appears very unusual, both in terms of depth and long-term homogeneity in sedimentation. This

problem is likely to be encountered in many estuarine sequences. Underlying this difficulty is the sensitive sedimentary response of estuaries to a number of factors, both regional, such as changes in base-level, and individual, such as sediment supply from the catchment, fluvial discharge and inherited topography.

10 Conclusions

This thesis presents the results of sediment and pollen analyses from Late-glacial and Holocene estuarine sediment sequences of the Algarve province of southern Portugal. This study represents the first attempt in this region to study the vegetation development since the Late-glacial. The study also adopts an unconventional approach in the use of estuarine sediments, necessitated by the absence of natural lakes and lacustrine sediment sequences in the region. Three sites have been investigated in the course of this study, one from the Guadiana estuary in the eastern Algarve, and two from the Boina-Arade estuary in the western Algarve. Core CM5 from Guadiana estuary contains a *c.* 50 m sequence of Late-glacial and Holocene sediments, representing the infill of a small tributary valley of the Guadiana. Cores P2 and P5 from the Boina-Arade estuary contain Holocene sequences of *c.* 22 m and 20 m depth, respectively, which represent the estuarine fills of the Arade and Boina valleys.

Radiocarbon dates constrain the chronology of sedimentation at the sites, and provide an indication of long-term average sedimentation rates. Age-depth models for the history of sedimentation are proposed for the three sites. Given the likelihood that changes in depositional environment have been accompanied by changes in sedimentation rate, the

estimation of dates for lithostratigraphical and pollen assemblage biozone boundaries is tentative and in some cases problematic. Nevertheless, the radiocarbon-based site chronologies illustrate a general sedimentation trend which is common to the three sites. For the period prior to c. 7000 cal BP at the CM5 site, and for the period 8000–7000 cal BP at the Boina-Arade sites, high sedimentation rates in excess of 7 mm/yr are recorded. Around c. 7000 cal BP a deceleration to sedimentation rates between 1 and 1.5 mm/yr occurs at all sites. This sedimentation trend has also been identified in estuarine sedimentary sequences on the Huelva coast of southwestern Spain (Lario *et al.*, 2002a) and is considered to reflect a regional pattern of sea-level rise and the transition from a transgressive to sea-level highstand phase.

A combination of core lithological observations, sediment analyses (loss-on-ignition, particle-size analysis, magnetic susceptibility) and palynological evidence permit the identification of changes in the depositional environment during the period of infilling at the sites. High energy fluvial deposits compose the basal sediments at each site, and attest to a period of fluvial activity during the Pleistocene. Based on dating of comparative deposits from the Spanish coast (Dabrio *et al.*, 2000) and seismic stratigraphic evidence for an erosional phase succeeding the deposition of the gravels (Lobo *et al.*, 2003), these gravels are considered to have been deposited during the previous interglacial, and to have experienced weathering and erosion during the Last Glacial Maximum.

Estuarine infilling began c. 13000 cal BP in the Beliche tributary of the Guadiana, and after 8500 cal BP in the Boina-Arade estuary. The onset of estuarine infilling was controlled by the position of sea-level and the inherited topography of the palaeovalley systems. At the base of the CM5 Guadiana sequence, a series of laminated silty and sandy deposits of Late-glacial age (CM5s-2/3) relate to a transitional fluvial/estuarine phase. Although tidal sedimentary structures and brackish water indicators (dinoflagellates) are recorded, a strong fluvial influence and dominance of fluvially-derived coarse grained sediments is recorded. During the early Holocene, a thick sequence of transgressive deposits (CM5s-4) was

deposited under a calm, settling sedimentation regime and a reducing geochemical environment. At *c.* 9000 cal BP, a transition to more open estuarine conditions (CM5s-5) with increased tidal influence is recorded, with changes in sedimentary and palynological parameters. The impact of the decline in sedimentation rate after 7000 cal BP is not clearly evident in sedimentary parameters. After *c.* 5200 cal BP, the progressive infilling of the site is documented with palynological evidence for the expansion of saltmarshes, and from *c.* 2160 cal BP sedimentary evidence for oxidation.

In the Boina-Arade valley, cores P2 and P5 record a similar progression of changes in the depositional environment following the onset of Holocene sedimentation after *c.* 8500 cal BP. A first phase of intercalated coarse- and fine-grained sedimentation relates to a transitional phase from fluvial to estuarine conditions. This phase is more strongly developed in the Boina valley (core P5) where fluvial input from the high-gradient catchment is more important throughout the sedimentary sequence. A second phase documents open estuarine conditions and the maximum areal expansion of the Boina-Arade estuary, with the deposition of predominantly silty tidal sediments. In the upper part of the sequences a transition from low- to high-energy sedimentary environments is recorded at both sites with the deposition of sandy sediments. In the P2 Arade core, a tide-dominated channel setting is recorded; in the P5 Boina core, a fluvially-dominated deltaic setting is recorded. These changes are considered to have occurred around 6500 cal BP, although the timing is not tightly constrained by the available radiocarbon data. The changes are consistent with evidence from the wider region for changes in sedimentation associated with the transgressive/highstand sea-level transition and the subsequent diversification of estuarine sedimentary forms. However, new pollen data in this investigation presents evidence for a role of anthropogenic influence. Although only a small pollen dataset has been recovered from these upper deposits, it provides an indication of extensive human impact on the vegetation cover of the river catchments. Increased sediment supply from catchment soils as a result of deforestation may be implicated in the genesis of the coarse-grained, upper sedimentary fill recorded in the Boina-Arade estuary.

Pollen and spores contained within the sediments provide the first record of Late-glacial, early and mid-Holocene vegetation changes in the Algarve. The interpretation of estuarine pollen records is undoubtedly complicated by the potential overrepresentation of local pollen types, poorly defined pollen source areas, and changes in pollen composition arising from deposition in a dynamic and variable sedimentary environment. In light of these difficulties, efforts were undertaken to make a rigorous assessment of the pollen content of the studied sequences, and in particular to distinguish the record of dry ground pollen types from ambiguous to wetland pollen types. These efforts include large pollen counts, detailed taxonomic identification, presentation of pollen data as percentages (based on both the total sum of pollen and spores, and partial sums of dry ground/ wetland taxa) and concentration values, and the direct comparison of pollen and sediment stratigraphy.

The CM5 record from the Guadiana estuary provides the first dated Late-glacial pollen record for southern Portugal. A distinct Late-glacial pollen assemblage is recorded, with high levels of *Pinus*, *Juniperus*, and *Ephedra distachya* type. Within the Late-glacial sediments, a vegetation event is recorded with a decline of deciduous and evergreen *Quercus* and an expansion of dry- and cold-tolerant taxa. This vegetation event, supported by the radiocarbon dates, is considered an expression of climatic deterioration (cooling and drying) associated with the Allerød/Younger Dryas transition. The vegetation response to climate changes at the onset of the Holocene is not clear, due to the poor record of dry ground pollen types in the oldest sediments of Holocene age. However, a pollen assemblage from the early Holocene with *Pinus*, *Quercus*, Cistaceae and Ericaceae is tentatively interpreted as a mosaic of pinewood, oak forest and shrub communities. From c. 9800 cal BP, the presence of evergreen, sclerophyllous shrub taxa (*Olea*, *Phillyrea*, *Pistacia*) is recorded, and from c. 9000 cal BP, the dominance of *Quercus* forest. The phase of maximum Holocene forest development (c. 9000–5200 cal BP) is recorded at all three sites, presenting a regional picture of forests with deciduous and evergreen *Quercus* (including *Q. suber*), thickets of sclerophyllous taxa, and well-developed riparian woodlands of *Alnus* and *Fraxinus*. In

contrast with other arboreal taxa, the contribution of *Pinus* declines in importance, in part reflecting a contraction of *P. sylvestris* populations. During this period, a possible early anthropogenic clearance event is recorded with an expansion of scrub and open ground taxa in the CM5 record (CM5-IVb) at *c.* 7800–7400 cal BP, which is followed by a regeneration of arboreal taxa.

From 5200 cal BP, major changes in the vegetation cover are detected with the widespread replacement of forest by scrub communities and open ground. In the CM5 record, a series of changes is recorded which suggests a progressive intensification of anthropogenic pressure. Between *c.* 5200 and 4100 cal BP, an expansion of *Quercus coccifera* type pollen is interpreted as the development of tall thickets or maquis in response to forest clearance. Between *c.* 4100 and 2500 cal BP, the maximum development of *Cistus* shrublands is recorded, suggesting impacts from pastoral activities (grazing and burning) and the widespread development of scrub and heath vegetation communities. Between *c.* 2500 and 1400 cal BP, the expansion of open ground indicators such as *Plantago lanceolata* accompanied by declines in both arboreal and some shrub taxa, indicates the further intensification of human activities. In the P2 and P5 records, changes in the sedimentary environments prohibit palynological investigation of changes occurring during this period. However, the recovery of pollen from a small number of samples in the upper part of the cores permits a ‘snapshot’ of vegetation conditions for a date *c.* 5100 cal BP from the Arade core, and *c.* 3400 cal BP in the Boina core. At both sites, a major development of scrub, heath and open ground vegetation communities is recorded, suggesting deforestation and human pressure on the landscapes of the Boina-Arade basin.

Although there is not a wealth of comparative material from the southwestern sector of the Iberian peninsula, some insights into wider patterns of vegetation development emerge from comparison of the pollen records developed in this study with the pollen records from the Alentejo coast, southwestern Spain, and important records from the more distant sites of the Serra da Estrela and Padul. Comparison with the Alentejo records suggest a coherent

picture of vegetation changes in southern Portugal since the Late-glacial. An expansion of xeric scrub and steppe during the Younger Dryas, an early Holocene landscape in which pinewoods played a major role, and a change in forest dominance in the mid-Holocene from *Pinus* to *Quercus* are identified in both the Alentejo and the Algarve. Wider parallels with the Serra da Estrela and Padul suggest the importance of climatic controls on vegetation development during these periods, with cool, dry conditions during the Younger Dryas and warm, moist conditions in the Holocene, with increased moisture in the mid-Holocene after 9000 cal BP. Anthropogenic impacts are more marked in the last 5000 years. The expansion of scrub and heath communities recorded in the sites studied here has parallels at other southern Portuguese sites, as well as in the Serra da Estrela. Evidence for deforestation is recorded during the period from 5000 to 3000 cal BP, although the timing varies between sites. Comparison of dates for the expansion of shrublands, particularly heathlands, across southern and central Portugal suggests a particularly early human impact on forest cover in the Algarve. The evidence for a late Holocene development of *Quercus* in a managed woodland landscape, as recorded in southwest Spain, is not encountered.

Finally, this study highlights the potential for further development of the vegetation history of southern Portugal through the study of estuarine deposits, which, in contrast with lacustrine records, are widely preserved in the region. Although the challenges for interpretation of pollen records from these dynamic and sensitive sedimentary environments constitute a disadvantage compared with traditional lake settings, the potential to illustrate and evaluate environmental changes in both the coastal and upland zones is a distinct advantage. The information that results from this investigation contributes to our understanding of environmental change at the intersection of the terrestrial, fluvial and coastal domains.

Bibliography

- Adam, D.P. & P.J. Mehringer, Jr. 1975. Modern pollen surface samples — an analysis of subsamples, *Journal of Research of the U.S. Geological Survey* 3(6): 733-736.
- Allen, H.D. 2001. *Mediterranean Ecogeography*. Harlow: Prentice Hall.
- Allen, H.D. 2003. A transient coastal wetland: from estuarine to supratidal conditions in less than 2000 years - Boca do Rio, Algarve, Portugal *Land Degradation and Development* 14: 265-283
- Allen, J.R.L., 1996. Shoreline movement and vertical textural patterns in salt marsh deposits: implications of a simple model for flow and sedimentation over tidal marshes, *Proceedings of the Geologists' Association* 107: 15-23.
- Allen, J.R.L. 2000. Morphodynamics of Holocene salt marshes: a review sketch from the Atlantic and Southern North Sea coasts of Europe, *Quaternary Science Reviews* 19: 1155-1231.
- Allen, J.R.L. & D.M. Thornley. 2004. Laser granulometry of Holocene estuarine silts: effects of hydrogen peroxide treatment, *The Holocene* 14(2): 290-295.
- Allen, T. 1997. *Particle Size Measurement*. Volume 1, 5th edition. London: Chapman & Hall.
- Aller, R.C. 1982. Carbonate dissolution in nearshore terrigenous muds: the role of physical and biological reworking, *Journal of Geology* 90: 79-95.
- Anderson, N.J. & B. Rippey. 1988. Diagenesis of magnetic minerals in the recent sediments of a eutrophic lake, *Limnology and Oceanography* 33(6): 1476-1492
- Andrieu-Ponel, V., P. Ponel, A.J.T. Jull, J.-L. de Beaulieu, H. Bruneton & P. Leveau. 2000. Towards the reconstruction of the Holocene vegetation history of Lower Provence: two new pollen profiles from Marais des Baux, *Vegetation History and Archaeobotany* 9: 71-84.
- Ball, D.F. 1964. Loss-on-ignition as an estimate of organic matter and organic carbon in non-calcareous soils, *Journal of Soil Science* 15: 84-92.
- Bao, R., M.C. Freitas & C. Andrade. 1999. Separating eustatic from local environmental effects: a late-Holocene record of coastal change in Albufeira lagoon, Portugal, *The Holocene* 9: 341-352.
- Barbéro, M., R. Loisel, P. Quezel, D.M. Richardson & F. Romane. 1998. Pines of the Mediterranean basin. In D.M. Richardson (ed.), *Ecology and Biogeography of Pines*, 153-170. Cambridge: Cambridge University Press.
- Bard, E., B. Hamelin, M. Arnold, L. Montaggioni, G. Cabioch, G. Faure & F. Rougerie. 1996. Deglacial sea-level record from Tahiti corals and the timing of global meltwater discharge, *Nature* 382: 241-244.
- Barefoot, A. C. & F. W. Hankins. 1982. *Identification of Modern and Tertiary Woods*. Oxford: Clarendon Press.

- Bartlein, P.J., M.E. Edwards, S.L. Shafer & E.D. Barker, Jr. 1995. Calibration of radiocarbon ages and the interpretation of palaeoenvironmental records, *Quaternary Research* 44: 417-424.
- Behre, K.E. 1990. Some reflections on anthropogenic indicators and the record of prehistoric occupation phases in pollen diagrams from the Near East. In, S. Bottema, G. Entjes-Nieborg & W. van Zeist (eds.), *Man's Role in the Shaping of the Eastern Mediterranean Landscape*: 219-230. Rotterdam: A.A. Balkema.
- Bengtsson, L. & M. Enell. 1986. Chemical analysis. In B.E. Berglund (ed.), *Handbook of Holocene palaeoecology and palaeohydrology*: 433-436. London: John Wiley & Sons.
- Bennett, K.D. & K.J. Willis. 2001. Pollen. In J.P. Smoll, H.J.B Birks & W.M Last (eds.), *Tracking Environmental Change Using Lake Sediments. Volume 3: Terrestrial, Algal and Siliceous Indicators*. Dordrecht, the Netherlands: Kluwer Academic Publishers.
- Bennett, K.D. 1994. Confidence intervals for age estimates and deposition times in late-Quaternary sediment sequences, *The Holocene* 4(4): 337-348.
- Bennett, K.D. 1994. 'psimpoll' version 2.23: a C program for analysing pollen data and plotting pollen diagrams, *INQUA Commission for the study of the Holocene: Working group on data-handling methods, Newsletter* 11: 4-6.
- Bennett, K.D. 1996. Determination of the number of zones in a biostratigraphical sequence, *New Phytologist* 132: 155-170.
- Bennett, K.D., G. Whittington & K.J. Edwards. 1994. Recent plant nomenclatural changes and pollen morphology in the British Isles, *Quaternary Newsletter* 73: 1-6.
- Bennett, K.D., P.C. Tzedakis & K.J. Willis. 1991. Quaternary refugia of north European trees, *Journal of Biogeography* 18: 103-115.
- Bennett, K.D., P.C. Tzedakis & K.J. Willis. 1991. Quaternary refugia of north European trees, *Journal of Biogeography* 18: 103-115.
- Berglund, B.E. & M. Ralska-Jasiewiczowa. 1986. Pollen analysis and pollen diagrams. In B.E. Berglund (ed.), *Handbook of Holocene palaeoecology and palaeohydrology*: 455-484. London: John Wiley & Sons.
- Berner, R.A. 1984. Sedimentary pyrite formation: an update, *Geochimica et Cosmochimica Acta* 48: 605-615.
- Berthet, P. & M. Lecocq. 1977. Morphologie sporale des espèces françaises du genre *Isoetes* L., *Pollen et Spores* 19(3): 325-359.
- Bicho, N.F. 1994. The end of the Paleolithic and the Mesolithic in Portugal, *Current Anthropology* 35(5): 664-674.
- Birks H.J.B. & A.D. Gordon. 1985. *Numerical methods in Quaternary pollen analysis*. London: Academic Press.
- Bisutti, I., I. Hilke & M. Raessler. 2004. Determination of total organic carbon – an overview of current methods, *Trends in Analytical Chemistry*, Vol. 23, No. 10–11, 2004

- Björck, S., M.J.C. Walker, L.C. Cynar, S. Johnsen, K.-L. Knudsen, J.J. Lowe, B. Wohlfarth & INTIMATE members. 1998. An event stratigraphy for the Last Termination in the North Atlantic region based on the Greenland ice-core record: a proposal by the INTIMATE group, *Journal of Quaternary Science* 13(4): 283-292.
- Blackmore, S. 1984. The Northwest European pollen flora, 32: Compositae – Lactucaee, *Review of Palaeobotany and Palynology* 42: 45-85.
- Blanchard, A. 1960. The thermal oxidation of graphite. In M.H. Dodson (ed.) *The Depth of Oxidation of Graphite: A Theoretical Approach*, UKAEA Report DEG 148 (CA).
- Blondel, J. & J. Aronson. 1999. *Biology and Wildlife of the Mediterranean*. Oxford: Oxford University Press.
- Boessenkool, K.P., H. Brinkhuis, J. Schönfeld & J. Targarona. 2001. North Atlantic sea-surface temperature changes and the climate of western Iberia during the last deglaciation; a marine palynological approach, *Global and Planetary Change* 30: 33-39.
- Bond, G., W. Showers, M. Cheseby, R. Lotti, P. Almasi, P. Menocla, P. Priore, H. Cullen, I. Hajdas & G. Bonani. 1997. A pervasive millennial-scale cycle in North Atlantic Holocene and glacial climates. *Science* 278: 1257-1266.
- Bonny, A.P. 1978. The effect of pollen recruitment processes on pollen distribution over the sediment surface of a small lake in Cumbria, *Journal of Ecology* 66: 385-416.
- Borrego, J., J.A. Morales & J.G. Pendón. 1993. Holocene filling of an estuarine lagoon along the mesotidal coast of Huelva: the Piedras river mouth, southwestern Spain, *Journal of Coastal Research* 9(1): 242-254.
- Borrego, J., J.A. Morales & J.G. Pendón. 1995. Holocene estuarine facies along the mesotidal coast of Huelva, south-western Spain. In B.W. Flemming (ed.), *Tidal Signatures in Modern and Ancient Sediments*: 151-170. Special Publication of the International Association of Sedimentologists, No. 24. Oxford: Blackwell Science.
- Borrego, J., M. Lopez, J.G. Pendón & J.A. Morales. 1998. C/S ratios in estuarine sediments of the Odiel river-mouth, S.W. Spain, *Journal of Coastal Research* 14(4): 1276-1283.
- Borrego, J., F. Ruiz, M.L. Gonzalez-Regalado, J.G. Pendón & J.A. Morales. 1999. The Holocene transgression into the estuarine central basin of the Odiel River mouth (Cadiz gulf, SW Spain): lithology and faunal assemblages, *Quaternary Science Reviews* 18: 769-788.
- Boski, T., D. Moura, C. Veiga-Pires, S. Camacho, D. Duarte, D.B. Scott & S.G. Fernandes. 2002. Postglacial sea-level rise and sedimentary response in the Guadiana Estuary, Portugal/Spain border, *Sedimentary Geology* 150: 103-122.
- Bottema, S. & H. Woldring. 1990. Anthropogenic indicators in the pollen record of the Eastern Mediterranean. In S. Bottema, G. Entjes-Nieborg & W. van Zeist (eds.), *Man's Role in the Shaping of the Eastern Mediterranean Landscape*: 231-264. Rotterdam: A.A. Balkema.
- Bradshaw, R.H.W. 1981. Modern pollen-representation factors for woods in south-east England. *Journal of Ecology*, 69: 45-70.

- Braun-Blanquet, J., A.R. Pinto da Silva & A. Rozeira. 1956. Resultats de deux excursions géobotaniques à travers le Portugal septentrional et moyen. II. Chenaies a feuilles caduques (Quercion occidentale) et chenaies a feuilles persistantes (Quercion fagineae) au Portugal. *Agronomia Lusitana* 18:167-234.
- Braun-Blanquet, J., A.R. Pinto da Silva & A. Rozeira. 1964. Resultats de trois excursions géobotaniques à travers le Portugal septentrional et moyen. III. Landes à cistes et ericacées (Cisto-Lavanduletea et Calluno-Ulicetea). *Agronomia Lusitana* 23:229-313.
- Brush, G.S. & L.M. Brush. 1972. Transport of pollen in sediment-laden channel: a laboratory study, *American Journal of Science* 272: 359-381.
- Brush, G.S. & L.M. Brush. 1994. Transport and deposition of pollen in an estuary: signature of the landscape. In A. Traverse (ed.), *Sedimentation of Organic Particles*: 33-46. Cambridge: Cambridge University Press.
- Burrin, P.J. & R.G. Scaife. 1984. Aspects of Holocene valley sedimentation and floodplain development in southern England, *Proceedings of the Geologists' Association* 95: 81-96.
- Calado, D., F. Nocete, M.D. Cámalich, D. Martín, J.M Nieto, E. Alex & M. Bayona. 2003. Los poblados con menhires del Algarve occidental: Nuevas perspectivas para la explicación del origen e implicaciones históricas sobre las primeras sociedades sedentarias en el suroeste peninsular, *Jornadas Temáticas Andaluzas de Arqueología: Sociedades Recolectoras y Primeros Productores*. Ronda, Málaga: Junta de Andalucía, Consejería de Cultura.
- Camoin, G.F., L.F. Montaggioni & C.J.R. Braithwaite. 2004. Late glacial to post glacial sea levels in the Western Indian Ocean, *Marine Geology* 206: 119-146.
- Campbell, I.D. 1991. Experimental mechanical destruction of pollen grains, *Palynology* 15: 29-33.
- Campbell, I.D. & C. Campbell. 1994. Pollen preservation: experimental wet-dry cycles in saline and desalinated sediments, *Palynology* 18: 5-10.
- Campbell, I.D. & G.L. Chmura. 1994. Pollen distribution in the Atchafalaya River, U.S.A., *Palynology* 18: 55-65.
- Canfield, D.E. & R.A. Berner. 1987. Dissolution and pyritization of magnetite in anoxic marine sediments, *Geochimica et Cosmochimica Acta* 51: 645-659.
- Capelo, J.H. 1996. Esboço da paisagem vegetal da bacia Portuguesa do Rio Guadiana, *Silva Lusitana* IV (numero especial): 13-64.
- Cardoso, J.L., A.F. Carvalho & J. Norton. 1998. A estação do Neolítico Antigo de Cabranosa (Sagres, Vila do Bispo): estudo dos materiais e integração cronológico-cultural, *O Arqueólogo Português*, Serie IV, 16: 55-96.
- Carrion, J.S, C. Navarro, J. Navarro & M. Munuera. 2000. The distribution of cluster pine (*Pinus pinaster*) in Spain as derived from palaeoecological data: relationships with phytosociological classification, *The Holocene* 10(2): 243-252.

- Carrion, J.S, A. Andrade, K.D. Bennett, C. Navarro & M. Munuera. 2001. Crossing forest thresholds: inertia and collapse in a Holocene sequence from south-central Spain, *The Holocene* 11(6): 635-653.
- Carson, B., K.F. Carney & A.J. Meglis. 1988. Sediment aggregation in a salt-marsh complex, Great Sound, New Jersey, *Marine Geology* 82: 83-96.
- Catto, N.R. 1985. Hydrodynamic distribution of palynomorphs in a fluvial succession, Yukon, *Canadian Journal of Earth Science* 22: 1552-1556.
- Cearreta, A. & J.W. Murray. 2000. AMS 14C dating of Holocene estuarine deposits: consequences of high-energy and reworked foraminifera, *The Holocene* 10(1): 155-159.
- Chester, D.K. & P.A. James. 1991. Holocene alluviation in the Algarve, Southern Portugal: The case for an anthropogenic cause. *Journal of Archaeological Science* 18: 73-87.
- Chaster, D.K. & P.A. James. 1995. The Pleistocene Faro/Quarteira formation of the Algarve region, southern Portugal, *Geomorphology* 12: 133-149.
- Chester, D.K. & P.A. James. 1999. Late Pleistocene and Holocene Landscape Development in the Algarve, Portugal, *Journal of Mediterranean Archaeology* 12: 169-196.
- Chmura, G.L. 1994. Palynomorph distribution in marsh environments in the modern Mississippi Delta plain, *Geological Society of America Bulletin* 106: 705-714.
- Chmura, G.L. & K.B. Liu. 1990. Pollen in the Lower Mississippi River, *Review of Palaeobotany and Palynology* 64: 253-261.
- Chmura, G.L. & D. Eisma. 1995. A palynological study of surface and suspended sediments on a tidal flat: implications for pollen transport and deposition in coastal waters, *Marine Geology* 128: 183-200.
- Chmura, G.L., A. Smirnov & I.D. Campbell. 1999. Pollen transport through distributaries and depositional patterns in coastal waters, *Palaeogeography, Palaeoclimatology, Palaeoecology* 149: 257-270.
- Clark, J.S. & W.A. Patterson III. 1985. The development of a tidal marsh: upland and oceanic influences, *Ecological Monographs (Ecological Society of America)* 55(2): 189-217
- Clarke, G.C.S. & M.R. Jones. 1980. Aceraceae. In W. Punt & G.C.S. Clarke (eds.), *The Northwest European pollen flora, II*: 181-193. Amsterdam: Elsevier Scientific Publishing Company.
- Clarke, G.C.S. & M.R. Jones. 1981. Dipsacaceae. In W. Punt & G.C.S. Clarke (eds.), *The Northwest European pollen flora, III*: 1-25. Amsterdam: Elsevier Scientific Publishing Company.
- Clarke, G.C.S. 1980. Boraginaceae. In W. Punt & G.C.S. Clarke (eds.), *The Northwest European pollen flora, II*: 59-101. Amsterdam: Elsevier Scientific Publishing Company.
- Clarke, G.C.S., W. Punt & P.P. Hoen. 1991. The Northwest European Pollen Flora, 51. Ranunculaceae, *Review of Palaeobotany and Palynology* 69: 117-271.

- Collins, P.E.F., S.D. Turner & A.B. Cundy. 2001. High-resolution reconstruction of recent vegetation dynamics in a Mediterranean microtidal wetland: implications for site sensitivity and palaeoenvironmental research, *Journal of Coastal Research* 17(3): 684-693.
- Colman, S.M., J.P. Halka & C.H. Hobbs. 1992. Patterns and rates of sediment accumulation in the Chesapeake Bay during the Holocene rise in sea level. In C. Fletcher & J.F. Wehmiller (eds.), *Quaternary Coasts of the United States: Marine and Lacustrine Systems*: 101-111. Society of Economic Palaeontologists and Mineralogists (SEPM) Special Publication No. 48.
- Colman, S.M., P.C. Baucom & J.F. Bratton. 2002. Radiocarbon dating, chronologic framework, and changes in accumulation rates of Holocene estuarine sediments from Chesapeake Bay, *Quaternary Research* 57: 58-70.
- Coutinho, A.X.P., 1939. *Flora de Portugal (Plantas Vasculares)*. 2a Edição. Lisbon: Bertrand (Irmãos), Ltd.
- Dabrio, C.J., C. Zazo, J.L. Goy, F.J. Sierro, F. Borja, J. Lario, J.A. González & J.A. Flores. 2000. Depositional history of estuarine infill during the last postglacial transgression (Gulf of Cadiz, Southern Spain), *Marine Geology* 162: 381-404.
- Dafni, A. 1992. *Pollination Ecology: A Practical Approach*. Oxford: Oxford University Press.
- Dalrymple, R.W. 1992. Tidal depositional systems. In R.G. Walker & N.P. James (eds.), *Facies models: response to sea level change*: 195-218. St. John's : Geological Association of Canada.
- Dalrymple, R.W., B.A. Zaitlin & R. Boyd. 1992. Estuarine facies models: conceptual basis and stratigraphic implications, *Journal of Sedimentology* 62(6): 1130-1146.
- Dark, P. & J.R.L. Allen. 2005. Seasonal deposition of Holocene banded sediments in the Severn Estuary Levels (southwest Britain): palynological and sedimentological evidence, *Quaternary Science Reviews* 24: 11-33.
- Davies, B.E. 1974. Loss-on-ignition as an estimate of soil organic matter, *Proceedings of the Soil Science Society of America* 38: 150-151.
- Davis, M.B. 1963. On the theory of pollen analysis, *American Journal of Science* 261: 897-912.
- Davis, R.A. Jr. & H.E. Clifton. 1987. Sea-level change and the preservation potential of wave-dominated and tide-dominated coastal sequences. In D. Nummedal, O.H. Pilkey & J.D. Howard (eds.), *Sea-level fluctuation and coastal evolution*: 167-178. Special Publication of The Society of Economic Palaeontologists and Mineralogists (SEPM) no. 41.
- Davis, R.A. Jr. & M.O. Hayes. 1984. What is a wave-dominated coast?, *Marine Geology* 60: 313-329.
- Dawson, A.G., R.A. Hindson, C. Andrade, C. Freitas, R. Parish & M. Bateman. 1995. Tsunami sedimentation associated with the Lisbon earthquake of 1 November AD 1755: Boca do Rio, Algarve, Portugal. *The Holocene*, 5 (2), 209-215.
- Dean, W.E. Jr. 1974. Determination of carbonate and organic matter in calcareous sediments and sedimentary rocks by loss on ignition: comparison with other methods, *Journal of Sedimentary Petrology* 44(1): 242-248.

- Dearing, J. 1999. Magnetic susceptibility. In J. Walden, F. Oldfield & J.P. Smith (eds.), *Environmental Magnetism: a practical guide*: 35-62. Technical Guide, No. 6. London: Quaternary Research Association.
- Dearing, J.A., R.J.L. Dann, K. Hay, J.A. Lees, P.J. Loveland, B.A. Maher & K.O'Grady. 1996a. Frequency-dependent susceptibility measurements of environmental materials, *Geophysical Journal International* 124: 228-240.
- Dearing, J.A., K.L. Hay, S.M.J. Baban, A.S. Huddleston, E.M.H. Wellington & P.J. Loveland. 1996b. Magnetic susceptibility of soil: an evaluation of conflicting theories using a national data set, *Geophysical Journal International* 127: 728-734.
- Dearing, J.A., P.M. Bird, R.J.L. Dann & S.F. Benjamin. 1997. Secondary ferrimagnetic minerals in Welsh soils: a comparison of mineral magnetic detection methods and implications for mineral formation, *Geophysical Journal International* 130: 727-736.
- Dearing, J.A., J.F. Boyle, P.G. Appleby, A.W. Mackay & R.J. Flower. 1998. Magnetic properties of recent sediments in Lake Baikal, Siberia, *Journal of Paleolimnology* 20: 163-173.
- Dearing, J.A., Y. Hu, P. Doody, P.A. James & A. Brauer. 2001. Preliminary reconstruction of sediment-source linkages for the past 6000 yrs at the Petit Lac d'Annecy, France, based on mineral magnetic data, *Journal of Paleolimnology* 25: 245-258.
- Debenay, J.P., P. Carbonel, M.-T. Morzadec-Kerfourn, A. Cazaubon, M. Denèfle & A.-M. Lézine. 2003. Multi-bioindicator study of a small estuary in Vendée (France), *Estuarine, Coastal and Shelf Science* 58: 843-860.
- Dekkers, M.J. 1997. Environmental magnetism: an introduction, *Geologie en Mijnbouw* 76: 163-182.
- Devereux, C.M. 1982. Climate speeds erosion of the Algarve's valleys, *Geographical Magazine* 54: 10-18.
- Devereux, C.M. 1983. Recent Erosion and Sedimentation in Southern Portugal. Unpublished Ph.D. thesis: University of London.
- Dias, J.M.A., T. Boski, A. Rodrigues & F. Magalhães. 2000. Coast line evolution since the Last Glacial Maximum until present — a synthesis, *Marine Geology* 170: 177-186.
- Dias, R.P. & J. Cabral. 2002. Interpretation of recent structures in an area of cryptokarst evolution - neotectonic versus subsidence genesis, *Geodinamica Acta* 15: 233-248.
- Diot, M.F. & J.P. Tastet. 1995. Paleo-environnements Holocenes et limites chrono-climatiques enregistrés dans un marais estuarien de la Gironde (France), *Quaternaire* 6(2): 63-75.
- Dorado Valiño, M., A. Valdeolmillos Rodríguez, M.B. Ruiz Zapata, M.J. Gil García & I. de Bustamante Gutiérrez. 2002. Climatic changes since the Late-glacial/Holocene transition in La Mancha Plain (south-central Iberian Peninsula, Spain) and their incidence on Las Tablas de Daimiel marshlands, *Quaternary International* 93-94: 73-84.
- Dyer, K.R. 1979. Estuaries and estuarine sedimentation. In K.R. Dyer (ed.), *Estuarine hydrography and sedimentation*: 1-18. Cambridge: Cambridge University Press.

- Dyer, K.R. 1998. The typology of intertidal mudflats. In K.S. Black, D.M. Paterson & A. Cramp (eds.), *Sedimentary Processes in the Intertidal Zone*: 11-24. London: Geological Society Special Publication no. 139.
- Eisma, D. 1986. Flocculation and de-flocculation of suspended matter in estuaries, *Netherlands Journal of Sea Research* 20(2/3): 183-199.
- Eisma, D., P. Bernard, G.C. Cadée, V. Ittekkot, J. Kalf, R. Laane, J.M. Martin, W.G. Mook, A. van Put & T. Schuhmacher. 1991a. Suspended-matter particle size in some west-European estuaries; Part I: Particle-size distribution, *Netherlands Journal of Sea Research* 28(3): 193-214.
- Eisma, D., P. Bernard, G.C. Cadée, V. Ittekkot, J. Kalf, R. Laane, J.M. Martin, W.G. Mook, A. van Put & T. Schuhmacher. 1991b. Suspended-matter particle size in some west-European estuaries; Part II: A review on floc formation and break-up, *Netherlands Journal of Sea Research* 28(3): 215-220.
- Emiroglu, S., D. Rey & N. Petersen. 2004. Magnetic properties of sediment in the Ría de Arousa (Spain): dissolution of iron oxides and formation of iron sulphides, *Physics and Chemistry of the Earth* 29: 947-959.
- Engel, M.S. 1980. Haloragaceae. In W. Punt & G.C.S. Clarke (eds.), *The Northwest European pollen flora, II*: 199-207. Amsterdam: Elsevier Scientific Publishing Company.
- Erdtman, G. 1969. *Handbook of Palynology*. Copenhagen: Munksgaard.
- Espejo, R. 1987. The soils and ages of the “Raña” surfaces related to the Villuercas and Altamira mountain ranges (Western Spain), *Catena* 14: 399-418.
- Eyre, J.K. 1997. Frequency dependence of magnetic susceptibility for populations of single-domain grains, *Geophysical Journal International* 129: 209-211.
- F. Ruiz, M.L. González-Regalado & J.A. Morales. 1996. Distribución y ecología de los foraminíferos y ostrácodos actuales del estuario mesomareal del Río Guadiana (S.O. España), *GEOBIOS* 29(5): 513-528.
- Faegri, K. & L. van der Pijl. 1971. *Principles of Pollination Ecology*. Oxford: Pergamon Press.
- Faegri, K., & J. Iversen. (Faegri, K., P.E. Kaland & K. Krzywinski). 1989. *Textbook of Pollen Analysis*. Fourth edition. Chichester: Wiley.
- Fairbanks, R.G. A 17,000 year glacio-eustatic sea level record: influence of glacial melting rates in the Younger Dryas event and deep-ocean circulation, *Nature* 342: 637-642.
- Fall, P.L. 1987. Pollen taphonomy in a canyon stream, *Quaternary Research* 28: 393-406.
- Fenies, H. & J.-P. Tastet, 1998. Facies and architecture of an estuarine tidal bar (the Trompeloup bar, Gironde estuary, SW France), *Marine Geology* 150: 149-169.
- Figueiral, I. & C. Carcaillet, in press. A review of Late Pleistocene and Holocene biogeography of highland Mediterranean pines (*Pinus* type *sylvestris*) in Portugal, based on wood charcoal, *Quaternary Science Reviews*.

- Fine, P., M.J. Singer & K.L. Verosub. 1992. Use of magnetic-susceptibility measurements in assessing soil uniformity in chronosequence studies, *Soil Science Society of America Journal* 56: 1195-1199.
- Fleming, K., P. Johnston, D. Zwart, Y. Yokoyama, K. Lambeck and J. Chappell. 1998. Refining the eustatic sea-level curve since the Last Glacial Maximum using far- and intermediate-field sites, *Earth and Planetary Science Letters* 163: 327-342.
- Flemming, B.W. 2000. A revised textural classification of gravel-free muddy sediments on the basis of ternary diagrams, *Continental Shelf Research* 20: 1125-1137.
- Fletcher, C.H. III, J.E. Van Pelt, G.S. Brush & J. Sherman. 1993. Tidal wetland record of Holocene sea-level movements and climate history, *Palaeogeography, Palaeoclimatology, Palaeoecology* 102: 177-213.
- Folk, R.L. & W.C. Ward. 1957. Brazos river bar: a study in the significance of grain size parameters. *Journal of Sedimentary Petrology* 27(1): 3-26.
- Freund, H., G. Gerdes, H. Streif, O. Dellwig & F. Watermann. 2004. The indicative meaning of diatoms, pollen and botanical macro fossils for the reconstruction of palaeoenvironments and sea-level fluctuations along the coast of Lower Saxony; Germany, *Quaternary International* 112: 71-87.
- Frey, R.W. & J.D. Howard. 1986. Mesotidal estuarine sequences: a perspective from the Georgia Bight, *Journal of Sedimentary Petrology* 56(6): 911-924.
- Gibbs, R.J., D.M. Tshudy, L. Konwar & J.M. Martin. 1989. Coagulation and transport of sediments in the Gironde estuary, *Sedimentology* 36: 987-999.
- Gil García, M.J., M. Dorado Valiño, A. Valdeolmillos Rodríguez & M.B. Ruiz Zapata. 2002. Late-glacial and Holocene palaeoclimatic record from Sierra de Cebollera (northern Iberian Range, Spain), *Quaternary International* 93-94: 13-18.
- Giralt, S., F. Burjachs, J.R. Roca & R. Julia. Late Glacial to Early Holocene environmental adjustment in the Mediterranean semi-arid zone of the Salines playa-lake (Alacante, Spain), *Journal of Paleolimnology* 21: 449-460.
- Gomes, M.V. 1995. A Idade do Bronze no Algarve. In *Catálogo da exposição A Idade do Bronze em Portugal: discursos de poder: 140-143*. Lisboa: SEC, IPM, MNA.
- Gómez-Casero, M.T., P. Hidalgo, H. García-Mozo; E. Domínguez & C. Galán. 2004. Pollen biology in four Mediterranean *Quercus* species, *Grana* 43(1): 22-30
- González, R., J.M.A. Dias, F. Lobo & I. Mendes. 2004. Sedimentological and paleoenvironmental characterisation of transgressive sediments on the Guadiana Shelf (Northern Gulf of Cadiz, SW Iberia), *Quaternary International* 120: 133-144.
- Griffiths, J.C. 1967. *Scientific method in analysis of sediments*. New York: McGraw-Hill Book Company.
- Grillas, P., P. Gauthier, N. Yavercovski & C. Perennou. 2004. *Mediterranean Temporary Pools, Volume 2: Species Information Sheets*. Le Sambuc, France: Station Biologique de la Tour du Valat.

- Grimley, D.A., N.K. Arruda & M.W. Bramstedt. 2004. Using magnetic susceptibility to facilitate more rapid, reproducible and precise delineation of hydric soils in the midwestern USA, *Catena* 58: 183-213.
- Grimm, E.C. 1987. CONISS: a FORTRAN 77 program for stratigraphically constrained cluster analysis by the methods of incremental sum of squares, *Computers and Geoscience* 13: 13-35.
- Groot, J.J. 1966. Some observations on pollen grains in suspension in the estuary of the Delaware River, *Marine Geology* 4: 409-416.
- Grove, A.T. & O. Rackham. 2001. *The Nature of Mediterranean Europe: An Ecological History*. New Haven: Yale University Press.
- Haslett, S.K. Davies, P., R.H.F. Curr; C.F.C. Davies, C.P. King, A.J. Margetts & K. Kennington. 1998. Evaluating late-Holocene relative sea-level change in the Somerset Levels, southwest Britain, *The Holocene* 8(2): 197-207.
- Havinga, A.J. 1984. A 20-year experimental investigation into the differential corrosion susceptibility of pollen and spores in various soil types, *Pollen et Spores* 26(3-4): 541-558.
- Heap, A.D., S. Bryce & D.A. Ryan. 2004. Facies evolution of Holocene estuaries and deltas: a large-sample statistical study from Australia, *Sedimentary Geology* 168: 1-17.
- Heier-Nielsen, S., J. Heinemeier, H. L. Nielsen and N. Rud. 1995. Recent Reservoir Ages for Danish Fjords and Marine Waters, *Radiocarbon* 37: 875-882.
- Heiri, O., A.F. Lotter & G. Lemcke. 2001. Loss on ignition as a method for estimating organic and carbonate content in sediments: reproducibility and comparability of results, *Journal of Paleolimnology* 25: 101-110.
- Heusser, L. 1978. Spores and pollen in the marine realm. In B.U. Haq & A. Boersma (eds.), *Introduction to Marine Micropaleontology*: 327-339. New York: Elsevier.
- Hewlett, R. & J. Birnie. 1996. Holocene environmental change in the inner Severn estuary, UK: an example of the response of estuarine sedimentation to relative sea-level change, *The Holocene* 6(1): 49-61.
- Heyvaert, F. 1980. Première contribution à l'étude palynologique des spectres récents dans les vases salées des estuaires Picards (Somme et Pas-de-Calais), *Bulletin de l'Association française pour l'Etude du Quaternaire* 1-2:35-39
- Hilton, J., J.P. Lishman & J.S. Chapman. 1986. Magnetic and chemical characterisation of a diagenetic magnetic mineral formed in sediments of productive lakes, *Chemical Geology* 56: 325-333.
- Holmes, P.L. 1990. Differential transport of spores and pollen: a laboratory study, *Review of Palaeobotany and Palynology* 64: 289-296.
- Hooghiemstra, H., H. Stalling, C.O.C. Agwu & L.M. Dupont. 1992. Vegetational and climatic changes at the northern fring of the Sahara 250,000-5000 years BP: evidence from 4 marine pollen records located between Portugal and the Canary Islands, *Review of Palaeobotany and Palynology* 74: 1-53. et al., 1992; Turon et al., 2003

- Hughen, K.A., M.G.L. Baillie, E. Bard, A. Bayliss, J.W. Beck, C. Bertrand, P.G. Blackwell, C.E. Buck, G. Burr, K.B. Cutler, P.E. Damon, R.L. Edwards, R.G. Fairbanks, M. Friedrich, T.P. Guilderson, B. Kromer, F.G. McCormac, S. Manning, C. Bronk Ramsey, P.J. Reimer, R.W. Reimer, S. Remmele, J.R. Southon, M. Stuiver, S. Talamo, F.W. Taylor, J. van der Plicht, and C.E. Weyhenmeyer. 2004. Marine04 Marine Radiocarbon Age Calibration, 0–26 Cal Kyr BP, *Radiocarbon* 46: 1059-1086.
- Huntley, B. 1988. Europe. In B. Huntley & T. Webb (eds.), *Vegetation History*: 341-384. Dordrecht, Boston & London: Kluwer Academic Publishers.
- Huntley, B. & I.C. Prentice. 1993. Holocene Vegetation and Climates of Europe. In H.E. Wright Jr., J.E. Kutzbach, T. Webb III, W.F. Ruddiman, F.A. Street-Perrot & P.J. Bartlein (eds.), *Global Climates*: 136-168. Minneapolis: University of Minnesota Press.
- INAG (Instituto da Agua) 2000. *Plano de Bacia Hidrográfica das Ribeiras do Algarve*. Ministério do Ambiente e do Ordenamento do Território. Online: http://www.inag.pt/inag2004/port/a_intervencao/planeamento/pbh/pbh.html (13/07/05).
- Jackson, S.T. 1994. Pollen and spores in Quaternary lake sediments as sensors of vegetation composition: theoretical models and empirical evidence. In A. Traverse (ed.), *Sedimentation of Organic Particles*: 253-286. Cambridge: Cambridge University Press.
- Jahn, R, D. Pfannschmidt & K. Stahr. 1989. Soils from limestone and dolomite in the central Algarve (Portugal), their qualities in respect to groundwater recharge, runoff, erodibility and present erosion, *Catena* Supplement 14: Arid and semi-arid environments: geomorphological and pedological aspects: 25-42.
- Jalut, G., A.E. Amat, L. Bonnet, T. Gauquelin & M. Fontugne. 2000. Holocene climatic changes in the Western Mediterranean, from south-east France to south-east Spain, *Palaeogeography, Palaeoclimatology, Palaeoecology* 160: 255-290.
- James, P.A. & D.K. Chester, 1995. Soils of Quaternary river sediments in the Algarve. In J. Lewin, M.G. Macklin & J.C. Woodward (eds.), *Mediterranean Quaternary River Environments*: 245-262. Rotterdam: Balkema.
- Janssen, C.R. 1966. Pollen spectra from the deciduous and coniferous forests of northeastern Minnesota, *Ecology* 47: 804-835.
- Jennings, S.C., R.W.G. Carter & J.D. Orford. 1993. Late Holocene salt marsh development under a regime of rapid relative-sea-level rise: Chezzetcook Inlet, Nova Scotia. Implications for the interpretation of paleomorph sequences, *Canadian Journal of Earth Science* 30: 1374-1384.
- Jones, M.R. & G.C.S. Clarke. 1981. Nymphaeaceae. In W. Punt & G.C.S. Clarke (eds.), *The Northwest European pollen flora, III*: 57-67. Amsterdam: Elsevier Scientific Publishing Company.
- Kalb, P. 1989. O megalitismo e a Neolitização no oeste da península Ibérica, *Arqueologia (Grupo de Estudos Arqueológicos do Porto)* 20: 33-48.
- Kalis, A.J. 1980. Papaveraceae. In W. Punt & G.C.S. Clarke (eds.), *The Northwest European pollen flora, II*: 209-260. Amsterdam: Elsevier Scientific Publishing Company.
- Karlin, R. & S. Levi. 1983. Diagenesis of magnetic minerals in recent hemipelagic sediments, *Nature* 303: 327-330.

- Karlin, R. & S. Levi. 1985. Geochemical and sedimentological control of the magnetic properties of hemipelagic sediments, *Journal of Geophysical Research* 90(B12): 10373-10392.
- Keeling, P.S. 1962. Some experiments on the low-temperature removal of carbonaceous material from clays, *Clay Minerals Bulletin* 28: 155-158.
- Konen, M.E., P.M. Jacobs, C.L. Burras, B.J. Talaga & J.A. Mason. 2002. Equations for predicting soil organic carbon using loss-on-ignition for north central U.S. soils, *Soil Science Society of America Journal* 66: 1878-1881.
- Krom, M.D. & R.A. Berner. 1983. A rapid method for the determination of organic and carbonate carbon in geological samples, *Journal of Sedimentary Petrology* 53: 660-663.
- Lajeunesse, P & M. Allard. 2002. Sedimentology of an ice-contact glaciomarine fan complex, Nastapoka Hills, eastern Hudson Bay, northern Québec, *Sedimentary Geology* 152: 201-220.
- Lario, J., C. Zazo, A.J. Plater, J.L. Goy, C.J. Dabrio, F. Borja, F.J. Sierro & L. Luque. 2001. Particle size and magnetic properties of Holocene estuarine deposits from the Doñaña National Park (SW Iberia): evidence of gradual and abrupt coastal sedimentation, *Zeitschrift für Geomorphologie* 45: 33-54.
- Lario, J., C. Zazo, J.L. Goy, C.J. Dabrio, F. Borja, P.G. Silva, F. Sierro, A. González, V. Soler & E. Yll. 2002a. Changes in sedimentation trends in SW Iberia Holocene estuaries (Spain), *Quaternary International* 93-94: 171-176.
- Lario, J., C. Spencer, A.J. Plater, C. Zazo, J.L. Goy & C.J. Dabrio. 2002b. Particle size characterisation of Holocene back-barrier sequences from North Atlantic coasts (SW Spain and SE England), *Geomorphology* 42: 25-42.
- Lawson, I., M. Frogley, C. Bryant, R. Preece & P. Tzedakis. 2004. The Lateglacial and Holocene environmental history of the Ioannina basin, north-west Greece, *Quaternary Science Reviews* 23: 1599-1625.
- Le Borgne, E. 1955. Susceptibilité magnétique anormale du sol superficiel, *Annales de Géophysique* 11: 399-419.
- Lees, J.A., R.J. Flower, D. Ryves, E. Vologina & M. Sturm. 1998. Identifying sedimentation patterns in Lake Baikal using whole core and surface scanning magnetic susceptibility, *Journal of Paleolimnology* 20: 187-202.
- Libes, S.M. 1992. *An introduction to Marine Biogeochemistry*. New York: John Wiley & Sons, Inc.
- Lobo, F.J., J.M.A. Dias, R. González, F.J. Hernández-Molina, J.A. Morales & V. Díaz del Río. 2003. High-resolution seismic stratigraphy of a narrow, bedrock-controlled estuary: the Guadiana estuarine system, SW Iberia, *Journal of Sedimentary Research* 73(6): 973-986.
- Lobo, F.J., R. Sánchez, R. González, J.M.A. Dias, F.J. Hernández-Molina, L.M. Fernández-Salas, V. Díaz del Río & I. Mendes. 2004. Contrasting styles of the Holocene highstand sedimentation and sediment dispersal systems in the northern shelf of the Gulf of Cadiz, *Continental Shelf Research* 24: 461-482.

- Long, A.J., A.J. Plater, M.P. Waller & J.B. Innes. 1996. Holocene coastal sedimentation in the eastern English Channel: new data from the Romney Marsh region, United Kingdom, *Marine Geology* 136: 97-120.
- Loureiro, J.M. 1983. *Monografia Hidrológica do Algarve*. Faro: Universidade do Algarve. Direcção-Geral dos Recursos e Aproveitamentos Hidráulicos.
- Loureiro, N.S. & M.A. Coutinho, 1995. Rainfall changes and rainfall erosivity increase in the Algarve (Portugal), *Catena* 24: 55-67.
- Lousã, M.F. 1986. *Comunidades Halofílicas da Reserva de Castro Marim*. Lisboa: Universidade Técnica de Lisboa, Instituto Superior de Agronomia.
- Lowe, J.J. & M.J.C Walker. 2000. Radiocarbon dating the last Glacial-Interglacial transition (ca. 14-9 14C ka BP) in terrestrial and marine records: the need for new quality assurance protocols, *Radiocarbon* 42(1): 53-68.
- Luczak, C., M.A. Janquin & A. Kupka. 1997. Simple standard procedure for the routine determination of organic matter in marine sediment, *Hydrobiologia* 345: 87-94.
- Mabberley, D.J. & P.J. Placito. 1993. *Algarve Plants and Landscape*. Oxford: Oxford University Press.
- Magny, M., C. Miramont & O. Sivan. 2002. Assessment of the impact of climate and anthropogenic factors on the Holocene Mediterranean vegetation in Europe on the basis of palaeohydrological records, *Palaeogeography, Palaeoclimatology, Palaeoecology* 186: 47-59
- Maher, B.A. & R. Thompson. 1992. Paleoclimate significance of the mineral magnetic record of the Chinese loess and paleosols, *Quaternary Research* 37: 155-170.
- Malato Beliz, J. 1982. *A Serra de Monchique: Flora e Vegetação*. Lisbon: Serviço Nacional de Parques, Reservas e Património Paisagístico.
- Mangerud, J., S.T. Andersen, B.E. Berglund & J.J. Donner. 1974. Quaternary stratigraphy of Norden, a proposal for terminology and classification. *Boreas* 4: 109-128.
- Manupella, G. 1992. *Carta Geológica da Região do Algarve, 1:100,000*. Lisboa: Serviços Geológicos de Portugal.
- Marret, F. & J.-L. Turon. 1994. Paleohydrology and paleoclimatology off Northwest Africa during the last glacial-interglacial transition and the Holocene: Palynological evidences, *Marine Geology* 118: 107-117.
- Mateus, J. 1989. Lagoa Travessa. A Holocene pollen diagram from the South-West coast of Portugal, *Revista de Biologia* 14:17-94.
- Mateus, J. 1989. Pollen morphology of Portuguese Ericales, *Revista de Biologia* 14: 135-208.
- Mayer, L.M. 1994. Relationships between mineral surfaces and organic carbon concentrations in soils and sediments, *Chemical Geology* 114: 347-363.
- McLaren, P. 1981. An interpretation of trends in grain size measures, *Journal of Sedimentary Petrology* 51(2): 611-624.

- McManus, J. 1988. Grain size determination and interpretation. In M. Tucker (ed.) *Techniques in Sedimentology*: 63-85. Oxford: Blackwell Scientific Publications.
- Mendes, I., R. González, J.M.A. Dias, F. Lobo & V. Martins. 2004. Factors influencing recent benthic foraminifera distribution on the Guadiana shelf (southwestern Iberia), *Marine Micropalaeontology* 51: 171-292.
- Mikkelsen, O. & M. Pejrup, 1998. Comparison of flocculated and dispersed suspended sediment in the Dollard estuary. In K.S. Black, D.M. Paterson & A. Cramp (eds.), *Sedimentary Processes in the Intertidal Zone*: 199-209. London: Geological Society Special Publication no. 139.
- Milne, G.A., A.J. Long & S.E. Bassett. 2005. Modelling Holocene relative sea-level observations from the Caribbean and South America, *Quaternary Science Reviews* 24(10/11): 1183-1202.
- Mook, D.H. & C.M. Hoskin. 1982 Organic determination by ignition: caution advised, *Estuarine, Coastal and Shelf Science* 15: 697-699.
- Moore, P.D., J.A. Webb & M.E. Collinson. 1991. *Pollen Analysis*. Oxford: Blackwell Scientific Publications.
- Morales, J.A. 1993. *Sedimentología del estuario de Guadiana (S.W. España-Portugal)*. Ph.D. thesis: University of Sevilla, Sevilla, Spain, 274pp.
- Morales, J.A. 1997. Evolution and facies architecture of the mesotidal Guadiana River delta (S.W. Spain – Portugal), *Marine Geology* 138: 127-148.
- Morales, J.A., F. Ruiz & I. Jiménez. 1997. Papel de la sedimentación estuarina en el intercambio sedimentario entre el continente y el litoral: el estuario del Río Guadiana (S.O. España-Portugal), *Revista de la Sociedad Geológica de España* 10(3-4): 118-135.
- Morzadec-Kerfourn, M.T. 1992. Upper Pleistocene and Holocene dinoflagellate cyst assemblages in marine environments of the Mediterranean Sea and the northwest Atlantic coast of France. In M.J. Head & J.H. Wrenn (eds.), *Neogene and Quaternary Dinoflagellate Cysts and Acritarchs*: 121-132. Dallas: American Association of Stratigraphic Palynologists Foundation.
- Morzadec-Kerfourn, M.T. 2005. Interaction between sea-level changes and the development of littoral herbaceous vegetation and autotrophic dinoflagellates, *Quaternary International* 133–134: 137–140
- Moura, D. & T. Boski. 1999. Pliocene and Pleistocene lithostratigraphic units in the the Algarve, *Comunicações, Instituto Geológico e Mineiro* 86: 85-106.
- Moura, D., T. Boski, D. Duarte, C. Veiga-Pires, P. Pedro, N. Lourenço & F. Diniz. 2000. A subida do nível do mar durante o Holocénico no Golfo de Cadiz – tendência regional e diferenças locais. In J.A. Dias & O. Ferreira (eds.) *3rd Symposium on the Atlantic Iberian Continental Margin*: 207-208. Faro: Universidade do Algarve.

- Mudie, P.J. & R. Byrne, 1980. Pollen evidence for historic sedimentation rates in California coastal marshes, *Estuarine and Coastal Marine Science* 10: 305-316.
- Múgica, F.F., M. García Antón & H. Sainz Ollero. 1998. Vegetation dynamics and human impact in the Sierra de Guadarrama, Central System, Spain, *The Holocene* 8(1): 69-82.
- Muñoz Sobrino, C., P. Ramil-Rego & M. Rodríguez Guitián. 1997. Upland vegetation in the north-west Iberian peninsula: forest history and deforestation dynamics, *Vegetation History and Archaeobotany*, 6: 215-233.
- Muto, T. & R.J. Steel. 2000. The accommodation concept in sequence stratigraphy: some dimensional problems and possible redefinition, *Sedimentary Geology* 130: 1-10.
- Nombela, M.A., F. Vilas & G. Evans. 1995. Sedimentation in the mesotidal Rías Bajas of Galicia (north-western Spain): Ensenada de San Simón, Inner Ría de Vigo. In B.W. Flemming (ed.), *Tidal Signatures in Modern and Ancient Sediments*: 133-149. Special Publication of the International Association of Sedimentologists, No. 24. Oxford: Blackwell Science.
- Oldfield, F. 1992. The source of fine-grained 'magnetite' in sediments, *The Holocene* 2(2): 180-182.
- Oldfield, F. 1994. Toward the discrimination of fine-grained ferrimagnets by magnetic measurements in lake and near-shore sediments, *Journal of Geophysical Research* 99(B5): 9045-9050.
- Oldfield, F., B.A. Maher, J. Donoghue & J. Pierce. 1985. Particle-size related, mineral magnetic source sediment linkages in the Rhode River catchment, Maryland, USA, *Journal of the Geological Society of London* 142: 1035-1046.
- Oldfield, F., I. Darnley, G. Yates, D.E. France & J. Hilton. 1992. Storage diagenesis versus sulphide authigenesis: possible implications in environmental magnetism, *Journal of Paleolimnology* 7: 179-189.
- Oldfield, F. & L. Yu. 1994. The influence of particle size variations on the magnetic properties of sediments from the northeastern Irish Sea, *Sedimentology* 41: 1093-1108.
- Pais, J. 1989. Evolução do coberto florestal em Portugal no Neogénico e no Quaternário, *Comunicações dos Serviços Geológicos de Portugal* 75: 67-72.
- Pais, J., P. Legoinha, H. Elderfield, L. Sousa & M. Stevens. 2000. The Neogene of Algarve (Portugal), *Ciências da Terra (UNL)*, 14: 277-288.
- Pantaléon Cano, J., E.I. Yll, R. Pérez-Obiol & J.M Roure. 2003. Palynological evidence for vegetational history in semi-arid areas of the western Mediterranean (Almería, Spain), *The Holocene* 13(1): 109-119.
- Peck, R.M. 1974. Pollen budget studies in a small Yorkshire catchment. In H.J.B. Birks & R.G. West (eds.), *Quaternary Plant Ecology*: 43-60. Oxford: Blackwell.
- Pejrup, M. 1988. The triangular diagram used for classification of estuarine sediments: a new approach. In P.L. de Boer, A. van Gelder & S.D. Nio (eds.), *Tide-Influenced Sedimentary Environments and Facies*: 289-300. Dordrecht, Holland: D. Reidel Publishing Company.

- Pendón, J.G. & J.A. Morales. 1997. Facies deposicionales Holocenas de la Costa de Huelva: propuesta de nomenclatura para litofacies estuarinas, *Cuadernos de Geología Ibérica* 22: 165-190.
- Pendón, J.G., J.A. Morales, J. Borrego, I. Jimenez & M. Lopez. 1998. Evolution of estuarine facies in a tidal channel environment, SW Spain: evidence for a change from tide- to wave-domination, *Marine Geology* 147: 43-62.
- Pinto-Gomes, C.J., A.García Fuentes, A.M.A. Leite & P.C.C. Gonçalves. 1999. Charcos temporários mediterrânicos do Barrocal Algarvio: diversidade e conservação. *Quercetea* 1: 53-64
- Planchais, N. 1987. Impact de l'homme lors du remplissage de l'estuaire du Lez (Palavas, Hérault) mis en évidence par l'analyse pollinique, *Pollen et Spores* 29(1): 73-88.
- Polach, H.A. & J. Golson. 1966. *Collection of specimens for radiocarbon dating and interpretation of results*. Australian Institute of Aboriginal Studies Manual No.2. Australian National University, Canberra.
- Polunin, O. & B.E. Smythies, 1973. *Flowers of South-West Europe: a field guide*. Oxford: Oxford University Press.
- Pons, A. & M. Reille. 1988. The Holocene and Upper Pleistocene pollen record from Padul (Granada, Spain): a new study, *Palaeogeography, Palaeoclimatology, Palaeoecology* 66: 243-263.
- Pope, R.J.J. & A.C. Millington. 2000. Unravelling the patterns of alluvial fan development using mineral magnetic analysis: examples from the Sparta basin, Lakonia, Southern Greece, *Earth Surface Processes and Landforms* 25: 601-615.
- Psuty, N.P. & M.E.S.A. Moreira. 2000. Holocene sedimentation and sea level rise in the Sado Estuary, Portugal, *Journal of Coastal Research* 16: 125-138.
- Pullan, R.A. 1988. *A Survey of Past and Present Wetlands of the western Algarve*. Portugal: Liverpool Papers in Geography, No. 2. Department of Geography, University of Liverpool.
- Punt, W. 1976. Typhaceae and Sparganiaceae. In W. Punt (ed.), *The Northwest European pollen flora, I*: 75-88. Amsterdam: Elsevier Scientific Publishing Company.
- Punt, W. & W. Neinhuis. 1976. Gentianaceae. In W. Punt (ed.), *The Northwest European pollen flora, I*: 89-123. Amsterdam: Elsevier Scientific Publishing Company.
- Punt, W. & P. den Breejen. 1981. Linaceae. In W. Punt & G.C.S. Clarke (eds.), *The Northwest European pollen flora, III*: 75-115. Amsterdam: Elsevier Scientific Publishing Company.
- Punt, W., J.S. de Leeuw van Weenen & W.A.P. van Oostrum. 1976a. Primulaceae. In W. Punt (ed.), *The Northwest European pollen flora, I*: 31-70. Amsterdam: Elsevier Scientific Publishing Company.
- Punt, W., Tj. Reitsma & A.A.M.L. Reuvers. 1976b. Caprifoliaceae. In W. Punt (ed.), *The Northwest European Pollen Flora, I*: 5-29. Amsterdam: Elsevier Scientific Publishing Company.
- Punt, W., J.A.A. Bos & P.P. Hoen. 1991. The Northwest European Pollen Flora, 45. Oleaceae, *Review of Palaeobotany and Palynology* 69: 23-47.

- Queiroz, P.F. 1989. A preliminary palaeoecological study at Estacada (Lagoa de Albufeira), *Revista de Biologia* 14: 3-16.
- Queiroz, P.F.R. 1999. *Ecologia histórica da paisagem do noroeste Alentejano*. Unpublished Ph.D. dissertation, Universidade de Lisboa.
- Queiroz, P.F. & J.E. Mateus. 1994. Preliminary palynological investigation on the Holocene deposits of Lagoa de Albufeira and Lagoa de Melides, Alentejo (Portugal), *Revista de Biologia* 15: 15-27.
- Quezel, P. 1998. La végétation des mares transitoires à *Isoetes* en region méditerranéenne, intérêt patrimonial et conservation, *Ecologia Mediterranea* 24(2): 111-117.
- Rabenhorst, M.C. 1988. Determination of organic and carbonate carbon in calcareous soils using dry combustion, *Soil Science Society of America Journal* 52: 965-969.
- Reaves, C.M. 1986. Organic matter metabolizability and calcium carbonate dissolution in nearshore marine muds, *Journal of Sedimentary Petrology* 56(4): 486-494.
- Reed, J.M, A.C. Stevenson & S. Juggins. 2001. A multi-proxy record of Holocene climatic change in southwestern Spain: the Laguna de Medina, Cádiz, *The Holocene*, 11(6): 707-719.
- Reille, M. 1992. *Pollen et Spores d'Europe et Afrique du Nord*. Marseille: Laboratoire de Botanique Préhistorique et Palynologie, URA CNRS.
- Reille, M. 1995. *Pollen et Spores d'Europe et Afrique du Nord, Supplement 1*. Marseille: Laboratoire de Botanique Préhistorique et Palynologie, URA CNRS.
- Reimer, P.J., M.G.L. Baillie, E. Bard, A. Bayliss, J.W. Beck, C. Bertrand, P.G. Blackwell, C.E. Buck, G. Burr, K.B. Cutler, P.E. Damon, R.L. Edwards, R.G. Fairbanks, M. Friedrich, T.P. Guilderson, K.A. Hughen, B. Kromer, F.G. McCormac, S. Manning, C. Bronk Ramsey, R.W. Reimer, S. Remmele, J.R. Southon, M. Stuiver, S. Talamo, F.W. Taylor, J. van der Plicht & C.E. Weyhenmeyer. 2004. IntCal04 Terrestrial Radiocarbon Age Calibration, 0–26 Cal Kyr BP, *Radiocarbon* 46: 1029-1058.
- Reineck, H.E. & F. Wunderlich. 1968. Classification and origin of flaser and lenticular bedding, *Sedimentology* 11: 99-104.
- Reitz, A., C. Hensen, S. Kasten, J.A. Funk & G.J. de Lange. 2004. A combined geochemical and rock-magnetic investigation of a redox horizon at the last glacial/interglacial transition. *Physics and Chemistry of the Earth* 29(13/14): 921-931.
- Rey, D., N. López-Rodríguez, B. Rubio, F. Vilas, K. Mohamed, O. Pazos & M.F. Bógalo 2000. Propiedades magnéticas de los sedimentos e tipo estuarino. El caso de las Rías Baixas, *Journal of Iberian Geology* 26: 151-169.
- Rey, D., K.J. Mohamed, A. Bernabeu, B. Rubio & F. Vilas. 2005. Early diagenesis of magnetic minerals in marine transitional environments: geochemical signatures of hydrodynamic forcing, *Marine Geology* 215(3/4): 215-236.

- Rivas-Martínez, S., M. Lousa, T.E. Díaz, F. Fernández-González & J.C. Costa. 1990. La vegetación del sur de Portugal (Sado, Alentejo y Algarve), *Itinera Geobotanica* 3: 5-126.
- Rivera Nuñez, D. & M.J. Walker. 1989. A review of palaeobotanical findings of early *Vitis* in the Mediterranean and of the origins of cultivated grape-vines, with special reference to new pointers to prehistoric exploitation in the western Mediterranean, *Review of Palaeobotany and Palynology* 61: 205-237.
- Roberts, A.P. & G.M. Turner. 1993. Diagenetic formation of iron sulphide minerals in rapidly deposited marine sediments, south Island, New Zealand, *Earth and Planetary Science Letters* 115: 257-273.
- Roberts, N., M.E. Meadows & J.R. Dodson. 2001. The history of mediterranean-type environments: climate, culture and landscape, *The Holocene* 11(6): 631-634.
- Rocha, R.B. 1976. Estudo estratigráfico e paleontológico do Jurássico do Algarve occidental, *Ciências da Terra* 2: 11-19.
- Rochon, A., A. de Vernal, J.-L. Turon, J. Matthiessen & M.J. Head. 1999. Distribution of recent dinoflagellate cysts in surface sediments from the North Atlantic Ocean and adjacent seas in relation to sea-surface parameters. American Association of Stratigraphic Palynologists, Contributions Series No. 35.
- Rodrigues, A., A. Magalhães & J.M.A. Dias. 1991. Evolution of the North Portuguese coast in the last 18,000 years, *Quaternary International* 9: 67-74.
- Rodrigues, A., J.A. Dias & A. Ribeiro. 2000. The North Portuguese shelf during the last Glacial Maximum and Younger Dryas. In J.A. Dias & O. Ferreira (eds.) *3rd Symposium on the Atlantic Iberian Continental Margin*: 207-208. Faro: Universidade do Algarve.
- Rodríguez-Ramírez, A., J. Rodríguez Vidal, L. Cáceres, L. Clemente, G. Belluomini, L. Manfra, S. Improta & J. Ramón de Andrés. 1996. Recent coastal evolution of the Doñana National Park (SW Spain), *Quaternary Science Reviews* 15: 803-809.
- Rouillard, P. 1991. *Les Grecs et la péninsule Ibérique, du VIIIe au IVe siècle avant Jésus-Christ*. Paris: Diffusion, De Boccard.
- Round, F.E. 1965. *The Biology of the Algae*. London: Edward Arnold (Publishers) LTD.
- Roure, J.M. 1985. Palinología Ibérica. Familias 1 a 20. Cupressaceae a Betulaceae, *Orsis* 1: 43-49.
- Roy, P.S., B.G. Thom & L.D. Wright. 1980. Holocene sequences on an embayed high-energy coast: an evolutionary model, *Sedimentary Geology* 25: 1-19.
- Ruiz, F., A. Rodríguez-Ramírez, L.M. Cáceres, J. Rodríguez Vidal, M.I. Carretero, L. Clemente, J.M. Muñoz, C. Yañez & M. Abad. 2004. Late Holocene evolution of the southwestern Doñana National Park (Guadalquivir Estuary, SW Spain): a multivariate approach, *Palaeogeography, Palaeoclimatology, Palaeoecology* 204: 47-64.
- Rummery, T.A. 1983. The use of magnetic measurements in interpreting the fire histories of lake drainage basins, *Hydrobiologia* 103: 53-58.

- Rybnícková, E. & K. Rybníček. 1971. The determination and elimination of local elements in pollen spectra from different sediments, *Review of Palaeobotany and Palynology* 11: 165-176.
- Saa Otero, M.P. & F. Diaz Fierros. 1990. Análisis polínico de cuatro sedimentos de fondo de Ría en Galicia (España), *Revue de Paléobiologie* 9(2): 283-289.
- Saad, S.I. 1986. Palynological studies in the genus *Plantago* L. (Plantaginaceae), *Pollen et Spores* 28(1): 43-60.
- Sáenz de Rivas, C. 1973. Estudios palinológicos sobre *Quercus* de la España mediterránea, *Boletín de la Real Sociedad Española de Historia Natural* 71: 315-329.
- Sánchez Goñi, M.F. 1996. Vegetation and sea level changes during the Holocene in the Estuary of the Bidasoa (Southern part of the bay of Biscay), *Quaternaire* 7(4): 207-219.
- Sánchez Goñi, M.F., J.L. Turon, F. Eynaud, N.J. Shackleton & O. Cayre. 2000. Direct land/sea correlation of the Eemian, and its comparison with the Holocene: a high-resolution palynological record off the Iberian margin, *Geologie en Mijnbouw/ Netherlands Journal of Geosciences* 79(2/3): 345-354.
- Sangster, A.G. & H.M. Dale. 1961. A preliminary study of differential pollen grain preservation, *Canadian Journal of Botany* 39: 35-43.
- Sangster, A.G. & H.M. Dale. 1963. Pollen grain preservation of underrepresented species in fossil spectra, *Canadian Journal of Botany* 42: 437-449.
- Santos, L., R. Bao & M.F. Sánchez Goñi. 2001. Pollen record of the last 500 years from the Doniños coastal lagoon (NW Iberian Peninsula): Changes in the pollinic catchment size versus palaeoecological interpretation, *Journal of Coastal Research* 17(3): 705-713.
- Santos, L. & M.F. Sánchez Goñi. 2003. Lateglacial and Holocene environmental changes in Portuguese coastal lagoons 3: vegetation history of the Santo André coastal area, *The Holocene* 13(3): 459-464.
- Scheffers, A. & D. Kelletat. 2005. Tsunami relics on the coastal landscape west of Lisbon, Portugal, *Science of Tsunami Hazards* 23(1): 3-16.
- Schumacher, B.A. 2002. Methods for the determination of total organic carbon (TOC) in soils and sediments. NCEA-C-1282/ERASC-001. U.S. Environmental Protection Agency, Las Vegas, NV.
- Shepard, F.P. 1954. Nomenclature based on sand-silt ratios. *Journal of Sedimentary Petrology* 24: 151-158.
- Simonson, W. & P. Sturgess. 1987. The vegetation and flora of cork oak woodland and sandstone heathland in the lowlands of the western Algarve, A Rocha Observatory Report for the year 1986: 59-73. Mexilhoeira Grande, Portimão, Portugal: A Rocha Trust.
- Simonson, W. 1994. The Flora of Picota, *The A Rocha Observatory report for the year 1993*: 6-28. Mexilhoeira Grande, Portimão, Portugal: A Rocha Trust.

- Smirnov, A., G.L. Chmura & M.F. Lapointe. 1996. Spatial distribution of suspended pollen in the Mississippi River as an example of pollen transport in alluvial channels, *Review of Palaeobotany and Palynology* 92: 69-81.
- Smith, J. 1999. An introduction to the magnetic properties of natural materials. In J. Walden, F. Oldfield & J.P. Smith (eds.), *Environmental Magnetism: a practical guide*: 5-25. Technical Guide, No. 6. London: Quaternary Research Association.
- Snowball, I. 1991. Magnetic hysteresis properties of greigite (Fe₃S₄) and a new occurrence in Holocene sediments from Swedish Lapland, *Physics of the Earth and Planetary Interiors*, 68: 32-40.
- Snowball, I.F. 1994. Bacterial magnetite and the magnetic properties of sediments in a Swedish lake, *Earth and Planetary Science Letters* 126: 129-142.
- Snowball, I. and R. Thompson. 1990. A stable chemical remanence in Holocene sediments, *Journal of Geophysical Research* 95(B4): 4471-4479.
- Soares, A.M.M. 1993. The ¹⁴C content of marine shells: evidence for variability in coast upwelling off Portugal during the Holocene. In, *Isotope techniques in the Study of Past and Current Environmental Changes in the Hydrosphere and Atmosphere (Proceedings)*: 471-485. Vienna: IAEA-SM-329/49.
- Spencer, C.D., A.J. Plater & A.J. Long. 1998. Rapid coastal change during the mid- to late holocene: the record of barrier estuary sedimentation in the Romney marsh region, southeast England, *The Holocene* 8(2): 143-163.
- Sperazza, M., J.N. Moore & M.S. Hendrix. 2004. High-resolution particle size analysis of naturally occurring very fine-grained sediment through laser diffractometry, *Journal of Sedimentary Research* 74(5): 736-743.
- Sprugel, D.G. 1991. Disturbance, equilibrium, and environmental variability: What is 'natural' vegetation in a changing environment?, *Biological Conservation* 58: 1-18.
- Stace, C. 1991. *New flora of the British Isles*. Cambridge: Cambridge University Press.
- Stafford, P.J. 1991. The Northwest European Pollen Flora, 44. Selaginellaceae, *Review of Palaeobotany and Palynology* 69: 1-22.
- Stafford, P.J. & S. Blackmore. 1991. The Northwest European Pollen Flora, 46. Geraniaceae, *Review of Palaeobotany and Palynology* 69: 49-78.
- Stevenson, A.C. 1984. Studies in the vegetational history of S.W. Spain. III. Palynological investigations at El Asperillo, Huelva, *Journal of Biogeography* 12:
- Stevenson, A.C. 1985a. Studies in the vegetational history of S.W. Spain. I. Modern pollen rain in the Doñana National Park, Huelva, *Journal of Biogeography* 12: 243-268.
- Stevenson, A.C. 1985b. Studies in the vegetational history of S.W. Spain. II. Palynological investigations at Laguna de las Madres, S.W. Spain, *Journal of Biogeography* 12: 293-314.
- Stevenson, A.C. 1988. Studies in the vegetational history of S.W. Spain. IV. Palynological investigations of a valley mire at El Acebron, Huelva, *Journal of Biogeography* 15: 339-361.

- Stevenson, A.C. & R.J. Harrison. 1992. Ancient forests in Spain: A model for land-use and dry forest management in South-west Spain from 4000 BC to 1900 AD, *Proceedings of the Prehistoric Society* 58: 227-247.
- Stevenson, J.C., L.G. Ward & M.S. Kearney. 1986. Vertical accretion in marshes with varying rates of sea level rise. In D. Wolf (ed.), *Estuarine Variability*: 241-259. New York: Academic Press.
- Stewart, H.B. Jr. 1958. Sedimentary reflections of depositional environment in San Miguel Lagoon, Baja California, Mexico, *Bulletin of the American Association of Petroleum Geologists* 42(11):2567-2618.
- Stiner, M.C., N.F. Bicho, J. Lindly & R. Ferring. 2003. Mesolithic to Neolithic transitions: new results from shell-middens in the western Algarve, *Antiquity* 77(295): 75-86.
- Stockmarr, J. 1971. Tablets with spores used in absolute pollen analysis, *Pollen et Spores* 13: 615-621.
- Straus, L.G. 1989. New chronometric dates for the prehistory of Portugal, *Arqueologia (Grupo de Estudos Arqueologicos do Porto)* 20: 73-76.
- Straus, L.G., J. Altuna, D. Ford, L. Marambat, J.S. Rhine, J.-H.P. Schawrcz & J.-L. Vernet. 1993. Early farming in the Algarve (southern Portugal): a preliminary view from two cave excavations near Faro, *Trabalhos de Antropologia e Etnologia* 32: 141-162.
- Stuiver, M. & P.J. Reimer. 1993. Extended ¹⁴C database and revised CALIB radiocarbon calibration program, *Radiocarbon* 35: 215-230.
- Stuiver, M. & T.F. Braziunas. 1993. Modeling atmospheric ¹⁴C influences and ¹⁴C ages of marine samples to 10,000 BC, *Radiocarbon* 35(1): 137-189.
- Stuiver, M., P.J. Reimer & T.F. Braziunas. 1998. High-precision radiocarbon age calibration for terrestrial and marine samples, *Radiocarbon* 40(3): 1127-1151.
- Sugita, S. 1994. Pollen representation of vegetation in Quaternary sediments. Theory and method in patchy vegetation, *Journal of Ecology* 82: 881-897.
- Sutherland, R.A. 1998. Loss-on-ignition estimates of organic matter and relationships to organic carbon in fluvial bed sediments, *Hydrobiologia* 389: 153-167.
- Tanaka, N., M.C. Monaghan & D.M. Rye. 1986. Contribution of metabolic carbon to mollusc and barnacle shell carbonate, *Nature* 320: 520-523.
- Tanner, W.F. 1991a. Suite statistics: the hydrodynamic evolution of the sediment pool. In J.P.M. Syvitski (ed.), *Principles, methods, and application of particle size analysis*: 225-236. Cambridge: Cambridge University Press.
- Tanner, W.F. 1991b. Application of suite statistics to stratigraphy and sea-level changes. In J.P.M. Syvitski (ed.), *Principles, methods, and application of particle size analysis*: 283-292. Cambridge: Cambridge University Press.
- Tauber, H. 1965. Differential pollen dispersion and the interpretation of pollen diagrams, *Danmarks Geologiske Undersøgelse IIR* 89:1-69.

- Telford, R.J., E Heegaard & H.J.B. Birks. 2004. The intercept is a poor estimate of a calibrated radiocarbon age, *The Holocene* 14(2): 296-298.
- Thompson, R. & F. Oldfield. 1986. *Environmental Magnetism*. London: Allen & Unwin.
- Traverse, A. 1988. *Paleopalynology*. Boston: Unwin Hyman.
- Traverse, A. 1990. Studies of pollen and sporese in rivers and other bodies of water, in terms of source-vegetation and sedimentation, with special reference to Trinity River and Bay, Texas, *Review of Palaeobotany and Palynology* 64: 297-303.
- Turon, J.-L., A.-M. Lézine, M. Denèfle. 2003. Land-sea correlations for the last glaciation inferred from a pollen and dinocyst record from the Portuguese margin, *Quaternary Research* 59: 88-96.
- Tutin, T.J. (ed.) 1964-1980. *Flora Europea*. 5 volumes. Cambridge: Cambridge University Press.
- van Benthem, F. G.C.S. Clarke & W. Punt. 1984. Fagaceae. In W. Punt & G.C.S. Clarke (eds.), *The Northwest European pollen flora, IV*: 1-5. Amsterdam: Elsevier Scientific Publishing Company.
- van den Brink, L.M., & C.R. Janssen. 1985. The effect of human activities during cultural phases on the development of montane vegetation in the Serra da Estrela, Portugal, *Review of Palaeobotany and Palynology* 44: 193-215.
- van der Knaap, W.O., & J.F.N. van Leeuwen. 1995. Holocene vegetation succession and degradation as responses to climatic change and human activity in the Serra da Estrela, Portugal, *Review of Palaeobotany and Palynology* 89: 153-211.
- van der Knaap, W.O., & J.F.N. van Leeuwen. 1997. Late Glacial and early Holocene vegetation succession, altitudinal vegetation zonation, and climatic change in the Serra da Estrela, Portugal, *Review of Palaeobotany and Palynology* 97(3/4): 239-28.
- van Helvoort, H.A.M. & W. Punt. 1984. Araliaceae. In W. Punt & G.C.S. Clarke (eds.), *The Northwest European pollen flora, IV*: 1-5. Amsterdam: Elsevier Scientific Publishing Company.
- van Leeuwaarden, W. & Janssen, C.R. 1985. A preliminary palynological study of peat deposits near an oppidum in the lower Tagus valley, *Actas (Grupo de trabalho Português para o estudo do Quaternário)* 2: 225-236.
- van Leeuwen, P., W. Punt & P.P. Hoen. 1988. The Northwest European Pollen Flora, 43. Polygonaceae, *Review of Palaeobotany and Palynology* 57: 81-151.
- Visset, L. 1985. Dernière données pollenanalytiques et radiométriques du golfe Briéron (Massif Armoricain, France), *Ecologia Mediterranea*, Tome XI (Fascicule 1):107-116.
- Visset, L. 1987. Étude pollenanalytique de quelques sites du marais Poitevin, *Bulletin de l'Association française pour l'étude du Quaternaire* 24: 81-91.
- Volkman, J.K., D. Rohjans, J.Rullkötter, B.M. Scholz-Böttcher & G. Liebezeit. 2000. Sources and diagenesis of organic matter in tidal flat sediments from the German Wadden Sea, *Continental Shelf Research* 20: 1139-1158.

- Webb, T. III. 1987. The appearance and disappearance of major vegetational assemblages: Long-term vegetational dynamics in eastern North America, *Vegetatio* 69: 177-187.
- Wheeler, A.J., F. Oldfield & J.D. Orford. 1999. Depositional and post-depositional controls on magnetic signals from saltmarshes on the north-west coast of Ireland, *Sedimentology* 46: 545-558.
- Williams, M. 1992. Evidence for the dissolution of magnetite in recent Scottish peats, *Quaternary Research* 37: 171-182.
- Willis, K.J. 1994. The vegetational history of the Balkans, *Quaternary Science Reviews* 13: 769-788.
- Willis, K.J. & K.D. Bennett. 1994. The Neolithic transition - fact or fiction? Palaeoecological evidence from the Balkans, *The Holocene* 4(3): 326-330.
- Wolanski, E. & R.J. Gibbs. 1995. Flocculation of suspended sediment in the Fly River Estuary, Papua New Guinea, *Journal of Coastal Research* 11(3): 754-762.
- Wright, H.E. Jr. 1967. The use of surface samples in Quaternary pollen analysis, *Review of Palaeobotany and Palynology* 2: 321-330.
- Yll, E.-I., R. Perez-Obiol, J. Pantaleon-Cano & J.M Roure. 1997. Palynological evidence for climatic change and human activity during the Holocene on Minorca (Balearic Islands), *Quaternary Research* 48: 339-347.
- Zazo, C., J.L. Goy, L. Somoza, C.J. Dabrio, G. Belluomini, S. Imbrota, J. Lario, T. Bardají & P.G. Silva. 1994. Holocene sequence of sea-level fluctuations in relation to climatic trends in the Atlantic-Mediterranean linkage coast, *Journal of Coastal Research* 10(4): 933-945.
- Zilhão, J. 2001. Radiocarbon evidence for maritime pioneer colonization at the origins of farming in west Mediterranean Europe, *Proceedings of the National Academy of Sciences of the United States of America* 98(24): 14180-14185.

Appendix A. Beliche surface pollen samples

Rationale

Surface pollen samples are a valuable aide in the interpretation of fossil pollen records, particularly in new geographic areas of investigation (Wright, 1967). Surface soil samples were collected from 12 sample locations along two short transects on the Beliche floodplain, marsh and adjacent hill-slope. The objectives of the exercise were: a) to aid familiarisation with pollen types occurring in the area through the identification of well-preserved modern material from a known vegetational setting, b) to observe the relative contribution of pollen types from different habitats to the assemblages from the sample locations, and, in particular, to determine the extent of over-representation of local pollen types, and c) to provide comparative data to aid in the interpretation of the fossil pollen and spores recovered from core samples.

Methods

Two transects were chosen with respect to two gradients: 1) the gradient from overall wet to dry conditions, beginning on the floodplain marsh, crossing the break of slope and rising onto the valley-side (transect A) and 2) the general decrease in soil salinity along the floodplain from east to west, beginning near the bank of the Guadiana and progressing inland (transect B). The transects and sample locations are shown in Figure A1.

Sample locations on the transects were chosen on the basis of floristic composition, so as to be a) representative of the wider pattern of distribution of different vegetation groups and/or land uses in the floodplain environment and surroundings, and b) internally homogeneous with respect to the species present. The characteristics of each sample location are summarised in Table A1.

10 x 10 m quadrats were set up at each sample location, and the main floristic elements recorded in terms of presence/absence. Five soil samples were collected from each quadrat,

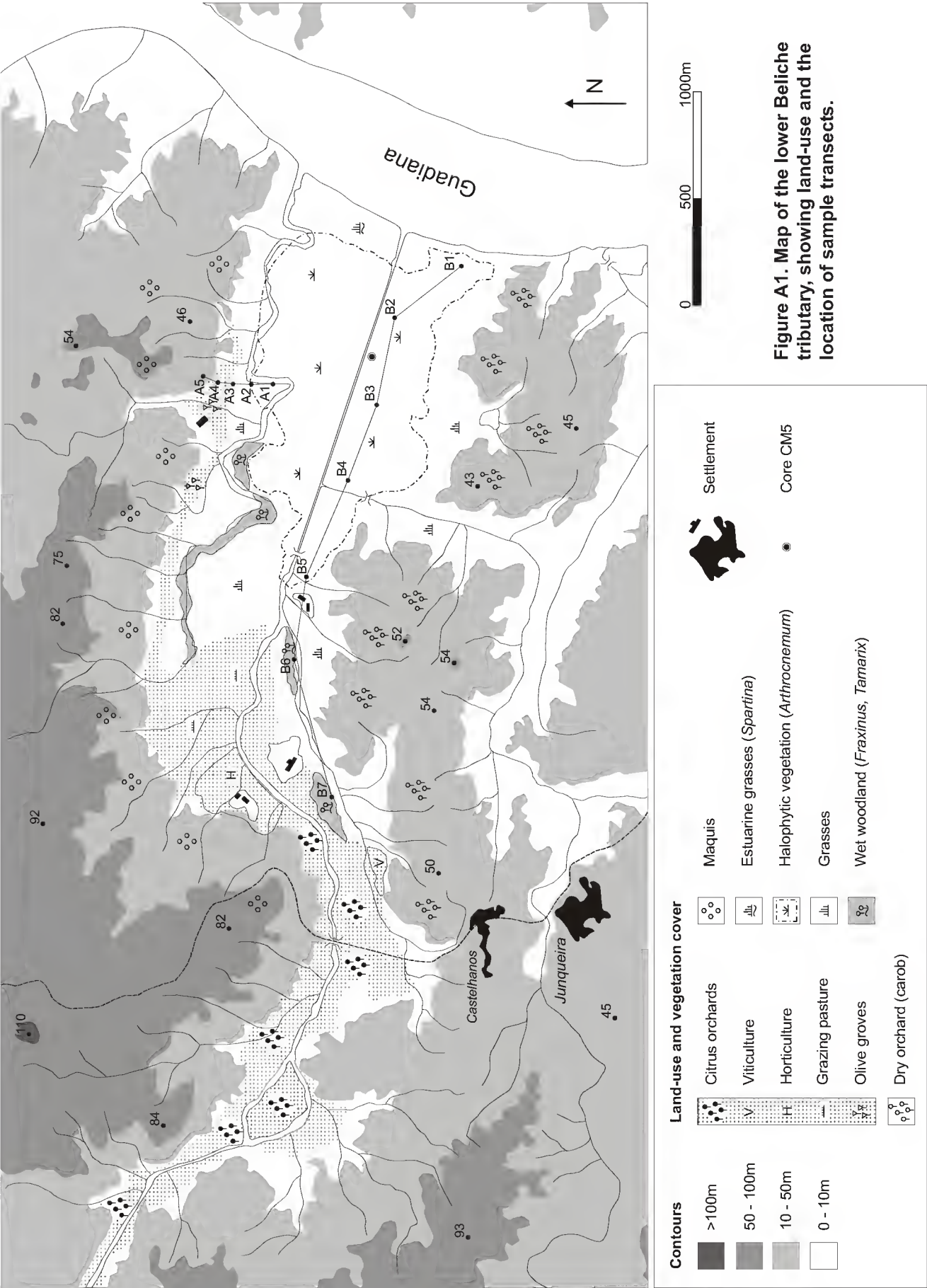


Figure A1. Map of the lower Beliche tributary, showing land-use and the location of sample transects.

Location	Description	Main floristic elements
A1	Upper saltmarsh	Halophytes (<i>Salicornia</i> , <i>Suaeda</i>), grasses, Asteraceae spp.
A2	Upper saltmarsh	Halophytes, grasses, Asteraceae spp., (<i>Plantago</i> , <i>Echium</i> , <i>Oxalis</i>)
A3	Alluvial meadow, site of abandoned cultivation	Grasses, Asteraceae spp., <i>Rumex</i> .
A4	Olive grove	Olive trees (<i>Olea</i>), grasses, Asteraceae and other flowering plants (<i>Echium</i> , Caryophyllaceae, <i>Plantago</i> , <i>Trifolium</i> .)
A5	<i>Cistus</i> scrub (<i>matos</i>)	<i>Cistus ladanifer</i> , <i>Cistus monspeliensis</i> , <i>Phillyrea</i> , <i>Genista</i> , <i>Lavandula</i> , grasses
B1	Lower saltmarsh	Halophytes (<i>Arthrocnemum</i> , <i>Salicornia</i> , <i>Halimione</i>), grasses
B2	Upper saltmarsh	Halophytes (<i>Arthrocnemum</i> , <i>Salicornia</i>), grasses, Asteraceae., <i>Trifolium</i> , <i>Plantago</i>
B3	Upper saltmarsh	Halophytes (<i>Arthrocnemum</i> , <i>Salicornia</i>), grasses, Asteraceae, <i>Trifolium</i> , <i>Echium</i> spp.
B4	Upper saltmarsh	Halophytes (<i>Arthrocnemum</i>), Asteraceae, grasses, <i>Trifolium</i> .
B5	Floodplain marsh	Grasses, <i>Juncus</i> , <i>Tamarix</i> , halophytes (<i>Arthrocnemum</i>),
B6	Floodplain marsh woodland fringe	Ash (<i>Fraxinus angustifolia</i>), <i>Juncus</i> , Apiaceae., Asteraceae., <i>Geranium</i> , <i>Plantago</i> , <i>Rumex</i> , halophytes (<i>Suaeda</i>)
B7	Woodland fringe	<i>Tamarix</i> , grasses, halophytes (<i>Suaeda</i>),

Table A1. Characterisation of sample locations.

distributed evenly across the quadrat (one near the centre and one towards each of the four corners). Soil samples were taken from the uppermost 2–3 cm.

In the laboratory, soil samples were mixed, and equal amounts of the five soil samples from each sample location were combined and mixed again. The generation of mixed samples has been shown is critical for the study of pollen from surface soil samples (Adam & Mehringer, 1975). The pollen content of individual soil samples at spot locations can occasionally deviate widely from the ‘average’ local pollen rain due to the contribution of fallen anthers from individual plants. The mixed pollen samples were subjected to a standard pollen preparation following the same methodology as for fossil pollen samples. Pollen slides were counted until total pollen and spore counts of ca. 1000 grains were achieved.

Results

The pollen content of the surface sample is displayed in full in Figure A2 and summarised by ecological groups in Figure A3. Overall, the observed pollen types reflect the vegetation

of the floodplain and its upland surroundings. Moreover, the strong representation of distinct local pollen types distinguishes clearly between samples of the marsh/floodplain and hill-slope settings. The results are discussed by ecological group in this section, and the provenance of the pollen in the following section.

Agroforestry, arboriculture

This group contains arboreal pollen taxa (*Eucalyptus*, *Pinus*, *Quercus suber* type, *Quercus undiff.*) which in the modern surroundings of the Beliche represent plantations, cultivated stands and scattered trees in areas of scrub. *Olea* is also placed in this group, because although wild olive trees are common, the abundance of *Olea* pollen clearly reflects the presence of the olive grove at location A4. This group is strongly represented at the hill-slope locations (A4, A5) and is recorded fairly consistently in lower abundances in the floodplain locations.

Thickets and scrub

This group contains pollen types of predominantly shrubby plants (e.g. *Phillyrea*, *Myrtus*, *Daphne* and *Cistus* types) which represent scrub vegetation growing on degraded soils typical of extensive areas of the Beliche catchment. Although included with the previous group, it is recognised that *Olea* and the *Quercus* types also reflect scattered arboreal elements of these scrub habitats. This group is strongly represented at location A5, within an area of *Cistus* scrub. However, the elements of this group are overall recorded sporadically and/or in low abundances at the other locations.

Cultivated and waste ground

Included in this group are pollen types of herbaceous plants generally associated with open ground and grassy areas. Many, such as the plantains (*Plantago lanceolata*/ *coronopus* types) and docks (*Rumex* types), or the non-native *Oxalis pes-caprae*, are ruderals, exploiting disturbed ground in areas of agricultural and pastoral activity. This group does not show a clear pattern of variation along the transects, which may reflect the tolerance of the included plants for different conditions encountered in the sampled area and/or that the sampled

Beliche Surface Pollen Samples

Analysis W. Fletcher

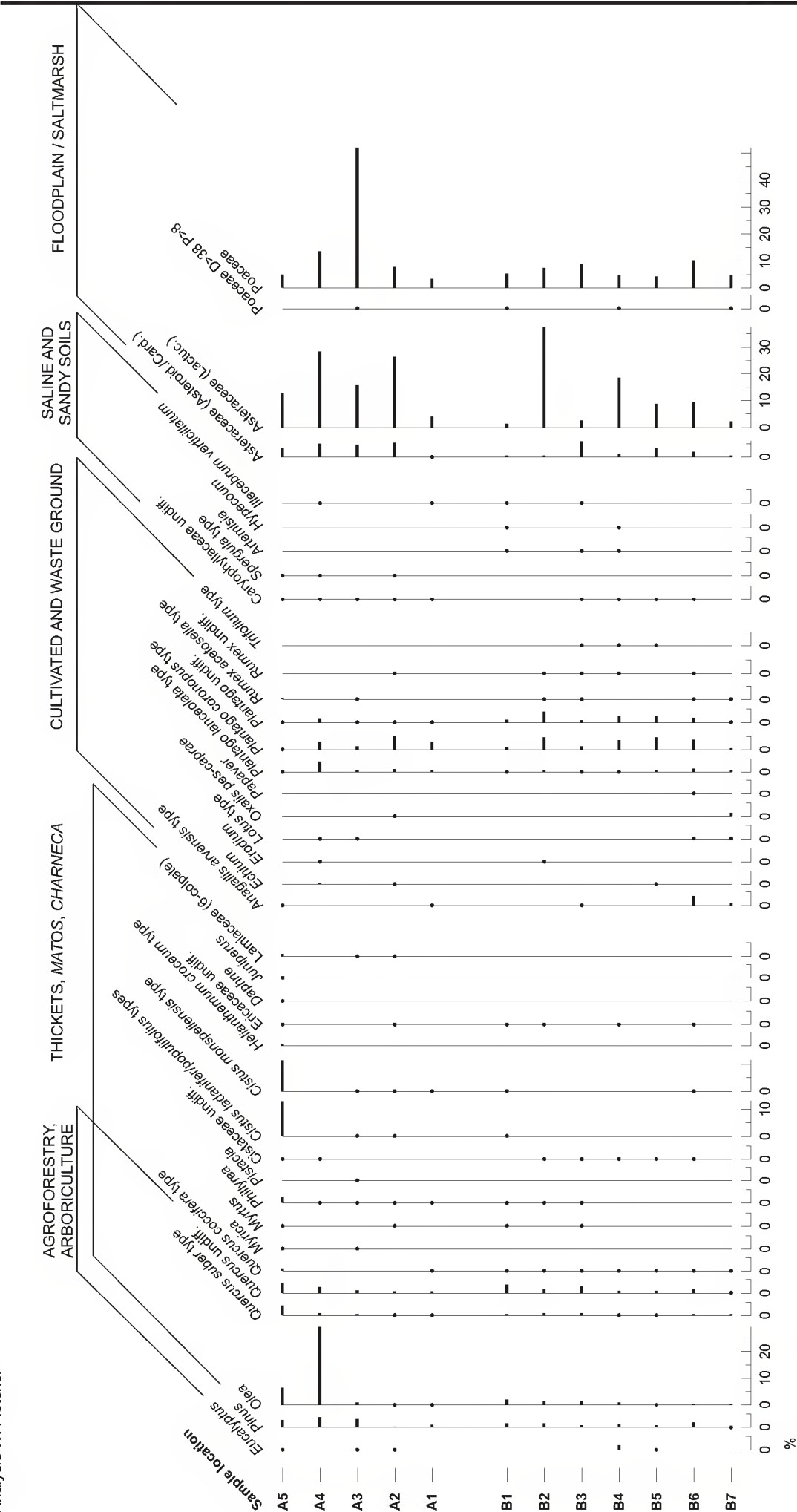


Figure A2. Percentage pollen diagram for Beliche surface samples, page 1 of 2.

Σ = Total pollen and spores
• represents values <0.5%

Figure A2. Percentage pollen diagram for Beliche surface samples, page 2 of 2.

transects do not include strong gradients for critical variables such as intensity of agricultural activity, disturbance regime, etc.

Within this group *Plantago* types are the most abundant, and are recorded at all locations. Different patterns of representation are noted for *P. lanceolata* and *P. coronopus* types, with *P. lanceolata* type reaching maxima at locations A4 and B6, and *P. coronopus* at locations A2 and B2. This contrast probably reflects the greater tolerance of *P. coronopus* for (high) saltmarsh conditions.

Saline and sandy soils

This group contains pollen types of generally herbaceous plants typical of sandy soils, particularly near the coast. This group is not strongly represented in the surface samples. Maximum values for the group occur at location A4, resulting from small maxima in *Spergula* type and Caryophyllaceae undiff., and at location B1, due to the occurrence of *Artemisia*, *Hypochaeris* and *Illecebrum verticillatum* types.

Open ground, floodplain and saltmarsh

The broad taxonomic pollen types of Asteraceae and Poaceae are included in this strongly-represented group. Reflecting the contribution of numerous species of marsh, floodplain and hill-slope environments, this group is ecologically ambiguous.

Asteraceae types are well represented at all sites except A1, B1 and, for Asteraceae (Lactucaee), B3. Poaceae pollen occurs in fairly consistent proportions at all locations, except at the meadow location A3, where Poaceae pollen represents >50% of the total assemblage.

Saltmarsh

Included in this group are Chenopodiaceae and Cyperaceae pollen types which represent primarily, though not exclusively, halophytic marsh vegetation. Chenopodiaceae pollen is abundant in all floodplain samples from transect B, and shows declining values along transect A. Maximum values occur for the lowest positions on each transect (A1, B1).

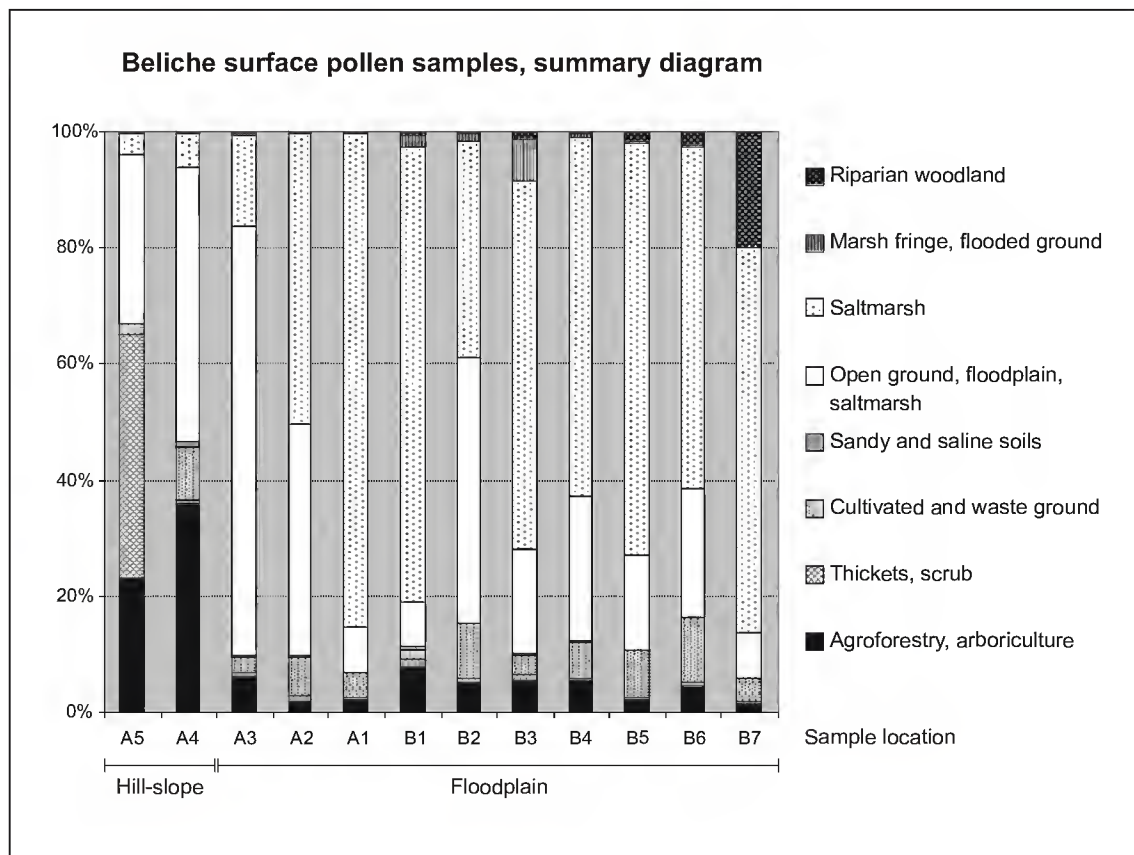


Figure A3. Summary pollen diagram showing relative proportions of several pollen groups associated with different habitats.

Marsh fringe and flooded ground

Included in this group are pollen types representing damp or seasonally flooded ground. *Isoetes* undiff. shows a clear pattern of increased values in the lower sample locations and with increased proximity to the Guadiana. *Ranunculus* type is included here because of the likely contribution of species inhabiting shallow and temporary pools (e.g. *R. peltatus*). Overall, this group makes a significant contribution only at locations B1, B2 and B3.

Aquatics

This group represents aquatic plants of fresh to brackish, stagnant or weakly flowing water. The group is very poorly represented overall, with only sporadic occurrences in the floodplain locations, and is excluded from Figure A3.

Riparian woodland

Pollen types representing damp woodland of the river floodplain (*Alnus*, *Fraxinus*, *Salix* types) are included in this group, together with *Tamarix*, a small tree or large shrub of riparian and marsh fringe settings, and *Scrophularia* type, a pollen type corresponding to herbaceous plants growing commonly, though not exclusively, in damp woodland. This group is best represented at sample locations in the inner areas of the Beliche floodplain (B5, B6, B7) situated close to small stands of *Tamarix* and *Fraxinus*.

Indeterminate

Included in this group are a number of pollen types such as Apiaceae undiff. and Liliaceae undiff. for which the taxonomic and ecological significance in relation to the modern day vegetation of the Beliche environment is either ambiguous or unknown. This group is excluded from Figure A3.

Pteridophytes

Spores of a fern (*Anogramma leptophylla*) and a clubmoss (*Selaginella denticulata*) were identified in the surface samples, along with indeterminate monolete and trilete spores. This group is represented in very low abundances in the samples and is excluded from Figure A3.

Comments on the pollen surface samples***Pollen sources***

The contribution of any given pollen type to a surface soil sample will be determined by a range of factors including pollen production, dispersal efficiency and distance from the source. The influence of the latter on the Beliche samples is considered here, employing the terminology of Janssen (1966).

A significant proportion of pollen deposited on the soil surface is expected to be derived from local plants — the local or gravity component. This component is deposited in the form of free pollen grains during dehiscence, but also intact anthers or entire flowers, and redeposited pollen grains trapped in leaves and branches. Local pollen should be

characterised by high pollen percentages, high variability over short distances, and rapid decline away from the source area (Janssen, 1966). A number of examples of strong local representation of pollen types derived from immediately local plants are observed in the Beliche data-set, and include *Olea* at location A4, *Cistus* at A5, *Poaceae* at A3, *Chenopodiaceae* at A1, A2 and B1–7, *Tamarix* at B7. Overall, the influence of strongly represented local pollen types accounts for the contrast in overall composition of the surface samples between the hill-slope and floodplain samples (Figure A3), and between the scrub (*matos*) and olive grove samples (A5, A4).

The case is particularly interesting with the *Cistus* pollen types, which are recorded in abundance within the *matos* sample location, but are poorly represented at all other locations, including the neighbouring sample location. This discrepancy suggests poor dispersal of the *Cistus* pollen grains, which may relate to the large size of the grains and the primary pollination mechanism of the Cistaceae, namely entomophily or pollination by insects.

A second component of the pollen samples is understood to be pollen that has been transported in the air some distance from its source. Included here are the extralocal component of pollen travelling relatively short distances from the source in a diffuse cloud near to the ground, and the regional component of pollen transported relatively long distances by air currents at altitude (Janssen, 1966). The extralocal and regional pollen components are expected not to show the high variability of local pollen. The contribution of an airborne component is detected in the Beliche samples. Notable examples include wind-pollinated *Pinus*, *Quercus* and *Olea* pollen types, which are recorded consistently across the floodplain surface, and — as would be expected of a mixed, airborne or atmospheric pollen source — in fairly even proportions (Figure A2).

A water-borne pollen component is also likely to have contributed to the composition of the surface pollen samples, at least for the floodplain sample locations. The floodplain surface will receive floodwaters carrying secondary pollen, remobilized and transported

from other sites of deposition, of both freshwater (Beliche) and tidal (Guadiana) origin. Pollen deposited on the floodplain may in turn be subject to further remobilization and redeposition. Possible indications of a waterborne pollen component include aquatic pollen types, *Myriophyllum* and *Potamogeton*, and *Pediastrum* colonies (a freshwater alga), recorded at locations B1 and B2 near the Guadiana. The presence of a water-borne pollen component will have the effect of broadening the pollen source area of the surface samples (Moore *et al.*, 1991)

Caution must be applied where a secondary pollen source is anticipated, because of the potential contribution of reworked, non-contemporary pollen and spores from catchment soils and sediments. Possible indications of a significant reworked component include a high proportion of crumpled, folded and otherwise degraded pollen grains, the presence of identifiable pre-Quaternary pollen and spores, and an abundance of resilient pollen types, generally in a poor state of preservation. These indicators were not encountered in the Beliche samples, with the possible exception of the latter. The abundance of Asteraceae (Lactucaee) — a type displaying particularly robust morphology (Havinga, 1984) — may reflect a secondary, reworked pollen component in the surface samples derived from catchment soils. However, other indicators are absent and the preservation state of pollen grains in the samples is very good overall. Therefore, in this case, the representation of the Asteraceae (Lactucaee) pollen type is taken as an example of local pollen dispersal, characterised by high pollen percentages and high variability over short distances.

Summary

The study of surface samples from the Beliche valley provides a number of insights into the transport of pollen into the floodplain/marsh environment with implications for the study of fossil pollen assemblages from estuarine settings. First, local vegetation occurring on different areas of the floodplain may be very strongly represented in the surface pollen assemblages. This is clearly demonstrated for halophytic vegetation with the abundance of Chenopodiaceae pollen at sample locations A1, A2 and B1–7. Similar effects are detected for elements of the riparian woodland (*Tamarix*) at location B7, and grasses (Poaceae) on

the alluvial meadow which fringes the saltmarsh (location A3). These effects support the view that in the study of fossil pollen assemblages from an estuarine setting, elements of saltmarsh and wetland vegetation must be excluded from the pollen sum so as to avoid the overrepresentation of a local vegetation signal and the consequent suppression of the regional signal.

Second, some common elements of the regional flora, notably wind-pollinated taxa such as *Pinus*, *Quercus* and *Olea*, are recorded consistently across the floodplain and probably reflect extralocal to regional sources. This observation does not hold, however, for certain pollen types indicative of scrub (*matos*) communities, notably members of the Cistaceae family which are poorly or inconsistently represented beyond their local domain (sample location A5). These observations suggest that the interpretation of these pollen taxa in fossil assemblages may not be equivalent; i.e. changes in pollen percentages for *Pinus*, *Quercus* and *Olea* may reflect vegetation events occurring over a wider area than changes in pollen percentages for Cistaceae.

Finally, the potential contribution of secondary pollen of fluvial, tidal and sedimentary origin is recognised. Water-borne pollen derived from surface runoff and of contemporary age may widen the source area of a pollen sample. This effect does not pose a significant problem for the identification of regional vegetation events from fossil pollen data. However, the redeposition of non-contemporaneous pollen eroded from soils and sediments may cause interpretive problems. The chief guard against errors introduced in this way is the careful consideration of the abundances of degraded and indeterminate grains, pre-Quaternary sporomorphs, and resilient pollen and spore types, all of which may indicate reworking.

Appendix B. Table of pollen types.

The following table contains a list of all pollen types encountered in the analysis of the CM5, P2 and P5 core samples and the Beliche surface pollen samples.

Accompanying each pollen type is an abbreviation of the published reference for the nomenclature and description of the pollen type. The details of the references are included at the end of the table.

Each pollen type is also accompanied by notes on the genera and species which, in light of knowledge of pollen morphology and the regional flora of the Algarve, may have contributed to the pollen record. Plant nomenclature follows Flora Europea (Tutin *et al.*, 1964-1980). A brief description of the common habitats of the species follows. The notes on likely species and their ecological or habitat preferences is derived from a range of sources, including Coutinho (1939), Tutin *et al.* (1964-1980), Malato Beliz (1982), and from observations in the field.

The purpose of this table is: 1) to make transparent the chain of interpretive reasoning between pollen types, plants and species-specific ecology which underlines pollen analysis and the the study of vegetation history, 2) to show the ecological significance of the pollen types, and/or the ambiguity resulting from multiple contributory species of different habitats, and 3) to highlight contrasts in ecological significance of some pollen types between northern Europe and southwestern Iberia.

Pollen/spore taxon	Reference	Notes on likely species	Habitats/Ecology
<i>Acer campestre</i> type	CJa	<i>Acer montpensulanum</i> L.	Woodland
<i>Alchemilla</i> type	MWC	<i>Aphanes arvensis</i> L., <i>Aphanes microcarpa</i> (Boiss. & Reuter) Rothm., <i>Aphanes cornucopioides</i> Lag.	Dry, sandy soils; fields and fallow ground
<i>Alisma</i>	MWC	<i>Alisma plantago-aquatica</i> L.	Ditches, river margins, marshes
<i>Alnus</i>	MWC	<i>Alnus glutinosa</i> (L.) Gaertner	River margins
<i>Anagallis arvensis</i> type	PLV	<i>Anagallis arvensis</i> L., <i>A. montelli</i> L.	Fallow and waste ground, gardens, vineyards, waysides
<i>Anagallis tenella</i> type	PLV	<i>Anagallis tenella</i> (L.) L.	Grassy places and humid ground close to springs and streams
<i>Anogramma leptophylla</i>	MWC	<i>Anogramma leptophylla</i> (L.) Link	Rocks, walls, hedges
<i>Anthemis</i> type	MWC	<i>Anthemis cotula</i> L., <i>A. arvensis</i> L., <i>Chamaemelum mixtum</i> (L.) All., <i>C. nobile</i> (L.) All., <i>C. fuscum</i> (Brot.) Vasc., <i>Achillea ageratum</i> L., <i>Chrysanthemum coronarium</i> L., <i>C. segetum</i> L., <i>Tanacetum annuum</i> L., <i>Anacyclus radiatus</i> Loisel.	Cultivated fields, fallow and waste ground, tracks
Apiaceae undiff.	MWC	Includes numerous Apiaceae spp.	Diverse
<i>Apium inundatum</i> type	MWC	<i>Apium inundatum</i> (L.) Reichenb. fil. in Reichenb. & Reichenb. fil., <i>A. nodiflorum</i> (L.) Lag., <i>A. graveolens</i> L.	Stagnant water
<i>Arbutus unedo</i>	M	<i>Arbutus unedo</i> L.	Woodland understory, scrub, pinewoods
<i>Armeria/Limonium</i>	MWC	<i>Armeria velutina</i> Welw. ex Boiss. & Reuter, <i>A. rouyana</i> Daveau, <i>A. macrophylla</i> Boiss. & Reuter, <i>A. pinifolia</i> (Brot.) Hoffmans. & Link, <i>A. littoralis</i> Willd.	Scrub on dry, sandy or gravelly soils, stony slopes, generally calcifuge
		<i>Armeria pungens</i> (Link) Hoffmans. & Link, <i>Limonium oleifolium</i> Miller, <i>L. ovalifolium</i> (Poiret) O. Kuntze, <i>L. echinoides</i> (L.) Miller	Maritime sands
		<i>Armeria gaditana</i> Boiss. in DC., <i>L. diffusum</i> (Pourret) O. Kuntze, <i>Limonium ramosissimum</i> (Poiret) Maire, <i>L. auriculae-ursifolium</i> (Pourret) Druce	Saltmarshes, coastal meadows, maritime sands
<i>Arnoseris minima</i> type	B	<i>Tolpis barbata</i> (L.) Gaertner	Fields, pasture, pinewoods, hedges, waste ground
<i>Artemisia</i>	MWC	<i>Artemisia arborescens</i> L., <i>A. caerulescens</i> L., <i>A. campestris</i> L.	Maritime sands, saline soils
<i>Asphodelus</i>	*	<i>Asphodelus fistulosus</i> L., <i>A. ramosus</i> L., <i>A. aestivus</i> Brot.,	Dry ground, scrub, pinewoods, waysides and field margins
<i>Aster</i> type	MWC	Numerous; includes <i>Aster</i> , <i>Bidens</i> , <i>Inula</i> , <i>Senecio</i> spp.	Various; notably open ground and saltmarsh
Asteraceae (Asteroideae/Cardueae) undiff.	BWE	Includes non-crested Asteraceae, not identified to one of the other groups; (formerly Compositae Tubuliflorae)	Diverse
Asteraceae (Lactuceae)	BWE	Numerous; includes <i>Leontodon</i> , <i>Sonchus</i> , <i>Lactuca</i> , <i>Scorzonera</i> , <i>Crepis</i> spp. (formerly Compositae Liguliflorae)	Diverse
<i>Betula</i>	MWC	<i>Betula pubescens</i> Ehrh.	Woodland
Boraginaceae undiff.	-	Includes pollen grains of Boraginaceae not identified to one of the other groups	Various
Brassicaceae	-	Numerous; includes all pollen grains belonging to Brassicaceae family	Various; especially open ground, cultivated and waste ground, maritime sands
<i>Callitriche</i>	MWC	<i>Callitriche stagnalis</i> Scop.	Ponds, ditches, rivers
<i>Calluna vulgaris</i>	M	<i>Calluna vulgaris</i> (L.) Hull	Charneacs (dwarf-scrub), dry places and waste ground
Caryophyllaceae trizonocolpate indet.	-	An unidentified type probably belonging to Caryophyllaceae, possibly <i>Corrigiola telephifolia</i> Pourr., <i>Paronychia cymosa</i> (L.) DC.	Unknown
Caryophyllaceae undiff.	-	Numerous; includes <i>Cerastium glomeratum</i> Thuill., <i>Silene</i> spp. (<i>S. colorata</i> Poiret, <i>S. apetala</i> Willd., <i>S. nocturna</i> L., <i>S. gallica</i> L.), and other Caryophyllaceae spp.	Sandy places, open and waste ground
<i>Castanea (=C. sativa type)</i>	VCP	<i>Castanea sativa</i> Miller	Woodland, cultivated stands
<i>Centaurea nigra</i> type	MWC	<i>Centaurea</i> spp.	Dry, open habitats
<i>Centaurea</i> , type unknown	*	An unknown <i>Centaurea</i> type, similar to <i>C. collina</i> L.	
<i>Centaureum (=C. pulchellum type)</i>	PN	<i>Centaureum maritimum</i> (L.) Fritsch, <i>C. erythraea</i> Rafn <i>C. pulchellum</i> (Swartz) Druce, <i>C. tenuiflorum</i> (Hoffmans. & Link) Fritsch, <i>C. spicatum</i> (L.) Fritsch	Dry grassland, pinewoods, scrub on sandy soils Damp grassy places near the sea
<i>Chamaerops</i>	*	<i>Chamaerops humilis</i> L.	Scrub
<i>Cheilanthes catanensis</i>	*	<i>Cheilanthes catanensis</i> (Cosent) H.P. Fuchs	Rocks, walls, usually calcareous
Chenopodiaceae	MWC	Numerous; includes <i>Beta</i> , <i>Chenopodium</i> , <i>Atriplex</i> , <i>Arthrocnemum</i> , <i>Salicornia</i> , <i>Suaeda</i> spp.	Predominantly saltmarsh, damp and saline terrain in the littoral zone, also dry ground in the interior

<i>Cicendia filiformis</i>	PN	<i>Cicendia filiformis</i> (L.) Delarbre	Humid <i>charnecas</i> (dwarf-scrub), scrub on damp, sandy or peaty ground, grassy places
<i>Cirsium</i> type	MWC	<i>Cirsium vulgare</i> (Savi) Ten.	Hedges, walls, field boundaries, rocky ground
Cistaceae undiff.	-	Includes grains of Cistaceae not identified to one of the other types.	<i>Charnecas</i> (dwarf-scrub), scrub, thickets, pinewoods
<i>Cistus</i> undiff. type	Q	<i>Cistus albidus</i> L., <i>C. crispus</i> L.	<i>Charnecas</i> (dwarf-scrub), scrub, pinewoods
<i>Cistus ladanifer</i> /populifolius types	Q	<i>Cistus ladanifer</i> L. (including <i>C. ladanifer</i> var. <i>sulcatus</i> , syn. <i>C. palinhiae</i> Ingram,), <i>C. populifolius</i> L.	Thickets, scrub, <i>charnecas</i> (dwarf-scrub), pinewoods
<i>Cistus monspeliensis</i> type	Q	<i>Cistus monspeliensis</i> L., <i>C. salvifolius</i> L.	Dry hills, <i>charnecas</i> (dwarf-scrub), scrub, pinewoods
<i>Colchicum</i>	MWC	<i>C. lusitanum</i> Brot.	Rocky terrain
<i>Convolvulus</i>	MWC	<i>Convolvulus tricolor</i> L., <i>C. arvensis</i> L.	Littoral sands, cultivated ground, waysides
<i>Coronilla</i> type	MWC	<i>Coronilla scorpioides</i> (L.) Koch, <i>C. repanda</i> (Poiret) Guss., <i>C. juncea</i> L., <i>C. valentina</i> L.	Dry ground, hills, moors, pinewoods
<i>Corylus</i>	MWC	<i>Corylus avellana</i> L.	Woodland
Crassulaceae	MWC	Numerous; includes <i>Sedum</i> spp.	Arid, sandy and rocky terrain
<i>Cynoglossum officinale</i> type	C	<i>Cynoglossum cheirifolium</i> L., <i>C. clandestinum</i> Desf., <i>C. creticum</i> Miller	Cultivated and waste ground, field margins and waysides; dry, open terrain
Cyperaceae	MWC	Numerous; includes <i>Scirpus</i> , <i>Helicoharis</i> , <i>Carex</i> spp.	Predominantly damp ground and marshes
<i>Daphne</i>	MWC	<i>Daphne gnidium</i> L. (possibly also <i>Thymelaea</i> spp.)	Dry places, <i>charnecas</i> (dwarf-scrub), pinewoods, scrub, wasteground
<i>Echium</i> (= <i>E. vulgare</i> type)	C	<i>Echium tuberculatum</i> Hoffmanns. & Link, <i>E. creticum</i> L., <i>E. plantagineum</i> L., <i>E. gaditanum</i> Boiss.	Sandy ground, scree, maritime sands, cultivated and waste ground, waysides
<i>Ephedra distachya</i> type	MWC	<i>Ephedra distachya</i> L.	
<i>Ephedra fragilis</i> type	MWC	<i>Ephedra fragilis</i> Desf.	Maritime scrub, sandy soils
<i>Erica arborea</i> type	M	<i>Erica arborea</i> L., <i>E. lusitanica</i> L.	Scrub, pinewoods, damp moorland of valleys and streamsides
<i>Erica australis</i> type	M	<i>Erica australis</i> L.	Scrub, <i>charnecas</i> (dwarf-scrub), pinewoods
<i>Erica erigena</i> type	M	<i>Erica erigena</i> R. Ross	Damp ground, marsh fringes
<i>Erica scoparia</i> type	M	<i>Erica scoparia</i> L.	Scrub, pinewoods, hills
<i>Erica umbellata</i> type	M	<i>Erica umbellata</i> L.	Dry places; <i>charnecas</i> (dwarf-scrub), scrub, pinewoods
Ericaceae undiff.	-	Includes pollen tetrads of Ericaceae, predominantly <i>Erica</i> spp., not identified to one of the other types.	Predominantly <i>charnecas</i> (dwarf-scrub), scrub and pinewoods, on dry or damp ground
<i>Erodium</i> (= <i>E. cicutarium</i> type)	StB	<i>Erodium cicutarium</i> (L.) L'Hér. in Aiton, <i>E. botrys</i> (Cav.) Bertol., <i>E. malacoides</i> L'Hér. in Aiton, <i>E. acule</i> (L.) Becherer & Thell., <i>E. chium</i> (L.) Willd.	Dry ground, field margins, waste ground and waysides, often on sandy soils
<i>Eryngium</i>	MWC	<i>Eryngium tenue</i> Lam., <i>E. dilatatum</i> Lam., <i>E. campestre</i> L., <i>Eryngium maritimum</i> L.	Dry, rocky or sandy ground, hills and fields
<i>Eucalyptus</i>	MWC	<i>Eryngium galioides</i> Lam., <i>E. corniculatum</i> Lam.	Maritime sands
<i>Euphorbia</i>	MWC	<i>Eucalyptus globulifera</i> Labill., <i>E. camaldulensis</i> Delnh.	Marshes, springs, damp or flooded ground
<i>Frankenia laevis</i> type	MWC	Numerous <i>Euphorbia</i> spp.	Roadside plantings, cultivated stands, agroforestry (introd.)
<i>Fraxinus</i>	PBH	<i>Frankenia laevis</i> L., possibly other <i>Frankenia</i> spp.	Various
Fabaceae, type unknown	-	<i>Fraxinus angustifolia</i> Vahl.	Saltmarshes and places close to the sea
Fabaceae undiff.	-	Includes grains of an unknown pollen type probably belonging to Fabaceae	River margins and woodland
<i>Fumaria officinalis</i> type	K	<i>Fumaria officinalis</i> L., <i>F. parviflora</i> Lam., <i>F. capreolata</i> L., <i>F. agraria</i> Lag., <i>F. muralis</i> Sonder ex Koch, <i>F. bastardii</i> Boreau	Unknown
<i>Galium</i> type	MWC	<i>Galium palustre</i> L., <i>G. helodes</i> Hoffmanns. & Link, <i>Cruciata laevipes</i> Opiz	Various
		<i>Galium divaricatum</i> Pourret ex Lam., <i>G. parisiense</i> L., <i>G. aparine</i> L., <i>G. murale</i> (L.) Ali., <i>G. tricornutum</i> Dandy, <i>G. verrucosum</i> Hudson, <i>Asperula arvensis</i> L., <i>A. hirsuta</i> Desf., <i>Sherardia arvensis</i> L., <i>Rubia peregrina</i> L., <i>Valantia muralis</i> L., <i>Crucianella maritima</i> L., <i>C. angustifolia</i> L.	Hedges, vineyards and fields, waste ground and waysides
<i>Geranium</i> (= <i>G. molle</i> type)	StB	<i>Geranium molle</i> L., <i>G. rotundifolium</i> L., <i>G. dissectum</i> L., <i>G. lucidum</i> L., <i>G. robertianum</i> L., <i>G. columbinum</i> L.	River margins, damp and shady ground
			Dry places, particularly fallow and waste ground, hedges and walls
<i>Gynandriris sisyrinchium</i>	*	<i>Gynandriris sisyrinchium</i> (L.) Parl.	Fields, orchards, irrigated ground; hedges, walls, waysides
			Dry places, especially near the coast

<i>Halimium halimifolium</i> type	Q	<i>Halimium halimifolium</i> (L.) Willk., <i>H. verticillatum</i> (Brot.) Sennen, <i>H. ocymoides</i> (Lam.) Willk., <i>H. lasianthum</i> (Lam.) Spach, <i>H. alyssoides</i> (Lam.) C. Koch, <i>Cistus libanotis</i> L., <i>Tuberaria globularifolia</i> (Lam.) Willk., <i>T. major</i> (Willk.) P. Silva & Rozeira	Sandy soils, pinewoods, <i>charnecas</i> (dwarf-scrub), scrub
<i>Halimium/Tuberaria</i>	Q	Includes grains which could not be ascribed with confidence to either <i>Halimium halimifolium</i> type or <i>Tuberaria guttata</i> type	<i>Charnecas</i> (dwarf-scrub), matos, especially on sandy soils
<i>Hedera helix</i>	VP	<i>Hedera helix</i> L.	Sebes, rochedos, walls, trees
<i>Helianthemum croceum</i> type	Q	<i>Helianthemum croceum</i> (Desf.) Pers., <i>H. nummularium</i> (L.) Miller, <i>H. oricanifolium</i> (Lam.) Pers, <i>H. aegypticum</i> (L.) Miller, <i>H. marifolium</i> (L.) Miller, <i>H. appeninum</i> (L.) Miller	Dry places, tracks, <i>charnecas</i> (dwarf-scrub)
<i>Helianthemum salicifolium</i> type	Q	<i>Helianthemum salicifolium</i> (L.) Miller	Dry places, tracks, <i>charnecas</i> (dwarf-scrub)
<i>Herniaria</i> type	MWC	<i>Herniaria hirsuta</i> L., <i>H. glabra</i> L.	Dry places, vineyards, waysides, walls
<i>Hypecoum</i>	MWC	<i>Hypecoum procumbens</i> L.	Sandy ground near the sea
		<i>Hypecoum inberbe</i> Sibth. & Sm.	Cultivated ground, waste ground
<i>Ilex aquifolium</i>	MWC	<i>Ilex aquifolium</i> L.	Woodland, hedges
<i>Illecebrum verticillatum</i> type	MWC	<i>Illecebrum verticillatum</i> L.	Damp, sandy places, river margins
<i>Isoetes histrix</i>	BL	<i>Paronychia echinulata</i> Chater, <i>P. argentea</i> Lam.	Dry, stony places, pinewoods, sands, waysides, <i>charnecas</i> (dwarf-scrub)
<i>Isoetes undiff.</i>	MWC	<i>Isoetes histrix</i> Bory	Terrestrial/semi-amphibious, pond margins, damp crevices
<i>Jastone montana</i> type	MWC	<i>Isoetes setacea</i> Lam., <i>I. velata</i> A. Braun in Bory & Durieu, <i>I. durieui</i> Bory, possibly some grains of <i>I. histrix</i> Bory, <i>I. boryana</i> Durieu	
<i>Juniperus</i>	MWC	<i>Jastone montana</i> L., <i>J. corymbosa</i> Poir.	Dry or sandy places, field margins and waysides
<i>Lamiaceae</i> (6-colpate)	-	<i>Juniperus phoenicea</i> L.	Sandy soils, particularly in the littoral zone: rocky places
	MWC	Numerous; includes <i>Thymus</i> , <i>Salvia</i> , <i>Lavandula</i> , <i>Mentha</i> spp.	Various; especially dry and rocky places, <i>charnecas</i> (dwarf-scrub), scrub
<i>Liliaceae</i> undiff.	-	<i>Lemna minor</i> L., <i>L. gibba</i> L.	Stagnant or weakly flowing water
<i>Linaria</i>	MWC	Numerous; includes <i>Altium</i> , <i>Asparagus</i> , <i>Scilla</i> spp. <i>Linaria anethystea</i> (Lam.) Hoffmans. & Link, <i>L. oblongifolia</i> (Boiss.) & Reuter, <i>L. saturojeoides</i> Boiss., <i>Linaria micrantha</i> (Cav.) Hoffmans. & Link, <i>L. hirta</i> (L.) Moench, <i>L. algarviana</i> Chav., <i>L. incarnata</i> (Vent.) Sprengel, <i>L. viscosa</i> (L.) Dum.-Courselet, <i>L. sparteae</i> (L.) Willd.	Various, dry places Dry, open habitats on sandy soils, fields and waste ground
		<i>Linaria lamarckii</i> Roxy, <i>L. pedunculata</i> (L.) Chaz.	Maritime sands
<i>Linum bienne</i> type	PB	<i>Linum bienne</i> Miller (<i>L. usitatissimum</i> L.)	Meadows, woods, waysides, littoral sands
<i>Linum catharticum</i> type	PB	<i>Linum trigynum</i> L., possibly <i>L. tenue</i> Desf.	Hills, <i>charnecas</i> (dwarf-scrub), rocky places, vineyards
<i>Linum</i> undiff.	-	Includes pollen grains of <i>Linum</i> spp. not identifiable to one of the other groups	Dry open habitats, especially on sandy soils
<i>Lotus</i> type	MWC	<i>Lotus edulis</i> L., <i>L. parviflorus</i> Desf., <i>L. subbiflorus</i> Lag., <i>L. corniculatus</i> L. <i>Lotus uliginosus</i> Schkuhr <i>Lotus arenarius</i> Brot., <i>L. creticus</i> L.	Predominantly damp, grassy places Marshes and wet grassland Maritime sands
<i>Lythrum salicaria</i> type	MWC	<i>Lythrum salicaria</i> L., <i>L. graefferi</i> L. = <i>L. junceum</i> Banks & Solander in A. Russell, <i>L. hyssopifolia</i> L., <i>L. thymifolia</i> L., <i>L. borysthenticum</i> (Schrank) Litv. in Majevski	River margins, damp and seasonally flooded places
Malvaceae	MWC	<i>Malva hispanica</i> L., <i>M. sylvestris</i> L., <i>M. nicaensis</i> All., <i>M. parviflora</i> L., <i>Lavatera trimestris</i> L., <i>L. olbia</i> L., <i>L. triloba</i> L., <i>L. cretica</i> L.	Waysides and fields, waste ground
<i>Mercurialis cf. annua</i>	MWC, *	<i>Mercurialis annua</i> L., possibly <i>M. elliptica</i> Lam.	Cultivated and waste ground, entulhos, walls, sebes
<i>Mercurialis cf. fomentosa</i>	MWC, *	<i>Mercurialis tomentosa</i> L.	Sebes, waysides, dry pasture
<i>Myrica</i>	MWC	<i>Myrica gale</i> L.	Damp ground and bogs
		<i>Myrica faya</i> Aiton.	Evergreen woodland, thickets
<i>Myriophyllum alterniflorum</i>	E	<i>Myriophyllum alterniflorum</i> DC. In Lam. & DC.	Stagnant or weakly flowing water
<i>Myriophyllum spicatum</i>	E	<i>Myriophyllum spicatum</i> L.	Stagnant or weakly flowing water
<i>Myrtus</i>	MWC	<i>Myrtus communis</i> L.	Woodland understory, scrub, hedges, <i>charnecas</i> (dwarf-scrub), pinewoods
<i>Nuphar</i>	JC	<i>Nuphar lutea</i> (L.) Sibth. & Sm.	Stagnant or weakly flowing water
<i>Nymphaea</i>	JC	<i>Nymphaea alba</i> L.	Stagnant or weakly flowing water
<i>Olea</i>	PBH	<i>Olea europaea</i> L.	Evergreen woodland, hedges, rocky and dry terrain
<i>Onobrychis</i> type	MWC	<i>Onobrychis peduncularis</i> (Cav.) DC.	Dry hills

<i>Ononis</i> type	MWC	<i>Ononis spinosa</i> L., <i>O. natrix</i> L., <i>O. mitissima</i> L., <i>O. cintrana</i> Brot., <i>O. pubescens</i> L., <i>O. viscosa</i> L. <i>Ononis baetica</i> Clemente, <i>O. diffusa</i> Ten., <i>O. variegata</i> L., <i>O. subspicata</i> Lag., <i>O. reclinata</i> L.	Dry terrain, hills, cultivated and waste ground Sandy ground, particularly near the coast
<i>Optiloglossum lusitanicum</i>	*	<i>Optiloglossum lusitanicum</i> L.	Seasonally flooded ground, damp depressions and small basins
<i>Osmunda regalis</i>	MWC	<i>Osmunda regalis</i> L.	River margins, damp places
<i>Oxalis pes caprae</i>	*	<i>Oxalis pes caprae</i> L.	Cultivated, disturbed and waste ground, field margins (introd.)
<i>Papaver rhoeas</i> type	K	<i>P. rhoeas</i> L., <i>P. hybridum</i> L., <i>P. rhoeas</i> L., <i>P. dubium</i> L.	Fields, fallow and waste ground
<i>Phillyrea</i>	PBH	<i>Phillyrea angustifolia</i> L. <i>Phillyrea latifolia</i> L.	Woodland understorey, scrub, <i>charnecas</i> (dwarf-scrub), pinewoods, hedges Woods, hedges, river margins
<i>Phytolaria globulifera</i>	MWC	<i>Phytolaria globulifera</i> L., <i>P. minuta</i> Durieu ex A. Braun	Seasonally wet hollows, marsh fringes, ditches
<i>Pinus</i> (Diploxylon type)	MWC	<i>Pinus pinaster</i> L., <i>P. pinaster</i> Alton, <i>P. halepensis</i> Miller <i>Pinus sylvestris</i> L.	Sandy soils, stable dunes Montane settings, predominantly extraregional
<i>Pistacia</i>	*	<i>Pistacia lentiscus</i> L., <i>P. terebinthus</i> L.	Thickets, hedges, scrub
<i>Plantago albicans</i> type	S	<i>Plantago albicans</i> L.	<i>Charnecas</i> (dwarf-scrub), arid terrain
<i>Plantago coronopus</i> type	S	<i>Plantago coronopus</i> L., possibly <i>P. serraria</i> L.	Cultivated and waste ground, waysides, walls, littoral sands
<i>Plantago lanceolata</i> type	S	<i>Plantago lanceolata</i> L., <i>P. lagopus</i> L., <i>P. bellardii</i> All.	Cultivated and waste, grassy places, field margins and waysides
<i>Plantago major</i> type	S	<i>Plantago major</i> L.	Ditches, damp or grassy places, waysides
<i>Plantago</i> undiff.	-	Includes grains of <i>Plantago</i> not identifiable to one of the other types	
Poaceae	MWC	Numerous	Diverse; dry, wetland and maritime habitats
Poaceae D>38 P>8	-	Poaceae pollen with grain diameter >38 and pore diameter > 8 µm; includes the cultivated grasses (Cerealia type), but possibly other large-grained Poaceae, e.g. <i>Glyceria fluitans</i> (L.) R. Brown	Arable fields (possibly ambiguous)
<i>Polygonum aviculare</i> type	MWC	<i>Polygonum aviculare</i> L., <i>P. maritimum</i> L., <i>P. equisetiforme</i> Sibth. & Sm., possibly other <i>Polygonum</i> spp.	Maritime sands, cultivated and waste ground, waysides
<i>Polygonum persicaria</i> type	MWC	<i>Polygonum hydropiper</i> L., <i>P. salicifolium</i> Brouss ex. Willd., <i>P. persicaria</i> L., <i>P. lapathifolium</i> L.	Ditches, river margins, damp terrain
<i>Polypodium vulgare</i> type	MWC	<i>Polypodium vulgare</i> L., <i>P. australe</i> Fée	Walls, rocks, trees, hedges
<i>Potamogeton</i> subg. <i>Potamogeton</i>	MWC	<i>Potamogeton natans</i> L., <i>P. nodosus</i> Poir et in Lam.	Ditches, marshes, rivers
<i>Pteropsida</i> (monolete) undiff.	BWE	Includes monolete spores not identified to one of the other types	Various
<i>Pteropsida</i> (trilete) undiff.	BWE	Includes trilete spores not identified to one of the other types	Various
<i>Quercus coccifera</i> type	SR	<i>Quercus coccifera</i> L.	Pinewoods, <i>charnecas</i> (dwarf-scrub), arid terrain
<i>Quercus</i> deciduous type	SR	<i>Quercus rotundifolia</i> Lam. <i>Quercus faginea</i> Lam., <i>Q. canariensis</i> Willd., possibly <i>Q. pyrenaica</i> Willd., <i>Q. robur</i> L.	Woodland, <i>montados</i> (parkland) Woodland on humus rich soils
<i>Quercus suber</i> type	SR	<i>Quercus lusitanica</i> Lam.	<i>Charnecas</i> (dwarf-scrub), scrub, pinewoods
<i>Quercus</i> undiff.	-	<i>Quercus suber</i> L.	Woodland, <i>montados</i> (parkland)
<i>Radiola</i>	MWC	Includes pollen grains of <i>Quercus</i> spp. not identifiable to one of the other types <i>Radiola tinoides</i> Roth.	Sandy soils, <i>charnecas</i> (dwarf-scrub), pinewoods
<i>Ranunculus</i> type (= <i>R. acris</i> group)	MWC (CPH)	Numerous <i>Ranunculus</i> spp.	Various; includes plants of dry ground and shallow water aquatics
<i>Rhamnus</i>	MWC	<i>Rhamnus alaternus</i> L., <i>R. lycioides</i> L.	Hedges, thickets, rocky places
<i>Rhododendron ponticum</i>	M	<i>Rhododendron ponticum</i> L.	Woodland, near streams
<i>Rhus</i>	MWC	<i>Rhus cortaria</i> L.	Rocky places, field boundaries and waysides
<i>Rosaceae</i> undiff.	-	Includes grains belonging to Rosaceae, not further identifiable	Various
<i>Rumex acetosa</i> type (= <i>R. acetosa</i> group)	MWC	<i>Rumex acetosa</i> L., possibly other <i>Rumex</i> spp.	Meadows, cultivated ground
<i>Rumex acetosella</i> type (= <i>R. acetosella</i> group)	MWC	<i>Rumex acetosella</i> L., <i>R. angiocarpus</i> Murb., <i>R. bucephalophorus</i> L., possibly also <i>R. intermedius</i> DC., <i>R. conglomeratus</i> Murray, <i>R. pulcher</i> L.	Dry and rocky terrain, cultivated and waste ground, waysides and walls
<i>Rumex</i> undiff.	-	Includes pollen grains of <i>Rumex</i> spp. not identified to one of the other groups	Various; predominantly open habitats on both dry or wet ground
<i>Salix</i>	MWC	<i>Salix alba</i> L., <i>S. salicifolia</i> Brot., <i>S. atrocinerea</i> Brot., possibly other <i>Salix</i> spp.	River margins and ditches, humid places
<i>Sambucus ebulus</i>	PRR	<i>Sambucus ebulus</i> L.	River margins, damp and shady places
<i>Samolus</i>	MWC	<i>Samolus valerandi</i> L.	River margins, marshes, damp places

<i>Sanguisorba minor</i>	MWC	<i>Sanguisorba minor</i> Scop.	Grassy places, waysides, muddy ground
<i>Scabiosa colombaria</i> type	CJb	<i>Scabiosa atropurpurea</i> L., <i>S. colombaria</i> L., <i>S. monspeliensis</i> Jacq.	Dry places, waste ground, vineyards, tracks
<i>Scrophularia</i> type	MWC	<i>Scrophularia auriculata</i> L., <i>S. scorodonia</i> L., <i>S. sambucifolia</i> L.	River margins, damp or flooded ground
		<i>Scrophularia canina</i> L.	Maritime sands
		<i>Verbascum virgatum</i> Stokes in With., <i>V. thapsus</i> L., <i>V. sinuatum</i> L.	Dry or sandy ground, scrub and waysides
<i>Selaginella denticulata</i>	St	<i>Selaginella denticulata</i> (L.) Link	Damp, shady places
<i>Serratula</i> type	MWC	<i>Serratula flavesces</i> (L.) Poir. in Lam., <i>S. pinnatifida</i> (Cav.) Poir. et, <i>S. alcalae</i> Cossou, <i>Carlina corymbosa</i> L., <i>C. racemosa</i> L., <i>Onopordum macracanthum</i> Schousboe	Thickets, scrub, waste ground and tracks, on dry, rocky terrain
		<i>Arctium minus</i> Bernh.	Fertile and shady ground, hedges, river margins
<i>Spergula</i> type	MWC	<i>Spergula arvensis</i> L., <i>Spergularia</i> spp. (<i>S. media</i> (L.) C. Presl, <i>S. rupicola</i> Lebel ex Le Jolis., <i>S. marina</i> (L.) Griseb.), <i>Loeflingia</i> spp. (<i>L. micrantha</i> Boiss & Reuter, <i>L. tavaresiana</i> Samp.), <i>Polycarpon tetraphyllum</i> (L.) L. and possibly others	Dry and saline soils, particularly near the coast; also waste ground, field margins, waysides
<i>Stachys</i> type (= <i>Stachys sylvatica</i> type)	MWC	<i>Stachys arvensis</i> (L.) L., <i>Lamium amplexicaule</i> L., <i>Ajuga iva</i> (L.) Schreber	Cultivated and waste ground, field margins and tracks
		<i>Stachys germanica</i> L.	Ditches, damp places, hedges
<i>Tamarix</i>	MWC	<i>Phlomis lychnitis</i> L., <i>P. purpurea</i> L.	Dry and rocky terrain
		<i>Tamarix africana</i> Poir. et, <i>T. canariensis</i> Willd.	Coastal marshes, river margins
<i>Teucrium</i>	MWC	<i>Teucrium pseudo-chamaepitys</i> L., <i>T. fruticosum</i> L.	Dry places, hedges
		<i>Teucrium scordium</i> L.	Humid places, marshes, river margins
<i>Trifolium</i> type	MWC	<i>Trifolium tomentosum</i> L., <i>T. scabrum</i> L., <i>T. arvense</i> L., <i>T. stellatum</i> L., <i>T. lappaceum</i> L., <i>Medicago orbicularis</i> (L.) Bartal., <i>M. rigidula</i> (L.) All., <i>M. aculeata</i> Gaertner, <i>M. truncatula</i> Gaertner, <i>M. minima</i> (L.) Bartal., <i>Medicago tornata</i> (L.) Miller	Fallow and waste ground, fields
		<i>Trifolium cheirleri</i> L., <i>T. glomeratum</i> L., <i>T. suffocatum</i> L., <i>T. bocconei</i> Savi, <i>T. liquisticum</i> Balbis ex Loisel., <i>T. angustifolium</i> L., <i>T. fragiferum</i> L., <i>T. aureum</i> Pollich	Open ground, grassy places, tracks and waysides
		<i>Trifolium micranthum</i> Viv., <i>T. isthmocarpum</i> Brot., <i>T. repens</i> L., <i>T. subterraneum</i> L., <i>T. striatum</i> L., <i>T. squamosum</i> L., <i>T. pratense</i> L., <i>T. spumosum</i> L., <i>Medicago arabica</i> (L.) Hudson	Damp, grassy places, meadows and river margins
		<i>Medicago marina</i> L., <i>M. littoralis</i> Rohde ex Loisel.	Maritime sands and marshes
<i>Tuberaria guttata</i> type	Q	<i>Tuberaria guttata</i> (L.) Fourr., <i>T. lignosa</i> (Sweet) Samp., <i>T. bupleurifolia</i> (Lam.) Willk., <i>Halimium commutatum</i> Pau	<i>Charnecas</i> (dwarf-scrub), pinewoods, sandy soils
<i>Typha latifolia</i> type	P	<i>Typha latifolia</i> L.	Marshes, ditches, ponds
<i>Typha/Sparganium</i> (= <i>S. emersum</i> / <i>S. erectum</i> types)	P	<i>Typha angustifolia</i> L., <i>Sparganium erectum</i> L.	Marshes, ditches, ponds
<i>Ulex</i> type	MWC	<i>Ulex europaeus</i> L., <i>U. minor</i> Roth, <i>U. argenteus</i> Welw. ex Webb, <i>U. parviflorus</i> Pourret, <i>Stauracanthus boivinii</i> (Webb) Samp., <i>S. genistoides</i> (Brot.) Samp., <i>Genista triacanthos</i> Brot., <i>G. hirsuta</i> Vahl, <i>G. polyanthos</i> R. de Roemer ex Willk., <i>Cytisus grandiflorus</i> DC., <i>C. scoparius</i> (L.) Link	<i>Charnecas</i> (dwarf-scrub), scrub, hedges, pinewoods
<i>Ulmus</i>	MWC	<i>Ulmus minor</i> Miller	River margins, hedges, woods
<i>Valerianella</i>	MWC	<i>Valerianella carinata</i> Loisel., <i>V. microcarpa</i> Loisel., <i>V. eriocarpa</i> Desv., <i>V. discoides</i> (L.) Loisel.	Cultivated fields, grassy places, waste ground
<i>Viburnum tinus</i>	PRR	<i>Viburnum tinus</i> L.	Woodland understorey, hedges, river margins
<i>Vitis vinifera</i>	MWC	<i>Vitis vinifera</i> L.	Woods, hedges; also cultivated

REFERENCES

[BL] Berthet & Lecocq, 1977; [B] Blackmore, 1984; [BWE] Bennett et al., 1994; [C] Clarke, 1980; [CJa] Clarke & Jones, 1980; [CJb] Clarke & Jones, 1981; [CPH] Clarke et al., 1991; [E] Engel, 1980; [JC] Jones & Clarke, 1981; [K] Kalis, 1980; [M] Mateus, 1989; [MWC] Moore et al., 1991; [P] Punt, 1976; [PLV] Punt et al., 1976; [PN] Punt & Neinhuis, 1976; [PRR] Punt et al., 1976b; [PB] Punt & den Breijer, 1981; [PBH] Punt et al., 1991; [Q] Queiroz, 1999; [S] Saad, 1986; [SR] Sáenz de Rivas, 1973; [SJ] Stafford 1991; [SB] Stafford & Blackmore, 1991; [VCP] van Benthem et al., 1984; [VPH] van Leeuwen et al., 1988; [VP] van Helvoort & Punt, 1984; [*] pollen taxon based on reference pollen slides and photographs in Reille (1992;1995)